MRR 2005-1

New Nouveau
Brunswick

Natural Resources
Minerals, Policy and Planning

Mineral Resource Report

GEOLOGICAL INVESTIGATIONS IN NEW BRUNSWICK FOR 2004

Gwen L. Martin, editor

2005

Mineral Resource Report 2005-1

GEOLOGICAL INVESTIGATIONS IN NEW BRUNSWICK FOR 2004

ISSN 0548-4014
ISBN 1-55396-354-7

Cover illustration:	*Natural rock arch in mafic volcanic flows of the Val d'Amour Formation, Inch Arran Park, New Brunswick* Photograph courtesy of Reginald A. Wilson
Preparation of figures:	Terry L. Leonard
Design and layout:	Gwen L. Martin
Translation:	Toutes les traductions ont été préparées par le Bureau de traduction, Ministère de l'Approvisionnement et des Services du Nouveau-Brunswick. All translations were provided by the Translation Bureau, New Brunswick Department of Supply and Services.

This report has been prepared by:

Minerals, Policy and Planning Division
Department of Natural Resources

Hon. Keith Ashfield
Minister of Natural Resources

October 2005

New Nouveau
Brunswick

Natural Resources
Minerals, Policy and Planning

GEOLOGICAL INVESTIGATIONS IN NEW BRUNSWICK FOR 2004

Gwen L. Martin, editor

ISSN 0548-4014
ISBN 1-55396-354-7

2005

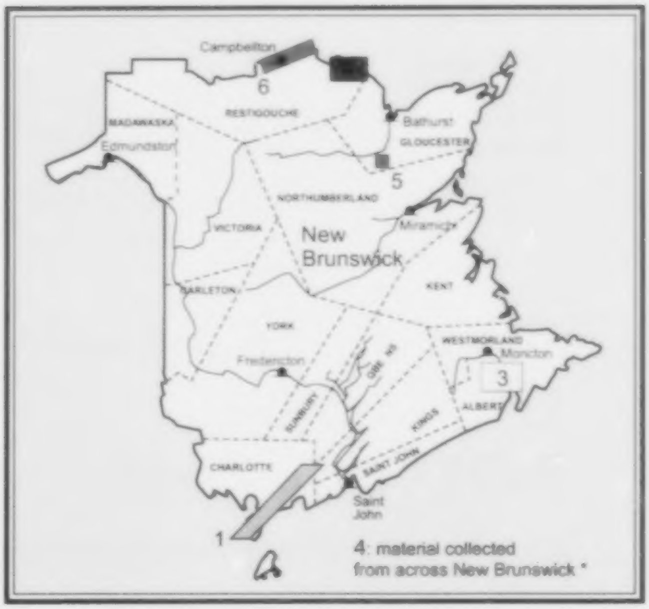
Campbellton
6
RESTIGOUCHE
MADAWASKA
Edmundston
Bathurst
GLOUCESTER
5
NORTHUMBERLAND
VICTORIA
New Brunswick
Miramichi
CARLETON
KENT
YORK
WESTMORLAND
Moncton
Fredericton
QUEENS
3
SUNBURY
KINGS
ALBERT
CHARLOTTE
SAINT JOHN
Saint John
1
4: material collected from across New Brunswick *

Map index to papers in this volume:

1. Distribution and petrochemistry of Late Neoproterozoic rocks in the southwestern New River Terrane, southern New Brunswick (Bartsch, Barr).
2. Geotechnical implications of bedrock characteristics in the Belledune area, northern New Brunswick (Dimitrov, McCutcheon).
3. Deformation of Lower Carboniferous rocks in the Rosevale to Saint-Joseph area, Albert and Westmorland counties, southeastern New Brunswick (Park, St. Peter).
4. Information values for trace elements in five New Brunswick till reference materials (Seaman, Boldon). *
5. Gilmour Brook South base-metal occurrence, Bathurst Mining Camp, northern New Brunswick (Walker).
6. Geology of the Val d'Amour Formation: revisiting the type area of the Dalhousie Group, northern New Brunswick (Wilson, Kamo, Burden).

Recommended citation:

Martin, G.L. (editor). 2005. Geological investigations in New Brunswick for 2004. New Brunswick Department of Natural Resources; Minerals, Policy and Planning Division, Mineral Resource Report 2005-1, 212 p.

Sample recommended citation for individual papers:

Bartsch, C.J., and Barr, S.M. 2005. Distribution and petrochemistry of Late Neoproterozoic rocks in the southwestern New River Terrane, southern New Brunswick. *In* Geological Investigations in New Brunswick for 2004. *Edited by* G.L. Martin. New Brunswick Department of Natural Resources; Minerals, Policy and Planning Division, Mineral Resource Report 2005-1, pp. 1–22.

TABLE OF CONTENTS

Pages

Distribution and petrochemistry of Late Neoproterozoic rocks in the southwestern New River Terrane, southern New Brunswick ◊ ☆ 1–22
C.J. BARTSCH[1] AND S.M. BARR[1]
[1] Department of Geology, Acadia University

Geotechnical implications of bedrock characteristics in the Belledune area, northern New Brunswick ☆ ▽ 23–44
I. DIMITROV[1] AND S.R. MCCUTCHEON[2]
[1] Department of Geology, University of New Brunswick
[2] Geological Surveys Branch, New Brunswick Department of Natural Resources

Deformation of Lower Carboniferous rocks in the Rosevale to Saint-Joseph area, Albert and Westmorland counties, southeastern New Brunswick ◊ 45–98
A.F. PARK[1] AND C.J. ST. PETER[2]
[1] Department of Geology, University of New Brunswick
[2] Geological Surveys Branch, New Brunswick Department of Natural Resources

Information values for trace elements in five New Brunswick till reference materials ◊ 99–126
A.A. SEAMAN[1] AND G.R. BOLDON[1]
[1] Geological Surveys Branch, New Brunswick Department of Natural Resources

Gilmour Brook South base-metal occurrence, Bathurst Mining Camp, northern New Brunswick ◊ 127–166
J.A. WALKER[1]
[1] Geological Surveys Branch, New Brunswick Department of Natural Resources

Geology of the Val d'Amour Formation: revisiting the type area of the Dalhousie Group, northern New Brunswick ◊ 167–212
R.A. WILSON[1], S. KAMO[2], AND E.T. BURDEN[3]
[1] Geological Surveys Branch, New Brunswick Department of Natural Resources
[2] Jack Satterly Geochronology Laboratory, Department of Geology, University of Toronto
[3] Department of Earth Sciences, Memorial University of Newfoundland

---

Funding:
◊ Geological Surveys Branch, New Brunswick Department of Natural Resources
☆ National Sciences and Engineering Research Council of Canada research grant
▽ Elmtree Resources Ltd.

106-01084/

DISTRIBUTION AND PETROCHEMISTRY OF LATE NEOPROTEROZOIC ROCKS IN THE SOUTHWESTERN NEW RIVER TERRANE, SOUTHERN NEW BRUNSWICK

CAMERON J. BARTSCH [1] AND SANDRA M. BARR [1]
[1] Department of Geology, Acadia University, Wolfville,
Nova Scotia, CANADA B4P 2R6 *(sandra.barr@acadiau.ca)*

Bartsch, C.J., and Barr, S.M. 2005. Distribution and petrochemistry of Late Neoproterozoic rocks in the southwestern New River Terrane, southern New Brunswick. *In* Geological Investigations in New Brunswick for 2004. *Edited by* G.L. Martin. New Brunswick Department of Natural Resources; Minerals, Policy and Planning Division, Mineral Resource Report 2005–1, pp. 1–22.

The narrow, fault-bounded New River Terrane contains the northwesternmost exposures of Neoproterozoic rocks known in southern New Brunswick. In 2004–2005, a mapping and petrological project was conducted to 1) clarify relationships among Neoproterozoic units in the southwestern part of the terrane, and 2) compare those rocks with units of similar age in the northeastern part of the terrane in the Long Reach area. As a result of this work, Neoproterozoic rocks in the southwestern New River Terrane are divided into ca. 620 Ma and ca. 555 Ma suites. The ca. 620 Ma suite consists of the Blacks Harbour Granodiorite and closely associated Beaver Harbour Porphyry. The ca. 555 Ma rocks are divided into the primarily volcanic Leavitts Head and McCallum Brook formations, and the comagmatic Little New River Granitoid Suite, Ragged Falls Granite, and Pull and Be Damned Granite. Both the ca. 620 Ma and ca. 555 Ma igneous rocks exhibit chemical signatures that are characteristic of formation in continental margin subduction settings. These suites correspond in ages and petrological characteristics to the Lingley Plutonic Suite and Lobster Brook Formation, respectively, which occur in the northeastern part of the New River Terrane.

Le terrane étroit, limité par des failles, de New River renferme les affleurements les plus au nord-ouest de roches néoprotérozoïques connus dans le Sud du Nouveau-Brunswick. On a réalisé en 2004-2005 un projet d'étude pétrologique et de cartographie dans le but de 1) clarifier les relations existant entre les unités néoprotérozoïques dans le sud-ouest du terrane et 2) de comparer ces roches avec des unités d'âge similaire dans le nord-est du terrane, dans le secteur du passage Long. Par suite de ces travaux, les roches néoprotérozoïques dans le sud-ouest du terrane de New River ont été subdivisées en cortèges d'environ 620 Ma et d'environ 555 Ma. Le cortège d'environ 620 Ma est constitué de la granodiorite de Blacks Harbour et du porphyre intimement associé de Beaver Harbour. Les roches d'environ 555 Ma ont été subdivisées en formations principalement volcaniques de Leavitts Head et de McCallum Brook ainsi qu'en plusieurs unités comagmatiques, soit le cortège granitique de la Petite rivière New, le granite des chutes Ragged et le granite Pull and Be Damned. Les roches ignées d'environ 620 Ma et 555 Ma présentent dans les deux cas des signatures chimiques caractéristiques d'une formation dans des environnements de subduction de marge continentale. Les âges et les caractéristiques pétrologiques de ces cortèges correspondent au cortège plutonique de Lingley et à la Formation de Lobster Brook, respectivement, qui se trouvent dans le nord-est du terrane de New River.

INTRODUCTION

The relationship of the New River Terrane in southwestern New Brunswick (Fig. 1) to the Avalon and Gander zones of Williams (1979) remains uncertain. Some rock units in the New River Terrane are Late Neoproterozoic and Cambrian, which suggests that the terrane may be part of the Avalon Zone. However, some other Cambrian components of the terrane are more similar to those in more inboard terranes of the Gander Zone (Johnson and McLeod 1996). Johnson (2001) interpreted the New River Terrane as a composite belt, in which fragments of both Avalon and Gander zones are separated by the Robin Hood Lake Fault (Johnson 2001). Other studies (e.g. Barr et al. 2003; King and Barr 2004) disputed the Avalonian affinity of parts of the terrane. Given this debate over its tectonic evolution, the New River Terrane plays an important role in interpretations of the northern Appalachian Orogen.

Mapping and petrological studies (Johnson 2001; Johnson and Barr 2004) have been conducted in the northeastern part of the New River Terrane in the Long Reach area (Fig. 1). The present study therefore focused on the southwestern part of the terrane (Fig. 1). The work consisted of re-examining lithological characteristics and relationships of Neoproterozoic units. This report describes the lithology and geochemistry of those units and compares them with units of similar age in the northeastern part of the terrane.

GEOLOGICAL SETTING

Southern New Brunswick is characterized by northeast-trending, fault-bounded belts of diverse pre-Carboniferous rocks. The tectonic belts form the eastern edge of the Appalachian Orogen in the province and originally were included in the Avalon and Gander zones of Williams (1979). They have since been divided (from east to west) into the Caledonia, Brookville, Kingston, New River, Mascarene, and St. Croix terranes (Fig. 1). The New River Terrane lies in the approximate centre of these belts, bounded on the southeast by the Belleisle Fault and on the northwest by the Back Bay Fault (Fig. 2).

The Caledonia Terrane contains Late Neoproterozoic volcanic and sedimentary rocks of the ca. 620 Ma Broad River Group and ca. 560–550 Ma Coldbrook Group, plus their cogenetic plutons, all of which are unconformably overlain by Cambrian–Ordovician

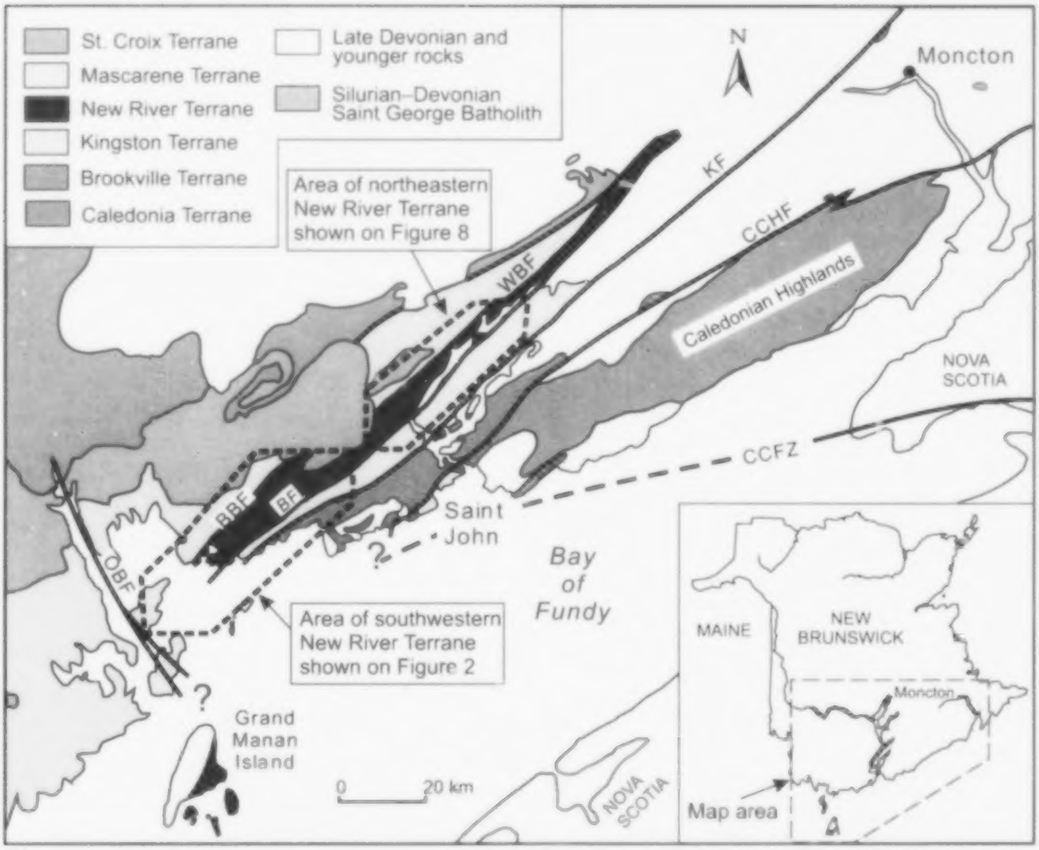
St. Croix Terrane
Mascarene Terrane
New River Terrane
Kingston Terrane
Brookville Terrane
Caledonia Terrane
Late Devonian and younger rocks
Silurian–Devonian Saint George Batholith
N
Moncton
KF
Area of northeastern New River Terrane shown on Figure 8
CCHF
WBF
Caledonian Highlands
NOVA SCOTIA
CCFZ
BBF
BF
Saint John
OBF
?
Bay of Fundy
Area of southwestern New River Terrane shown on Figure 2
Grand Manan Island
0
20 km
NOVA SCOTIA
MAINE
NEW BRUNSWICK
Moncton
Map area

Figure 1. Tectonostratigraphic subdivisions in southern New Brunswick (after Johnson and Barr 2004). BBF = Back Bay Fault, BF = Belleisle Fault, CCFZ = Cobequid–Chedabucto Fault Zone, CCHF = Caledonia–Clover Hill Fault, KF = Kennebecasis Fault, OBF = Oak Bay Fault, WBF = Wheaton Brook Fault.

sedimentary rocks (Barr and White 1999 and references therein). The adjacent Brookville Terrane comprises Neoproterozoic metasedimentary rocks, orthogneissic and paragneissic rocks, abundant ca. 550–525 Ma plutonic rocks, and minor volcanic rocks (White and Barr 1996; White et al. 2002 and references therein). The Kingston Terrane contains a succession of lowermost Silurian (ca. 442–435 Ma) volcanic rocks and cogenetic high-level plutons interpreted to have formed in a volcanic-arc setting along a continental margin (Barr et al. 2002). The Silurian rocks of the Kingston Terrane separate Neoproterozoic rocks of the Brookville and Caledonia terranes from those of the New River Terrane, described in more detail below. The Mascarene Terrane, northwest of the New River Terrane, consists of Ordovician–Devonian volcanic and sedimentary cover rocks and Silurian–Devonian plutons. The St. Croix Terrane contains Cambrian–Silurian sedimentary and minor volcanic rocks (Fyffe et al. 1999 and references therein).

The St. Croix, Mascarene, New River, and possibly Brookville terranes all have been interpreted to be linked to the Gander Zone and underlain by Ganderian basement rocks (van Staal and Fyffe 1995; van Staal et al. 1998; King and Barr 2004). However, the New River Terrane also displays broad similarities to the Caledonia Terrane in that both contain ca. 620 Ma and ca. 555 Ma igneous suites locally overlain by, or in faulted contact with, Cambrian–Ordovician rocks (Currie and Hunt 1991; Johnson and McLeod 1996; Currie and McNicoll 1999; Barr et al. 2003; McLeod et al. 2003; Johnson and Barr 2004). One notable difference is that Cambrian–Ordovician sequences in the New River Terrane contain volcanic rocks, whereas those in the Caledonia Terrane lack volcanic units (Tanoli and Pickerill 1988).

Ca. 620 Ma Units in the Southwestern New River Terrane

The ca. 620 Ma rocks in the southwestern New River Terrane are restricted to the area southeast of the Letang Harbour Fault of Donohoe (1978). They constitute the Blacks Harbour Granodiorite and Beaver Harbour Porphyry (Fig. 2).

Blacks Harbour Granodiorite

The Blacks Harbour Granodiorite was named the Blacks Harbour Granite by Helmstaedt (1968) but in the present study was found to have a predominantly intermediate composition and so is more appropriately termed the Blacks Harbour Granodiorite. McLeod et al. (1994) interpreted the unit as Neoproterozoic, an age that has since been substantiated by a U–Pb zircon date of 622 ± 2 Ma (Barr et al. 2003).

The Blacks Harbour Granodiorite consists of a grey to green to greenish-yellow, medium-grained granodiorite (Fig. 3) that is gradational to tonalite and locally granite. Granodiorite samples typically contain 70% to 80% plagioclase and quartz, as well as 20% to 30% K-feldspar phenocrysts, chlorite after biotite, and opaque minerals. Plagioclase has undergone variable degrees of saussuritization, resulting in abundant albite, sericite, epidote, and calcite in most samples. Overall, the degree of cataclasis increases westward toward Letang Harbour. This change is accompanied by increased limonite staining and the presence of abundant fault blocks containing maroon conglomerate and sandstone from the overlying Devonian Perry Formation.

Most contacts between the Blacks Harbour Granodiorite and surrounding units are faulted. Near the village of Blacks Harbour, however, the Blacks Harbour Granodiorite is disconformably overlain by the Perry Formation, which contains numerous granitoid clasts that clearly are derived from the granodiorite.

Beaver Harbour Porphyry

As mapped by Helmstaedt (1968) and modified herein, the Beaver Harbour Porphyry occurs as faulted slivers within the Blacks Harbour Granodiorite in the Deadmans Harbour–Beaver Harbour area and extends along the southeastern margin of the terrane to New River (Fig. 2). The unit is undated but has been assigned a ca. 620 Ma age, based on its spatial association with the Blacks Harbour Granodiorite.

The Beaver Harbour Porphyry includes two similar rock types that differ in grain size and phenocryst characteristics. One is feldspar porphyry that occurs mainly along the

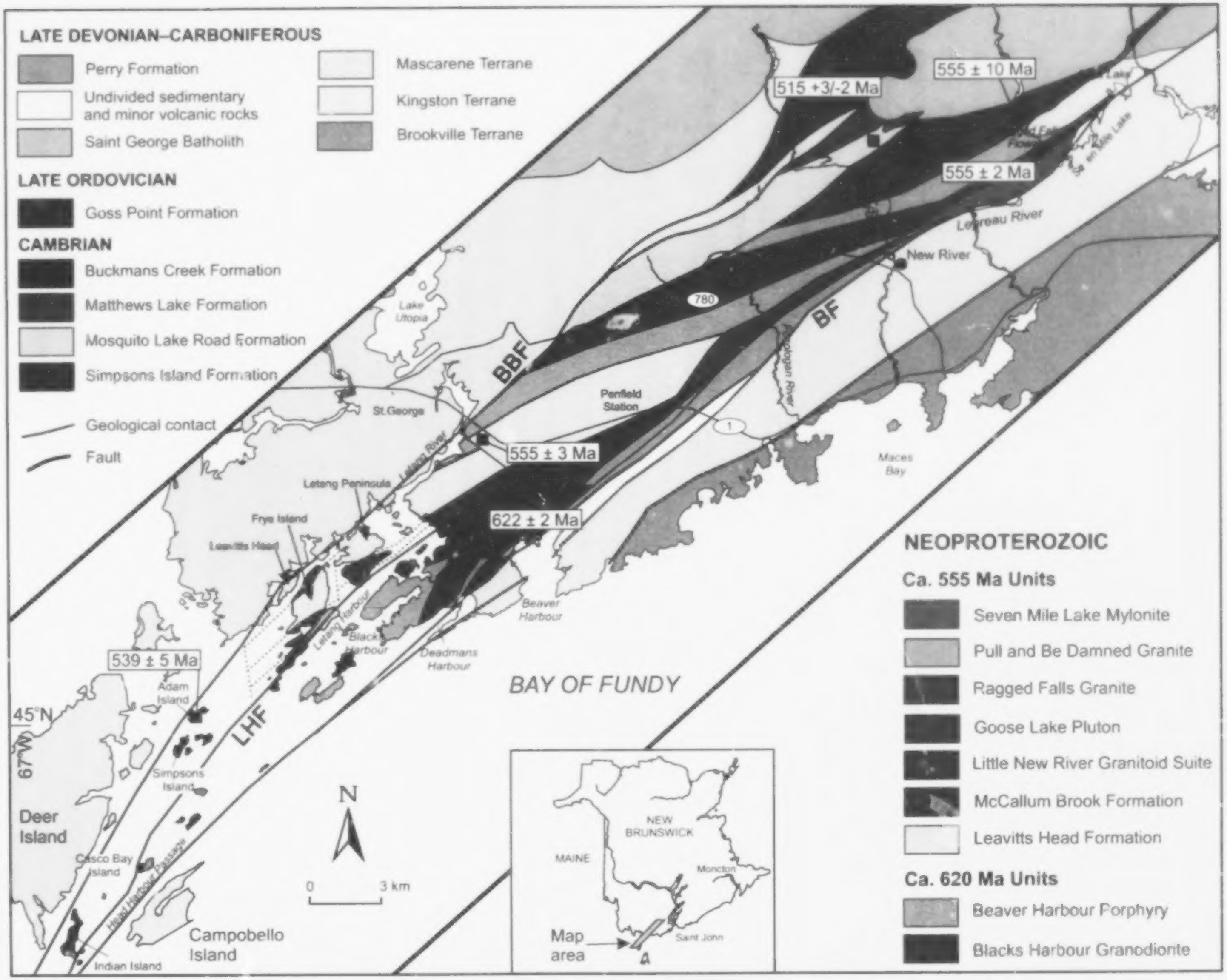
LATE DEVONIAN–CARBONIFEROUS
Perry Formation
Undivided sedimentary and minor volcanic rocks
Saint George Batholith
Mascarene Terrane
Kingston Terrane
Brookville Terrane
LATE ORDOVICIAN
Goss Point Formation
CAMBRIAN
Buckmans Creek Formation
Matthews Lake Formation
Mosquito Lake Road Formation
Simpsons Island Formation
Geological contact
Fault
515 +3/-2 Ma
555 ± 10 Ma
555 ± 2 Ma
555 ± 3 Ma
622 ± 2 Ma
539 ± 5 Ma
Lepreau River
New River
780
BF
BBF
Lake Utopia
Penfield Station
St.George
1
Maces Bay
Letang Peninsula
Frye Island
Leavitts Head
Letang Harbour
Blacks Harbour
Beaver Harbour
Deadmans Harbour
BAY OF FUNDY
45°N
67°W
Adam Island
LHF
Simpsons Island
Deer Island
Casco Bay Island
Head Harbour Passage
Campobello Island
Indian Island
N
0
3 km
NEW BRUNSWICK
MAINE
Moncton
Saint John
Map area
NEOPROTEROZOIC
Ca. 555 Ma Units
Seven Mile Lake Mylonite
Pull and Be Damned Granite
Ragged Falls Granite
Goose Lake Pluton
Little New River Granitoid Suite
McCallum Brook Formation
Leavitts Head Formation
Ca. 620 Ma Units
Beaver Harbour Porphyry
Blacks Harbour Granodiorite

Figure 2. Simplified geological map of the southwestern part of the New River Terrane, based on the present study and Smith et al. (2004). BBF = Back Bay Fault, BF = Belleisle Fault, LHF = Letang Harbour Fault. U–Pb ages in boxes are from sources cited in the text.

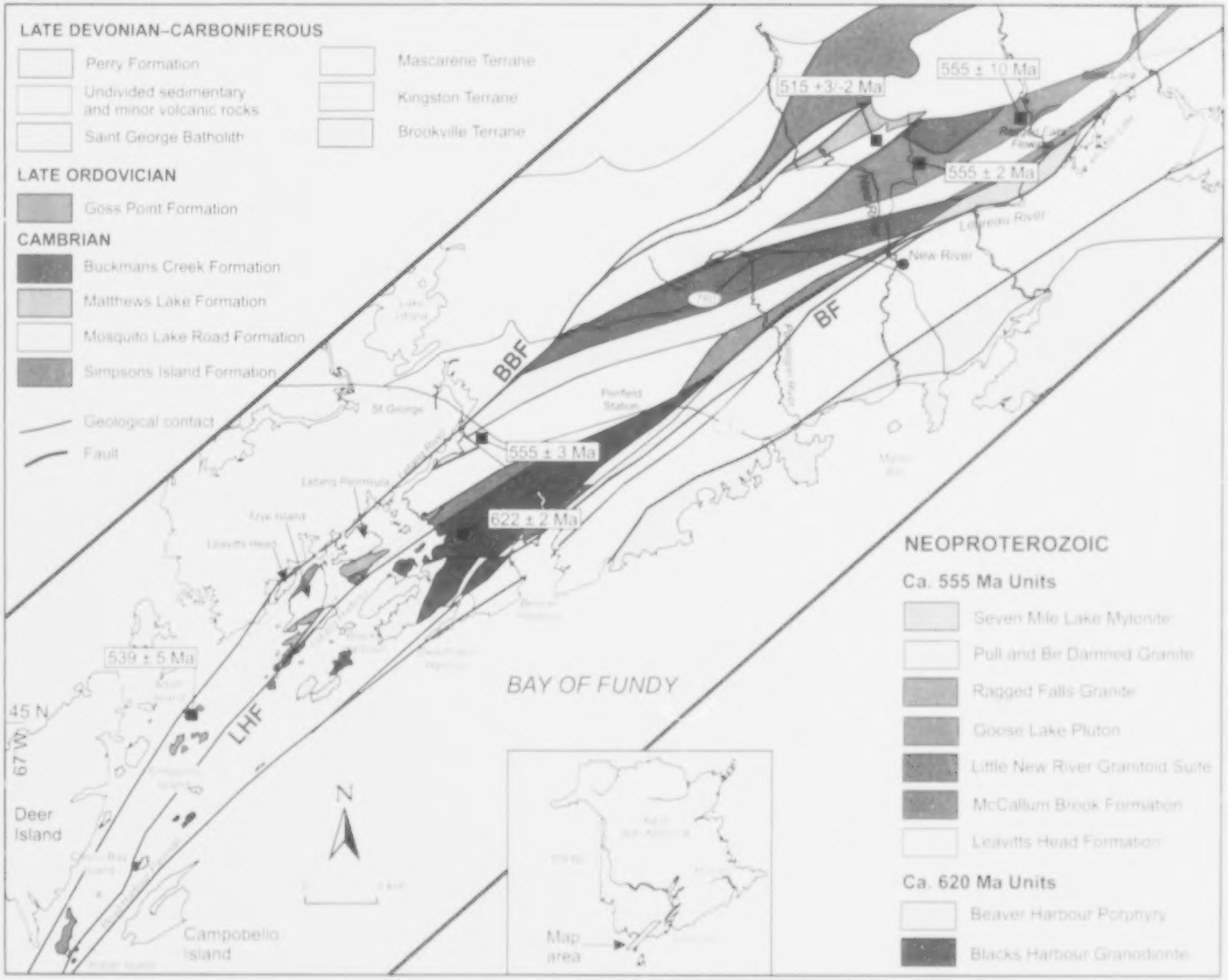
LATE DEVONIAN–CARBONIFEROUS
Perry Formation
Undivided sedimentary and minor volcanic rocks
Saint George Batholith
Mascarene Terrane
Kingston Terrane
Brookville Terrane
LATE ORDOVICIAN
Goss Point Formation
CAMBRIAN
Buckmans Creek Formation
Matthews Lake Formation
Mosquito Lake Road Formation
Simpsons Island Formation
Geological contact
Fault
NEOPROTEROZOIC
Ca. 555 Ma Units
Seven Mile Lake Mylonite
Pull and Be Damned Granite
Ragged Falls Granite
Goose Lake Pluton
Little New River Granitoid Suite
McCallum Brook Formation
Leavitts Head Formation
Ca. 620 Ma Units
Beaver Harbour Porphyry
Blacks Harbour Granodiorite
515 +3/-2 Ma
555 ± 10 Ma
555 ± 2 Ma
555 ± 3 Ma
622 ± 2 Ma
539 ± 5 Ma
BBF
BF
LHF
New River
Lepreau River
Pennfield Station
St George
Letang Peninsula
Frye Island
Leavitts Head
BAY OF FUNDY
45 N
67 W
Deer Island
Campobello Island
N
Map area

Figure 2. Simplified geological map of the southwestern part of the New River Terrane, based on the present study and Smith et al. (2004). BBF = Back Bay Fault, BF = Belleisle Fault, LHF = Letang Harbour Fault. U–Pb ages in boxes are from sources cited in the text.

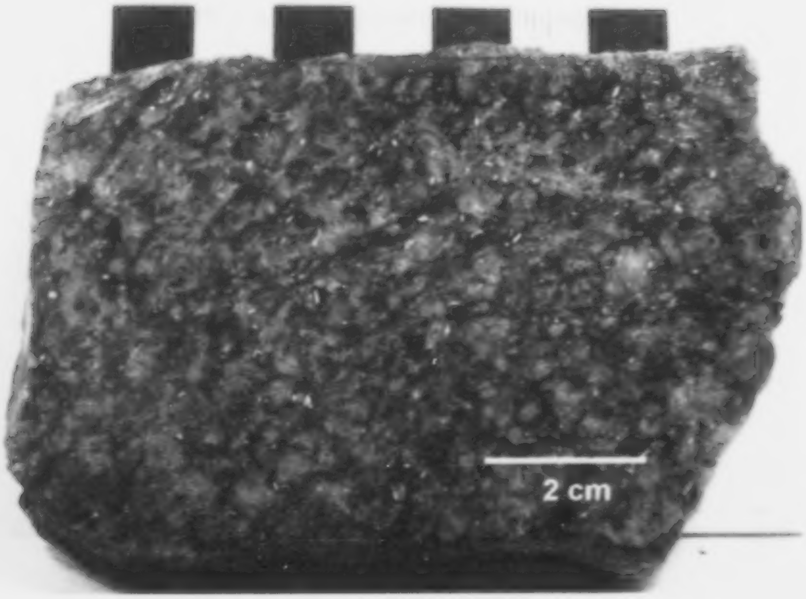

Figure 3. Photograph of hand sample typical of the Blacks Harbour Granodiorite.

north shore of Beaver Harbour. The rock contains yellowish-green, anhedral feldspar phenocrysts and minor, well rounded quartz phenocrysts in a dark brown to maroon, aphanitic groundmass. The other, more abundant, rock type also has a dark brown, aphanitic matrix but contains well rounded quartz phenocrysts ranging in size from 1 to 3 mm. Feldspar phenocrysts are also present but are less numerous than in the feldspar porphyry. Brown rhyodacite also assigned to the Beaver Harbour Porphyry appears on the western shore of Beaver Harbour and north of Deadmans Harbour.

In Beaver Harbour, moderate to steep, northwest-dipping faults separate the Beaver Harbour Porphyry from the Blacks Harbour Granodiorite. The contact between the Ragged Falls Granite and Beaver Harbour Porphyry is not exposed along Pocologan River but is inferred to be a fault. At the head of Deadmans Harbour (Fig. 2), the Perry Formation unconformably overlies the Beaver Harbour Porphyry; clasts derived from the porphyry occur in the Perry conglomerate.

Ca. 555 Ma Units in the Southwestern New River Terrane

The ca. 555 Ma igneous rocks of the southwestern New River Terrane have been divided into five units: the Leavitts Head Formation, McCallum Brook Formation, Little New River Granitoid Suite, Ragged Falls Granite, and Pull and Be Damned Granite. They occur in close association with an apparently in-part-equivalent mylonitic unit termed the Seven Lake Mylonite.

Leavitts Head Formation

Most volcanic rocks in the southwestern New River Terrane have been assigned to the Leavitts Head Formation (McLeod 1995). A rhyolite sample from the formation yielded an age of ca. 553 Ma (Johnson and McLeod 1996; McLeod et al. 2003).

Three subunits are recognized in the Leavitts Head Formation: 1) brown rhyolite to rhyodacite flows and crystal tuff, 2) green rhyolite flows and crystal tuff that previously were assigned to the Goss Point Formation (Johnson and McLeod 1996) or Simpsons Island Formation (Smith et al. 2004), and 3) felsite, tuffaceous felsite, and minor volcanogenic sedimentary rocks.

The brown rhyolite to rhyodacite makes up most of the Leavitts Head Formation and forms all of the formation north of Highway 1. It displays a range of textures from very fine grained and massive to porphyritic with quartz and feldspar phenocrysts to flow banded and locally tuffaceous. The brown rhyodacite and rhyolite flows and tuffs generally grade into, or are in faulted contact with, the green rhyolite and crystal tuff. The green colour seems to be confined to foliated and sheared rocks, suggesting that it may be an effect of alteration, rather than a separate rock type. The felsite unit typically weathers dark red to orange and ranges from massive to blocky. Fresh surfaces vary from white to light green. Small, well rounded quartz phenocrysts occur locally, and small vesicles are present on the eastern shore of Indian Island, commonly infilled with white carbonate minerals. Disseminated pyrite is typically present. Flow banding was observed in the more tuffaceous felsite on Popes and Frye islands. Volcanogenic agglomerate and siltstone overlie the felsite on one of the Park Islands.

McCallum Brook Formation

The McCallum Brook Formation, which was termed the Matthews Lake Brook Formation by Bartsch (2005), occurs at two locations in the study area. It is named for a brook that crosses the unit a few kilometres north of New River (Fig. 2).

The McCallum Brook Formation is composed of volcanic rocks and associated high-level intrusive rocks that include felsic flows, quartz–feldspar porphyry, and porphyritic dykes. The flows are black and aphanitic, have rhyolitic–dacitic compositions, and contain abundant lithophysae. The porphyry is greyish green to black, siliceous, and commonly contains xenoliths of felsic tuff. The associated small dykes are porphyritic and contain white, euhedral, randomly oriented K-feldspar phenocrysts in a black, aphanitic matrix. Both the flows and high-level intrusive rocks possess abundant biotite that likely resulted from contact metamorphism related to the intrusion of the nearby Mount Douglas Granite. The McCallum Brook Formation is distinguished from the Leavitts Head Formation on the basis of its colour and its abundant porphyry intrusions.

Xenoliths of what appear to be lithologies of the McCallum Brook Formation are present in the ca. 555 Ma Ragged Falls Granite, placing a Late Neoproterozoic age on the formation. The formation is unconformably overlain by the Matthews Lake Formation, an Early Cambrian succession of quartz arenite, quartzite-pebble conglomerate, and volcanogenic sedimentary rocks (Johnson 2001).

Little New River Granitoid Suite

The Little New River Granitoid Suite forms a narrow band approximately 1 km wide and 8 km long in the central part of the New River Terrane (Fig. 2). This heterogeneous unit consists of medium-grained gabbro to quartz diorite mingled with pink monzogranite and granodiorite (Fig. 4). The granitic component is porphyritic and displays euhedral phenocrysts of K-feldspar and plagioclase.

Poor exposure in this part of the New River Terrane has made it difficult to establish the relationship of the Little New River Granitoid Suite to other igneous units. The gabbroic and dioritic components of the suite distinguish it from other plutonic units in the terrane. Farther east, however, the granitic component seems to grade into the Ragged Falls Granite and Seven Mile Lake Mylonite (both described below). Based on this apparently gradational relationship, the Little New River Granitoid Suite is assigned an age of ca. 555 Ma. However, some gabbroic rocks in the unit are relatively unaltered and could be younger.

Ragged Falls Granite

The Ragged Falls Granite occurs in three areas that are separated from one another by parts of the Leavitts Head Formation, Little New River Granitoid Suite, and/or Pull and Be Damned Granite (Fig. 2).

The Ragged Falls Granite consists of red and green, medium-grained syenogranite that locally grades into granodiorite. The least deformed samples contain almost no mafic minerals and are dominated by large, pink K-feldspar crystals. Most samples exhibit dark foliation bands attributed to extensive deformation and shearing. Granite in the northern part of the unit appears to have been contact metamorphosed by the Mount Douglas Granite and shows a bleached appearance in hand sample. Granite from the Ragged Falls Flowage area yielded an age of ca. 555 ± 10 Ma (Currie and Hunt 1991), and granodiorite in the Mosquito Lake Road area also assigned to the Ragged Falls Granite gave an age of ca. 555 ± 3 Ma (Johnson and McLeod 1996).

The Ragged Falls Granite intrudes both the Leavitts Head and McCallum Brook formations. In the Pocologan River–New River area, a sliver of the unit appears to merge with, or be truncated by, the Seven Mile Lake Mylonite to the north and is inferred to be in faulted contact with the Beaver Harbour Porphyry to the south.

Pull and Be Damned Granite

The Pull and Be Damned Granite consists of granophyric alkali-feldspar granite (Fig. 5). It typically is pink, medium to fine grained, and contains well rounded quartz phenocrysts that display a distinctive quartz-eye appearance in hand specimen. The granite is leucocratic, and no primary mafic minerals are present. Pink to white rhyolite flows, crystal tuff, and green lapilli tuff commonly occur as xenoliths in the northern part of

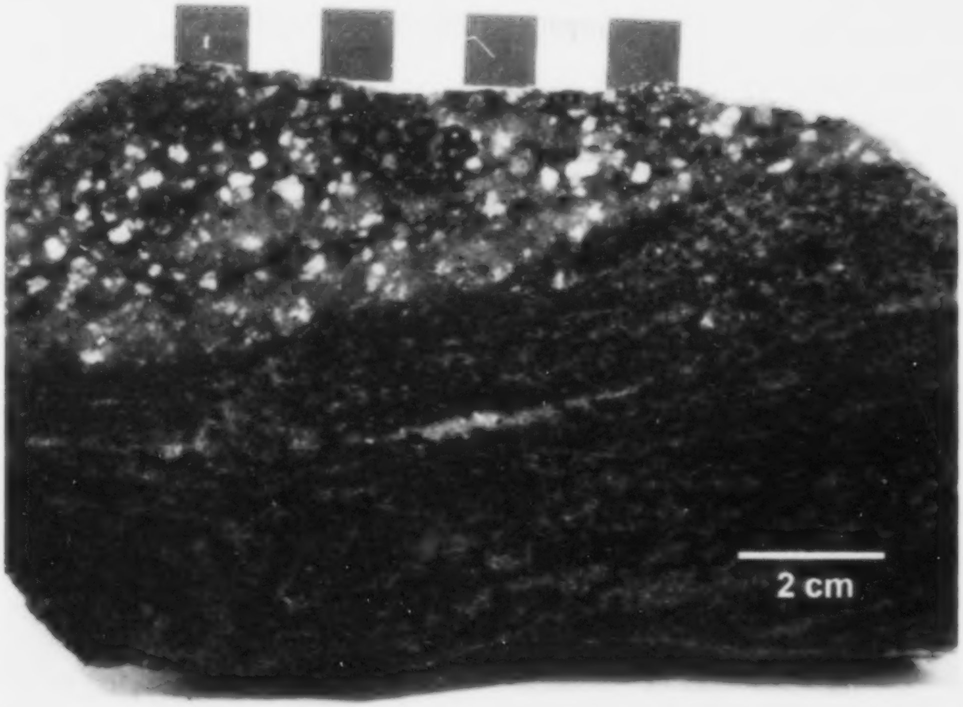

Figure 4. Photograph of hand sample showing mingled gabbro and granodiorite from the Little New River Granitoid Suite.

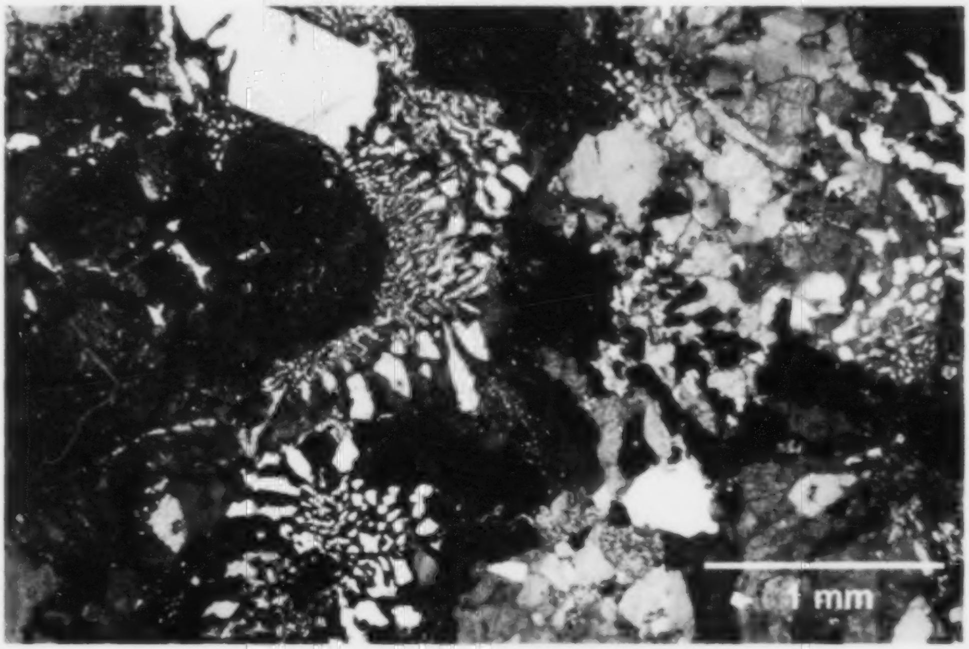

Figure 5. Photomicrograph of granophyric alkali-feldspar granite typical of the Pull and Be Damned Granite.

the unit. Numerous fault blocks of brown rhyolite and crystal tuff from the Leavitts Head Formation are present in the more southern part.

Near Frye Island and Letang River, contacts between the Pull and Be Damned Granite and surrounding units are faults that dip steeply to the east. At numerous locations near the head of the Letang River and on Highway 780, the granite contains faulted slivers of the Leavitts Head Formation.

In many locations, the Pull and Be Damned Granite is closely associated with the Ragged Falls Granite, as was noted earlier by Currie (1988). East of Mosquito Lake Road, the two units appear to pass gradationally into one another and into overlying felsic volcanic rocks of the Leavitts Head Formation. This proximity leaves little doubt that the two granitic units and the volcanic rocks belong to the same magmatic system. The two granites are distinguished on the basis of textural differences. The medium-grained Ragged Falls Granite likely crystallized at greater depth than did the medium- to fine-grained and granophyric Pull and Be Damned Granite.

Seven Mile Lake Mylonite

The Seven Mile Lake Mylonite (Garnett and Brown 1973) comprises mylonitized granitic and less abundant volcaniclastic and sedimentary rocks. The unit is situated northwest of the Belleisle Fault in the northeastern part of the map area (Fig. 2). Good exposures occur along the shore of Seven Mile Lake. They also are visible at Lepreau River and New River, where granitic rocks are sheared in with slivers of tuffaceous volcaniclastic rocks.

The protoliths of the Seven Mile Lake Mylonite cannot be clearly defined everywhere. However, the granitic component of the mylonite contains red to orange K-feldspar porphyroblasts surrounded by a strongly recrystallized, dark-green matrix; similar characteristics appear in the eastern part of the Little New River Granitoid Suite where Highway 780 crosses Little New River. Along Little New River, strongly protomylonitic textures occur in rocks of the granitoid suite near the contact with the mylonite, which supports the interpretation of a gradational (rather than a faulted) relationship between the two units. The volcanic component of the mylonite appears to most closely resemble rocks in the Leavitts Head Formation.

GEOCHEMISTRY

As part of the present study, 51 samples collected from the southwestern New River Terrane were analyzed for major and trace elements. The new analyses were added to the existing database containing analyses from Greenough et al. (1985), Johnson and McLeod (1996), and Barr et al. (2003). The complete database of 75 analyses and sample locations were presented by Bartsch (2005).

Analyses of ca. 620 Ma Samples

Samples from the Blacks Harbour Granodiorite plot in two clusters on most major-element diagrams (Fig. 6). One cluster contains from 64% to 69% SiO_2, and the other contains from 73% to 78% SiO_2. The difference in SiO_2 content is consistent with petrographic observations that indicate both granodioritic to tonalitic and granitic components in the Blacks Harbour Granodiorite. Although the analyzed samples show a gap of about 3% in SiO_2 content, field observations suggest that the granodiorite is gradational to granite and that the two components are related by fractional crystallization.

The Beaver Harbour Porphyry is represented by only two analyzed samples, but chemically they resemble the granodioritic to tonalitic samples of the Blacks Harbour Granodiorite (Fig. 6).

The samples plot mainly in the subalkaline field on the Zr/TiO_2 vs Nb/Y discrimination diagram (Fig. 7a), although four samples of Blacks Harbour Granodiorite with anomalously low Y contents (Fig. 6f) plot on or over the subalkalic–alkalic boundary (Fig. 7a). The I-type character of the rocks is evident in the Nb vs Ga/Al plots (Fig. 7b). The Rb vs Y + Nb and TiO_2 vs Zr discrimination diagrams (Fig. 7c, d) clearly show a volcanic-arc signature.

Analyses of ca. 555 Ma Samples

All analyzed samples of the ca. 555 Ma units contain high concentrations of SiO_2, mainly between 70% and 80% (Fig. 6). The Leavitts Head Formation and Ragged Falls Granite have the widest range in major- and trace-element concentrations, whereas the Pull and Be Damned Granite and the granitic component of the Little New River Granitoid Suite show a narrower spread (Fig. 6). No analyses were obtained from the gabbroic and dioritic components of the suite, due to their heterogeneity. The varied major-element concentrations generally reflect differing mineralogies of the individual units. The Little New River Granitoid Suite and some parts of the Ragged Falls Granite and the Leavitts Head Formation contain abundant plagioclase and mafic minerals (biotite, hornblende, and pyroxene). The Pull and Be Damned Granite, however, consists primarily of quartz and K-feldspar and thus has a narrower compositional range.

These varied compositional ranges in intermediate to felsic units support the interpretation that the ca. 555 Ma units are related through fractional crystallization of plagioclase and mafic minerals. The linear trends in most major-element oxide plots (Fig. 6a–c) also indicate the involvement of fractional crystallization.

The ca. 555 Ma samples show a wider range in, and generally higher values of, the trace elements Zr, Y, and Nb (Fig. 6d–f) than do samples of the ca. 620 Ma Blacks Harbour Granodiorite containing similar SiO_2 contents. Nonetheless, the chemical differences between the two ages of rocks are not substantial. Both igneous suites plot in the subalkalic and I-type fields (Fig. 7a, b) and likely formed in a volcanic-arc setting (Fig.

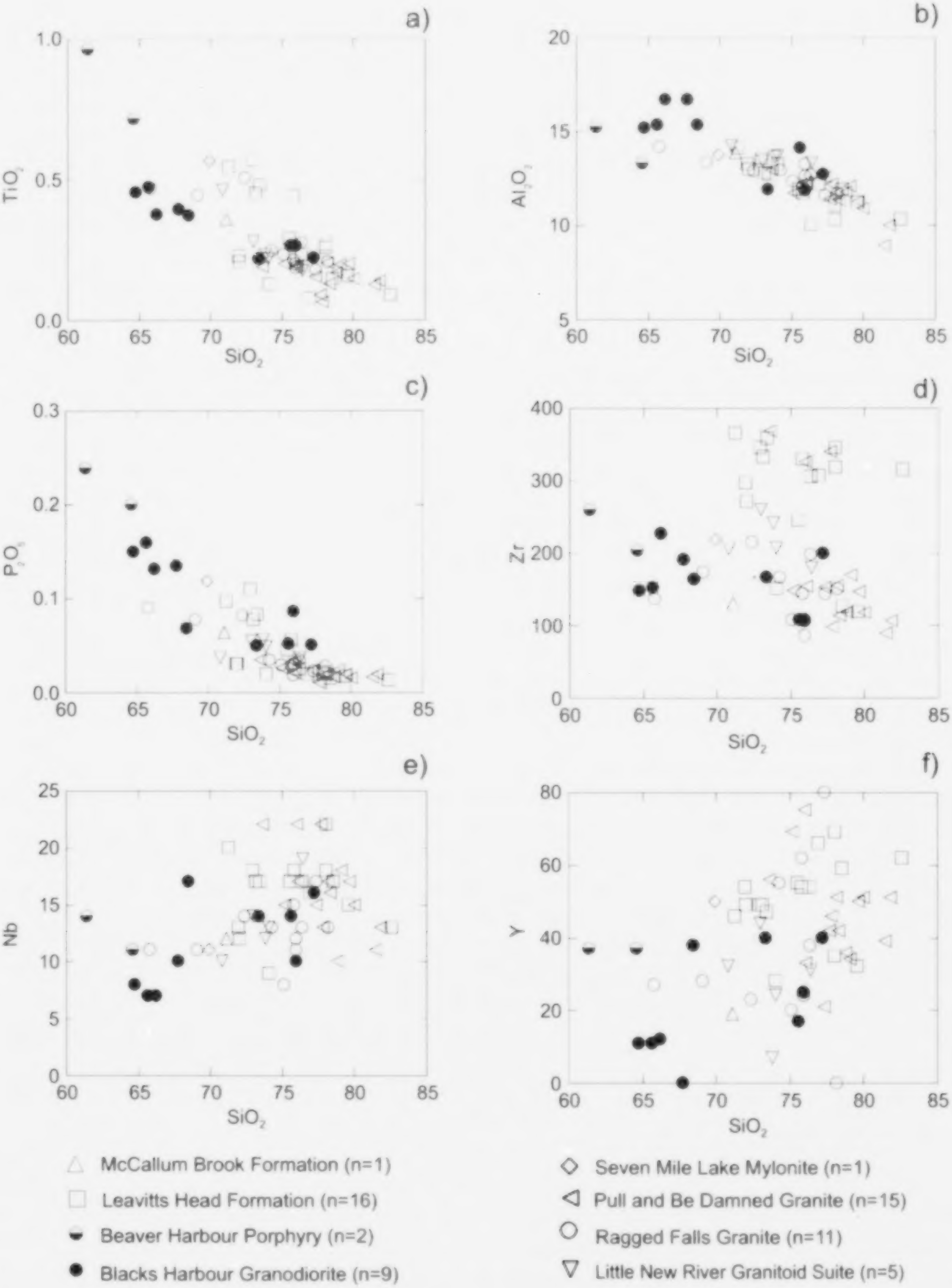

Figure 6. Selected SiO_2 variation diagrams of analyzed samples from Neoproterozoic units in the southwestern New River Terrane. Data and sample locations are in Bartsch (2005).

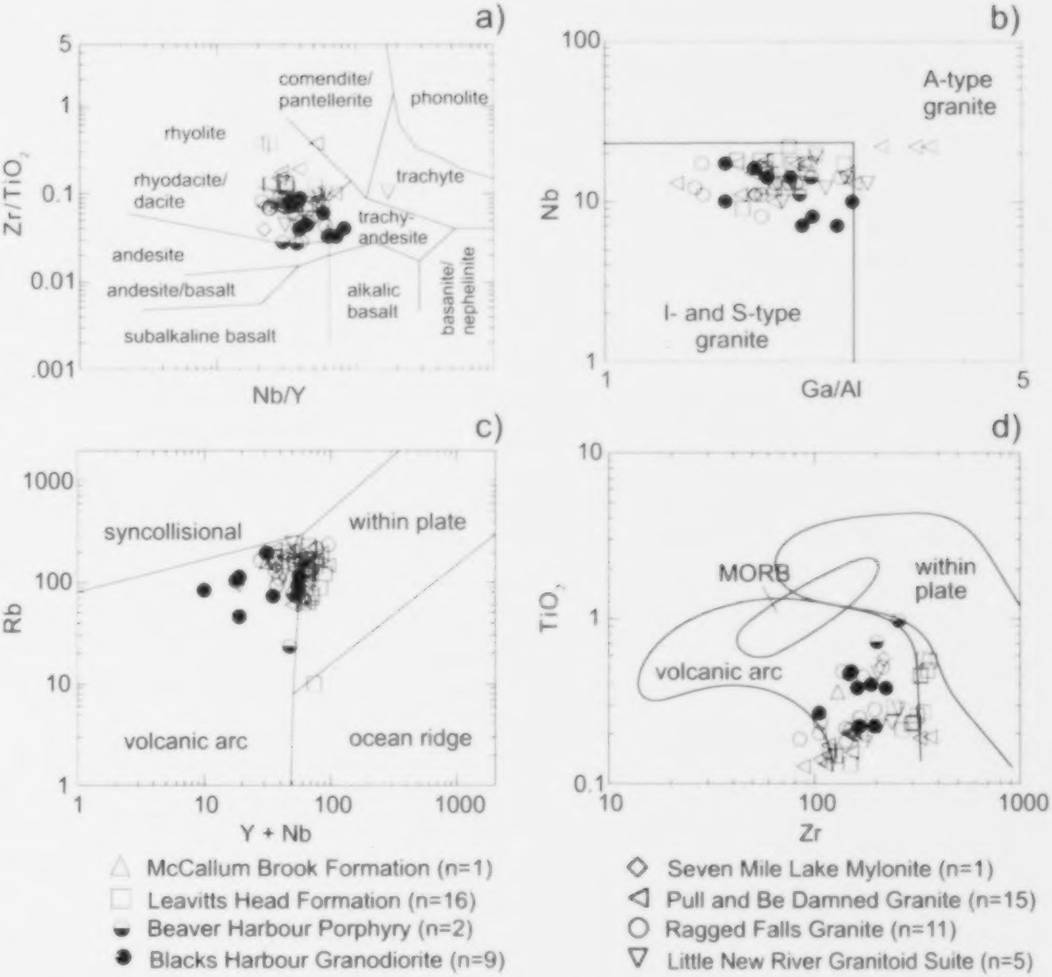

Figure 7. Discrimination diagrams for samples from Neoproterozoic units in the southwestern New River Terrane. Field in a) is from Winchester and Floyd (1977). Field in b) is from Whalen et al. (1987). Field in c) is from Pearce et al. (1984). Field in d) is from Pearce (1982).

7c, d). The ca. 555 Ma units are interpreted to represent a highly evolved, felsic I-type suite formed at an active continental margin during the late stages of orogeny, whereas the ca. 620 Ma rocks may represent a less mature, continental margin arc environment. Even so, the two suites display notably similar chemical signatures; without the geochronological data, their age difference might not have been suspected.

CORRELATIONS WITH THE NORTHEASTERN NEW RIVER TERRANE

The Robin Hood Lake Fault (Fig. 8) separates the northeastern part of the New River Terrane from the southwestern part of the terrane. Units southeast of the fault include 1) ca. 620 Ma granitic and other felsic to intermediate plutonic and minor volcanic rocks of the Lingley Plutonic Suite, and 2) ca. 555 Ma rhyolite, rhyolite porphyry, ash tuff, and minor microgranite porphyry of the Lobster Brook Formation. Johnson (2001) interpreted this entire rock assemblage, together with the ca. 620 Ma Blacks Harbour Granite, to be

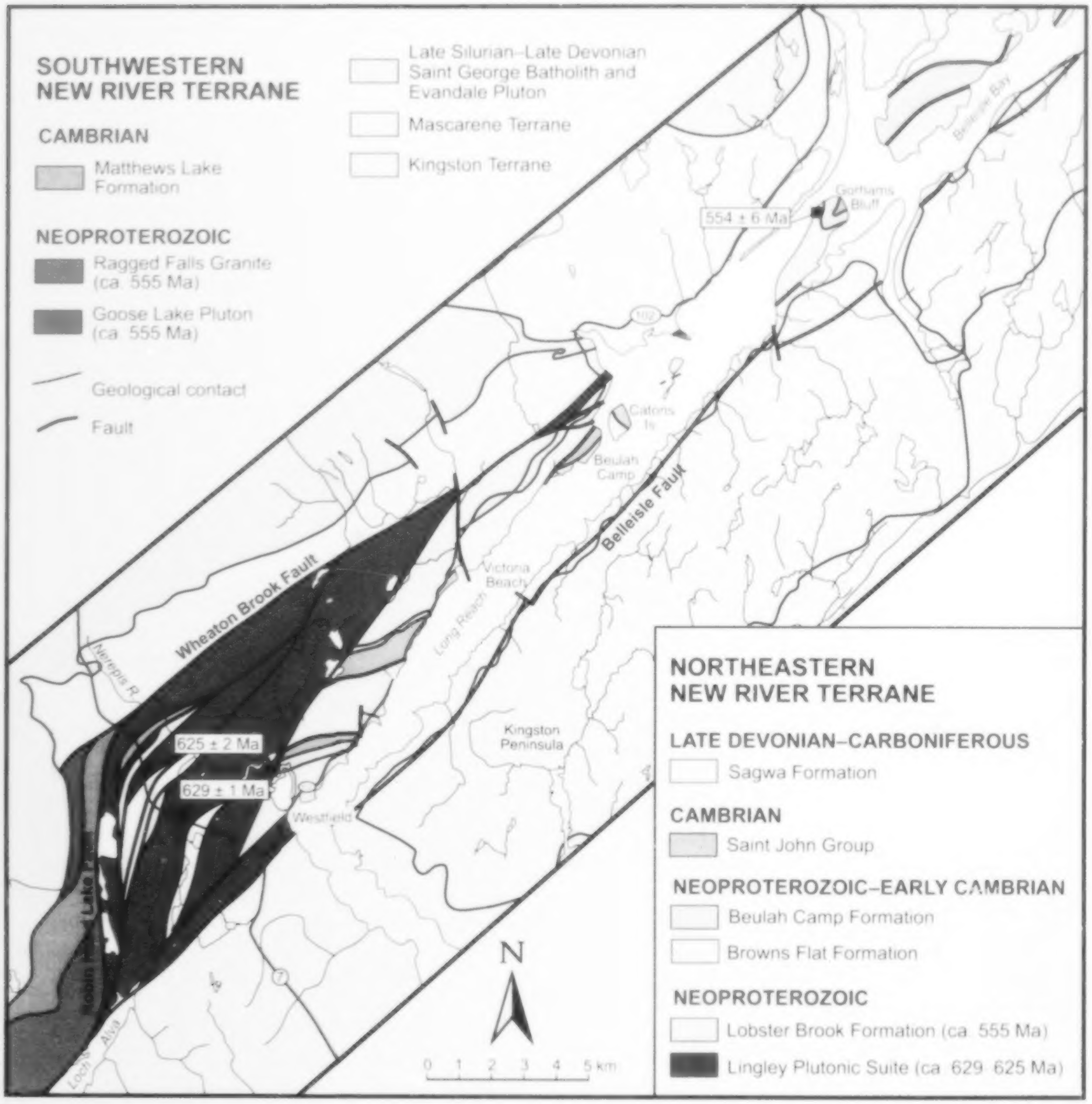
SOUTHWESTERN NEW RIVER TERRANE
CAMBRIAN
Matthews Lake Formation
NEOPROTEROZOIC
Ragged Falls Granite (ca. 555 Ma)
Goose Lake Pluton (ca. 555 Ma)
Geological contact
Fault
Late Silurian–Late Devonian Saint George Batholith and Evandale Pluton
Mascarene Terrane
Kingston Terrane
Belleisle Bay
Gorhams Bluff
554 ± 6 Ma
102
Catons Is.
Beulah Camp
Belleisle Fault
Victoria Beach
Wheaton Brook Fault
Long Reach
Nerepis R.
625 ± 2 Ma
629 ± 1 Ma
Westfield
Kingston Peninsula
Robin Hood Lake
Loch Alva
7
N
0 1 2 3 4 5 km
NORTHEASTERN NEW RIVER TERRANE
LATE DEVONIAN–CARBONIFEROUS
Sagwa Formation
CAMBRIAN
Saint John Group
NEOPROTEROZOIC–EARLY CAMBRIAN
Beulah Camp Formation
Browns Flat Formation
NEOPROTEROZOIC
Lobster Brook Formation (ca. 555 Ma)
Lingley Plutonic Suite (ca. 629–625 Ma)

Figure 8. Geological map of the northeastern New River Terrane in the Long Reach area. Map is based on Johnson (2001) and Johnson and Barr (2004).

affiliated with the Avalon Zone. She further suggested that rocks northwest of the Robin Hood Lake Fault belong to the Gander Zone and that the fault juxtaposed rocks of different tectonic affinities.

In this section, the ca. 620 Ma Lingley Plutonic Suite from the Long Reach area is compared with the Blacks Harbour Granodiorite and Beaver Harbour Porphyry from the southwestern part of the terrane; and the ca. 555 Ma Lobster Brook Formation from the Long Reach area is compared with the Leavitts Head Formation from the southwestern part of the terrane.

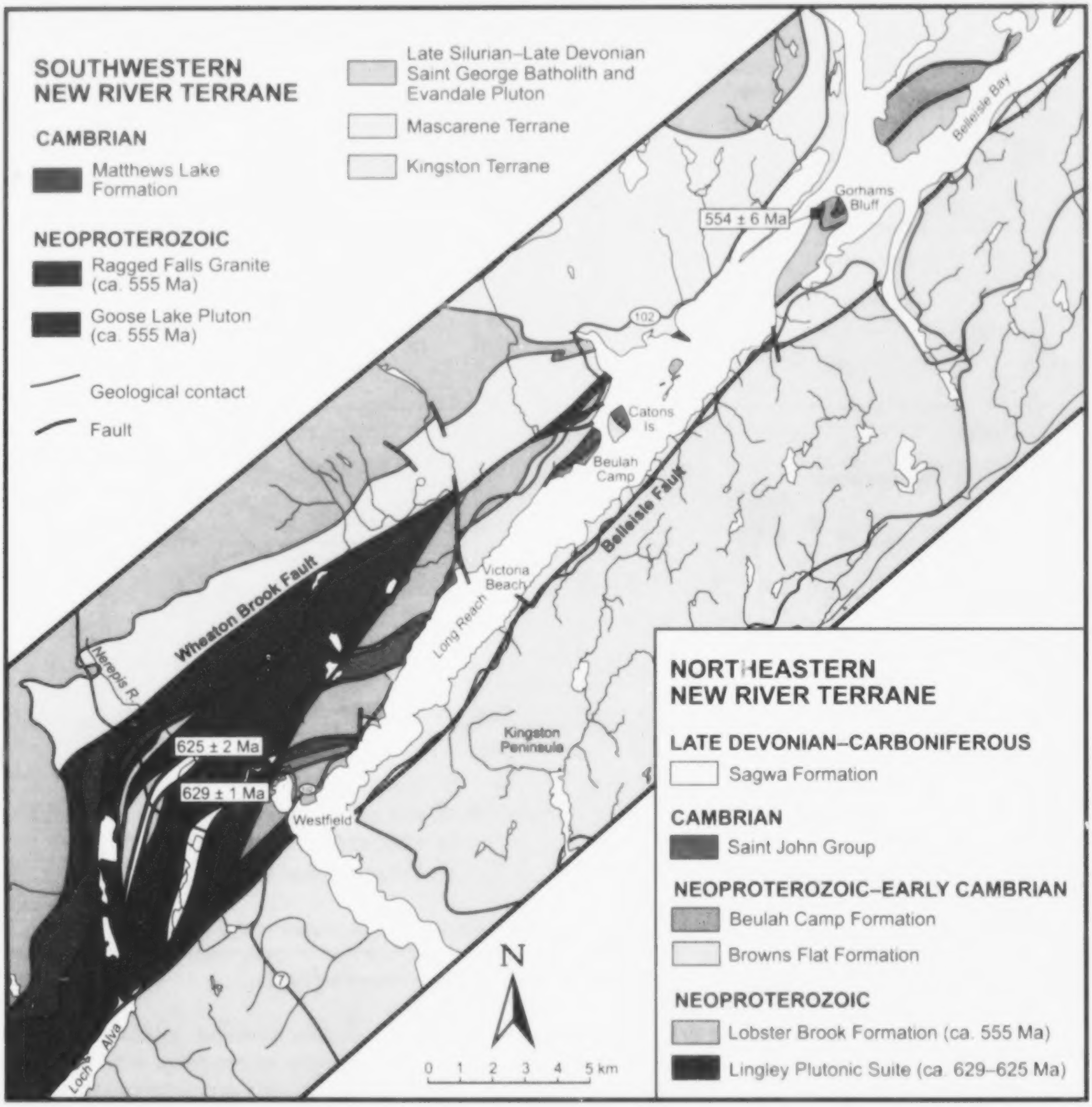
SOUTHWESTERN NEW RIVER TERRANE
CAMBRIAN
Matthews Lake Formation
NEOPROTEROZOIC
Ragged Falls Granite (ca. 555 Ma)
Goose Lake Pluton (ca. 555 Ma)
Geological contact
Fault
Late Silurian–Late Devonian Saint George Batholith and Evandale Pluton
Mascarene Terrane
Kingston Terrane
NORTHEASTERN NEW RIVER TERRANE
LATE DEVONIAN–CARBONIFEROUS
Sagwa Formation
CAMBRIAN
Saint John Group
NEOPROTEROZOIC–EARLY CAMBRIAN
Beulah Camp Formation
Browns Flat Formation
NEOPROTEROZOIC
Lobster Brook Formation (ca. 555 Ma)
Lingley Plutonic Suite (ca. 629–625 Ma)
Belleisle Bay
Gorhams Bluff
554 ± 6 Ma
102
Catons Is
Beulah Camp
Belleisle Fault
Victoria Beach
Long Reach
Wheaton Brook Fault
Nerepis R.
Kingston Peninsula
625 ± 2 Ma
629 ± 1 Ma
Westfield
7
Loch Alva
N
0 1 2 3 4 5 km

Figure 8. Geological map of the northeastern New River Terrane in the Long Reach area. Map is based on Johnson (2001) and Johnson and Barr (2004).

affiliated with the Avalon Zone. She further suggested that rocks northwest of the Robin Hood Lake Fault belong to the Gander Zone and that the fault juxtaposed rocks of different tectonic affinities.

In this section, the ca. 620 Ma Lingley Plutonic Suite from the Long Reach area is compared with the Blacks Harbour Granodiorite and Beaver Harbour Porphyry from the southwestern part of the terrane; and the ca. 555 Ma Lobster Brook Formation from the Long Reach area is compared with the Leavitts Head Formation from the southwestern part of the terrane.

Ca. 620 Ma Units in the Long Reach Area

Currie (1988) and Currie and McNicoll (1999) subdivided plutonic rocks of the Long Reach area into tonalite and hornblende granodiorite of the Brittain Creek Pluton; and quartz–feldspar porphyry and associated felsic volcanic and minor sedimentary rocks of the Lingley Plutonic Suite. They reported U–Pb zircon dates of 625 ± 2 Ma and 629.3 ± 0.9 Ma, respectively, for these plutons. The spatial proximity and similar ages of these porphyritic- and granitic-textured rocks, however, led some workers to include both units in the Lingley Plutonic Suite (Johnson 2001; Johnson and Barr 2004).

Rocks from the Lingley Plutonic Suite, as defined by Johnson (2001), were examined during the present study (Bartsch 2005). Some Lingley samples resemble rocks of the Blacks Harbour Granodiorite, showing a gradation between dark green/pink granite and greenish-grey granodiorite containing minor to abundant K-feldspar phenocrysts. Other Lingley samples are quartz porphyry and quartz–feldspar porphyry, which are similar to rocks from the Beaver Harbour Porphyry. Samples from both porphyry units have a light brown, fine-grained groundmass and rounded, embayed quartz and euhedral feldspar phenocrysts. Hence, based on petrographic features, the Blacks Harbour Granodiorite and Beaver Harbour Porphyry are similar to the Lingley Plutonic Suite.

The Lingley Plutonic Suite also shows chemical similarities to both the Blacks Harbour Granodiorite and Beaver Harbour Porphyry. The SiO_2 content of Lingley rocks ranges from 57% to 77%, similar to the 60% to 78% range for the Blacks Harbour and Beaver Harbour units (Fig. 9a–c). Plots of major-element oxides for the three units show a similar compositional range (Fig. 9a, b), displaying well developed trends of decreasing TiO_2 and P_2O_5 with increasing SiO_2. Trace-element trends are less obvious, but Zr, for example, decreases with increasing SiO_2 in all three units (Fig. 9c).

Johnson and Barr (2004) interpreted linear trends in the Lingley Plutonic Suite to indicate crystal fractionation in a comagmatic suite. Data from the Blacks Harbour Granodiorite and Beaver Harbour Porphyry support this interpretation and suggest that all three units may be related, although the Lingley Plutonic Suite may be slightly older based on its ca. 29 Ma and ca. 625 Ma ages. Most samples plot in the calc-alkaline and volcanic-arc fields, and their Ga–Al ratios and Nb concentrations are consistent with those of fractionated I-type granite formed at an active continental margin (Fig. 9d–f).

Ca. 555 Ma Units in the Long Reach Area

Like ca. 555 Ma units in the southwestern part of the terrane, the Lobster Brook Formation of the Long Reach area (Fig. 8) consists of felsic extrusive to high-level intrusive rocks including rhyolite, rhyolite crystal tuff, lithic–crystal tuff, volcanic debris flows, rhyolite porphyry, and minor microgranite porphyry (Johnson 2001; Johnson and Barr 2004). Samples of the rhyolite, rhyolite crystal tuff, and rhyolite porphyry were

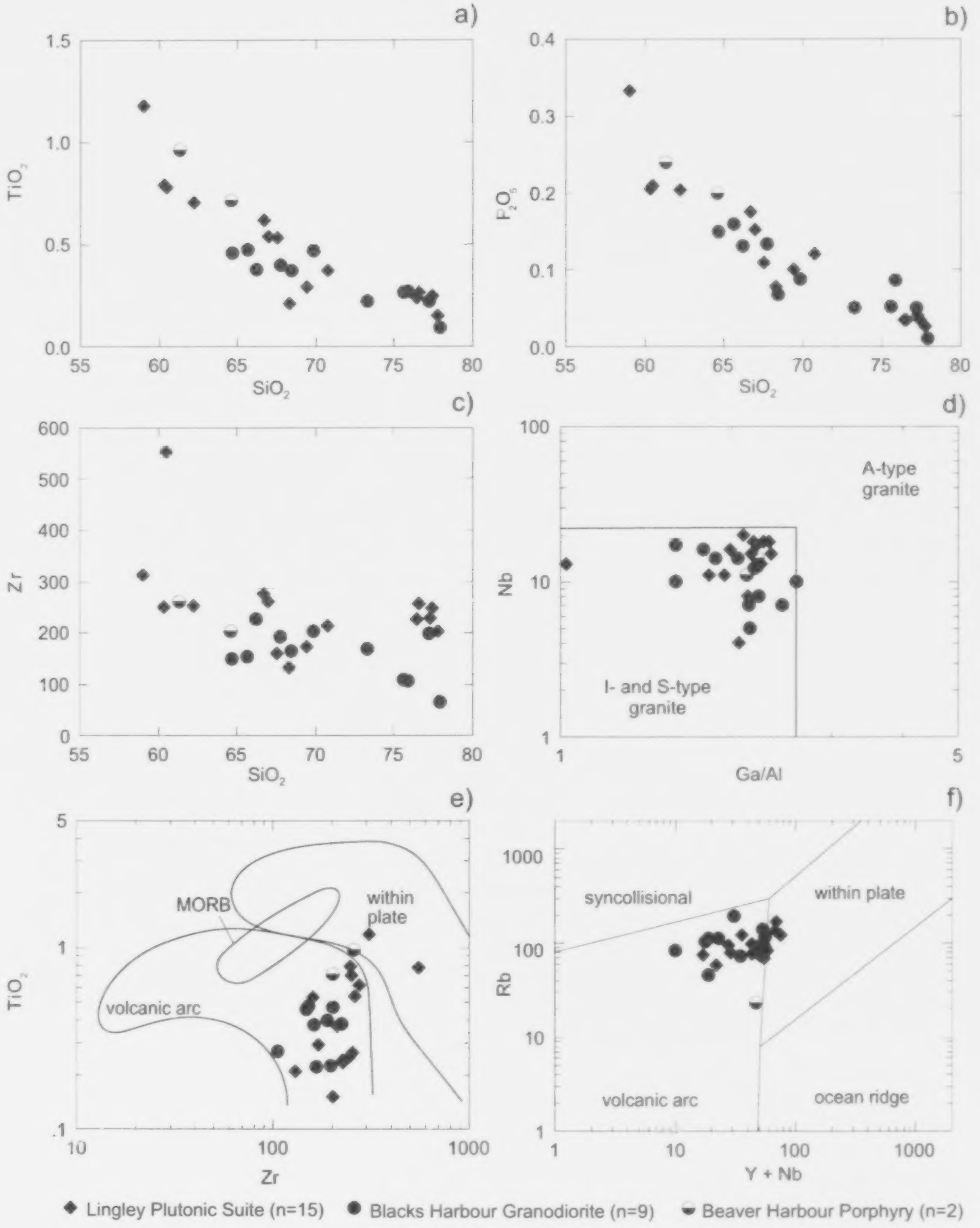

Figure 9. Selected SiO_2 variation and discrimination diagrams for the Lingley Plutonic Suite, Blacks Harbour Granodiorite, and Beaver Harbour Porphyry. Data are from the present study and Johnson and Barr (2004). Field in d) is from Whalen et al. (1987). Field in e) is from Pearce (1982). Field in f) is from Pearce et al. (1984). MORB = mid-oceanic-ridge basalt.

examined during this study (Bartsch 2005). The rhyolite is dark brown to maroon and features abundant rounded and embayed quartz and subhedral plagioclase phenocrysts.

Its groundmass locally is spherulitic but more commonly is equigranular; some samples display prominent flow banding in a fine-5grained, red groundmass. The rhyolite crystal tuff is also dark brown to maroon and contains many broken quartz and feldspar crystals set in an aphanitic quartzo–feldspathic matrix. The presumably intrusive rhyolite porphyry is reddish maroon to tan and has few phenocrysts in its equigranular quartzo–feldspathic groundmass.

A sample of rhyolite crystal tuff from the Lobster Brook Formation gave a U–Pb zircon age of 554 ± 6 Ma, identical to the 554 ± 3 Ma age reported for felsic tuff in the Leavitts Head Formation (McLeod et al. 2003). The lithological ranges of the two formations are also similar, although they differ in that the abundant hematite responsible for the maroon coloration of some Lobster Brook samples is mainly absent from the Leavitts Head rocks.

Samples of the Leavitts Head and Lobster Brook formations yielded comparable major- and trace-element analyses. Their SiO_2 contents plot between 70% and slightly over 80%, representing a compositional range of rhyolite to rhyodacite (Fig. 10). Samples from both formations show decreasing TiO_2 and Al_2O_3 with increasing SiO_2 (Fig. 10a, b). Trace-element concentrations are also similar, although Leavitts Head samples generally contain higher Zr (Fig. 10c). Plots of both sample sets lie near the granite-type boundary on the Nb vs Ga/Al diagram (Fig. 10d), which is consistent with a highly fractionated, felsic I-type magma. On the TiO_2 vs Zr diagram (Fig. 10e), Lobster Brook samples plot in the volcanic-arc field, directly over the highest concentration of Leavitts Head samples.

The evolved compositions of the ca. 555 Ma rocks (Fig. 10f) suggest that they formed in a volcanic-arc setting along an active continental margin, late in the orogenic cycle. This interpretation differs from that of Johnson and Barr (2004) who, using a more limited data set, suggested a within-plate, anorogenic setting.

DISCUSSION

The information presented here supports the interpretation that ca. 625–620 Ma and ca. 555 Ma igneous units can be correlated throughout the New River Terrane, as was suggested by previous workers (e.g. Johnson 2001; Johnson and Barr 2004). In the southwestern part of the terrane, the ca. 625–620 Ma and ca. 555 Ma units are separated by the Letang Harbour Fault. However, in the northeastern part, units of both ages occur southeast of the Robin Hood Lake Fault (Fig. 8). If the unit correlations proposed here are correct, then correlative ca. 555 Ma units also occur northwest of the Robin Hood Lake Fault. This implies that the fault does not separate Avalon-like and Gander-like units, as was proposed by Johnson (2001).

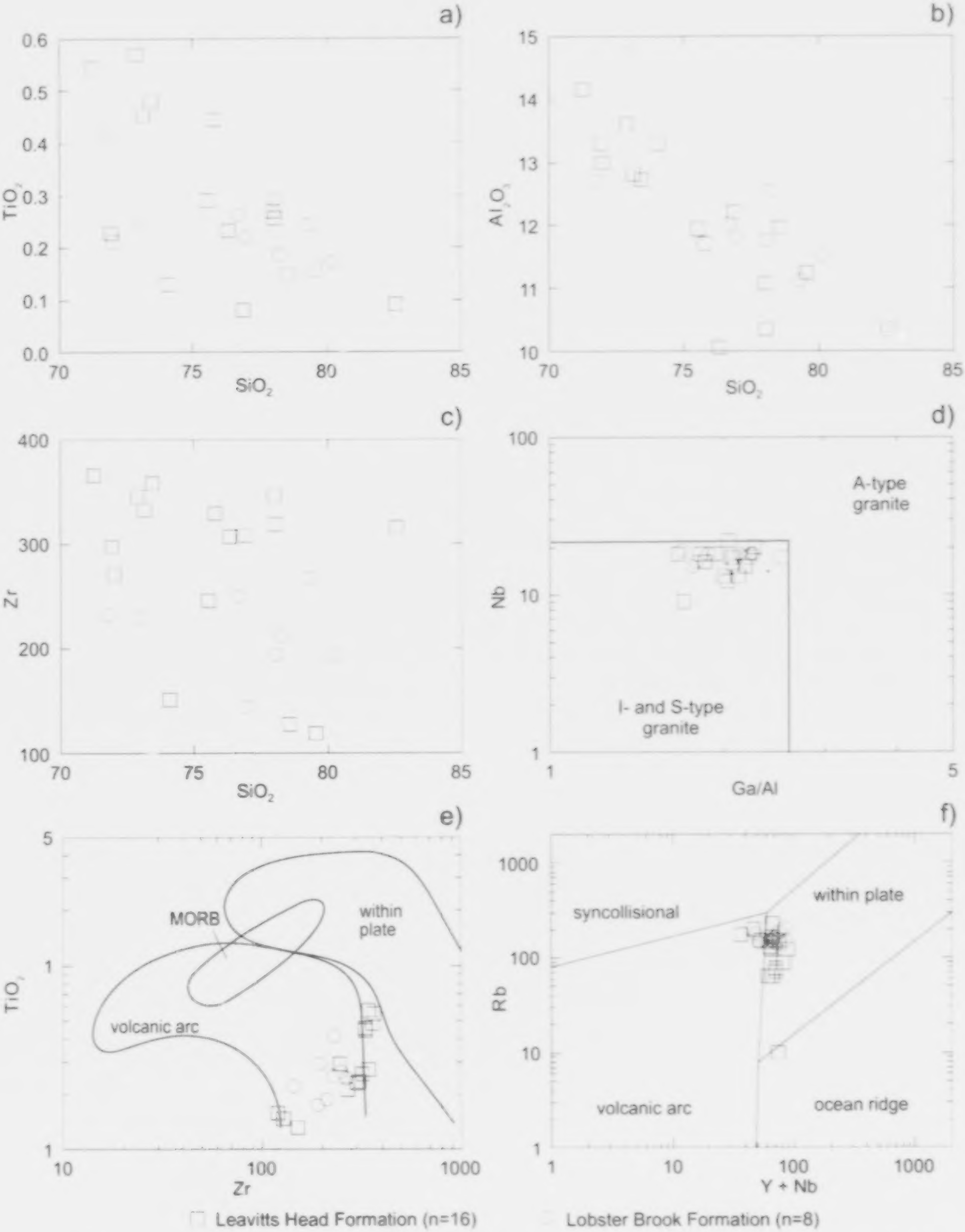

Figure 10. Selected SiO$_2$ variation and discrimination diagrams for the Lobster Brook and Leavitts Head formations. Data are from the present study and Johnson and Barr (2004). Field in d) is from Whalen et al. (1987). Field in e) is from Pearce (1982). Field in f) is from Pearce et al. (1984).

Bartsch (2005) presented a tectonic model for the southwestern New River Terrane, in which the ca. 625–620 Ma and ca. 555 Ma rocks were formed in two separate, unrelated subduction zones that were juxtaposed at the Letang Harbour Fault as late as the Devonian, when the Perry Formation was deposited. This model appears not to apply to the Long Reach area, where units of both ages show close spatial association (Fig. 8).

The ca. 620 Ma units of the Avalonian Caledonia Terrane formed in a continental margin arc environment, as did those of corresponding age from the New River Terrane. However, the ca. 560–550 Ma volcanic and plutonic rocks of the Caledonia Terrane have been interpreted as forming in an extensional setting (e.g. Barr and White 1999; Barr et al. 2003), whereas the ca. 555 Ma rocks of the New River Terrane (as suggested here) appear to have formed in an arc setting. Moreover, both the ca. 620 Ma and ca. 555 Ma suites of the New River Terrane differ from units of corresponding ages in the Caledonia Terrane in their overall lithological assemblages, particularly in the lack of sedimentary rocks in the New River Terrane (Barr et al. 2003; Bartsch 2005). The significance of these discrepancies has yet to be determined.

CONCLUSIONS

Geological mapping in the southwestern New River Terrane has further clarified distribution of ca. 620 Ma and ca. 555 Ma rocks in the area. The ca. 620 Ma units (the Blacks Harbour Granodiorite and Beaver Harbour Porphyry) are restricted to southeast of the Letang Harbour Fault. The ca. 555 Ma rocks occur as six units:

- Leavitts Head Formation (rhyolite, rhyolitic crystal tuff, and lithic–crystal tuff);
- McCallum Brook Formation (quartz–feldspar porphyry and associated lithophysae-rich volcanic rocks);
- Little New River Granitoid Suite (medium-grained gabbro to quartz diorite, pink monzogranite, and granodiorite);
- Ragged Falls Granite (medium-grained syenogranite and altered syenogranite);
- Pull and Be Damned Granite (granophyric alkali-feldspar granite); and
- Seven Mile Lake Mylonite (mylonite derived from Little New River Suite, Leavitts Head Formation, and possibly other units).

Field observations and petrochemical data suggest that the ca. 555 Ma units are comagmatic, as does the close spatial association of the intrusive and extrusive components. Petrological and geochemical evidence also indicates that both the ca. 555 Ma and ca. 620 Ma suites formed in active continental margin subduction settings.

This study has better defined the distribution and characteristics of Neoproterozoic rock units in the southwestern New River Terrane. Nonetheless, the original relationships among the various units, and their relationship to the Avalonian Caledonia Terrane and to more inboard Ganderian terranes, remain enigmatic.

ACKNOWLEDGEMENTS

Results presented in this paper were derived from an M.Sc. project undertaken by the first author at Acadia University in Wolfville, Nova Scotia. We thank Heather Wolczanski for assistance in the field, and Malcolm McLeod, Susan Johnson, and Chris White for helpful comments during the project. Project funding was provided in part by the New Brunswick Department of Natural Resources and in part by a Natural Sciences and Engineering Research Council (NSERC) Discovery Grant to S.M. Barr. We thank reviewer Chris White and editor Steve McCutcheon for helpful suggestions that improved the manuscript.

REFERENCES

Barr, S.M., and White, C.E. 1999. Field relations, petrology, and structure of Neoproterozoic rocks in the Caledonian Highlands, southern New Brunswick, Canada. Geological Survey of Canada Bulletin, **503**: 101 p.

Barr, S.M., White, C.E., and Miller, B.V. 2002. The Kingston Terrane, southern New Brunswick, Canada: evidence for an Early Silurian volcanic arc. Geological Society of America Bulletin, **114**: 964–982.

Barr, S.M., White, C.E., and Miller, B.V. 2003. Age and geochemistry of Late Neoproterozoic and Early Cambrian igneous rocks in southern New Brunswick: similarities and contrasts. Atlantic Geology, **39**: 55–73.

Bartsch, C. 2005. Constraints on the tectonic evolution of the southern New River Terrane and its relationship to other terranes in southern New Brunswick. Unpublished M.Sc. thesis, Acadia University, Wolfville, Nova Scotia, Canada, 169 p.

Currie, K.L. 1988. The western end of the Avalon Zone in southern New Brunswick. Maritime Sediments and Atlantic Geology, **24**: 339–352.

Currie, K.L., and Hunt, P.A. 1991. Latest Precambrian igneous activity near Saint John, New Brunswick. *In* Radiogenic Age and Isotopic Studies: Report 4. Geological Survey of Canada, Paper 90-2, pp.11–17.

Currie, K.L., and McNicoll, V.J. 1999. New data on the age and geographic distribution of Neoproterozoic plutons near Saint John, New Brunswick. Atlantic Geology, **35**: 157–166.

Donohoe, H.V. 1978. Analysis of structures in the St. George area, Charlotte County, New Brunswick. Unpublished Ph.D. thesis, University of New Brunswick, Fredericton, New Brunswick, Canada, 227 p.

Fyffe, L.R., Pickerill, R.K., and Stringer, P. 1999. Stratigraphy, sedimentology, and structure of the Oak Bay and Waweig formations, Mascarene Basin: implications for the paleotectonic evolution of southwestern New Brunswick. Atlantic Geology, **35**: 59–84.

Garnett, J.A., and Brown, R.L. 1973. Fabric variation in the Lubec–Belleisle Zone of southern New Brunswick. Canadian Journal of Earth Sciences, **10**: 1591–1599.

Greenough, J.D., McCutcheon, S.R., and Papezik, V.S. 1985. Petrology and geochemistry of the Cambrian volcanic rocks from the Avalon Zone in New Brunswick. Canadian Journal of Earth Sciences, **22**: 881–892.

Helmstaedt, H. 1968. Structural analysis of the Beaver Harbour area, Charlotte County, New Brunswick. Unpublished Ph.D. thesis, University of New Brunswick, Fredericton, New Brunswick, Canada, 195 p.

Johnson, S.C. 2001. Contrasting geology of the Pocologan River and Long Reach areas: implications for the New River belt and correlations in southern New Brunswick and Maine. Atlantic Geology, **37**: 61–79.

Johnson, S.C., and Barr, S.M. 2004. New chemical data from Neoproterozoic–Cambrian igneous rocks in the Long Reach area, southern New Brunswick. *In* Geological Investigations in New Brunswick for 2003. *Edited by* G.L. Martin. New Brunswick Department of Natural Resources; Minerals, Policy and Planning Division, Mineral Resource Report 2004-4, pp. 75–94.

Johnson, S.C., and McLeod, M.J. 1996. The New River belt: a unique segment along the western margin of the Avalon composite terrane, southern New Brunswick, Canada. *In* Avalonian and Related Peri-Gondwanan Terranes of the Circum-North Atlantic. *Edited by* R.D. Nance and M.D. Thompson. Geological Society of America, Special Paper 304, pp. 149–164.

King, M.S., and Barr, S.M. 2004. Magnetic and gravity models across terrane boundaries in southern New Brunswick, Canada. Canadian Journal of Earth Sciences, **41**: 1027–1047.

McLeod, M.J. 1995. Bedrock geology and metallic occurrences in the Letang–Head Harbour Passage area, Charlotte County, New Brunswick. *In* Current Research 1994. *Edited by* S.A.A. Merlini. New Brunswick Department of Natural Resources and Energy; Minerals and Energy Division, Miscellaneous Report 18, pp. 141–156.

McLeod, M.J., Nowlan, G.S., and McCracken, A.D. 1994. Tectonic and economic significance of an Ordovician conodont discovery in southwestern New Brunswick. *In* Current Research 1993. *Edited by* S.A.A. Merlini. New Brunswick Department of Natural Resources and Energy; Minerals and Energy Division, Miscellaneous Report 12, pp. 121–128.

McLeod, M.J., Johnson, S.C., and Krogh, T.E. 2003. Archived U–Pb data from southern New Brunswick. Atlantic Geology, **39**: 209–225.

Pearce, J.A. 1982. Trace-element characteristics of lavas from destructive plate boundaries. *In* Andesites. *Edited* by R.S. Thorpe. John Wiley and Sons, New York, pp. 525–548.

Pearce, J.A., Harris, N.B.W., and Tindle, A.G. 1984. Trace-element discrimination diagrams for the tectonic interpretation of granitic rocks. Journal of Petrology, **25**: 956–983.

Smith, E.A., Johnson, S.C., and McLeod, M.J. 2004. Bedrock geological compilation of the St. George area (NTS 21 G/02), Charlotte County, New Brunswick. New Brunswick Department of Natural Resources; Minerals, Policy and Planning Division (in press).

Tanoli, S.K., and Pickerill, R.K. 1988. Lithostratigraphy of the Cambrian–Lower Ordovician Saint John Group, southern New Brunswick. Canadian Journal of Earth Sciences, **25**: 669–690.

van Staal, C.R, and Fyffe, L.R. 1995. Gander Zone — New Brunswick. *In* Geology of the Appalachian–Caledonian Orogen in Canada and Greenland. *Edited by* H. Williams. Geological Survey of Canada, Geology of Canada, No. 6, pp. 216–223.

van Staal, C.R., Dewey, J.F., MacNiocaill, C., and McKerrow, W.S. 1998. The Cambrian–Silurian tectonic evolution of the northern Appalachians and British Caledonides: history of a complex west and southwest Pacific-type segment of Iapetus. *In* Lyell: The Past is the Key to the Present. *Edited by* D.J. Blundell and A.C. Scott. Geological Society of London, Special Publication 143, pp. 199–242.

Whalen, J.B., Currie, K., and Chappell, B.W. 1987. A-type granites: geochemical characteristics, discrimination, and petrogenesis. Contributions to Mineralogy and Petrology, **95**: 407–419.

White, C.E., and Barr, S.M. 1996. Geology of the Brookville Terrane, southern New Brunswick, Canada. In Avalonian and Related Peri-Gondwanan Terranes of the Circum-North Atlantic. Edited by R.D. Nance and M.D.Thompson. Geological Society of America, Special Paper 304, pp. 133–147.

White, C.E., Barr, S.M., Miller, B.V., and Hamilton, M.A. 2002. Granitoid plutons of the Brookville Terrane, southern New Brunswick: petrology, age, and tectonic setting. Atlantic Geology, **39**: 53–74.

Williams, H. 1979. Appalachian Orogen in Canada. Canadian Journal of Earth Sciences, **16**: 792–807.

Winchester, J.A., and Floyd, P.A. 1977. Geochemical discrimination of different magma series and their differentiation products using immobile elements. Chemical Geology, **20**: 325–343.

GEOTECHNICAL IMPLICATIONS OF BEDROCK CHARACTERISTICS IN THE BELLEDUNE AREA, NORTHERN NEW BRUNSWICK

IVAN DIMITROV [1] AND STEVEN R. MCCUTCHEON [2]
[1] Department of Geology, University of New Brunswick, P.O. Box 4400,
Fredericton, New Brunswick, CANADA E3B 5A3 (*d7z85@unb.ca*)
[2] Geological Surveys Branch, New Brunswick Department of Natural Resources,
P.O. Box 50, Bathurst, New Brunswick, CANADA E2A 3Z1

Dimitrov, I., and McCutcheon, S.R. 2005. Geotechnical implications of bedrock characteristics in the Belledune area, northern New Brunswick. *In* Geological Investigations in New Brunswick for 2004. *Edited by* G.L. Martin. New Brunswick Department of Natural Resources; Minerals, Policy and Planning Division, Mineral Resource Report 2005-01, pp. 23–44.

The district around the Port of Belledune, located beside Chaleur Bay in northern New Brunswick, hosts major industrial facilities including a smelter and a power generating station. Bedrock underlying the area varies considerably in lithological composition and structural complexity. Anisotropic features such as bedding contacts and fault boundaries potentially can affect the mechanical strength of rock. At present, little information is available on the geotechnical properties of bedrock in the Belledune area. To fill this knowledge gap, a survey was conducted in the summer of 2004 to obtain geological data that could prove useful in assessing the engineering integrity of construction sites in the region.

The geological survey delineated several lithological and structural features that could represent potential zones of weakness in the bedrock. The lithological features include mudstone interbeds in the Weir Formation, karst topography in the La Vieille Formation, weathered tuff layers in the South Charlo Formation, and calcrete pockets in the Bonaventure Formation. The survey also identified the existence of numerous steeply dipping faults that have the potential to slip during loading. Other structural features such as cleavage and jointing generally are not well developed in the bedrock. They likely pose little engineering risk but nonetheless should be examined on a site-specific basis.

Le district voisin du port de Belledune, situé au bord de la baie des Chaleurs dans le Nord du Nouveau-Brunswick, abrite des installations industrielles importantes, dont une fonderie et une centrale énergétique. Le substrat rocheux sous-jacent au secteur présente une composition lithologique et une complexité structurale qui varient considérablement. Les particularités anisotropes comme les contacts de stratification et les limites des failles peuvent affecter la solidité mécanique de la roche. On dispose à l'heure actuelle de peu de renseignements au sujet des propriétés géotechniques du substrat rocheux dans le secteur de Belledune. Pour combler cette lacune, on a réalisé un levé au cours de l'été 2004 en vue d'obtenir des données géologiques qui pourraient s'avérer utiles dans l'évaluation de l'intégrité technique des chantiers de construction dans la région.

Le levé géologique a délimité plusieurs particularités lithologiques et structurales qui pourraient représenter des zones éventuelles de faiblesse dans le substrat rocheux. Les particularités lithologiques relevées comprennent des couches interstratifiées de mudstone dans la Formation de Weir, un relief karstique dans la Formation de La Vieille, des couches de tuf météorisé dans la Formation de South Charlo, et des poches de calcrète dans la Formation de Bonaventure. Le levé a en plus relevé l'existence de nombreuses failles abruptement inclinées qui pourraient s'effondrer pendant le chargement. Les autres particularités structurales comme les schistosités et les fissurations ne sont généralement pas très développées dans le substrat rocheux. Elles posent vraisemblablement peu de risque technique, mais il faudrait néanmoins examiner chacune de ces zones.

INTRODUCTION

The Port of Belledune and its industrial environs are situated beside Chaleur Bay in northern New Brunswick (Fig. 1). The area in and around the town hosts major industrial complexes including a smelter, power generating station, soil treatment plant, gypsum plant, and deepwater port. These facilities are constructed over Silurian and Carboniferous bedrock that generally is well lithified and has good geotechnical properties (Fig. 1). However, the gravitational load of some man-made installations potentially could shear weak layers in the bedrock, or could reactivate geological structures that have a specific orientation. Features such as faults, joints, or bedrock with low shear strength thus should be examined when assessing the mechanical integrity of industrial construction projects.

During the summer of 2004, a survey was conducted in the Belledune area to clarify the structural geometry of local bedrock and to determine features affecting bedrock strength. The research involved no quantitative geotechnical assessment, because such work usually focuses on a particular engineering project. Instead, the study simply identified bedrock features for geological and other engineers to consider when evaluating geotechnical properties of specific sites in the region.

REGIONAL OVERVIEW

The geology of the survey area has been mapped and described by Alcock (1935), Greiner (1970), Noble (1976), Irrinki (1990), Walker et al. (1993a, b), and Walker and McCutcheon (1995). The oldest rocks (Fig. 1) comprise an uplifted block of Ordovician deep marine basalt and gabbro (Fournier Group) that represent remnants of an ancient

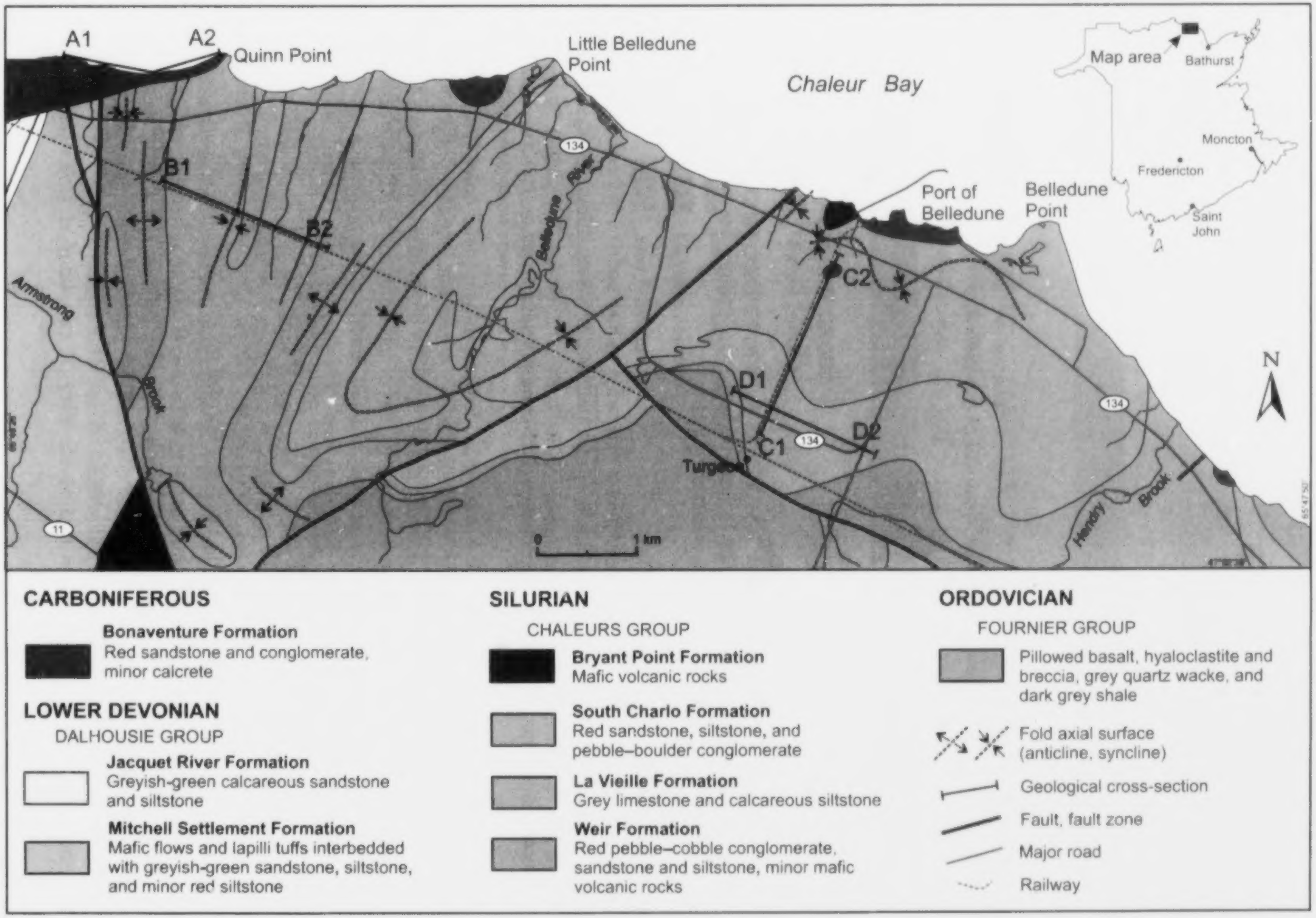
A1
A2
Quinn Point
Little Belledune Point
Chaleur Bay
Map area
Bathurst
Moncton
Fredericton
Saint John
Port of Belledune
Belledune Point
B1
B2
C1
C2
D1
D2
134
11
Belledune River
Armstrong Brook
Hendry Brook
Turgeon
N
0
1 km
CARBONIFEROUS
Bonaventure Formation
Red sandstone and conglomerate, minor calcrete
LOWER DEVONIAN
DALHOUSIE GROUP
Jacquet River Formation
Greyish-green calcareous sandstone and siltstone
Mitchell Settlement Formation
Mafic flows and lapilli tuffs interbedded with greyish-green sandstone, siltstone, and minor red siltstone
SILURIAN
CHALEURS GROUP
Bryant Point Formation
Mafic volcanic rocks
South Charlo Formation
Red sandstone, siltstone, and pebble–boulder conglomerate
La Vieille Formation
Grey limestone and calcareous siltstone
Weir Formation
Red pebble–cobble conglomerate, sandstone and siltstone, minor mafic volcanic rocks
ORDOVICIAN
FOURNIER GROUP
Pillowed basalt, hyaloclastite and breccia, grey quartz wacke, and dark grey shale
Fold axial surface (anticline, syncline)
Geological cross-section
Fault, fault zone
Major road
Railway

Figure 1. Bedrock geological map of the Belledune area, northern New Brunswick (modified after Walker et al. 1993a, b).

ocean floor (Noble 1976; Pajari et al. 1977; Fyffe and Noble 1985; van Staal et al. 1988). Silurian and Lower Devonian sedimentary and volcanic rocks of the Chaleurs and Dalhousie groups were deposited in a shallow marine environment along the margin of the Ordovician uplift. The Ordovician–Devonian sequences were folded and transected by faults during tectonic events related to collision of the Appalachian Orogen with the ancient North American continental margin (van Staal and de Roo 1995). Mainly flat-lying Carboniferous conglomerate and sandstone unconformably overlie the older deformed rocks along Chaleur Bay.

The main industrial complexes in the Belledune area are situated on ground that is underlain by Silurian and Carboniferous bedrock of the Weir, La Vieille, South Charlo, and Bonaventure formations (Fig. 1). This paper outlines basic lithological and structural characteristics of the four bedrock units. It also suggests how some of those features might represent weak zones in the bedrock that could affect its mechanical integrity.

LITHOLOGICAL FEATURES

Several lithological characteristics influence the geotechnical properties and mechanical strength of bedrock. They include mineral composition, degree of diagenetic lithification, lithological contacts, and weathering intensity.

Weir Formation

The Silurian Weir Formation comprises a sequence of interbedded red conglomerate, sandstone, and minor mudstone. Clasts in the conglomerate include shale, mafic volcanic rocks, quartz, jasper, and chert. The formation is well exposed on Highway 134 just northeast of Turgeon (Fig. 2: cross-section D1–D2) and at Quinn Point.

About 600 m west of Quinn Point, dark grey, feldspar-phyric mafic flows (Fig. 3) are interbedded with sandstone of the Weir Formation. A boulder conglomerate located slightly north of the mafic outcrops contains clasts up to 30 cm in diameter that obviously were derived from these flows. Beds in the lower part of the formation are thick bedded to very thick bedded, poorly sorted, and coarser grained. Bedding characteristics gradually alter upsection until, in the upper part, they are crossbedded, well sorted, and finer grained. Upper beds of the Weir Formation feature sandstone rich in quartz and pink alkali feldspar and cemented by abundant, diagenetic calcite. The calcite cement increases upsection such that sandstone grades consecutively into sandy shale, shaly limestone, and nodular limestone of the overlying La Vieille Formation.

If acidified groundwater, or water undersaturated in calcite, percolated through the sandstone beds, the calcite cement could dissolve, which would greatly decrease strength of the sandstone. As well, the sandstone layers have regular interbeds (up to 10 cm thick)

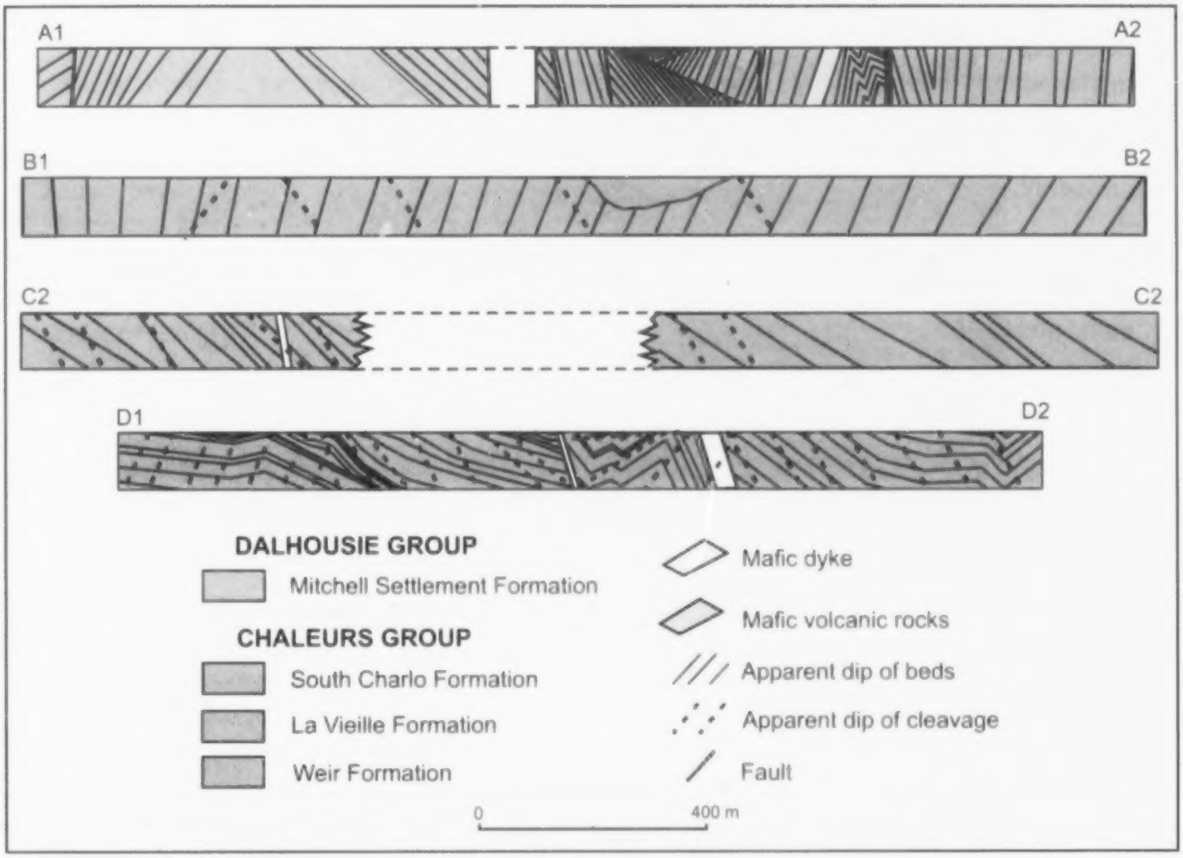
A1
A2
B1
B2
C2
C2
D1
D2
DALHOUSIE GROUP
Mitchell Settlement Formation
CHALEURS GROUP
South Charlo Formation
La Vieille Formation
Weir Formation
Mafic dyke
Mafic volcanic rocks
Apparent dip of beds
Apparent dip of cleavage
Fault
0
400 m

Figure 2. Geological cross-sections of bedrock in the Belledune area. Section lines A1–A2, B1–B2, C1–C2, and D1–D2 are marked on Figure 1. A thin cover of Carboniferous strata overlies A1–A2 and C1–C2 but is not shown here.

of clay-rich mudstone. Mudstone is easily weathered and can significantly lower bedrock strength. The clay-rich mudstone and sandstone of the Weir Formation is soft enough to be readily scratched with a hammer or fingernail.

La Vieille Formation

The Silurian La Vieille Formation comprises highly fossiliferous, light to dark grey, nodular limestone (Fig. 4). Good exposures occur on Quinn Point and in a roadcut along Highway 134, approximately 2.5 km southwest of the Port of Belledune.

The limestone beds are well cemented and lithified and mechanically should be quite strong. The possibility exists, however, that these rocks may contain sinkholes. According to Lavoie (2005), the La Vieille Formation underwent a period of hydrothermal alteration associated with dolomitization, brecciation, leaching, and the development of porous intervals. An actual solution cavity can be seen in the La Vieille Formation south of Quinn Point. The cavity is known as "Crystal Cave" and is large enough to accommodate a person.

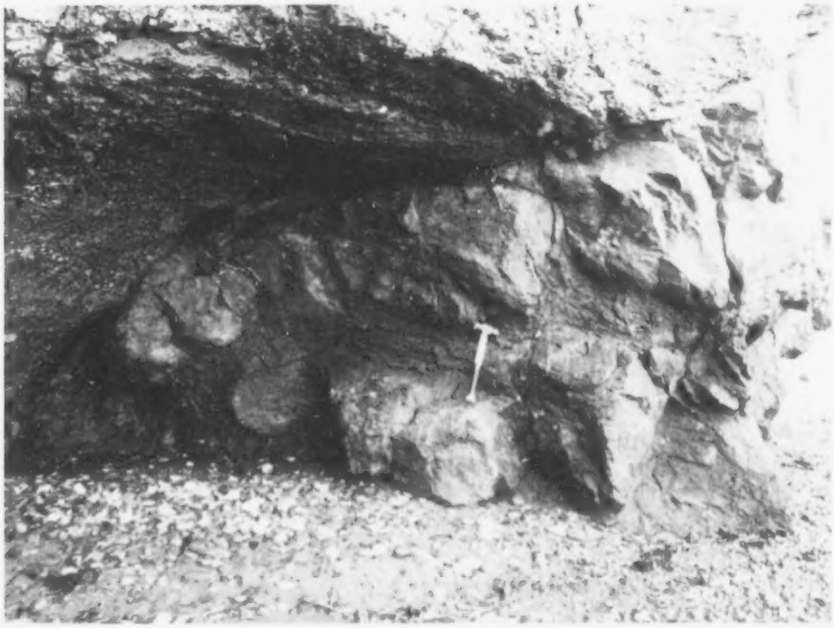

Figure 3. Mafic volcanic rocks of the Weir Formation unconformably overlain by coarse sandstone of the Bonaventure Formation west of Quinn Point. Hammer is 45 cm long.

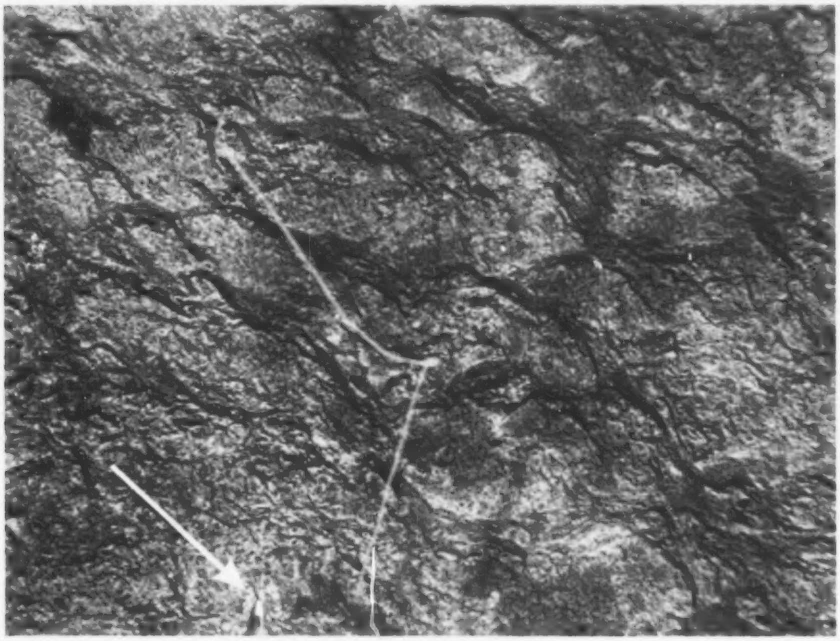

Figure 4. Nodular limestone of the La Vieille Formation along Highway 134 approximately 2.5 km southwest of Belledune. Pen tip (shown by arrow) is 3 mm long.

Karst topography may have developed in the La Vieille Formation during two distinct tectonic events, both of which are recorded in the Chaleur Bay region as geological unconformities. Southeast of the survey area, at Limestone Point near Petit Rocher, an unconformity exists between the La Vieille and South Charlo formations, indicating uplift and erosion in the mid-Silurian (Fyffe and Noble 1985; Dimitrov et al. 2004). The uplift could have been accompanied by the circulation of meteoric water and/or hydrothermal fluids and by the resulting formation of solution cavities.

The survey area contains no known exposures of such a mid-Silurian unconformity, but the unconformity's presence can be inferred by differences in bedding dips. Specifically, bedding in the La Vieille Formation dips more steeply than in the overlying South Charlo Formation. Limestone beds of the La Vieille Formation dip steeply to the west on both limbs of a syncline (Fig. 2: cross-section B1–B2), whereas conglomerate of the South Charlo Formation has a maximum dip of 40°. Moreover, the conglomerate occurs southeast of the syncline's core and thus must lie unconformably within a depression eroded into the limestone.

The second period of uplift and erosion is indicated by an unconformity between the Chaleurs Group (Weir Formation) and Bonaventure Formation (Alcock 1935). The unconformity can be seen west of Quinn Point, where folded strata of the Silurian Chaleurs Group and Lower Devonian Dalhousie Group lie below undeformed conglomerate of the Carboniferous Bonaventure Formation (Fig. 1, 3). The Siluro–Devonian basement has an uneven topography caused in part by karst depressions and the upward protrusion of resistant beds. Beds of Carboniferous boulder conglomerate in these erosional hollows exhibit a primary depositional dip of up to 20°.

Thus, it is possible that two periods of karst formation occurred in the region. One was related to mid-Silurian Salinic tectonism, and the other to mid-Devonian Acadian tectonism. Lavoie (2005) concluded that hydrothermal alteration occurred early in the depositional history of the La Vieille Formation and therefore was likely related to the mid-Silurian event.

South Charlo Formation

The South Charlo Formation comprises maroon to red, medium-bedded, medium-grained sandstone; red and green, thin-bedded, slightly calcareous siltstone; and red and green pebble–boulder conglomerate. The conglomerate contains moderately to well rounded clasts of mafic and felsic volcanic rocks, limestone, shale, chert, and sandstone. The abundant clasts of coarsely feldspar-phyric basalt appear to have been derived from the laterally interfingering Bryant Point Formation (Walker and McCutcheon 1995). The limestone clasts likely were obtained from the underlying La Vieille Formation (Fig. 5). In the coastal section just west of the Port of Belledune, rare clastic dykes of coarse sandstone have been injected into fractures in the conglomerate (Fig. 6).

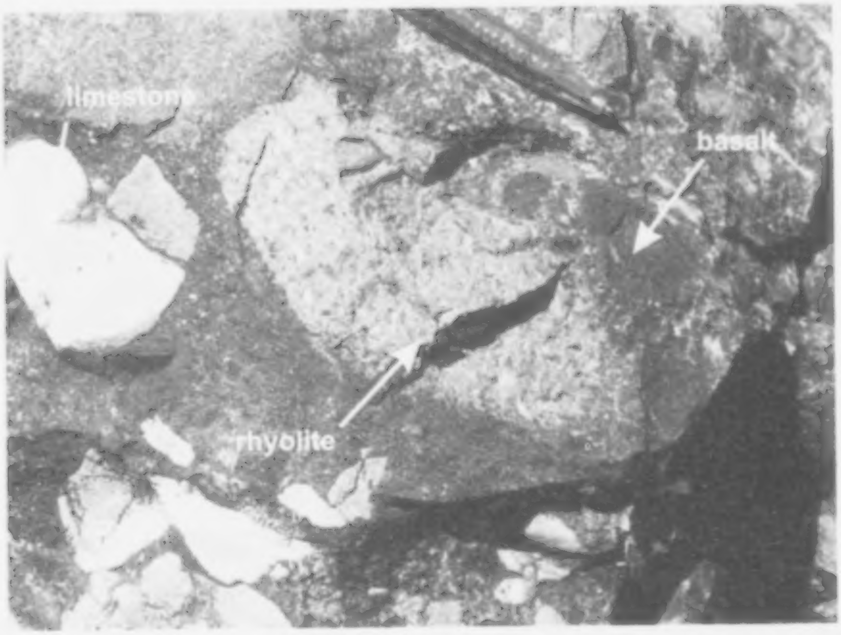
limestone
basalt
rhyolite

Figure 5. Conglomerate of the South Charlo Formation containing clasts of limestone, rhyolite, and basalt in an exposure along the railway into Belledune. Blue pen for scale.

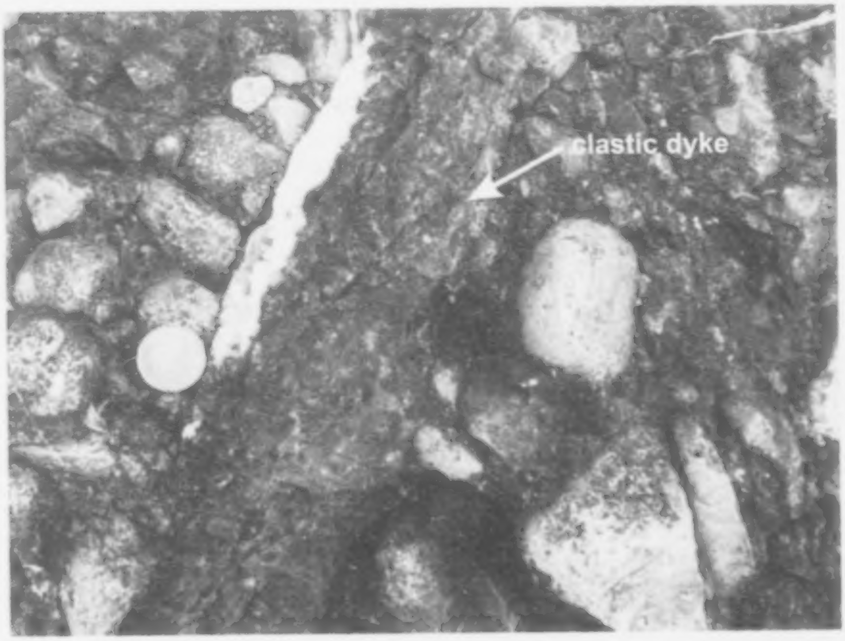
clastic dyke

Figure 6. Clastic dyke cutting conglomerate of the South Charlo Formation beside the Chaleur Bay coast west of Belledune. One-dollar coin for scale.

The clastic sedimentary beds of this formation grade laterally from poorly sorted conglomerate into sandstone and shale. Consequently, the characteristics of grain size, compressibility, and permeability vary significantly from one locale to another. As well, thin interbeds of tuffaceous sandstone in the conglomerate (Fig. 7) have weathered into layers of sage green bentonitic clay. These clay horizons could represent significant planes of weakness.

Bonaventure Formation

The Carboniferous Bonaventure Formation is restricted to a narrow, topographically flat belt along Chaleur Bay (Fig. 1). All rocks in the unit are red; they consist of coarse-grained sandstone, pebble conglomerate, and, locally, boulder conglomerate. Lithologically, the Bonaventure Formation resembles the Weir Formation. The Bonaventure rocks, however, are flat lying to gently dipping (less than 10°) and are the least lithified rocks in the survey area.

Poor lithification of the Bonaventure rocks has given them a low cohesive strength. On the other hand, the flat topography of the district does not feature steep, erosion-prone slopes where rock cohesion would become an issue. The rocks do display a lateral variation in grain size and permeability, factors that should be considered when assessing geotechnical properties of the formation. In addition, the Bonaventure Formation contains nodular calcrete in lenses that are up to 2 m thick. Calcrete (groundwater-transported accumulations of calcite) can leach out to form collapsible cavities when subjected to water action. Such lenses occur near the base of the formation in sections west of Quinn Point, along the railway track at Belledune (Fig. 8), and east of Hendry Brook. As with the other Bonaventure rocks, the calcrete tends to be red; acid testing therefore may be required to identify it.

STRUCTURAL FEATURES

Several structural features can be seen in Silurian and Carboniferous bedrock units underlying the Belledune area. These include folds, cleavage, faults, and joints, all of which potentially could influence the geotechnical properties and mechanical strength of regional bedrock. Reactivation of faults and other structural planes of weakness may take place, for example, when construction projects expose a rockface that is susceptible to mass flow in a given direction. This can occur when deep excavations are made for tunnels, building foundations, and trenches related to dam construction.

Folds

Silurian and Early Devonian rock sequences in the survey area have been affected by open to tight upright folds (Fig. 2). Fold geometry details are not well known because the district has sparse outcrop, except along the coast and in roadcuts. Three structural domains can be identified on the basis of regional variation in fold orientation: the western

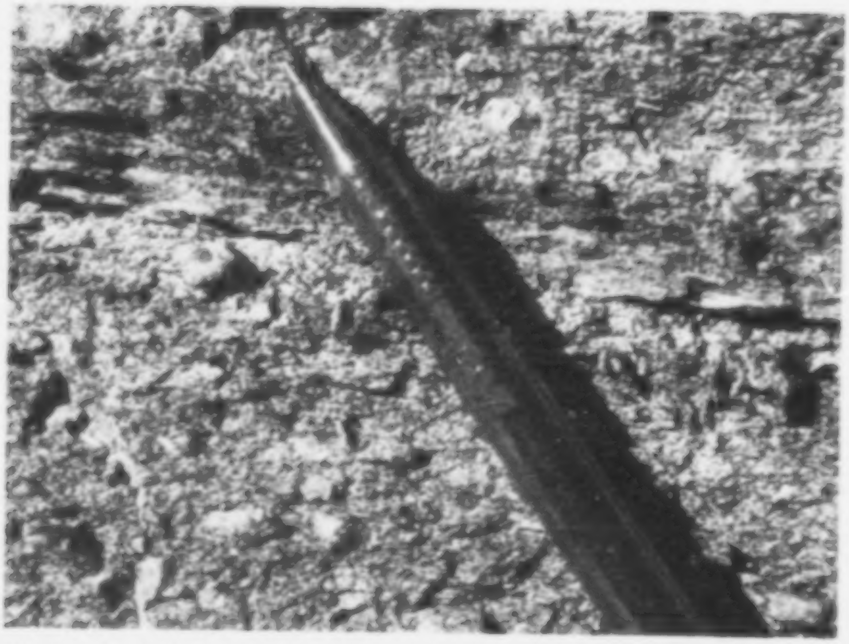

Figure 7. Tuffaceous sandstone interbedded with conglomerate of the South Charlo Formation on the Chaleur Bay coast west of Belledune. Blue pen for scale.

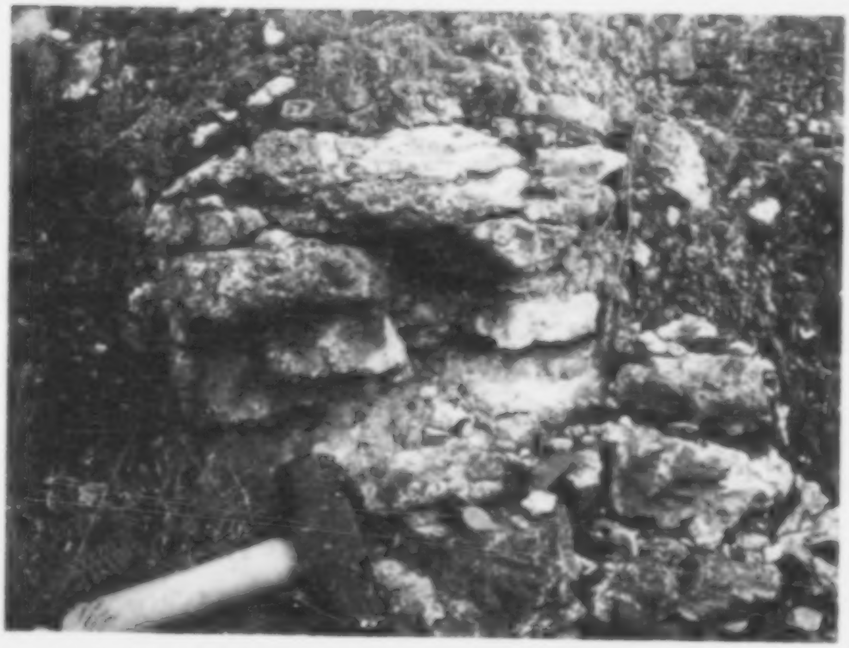

Figure 8. Calcrete of the Bonaventure Formation, preserved in a pocket eroded into conglomerate of the South Charlo Formation. Head of hammer is 10 cm long.

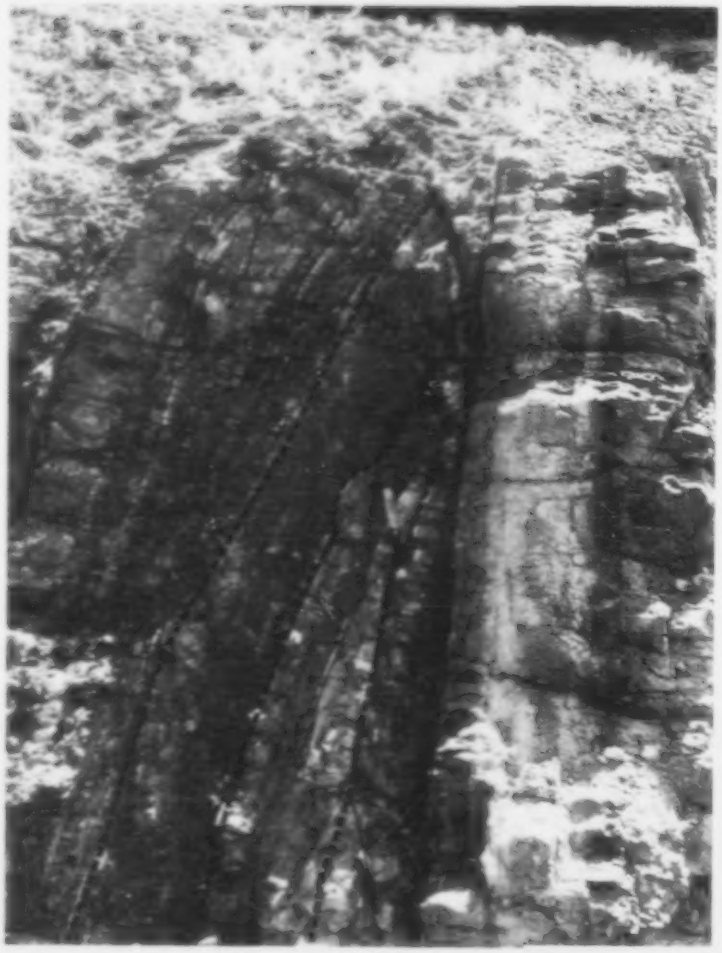

Figure 9. Tight fold in sandstone of the Weir Formation, west of Quinn Point. Hammer in the fold closure is 45 cm long. Red lines indicate small faults.

domain west of Quinn Point, the central domain between Quinn Point and Belledune, and the eastern domain between Belledune and Hendry Brook (Fig. 1).

In the western domain, the folding style is best demonstrated in the Weir and La Vieille formations west of Quinn Point (Fig. 9, 10). Both formations host north- to northeast-trending folds. Evidence of overturned bedding occurs locally in the La Vieille Formation (Fig. 11), but bedding is not inverted on a regional scale (see Fig. 2: cross-section A1–A2). In the central and eastern domains, around Belledune and Hendry Brook, the folds trend easterly and northeasterly. The mapped distribution pattern of Silurian strata suggests that two generations of folds (F_1 and F_2) exist. Indisputable mesoscopic F_1 folds have not yet been observed, however, and refolding thus has not been proven at the outcrop scale.

Fold structures in the western domain are fairly homogeneous, as indicated by the obvious girdle of poles to bedding and the tightly grouped axial planes in stereographic projection (Fig. 12a). Folds are upright, tight to isoclinal, and have subhorizontal axes that trend consistently north–south. Fold orientation in the central domain is more

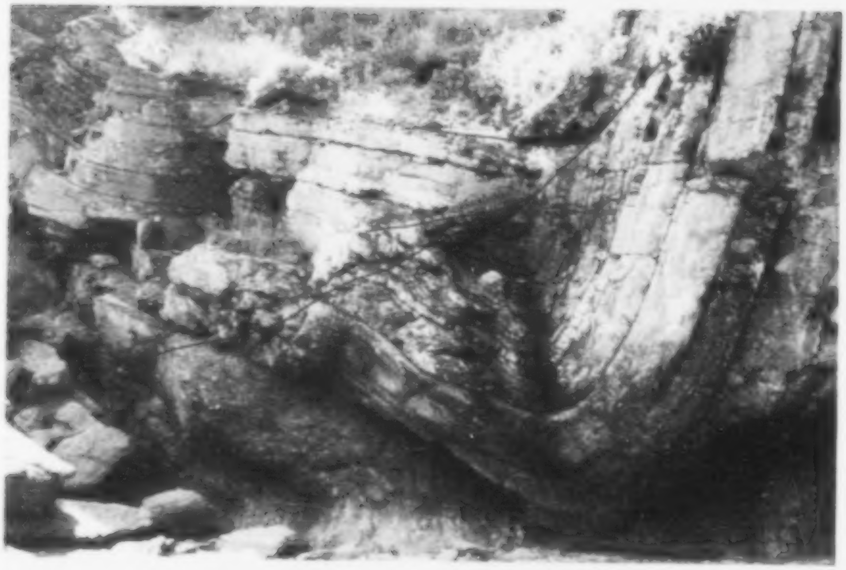

Figure 10. Folded strata west of Quinn Point, showing the core of a large syncline cut by a reverse fault in limestone of the La Vieille Formation. Vertical view is approximately 4 m. Arrow indicates an offset along the fault plane.

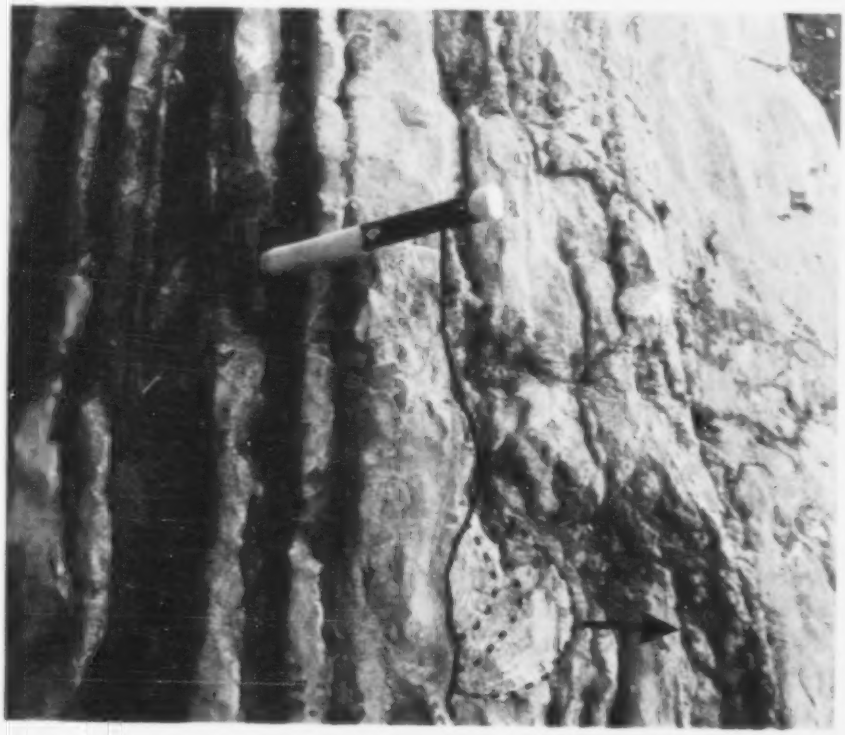

Figure 11. Fossil in the growth position in limestone of the La Vieille Formation, indicating that the beds are overturned. Hammer is 45 cm long.

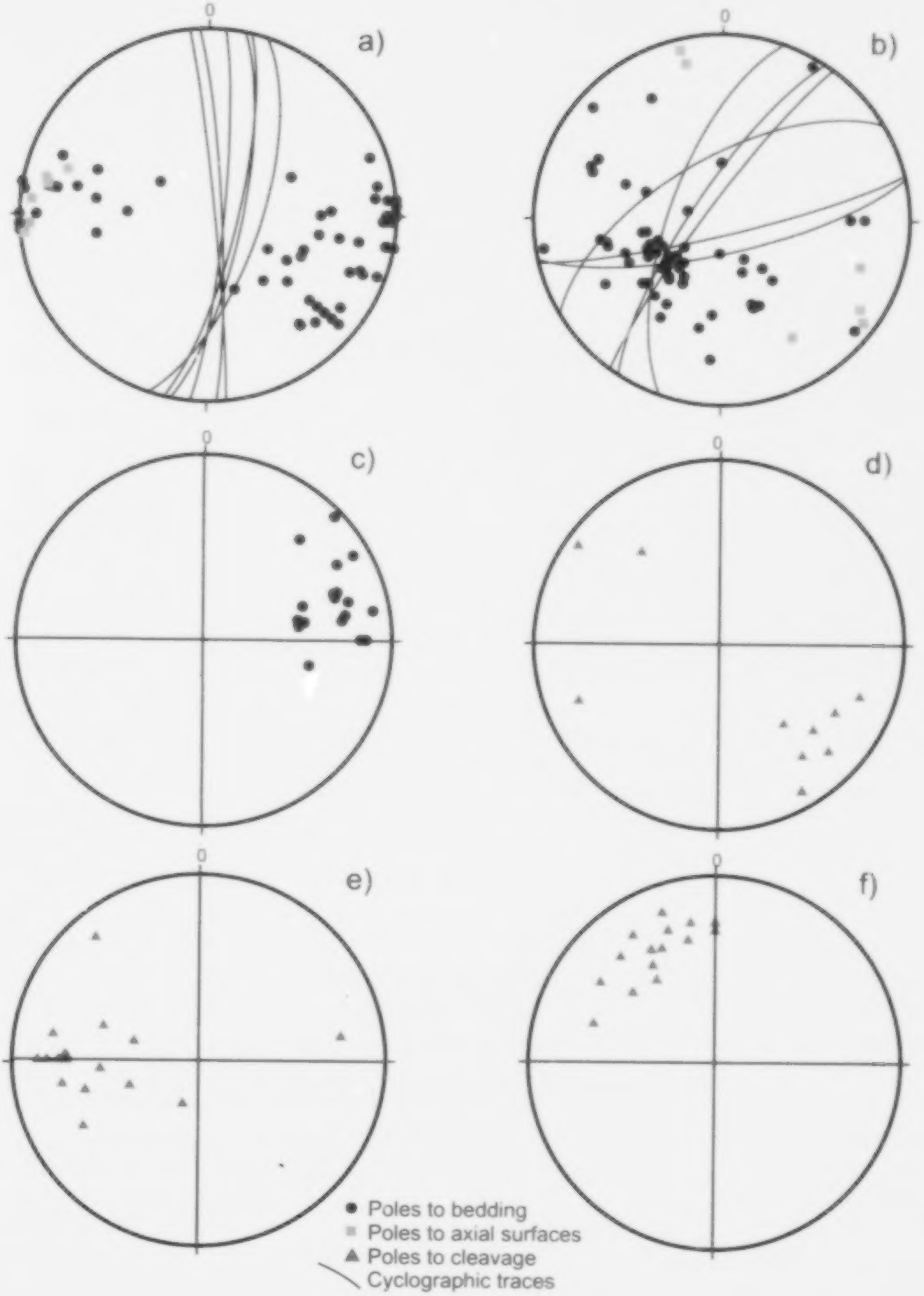

Figure 12. Equal area, lower hemisphere projection of bedding and cleavage planes for the three structural domains in the Belledune area (see Fig. 1). a) Poles to bedding and cyclographic traces (great circle projections) representing axial surfaces of folds measured in the western domain along sections A1–A2 and B1–B2. b) Poles to bedding and cyclographic traces representing axial surfaces of folds measured in the central domain along sections C1–C2 and D1–D2. c) Poles to bedding measured in the eastern domain along the coast near Hendry Brook. d) Poles to cleavage measured in the western domain. e) Poles to cleavage measured in the central domain. f) Poles to cleavage measured in the eastern domain.

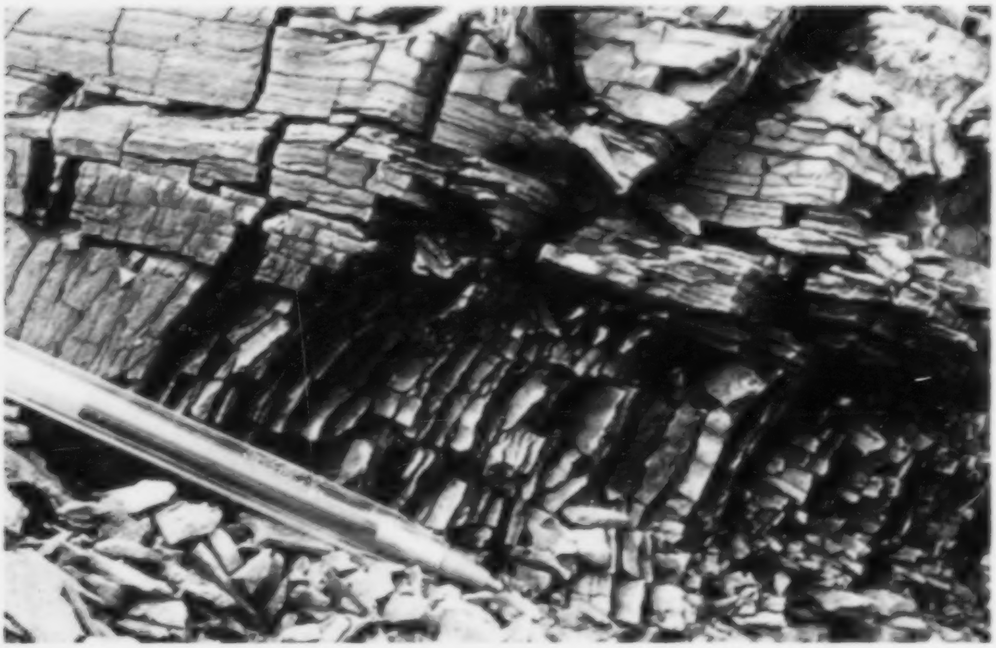

Figure 13. Fold and cleavage structures in sandstone of the Weir Formation west of Quinn Point. Two cleavages are displayed on the limb of a fold that has an axial plane dip-direction and dip of 101°/75°. The bedding-parallel fissility dips at approximately 300°/30°, and the fracture cleavage dips at approximately 120°/60°, subperpendicular to bedding. Blue pen for scale.

heterogeneous (Fig. 12b). The stereographic diagram for this domain indicates upright folds that plunge moderately northeasterly and seem more open than those in the western domain. On the other hand, some bedding attitudes are too steep for upright open folds; folding thus is probably polyclinal, which is consistent with the broad spread in the axial planes. The varying fold trends in this domain likely reflect an interference pattern between the map-scale, northwesterly trending folds and the smaller scale, open, northeasterly trending folds. Folds in the eastern domain have not been directly measured, but all of their poles to bedding (Fig. 12c) occur on the northern limb of a map-scale northwesterly trending syncline (Fig. 1).

Cleavage

Bedding-parallel fractures and fracture cleavage both are present in the survey area (Hobbs et al. 1976, p. 216), except in beds with a high sand content (Fig. 13). In argillaceous interbeds, the two features usually combine to form a pencil structure. The interbeds are quite thin, however, and their display of cleavage surfaces is limited. Penetrative cleavage rarely is observed in mesoscale in sandy rocks of the Weir Formation or in most limestone of the La Vieille Formation.

Cleavage in the district is not well developed; thus, the relationship between folds and cleavage remains unclear (Fig. 12d–f). In the western domain (Fig. 12d), northeasterly

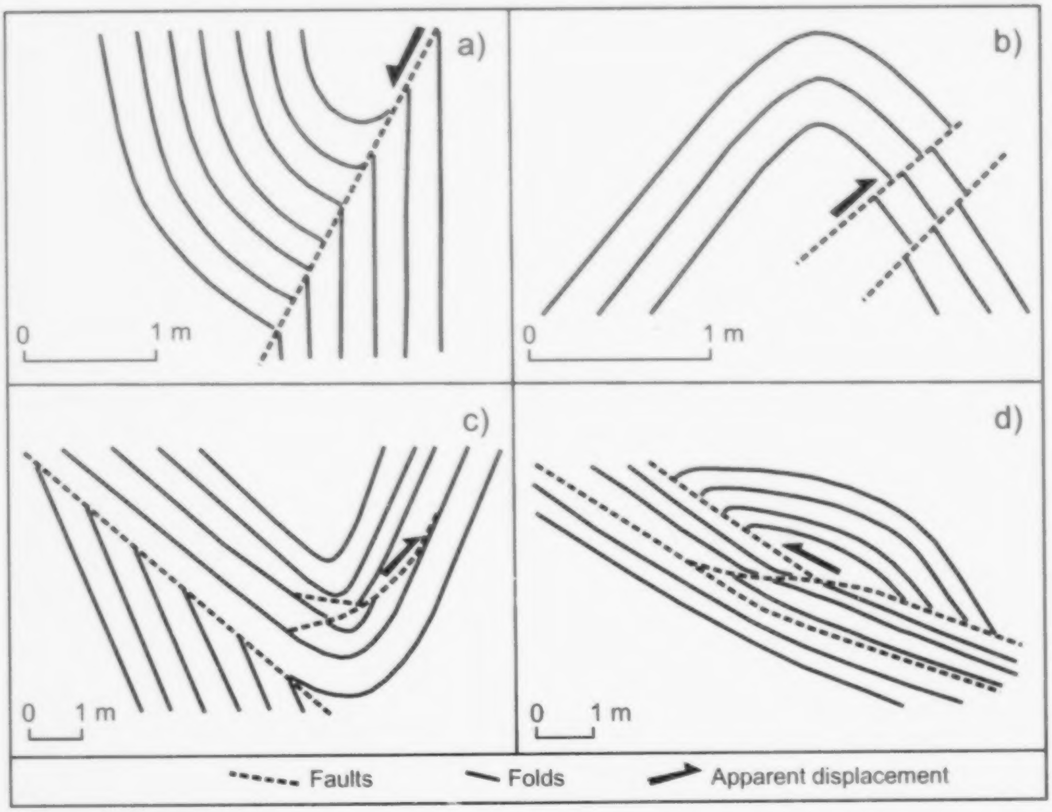

Figure 14. Sketches of relationships between folds and faults in vertical exposures around Belledune. a) Roadcut on Highway 11. b) and c) Coastal exposures near Quinn Point. d) Coastal exposure east of the mouth of Jacquet River.

trending cleavage transects the northerly trending fold axes (Fig. 12a). In the central domain, poles to cleavage (Fig. 12e) show either that the cleavage is folded or that more than one cleavage exists. In the eastern domain (Fig. 12f), the cleavage trends northeasterly to easterly. Cleavage in the central and eastern parts of the map area appears to be associated mainly with the northeasterly trending folds, whereas cleavage in the western area is roughly axial planar to the northerly trending folds.

Because fracture cleavage is poorly displayed in the survey area, it likely would have little impact on the geotechnical properties of bedrock in and around Belledune. Where cleavage is locally well developed, however, it might create significant planes of weakness. For instance, cleavage patterns in the La Vieille Formation potentially could decrease the mechanical strength of its limestone and create paths for water percolation.

Faults

Fold structures in the survey area are affected by numerous brittle faults. Many faults can be seen along Highway 11 and the Chaleur Bay coast (Fig. 14a–d); others are inferred from the regional map pattern. The Silurian sedimentary rocks are transected by diabasic dykes that likely intruded existing fault zones or acted as planes of weakness along which later faults developed (Fig. 2).

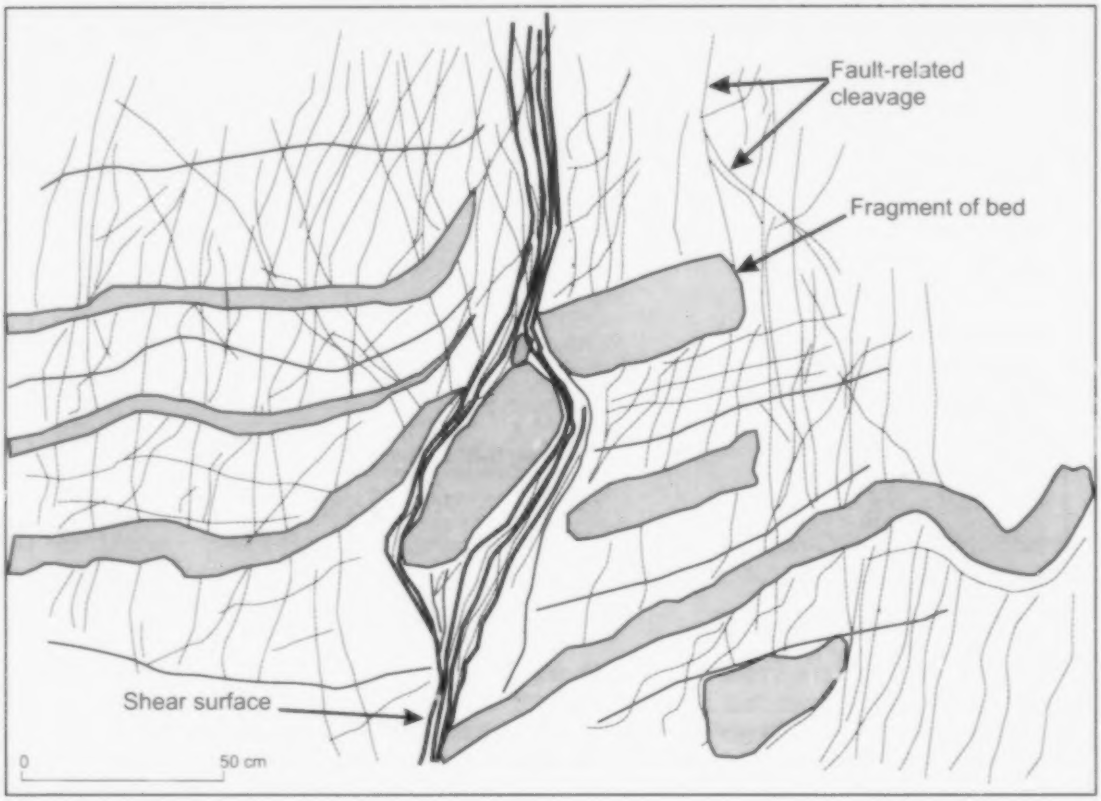

Figure 15. Sketch of easterly trending, subvertical fault zone developed in nodular limestone of the La Vieille Formation, 650 m southeast of Hendry Brook on Chaleur Bay.

The following descriptions are limited to faults that are visible in bedrock, that exhibit deformation zones thicker than 5 cm, and that reorient the bedding. Faults are classified here solely on a descriptive basis, as their relative ages generally are not known.

Subvertical Faults

The La Vieille Formation contains several subvertical fault zones that trend north-northeasterly. One such zone is well exposed on the Chaleur Bay coast approximately 650 m southeast of Hendry Brook (Fig. 1). It strikes northeasterly, is about 15 m wide, and contains distorted, thin-bedded, nodular limestone of the La Vieille Formation. The deformation zone is highly heterogeneous and is characterized by blocks of relatively undeformed limestone preserved between anastomosing fractures (Fig. 15). Individual fractures are subparallel to the general trend of the fault zone, except where they deflect around fragments of dismembered nodular beds. These fractures are locally concentrated, forming high-strain domains that can be traced for several metres. The limestone blocks show varied orientations of a weak Acadian cleavage, which indicates they have been rotated. The fault zone thus appears to be postcleavage and younger than the Acadian folding event.

Several other subvertical (10° to 20°) fault zones can be seen in the La Vieille Formation (Fig. 16a, b). These zones are narrower, have apparent offsets that do not exceed half a metre, and generally are associated with well developed fault-drag folds.

Geological structures with subvertical dips are of particular engineering concern, because they are subjected to large stresses when loaded (Dimitrov 2003). Consequently, these subvertical faults may be the most important regional anisotropy to consider when assessing engineering projects in the survey area. Complicating the situation is the fact that the faults are commonly obscured by a flat-lying veneer of Carboniferous strata. It is conceivably, therefore, that a foundation constructed on Carboniferous bedrock could be immediately underlain by a weak zone of fault gouge.

Bedding-Parallel Brittle Faults

Faults subparallel to bedding on the footwall and/or hanging wall have been identified along the Chaleur Bay coast. Most fault planes are inclined to bedding by 0° to 10° and have relatively steep dips of between 45° and 90°. Locally, the infilling is penetratively foliated parallel to the fault walls. As well, there can be synthetic and/or antithetic shear surfaces inclined at 10° to 30° to the fault walls. The fill zones are highly susceptible to weathering. The bedding-parallel faults trend mainly northeasterly (Fig. 16a, b) and are filled with breccia or gouge that ranges in thickness from 10 mm to 1.5 m. Faults that lie nearly parallel to bedding can be mistaken for clay seams or weak silty interbeds. In such cases, faults are recognized by the presence of secondary shears, angular breccia fragments in the gouge, or slight obliquity of the bedding to fracture surfaces.

Faults with slightly steeper dips also were observed. They trend mainly northeasterly and have dips that range from 30° to 45° (Fig. 16b, 17). They are interpreted as normal faults except in one exposure, where movement may be reversed. The fault-fill varies in thickness from several millimetres (where faults are parallel to bedding) to 1 m (where faults cut beds at higher angles).

Fault-fill ranges from coarse breccias or laminated fault gouge to relatively coherent domains affected by systematic synthetic and antithetic fractures. Fractures in these domains appear to indicate significant rotation toward the walls of the fault zone. The angle of intersection between fractures and fault zone boundaries indicates differing degrees of strain within the zone (Fig. 18). A larger angle coincides with less deformed fault-fill composed of large, lozenge-shaped fragments of apparently intact rock. A lower angle coincides with a more highly milled rock mass that contains smaller fragments elongated parallel to the fault zone. Evidence of large-scale thrusting related to shallowly dipping structures was not detected.

The age, magnitude, and displacement mode of these bedding-parallel shear surfaces cannot be clearly determined, as outcrop is sparse. The region's overall lack of Carboniferous cover makes it difficult to distinguish pre-Carboniferous faults from post-

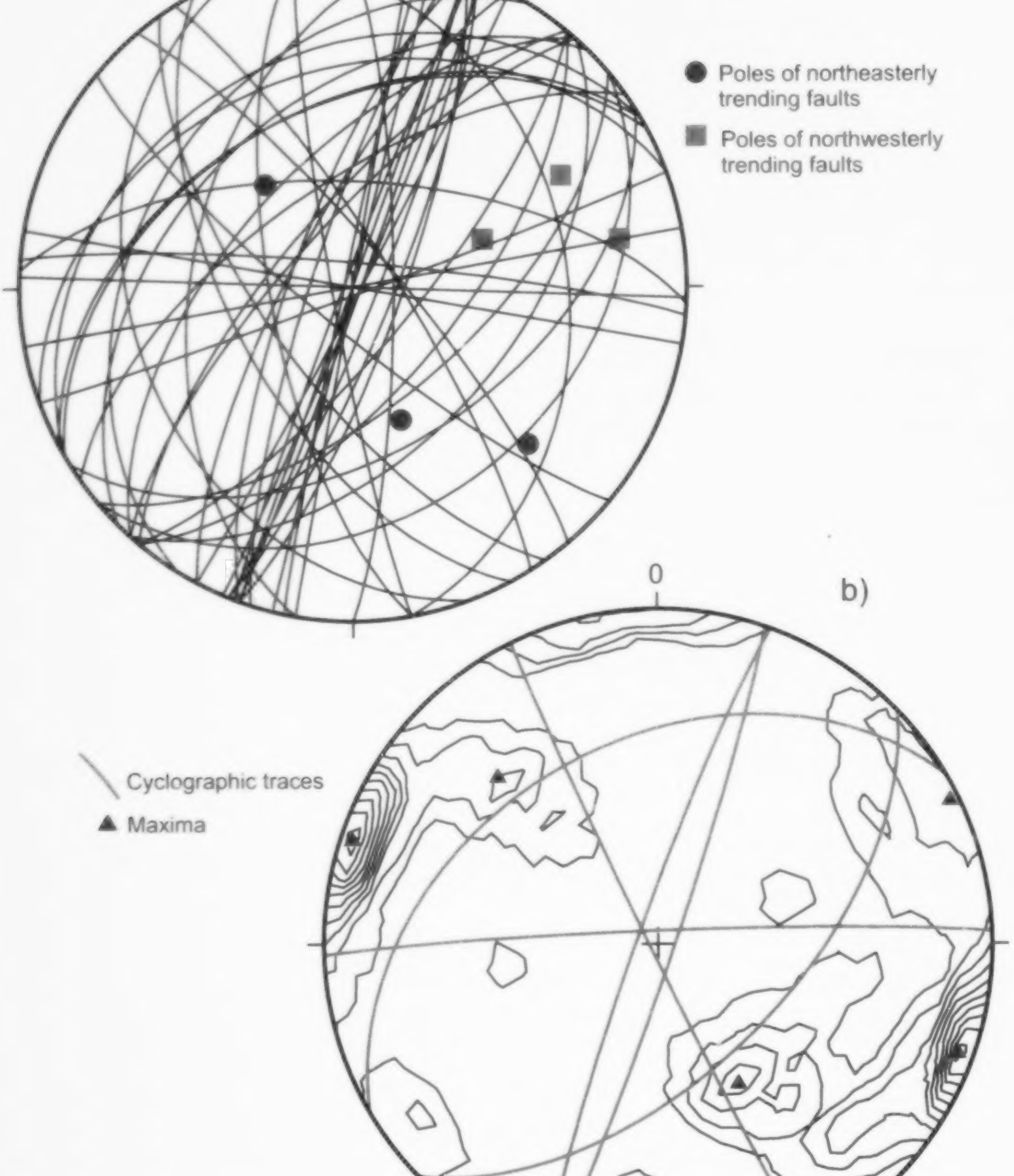
0
a)
● Poles of northeasterly trending faults
■ Poles of northwesterly trending faults
0
b)
Cyclographic traces
▲ Maxima

Figure 16. Equal area, lower hemisphere projection of faults in the Belledune area. a) Cyclographic traces show faults with an apparent offset of more than 30 cm; poles are shown only for faults covered by Carboniferous strata. b) Contoured poles to the faults show the maxima and the corresponding cyclographic traces. Density contours are expressed as a per cent per 1% area; lower and upper density boundaries are 0% and 10% respectively (computer application is from Duyster 2000).

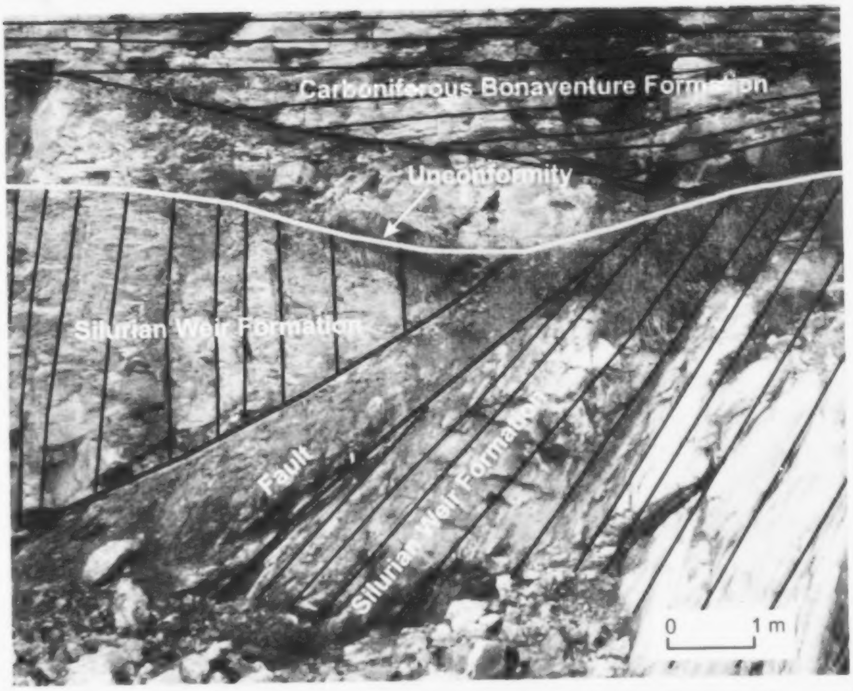
Carboniferous Bonaventure Formation
Unconformity
Silurian Weir Formation
Fault
Silurian Weir Formation
0
1 m

Figure 17. Fault in Silurian rocks of the Weir Formation, sealed by unconformably overlying Carboniferous strata of the Bonaventure Formation, approximately 1 km west of Quinn Point. Sandstone beds of the Weir Formation in the footwall are subparallel to the fault, which dips at 160°/35°. Beds in the hanging wall are oblique.

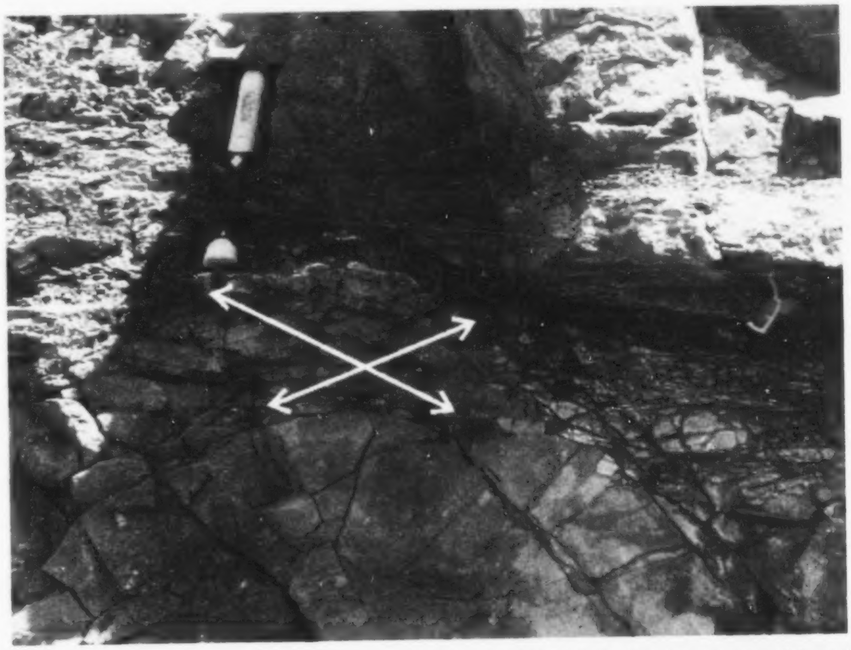

Figure 18. Shallowly dipping brittle fault east of Quinn Point. White lines represent two directions of fracture cleavage in the low-strain part of the fault zone. Laminated fracturing parallel to the walls of fault zone (on the right side of the photograph) indicates an increase in internal deformation. Hammer is 45 cm long.

Carboniferous faults in most locations. Three northeasterly trending faults and several northwesterly trending faults are truncated by the Carboniferous unconformity and thus are interpreted as Acadian structures (Fig. 16a, 17). In the northwestern part of the survey area, two shallowly dipping faults displace Carboniferous strata. Vertical separation of the bedding is 3 to 5 m, which may correspond to a true displacement of about 10 to 15 m.

Small Extensional Faults

A dense concentration of small extensional faults has been observed in Silurian sandstone of the South Charlo Formation east of Belledune. The faults are restricted to specific beds or groups of beds and indicate extension parallel to bedding. Most faults have straight, sharp surfaces that lie at high angles to bedding; others are listric or are transitional into pinch-and-swell bedding structures. Apparent offset does not exceed 10 cm. Morphologically, these faults resemble small faults in the Simpsons Field Formation near Petit Rocher (see Dimitrov et al. 2004).

Joints

Few outcrops in the survey area have well developed jointing. Joints that were measured show a predominant, average strike of 350° and a northeasterly to southwesterly dip. The statistical grouping is weak, and joint orientation varies significantly across the region. Nonetheless, joint patterns should be evaluated on a site-specific basis to ensure that their location and/or density will not compromise mechanical strength of the bedrock.

CONCLUSIONS

The present study has delineated several lithological and structural zones of potential weakness that should be considered when performing any geotechnical assessment of industrial projects in the Belledune area. These zones include mudstone interbeds in the Weir Formation, karst topography in the La Vieille Formation, weathered tuff layers in the South Charlo Formation, pockets of calcrete in the Bonaventure Formation, and subvertical faults transecting the older, deformed bedrock. Cleavage and jointing are not well developed in the area as a whole, but the location and concentration of both features should be analyzed on a site-specific basis, as needed.

ACKNOWLEDGEMENTS

This paper was critically reviewed by Paul Williams and Les Fyffe. Project funding was provided by Elmtree Resources Ltd. of Bathurst, New Brunswick, and by the Natural Sciences and Engineering Research Council of Canada (NSERC), Collaborative Research and Development Grant No. 261082-02-Project (CRDPJ).

REFERENCES

Alcock, F.J. 1935. Geology of the Chaleur Bay region. Geological Survey of Canada, Memoir 183, 146 p.

Dimitrov, I. 2003. Simple procedure for quantification of the gravitational stress field in fractured hard rock massifs. Engineering Geology, **68**: 397–400.

Dimitrov, I., McCutcheon, S.R., and Williams P.F. 2004. Stratigraphic and structural observations in Silurian rocks between Pointe Rochette and the Southeast Upsalquitch River, northern New Brunswick: a progress report. *In* Geological Investigations in New Brunswick for 2003. *Edited by* G.L. Martin. New Brunswick Department of Natural Resources; Minerals, Policy and Planning Division, Mineral Resource Report 2004-4, pp. 41–74.

Duyster, J.P. 2000. StereoNett version 2.46; www.geologynet.com.

Fyffe, L.R., and Noble, J.P.A. 1985. Stratigraphy and structure of the Ordovician, Silurian and Devonian of northern New Brunswick. *In* Fredericton '85, Field Excursions. *Edited by* R.K. Pickerill, C.K. Mawer, and L.R. Fyffe. Geological Association of Canada–Mineralogical Association of Canada, Excursion 4, No. 2, pp. 1–56.

Greiner, R.G. 1970. Geology of the Charlo area (21-0/16), Restigouche County, New Brunswick. New Brunswick Department of Natural Resources; Mineral Resources Branch, Map Series 70-2, 17 p.

Hobbs, B.E., Means, W.D., and Williams, P.F. 1976. An outline of structural geology. John Wiley & Sons, New York, 571 p.

Irrinki, R.R. 1990. Geology of the Charlo area, Restigouche County, New Brunswick. New Brunswick Department of Natural Resources and Energy; Minerals and Energy Division, Report of Investigation 24, 118 p.

Lavoie, D. 2005. Hydrothermal dolomitization in the Lower Silurian La Vieille Formation in northeastern New Brunswick: field evidence and implications for hydrocarbon exploration. Geological Survey of Canada, Current Research 2005-D1, 10 p.

Noble, J.P.A. 1976. Silurian stratigraphy and paleogeography, Pointe Verte area, New Brunswick, Canada. Canadian Journal of Earth Sciences, **13**: 537–546.

Pajari, G.E. Jr., Rast, N., and Stringer, P. 1977. Paleozoic volcanicity along the Bathurst–Dalhousie geotraverse, New Brunswick, and its relations to structure. *In* Volcanic Regimes in Canada, *Edited by* W.R.A. Baragar, L.C. Coleman, and J.M. Hall. Geological Association of Canada, Special Paper 16, pp. 111–124.

van Staal, C.R., and de Roo, J.A. 1995. Mid-Paleozoic tectonic evolution of the Appalachian Central Mobile Belt in northern New Brunswick, Canada: collision, extensional collapse and dextral transpression. *In* Current Perspectives in the Appalachian–Caledonian Orogen. *Edited by* J.P. Hibbard, C.R. van Staal, and P.A. Cawood. Geological Association of Canada, Special Paper 41, pp. 367–389.

van Staal, C.R., Langton J.P., and Sullivan, R.W. 1988. A U–Pb zircon age for the ophiolitic Deveraux Formation, Elmtree Terrane, northeastern New Brunswick. *In* Radiogenic Age and Isotopic Studies: Report 2. Geological Survey of Canada, Paper 88-2, pp. 37–40.

Walker, J.A., and McCutcheon, S.R. 1995. Siluro–Devonian stratigraphy of the Chaleur Bay Synclinorium, northern New Brunswick. *In* Current Research 1994. *Edited by* S.A.A. Merlini. New Brunswick Department of Natural Resources and Energy; Minerals and Energy Division, Miscellaneous Report 18, pp. 225–244.

Walker, J.A., Gower, S.J., and McCutcheon, S.R. 1993a. Geology of the Quinn Point area (NTS 21 P/13e), Gloucester and Restigouche counties, New Brunswick. New Brunswick Department of Natural Resources and Energy; Minerals and Energy Division, Plate 93-10.

Walker, J.A., Gower, S.J., and McCutcheon, S.R. 1993b. Geology of the Belledune area (NTS 21 P/13f), Gloucester County, New Brunswick. New Brunswick Department of Natural Resources and Energy; Minerals and Energy Division, Plate 93-11.

DEFORMATION OF LOWER CARBONIFEROUS ROCKS IN THE ROSEVALE TO SAINT-JOSEPH AREA, ALBERT AND WESTMORLAND COUNTIES, SOUTHEASTERN NEW BRUNSWICK

ADRIAN F. PARK[1] **AND CLINTON J. ST. PETER**[2]
[1] Department of Geology, University of New Brunswick,
P.O. Box 4400, Fredericton, New Brunswick, CANADA E3B 5A3 (*apark@unb.ca*)
[2] Geological Surveys Branch, New Brunswick Department of Natural Resources,
P.O. Box 6000, Fredericton, New Brunswick, CANADA E3B 5H1 (*Clint.St.Peter@gnb.ca*)

Park, A.F., and St. Peter, C.J. 2005. Deformation of Lower Carboniferous rocks in the Rosevale to Saint-Joseph area, Albert and Westmorland counties, southeastern New Brunswick. *In* Geological Investigations in New Brunswick for 2004. *Edited by* G.L. Martin. New Brunswick Department of Natural Resources; Minerals, Policy and Planning Division, Mineral Resource Report 2005-1, pp. 45–98.

Rocks of the Horton and Sussex groups in southeastern New Brunswick display a variety of deformation features in transects that are well exposed at Albert Mines, at Le Blanc Creek near Saint-Joseph, in coastal sections at Boudreau Village and Belliveau Village, and in the Peck Creek–Weldon Creek area. Early deformation is represented by predominantly bedding-parallel shear zones that generally are confined to shale layers and related to folds (F_1) with strongly curvilinear axes (locally sheath folds). The shear zones locally ramp through the bedding, forming duplex structures in which hanging wall antiform–synform pairs and footwall synforms can be recognized. Where kinematic indicators are present, and large-scale vergence can be determined, directions of movement associated with the bedding-parallel deformation, including the F_1 folds, indicate top-to-the-south (between south-southwest and south-southeast). This early deformation is most prevalent in the Horton Group (Albert Formation) but also is present in rocks of the Sussex Group, albeit with a more heterogeneous expression that includes a pair of very early cleavages.

Later, fault-related deformation overprints the earlier fold- and thrust-related features. The F_2 folds overprint the bedding-parallel shear zones and trend obliquely to the fold-thrust features. Significantly, both the F_1 and F_2 folds predate the latest Tournaisian–early Visean unconformity at the base of the Windsor Group (Hillsborough Formation). This deformation relates to north-northwest–south-southeast compression with a right-lateral component of transpression.

Les roches des groupes de Horton et de Sussex dans le Sud-Est du Nouveau-Brunswick affichent toute une variété de particularités de déformation dans des stratotypes affleurant nettement près d'Albert Mines, à proximité de Saint-Joseph, dans les stratotypes côtiers de Boudreau Village et de Belliveau Village, ainsi que le

long de la crique Peck et de la crique Weldon. Les premières manifestations se caractérisent par des zones de cisaillement à litage principalement parallèle qui sont généralement confinées aux couches de schiste et qui sont apparentées à des plis (F_1) aux axes fortement curvilignes (localement des plis en fourneau). On trouve par endroits des zones de cisaillement à litage parallèle s'inclinant à travers des structures duplex formant un litage dans lesquelles on peut repérer des paires de plis antiformes-synformes de lèvre supérieure et des synformes de lèvre inférieure. Lorsque des indicateurs cinématiques sont présents et qu'on peut déterminer une vergence à grande échelle, les orientations du mouvement associé à la déformation liée à un charriage, à litage parallèle, précoce (notamment les plis F_1) pointent le sommet vers le sud (entre le sud-sud-ouest et le sud-sud-est). Cette déformation est surtout courante au sein du groupe de Horton (Formation d'Albert), mais elle est aussi présente dans les roches du groupe de Sussex, bien que sous une forme d'expression plus hétérogène, notamment une paire de schistosités très précoces.

La déformation apparentée à des failles tardives se superpose à des particularités antérieures apparentées à des plis et à un charriage. Une partie de cette même déformation correspond à un ensemble de plis (F_2) se superposant à des zones de cisaillement à litage parallèle et orientées en oblique avec les manifestations de plissement-charriage. Il est significatif qu'on puisse démontrer que les plis F_1 et F_2 sont antérieurs à la discordance à la base de la Formation de Hillsborough (groupe de Windsor : Tournaisien le plus tardif au Viséen précoce). Cette déformation est liée à une compression nord-nord-ouest/sud-sud-est comportant une composante dextre de transpression.

INTRODUCTION AND GEOLOGICAL BACKGROUND

During the summer of 2004, a study of Lower Carboniferous (Tournaisian) rocks in southeastern New Brunswick (Fig. 1) was undertaken for the New Brunswick Department of Natural Resources. The general purpose was to document deformation in the sedimentary units and to show its relationship to the east- and east-northeast-trending faults that affect Carboniferous and older rocks in the area. The work did not entail regional remapping but instead involved identifying critical sections and transects for a more detailed structural analysis. Given the recent renewal of oil and gas exploration in southeastern New Brunswick, data on the timing and relationship of rock deposition, deformation, and subsequent fault movement have assumed a new importance.

Outcrops of Lower Carboniferous rocks and faults are sparse in the study area, and large, continuous sections of rock exposure are restricted to sites along a few creeks and tidal riverbanks. Good, semicontinuous outcrop does occur, however, in several transects from Rosevale in the west to Saint-Joseph in the east (Fig. 2). This has provided the opportunity to examine critical sections through most of the Lower Carboniferous

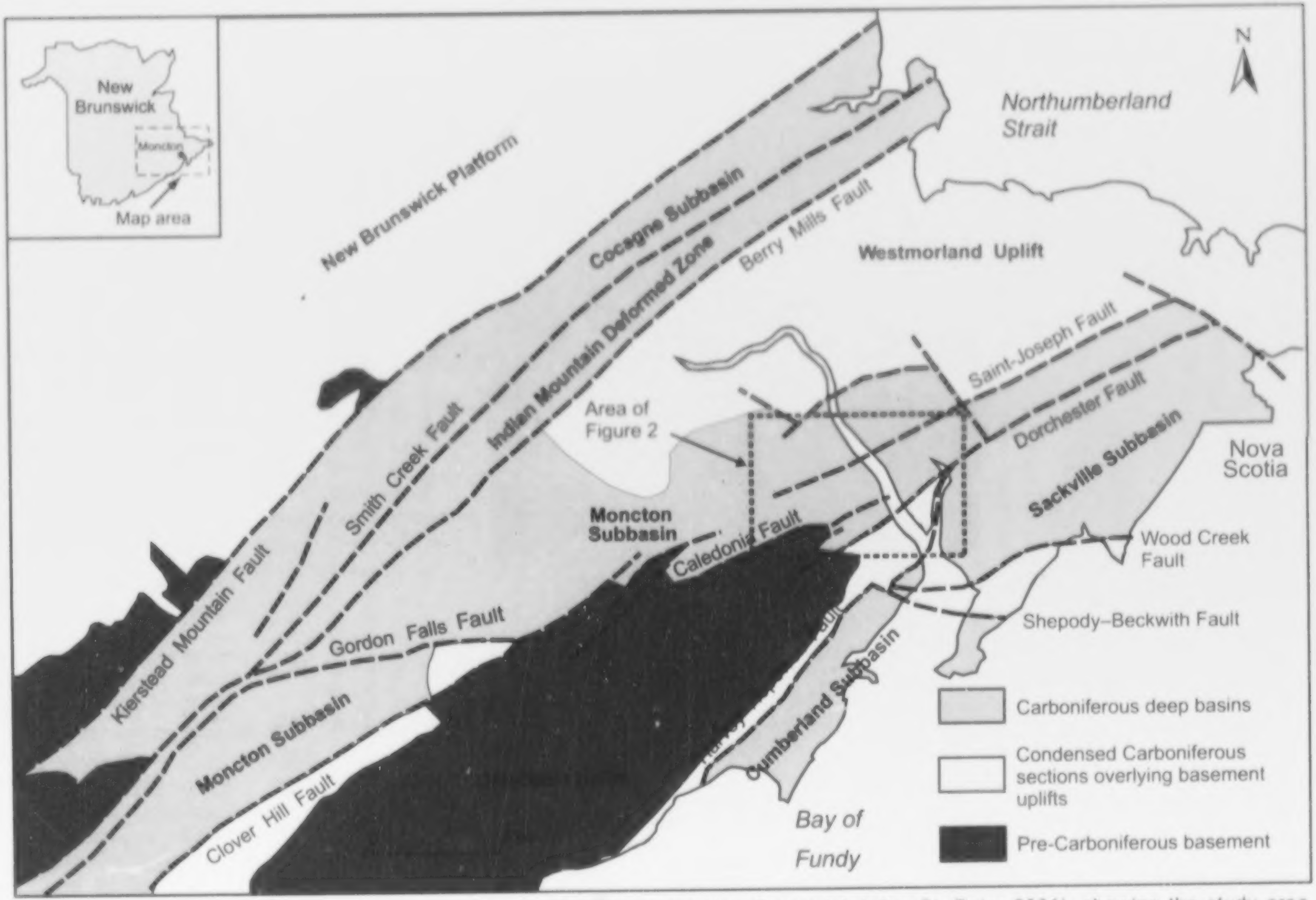
New Brunswick
Moncton
Map area
N
Northumberland Strait
New Brunswick Platform
Cocagne Subbasin
Berry Mills Fault
Westmorland Uplift
Indian Mountain Deformed Zone
Smith Creek Fault
Saint-Joseph Fault
Area of Figure 2
Dorchester Fault
Nova Scotia
Sackville Subbasin
Moncton Subbasin
Caledonia Fault
Wood Creek Fault
Kierstead Mountain Fault
Gordon Falls Fault
Shepody–Beckwith Fault
Moncton Subbasin
Cumberland Subbasin
Clover Hill Fault
Bay of Fundy
Carboniferous deep basins
Condensed Carboniferous sections overlying basement uplifts
Pre-Carboniferous basement

Figure 1. Lower Carboniferous subbasins and faults of southeastern New Brunswick (after St. Peter 2001), showing the study area detailed on Figure 2.

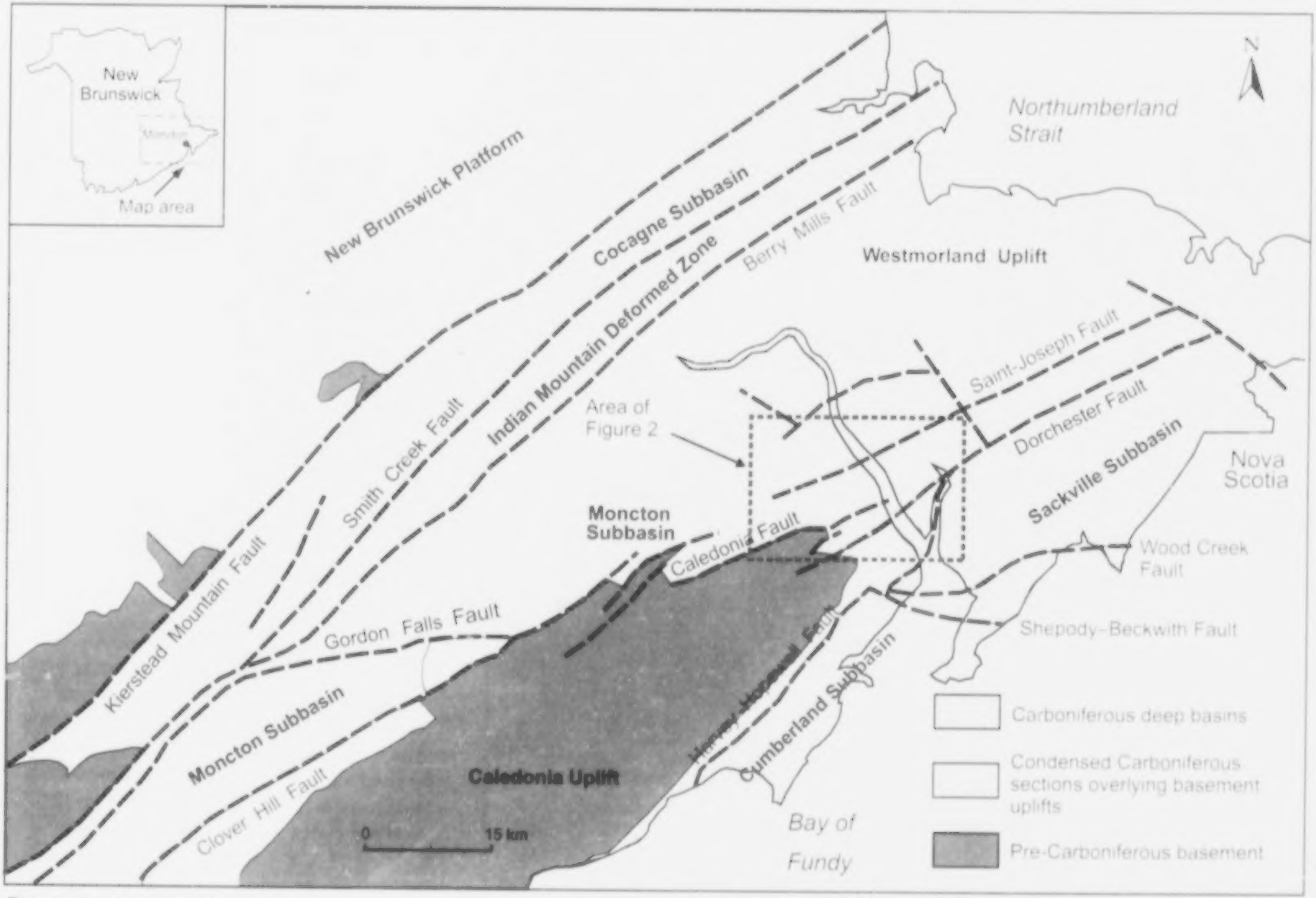

New Brunswick
Moncton
Map area
N
Northumberland Strait
New Brunswick Platform
Cocagne Subbasin
Indian Mountain Deformed Zone
Berry Mills Fault
Westmorland Uplift
Saint-Joseph Fault
Dorchester Fault
Sackville Subbasin
Nova Scotia
Area of Figure 2
Smith Creek Fault
Kierstead Mountain Fault
Moncton Subbasin
Caledonia Fault
Wood Creek Fault
Shepody–Beckwith Fault
Gordon Falls Fault
Moncton Subbasin
Harvey-Hopewell Fault
Cumberland Subbasin
Caledonia Uplift
Clover Hill Fault
0
15 km
Bay of Fundy
Carboniferous deep basins
Condensed Carboniferous sections overlying basement uplifts
Pre-Carboniferous basement

Figure 1. Lower Carboniferous subbasins and faults of southeastern New Brunswick (after St. Peter 2001), showing the study area detailed on Figure 2.

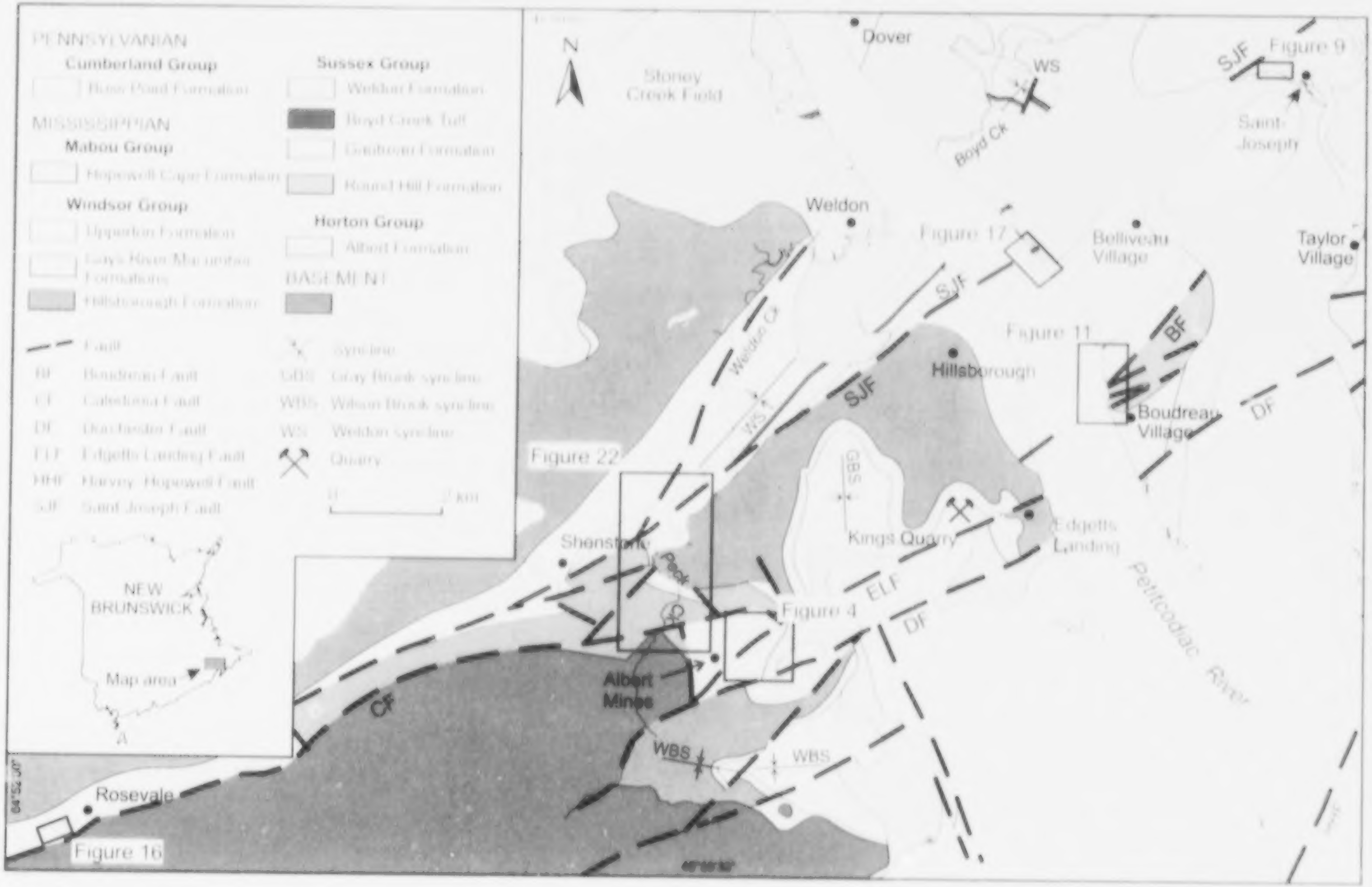
PENNSYLVANIAN
Cumberland Group
Boss Point Formation
MISSISSIPPIAN
Mabou Group
Hopewell Cape Formation
Windsor Group
Upperton Formation
Gays River-Macumber Formations
Hillsborough Formation
Sussex Group
Weldon Formation
Boyd Creek Tuff
Gautreau Formation
Round Hill Formation
Horton Group
Albert Formation
BASEMENT
Fault
BF Boudreau Fault
CF Caledonia Fault
DF Dorchester Fault
ELF Edgetts Landing Fault
HHF Harvey-Hopewell Fault
SJF Saint Joseph Fault
Syncline
GBS Gray Brook syncline
WBS Wilson Brook syncline
WS Weldon syncline
Quarry
0
2 km
NEW BRUNSWICK
Map area
N
Dover
Stoney Creek Field
WS
Boyd Ck
SJF
Figure 9
Saint-Joseph
Weldon
Figure 17
Belliveau Village
Taylor Village
SJF
Weldon Ck
WS
SJF
Hillsborough
Figure 11
BF
Boudreau Village
DF
Figure 22
GBS
Kings Quarry
Edgetts Landing
Shenstone
Peck
Figure 4
ELF
DF
Petitcodiac River
Albert Mines
CF
WBS
WBS
Rosevale
Figure 16

Figure 2. Geological map of the Rosevale–Hillsborough–Saint-Joseph area, southeastern New Brunswick (after St. Peter and Johnson 1997, 2004 revision; St. Peter 2004). Map area is outlined on Figure 1.

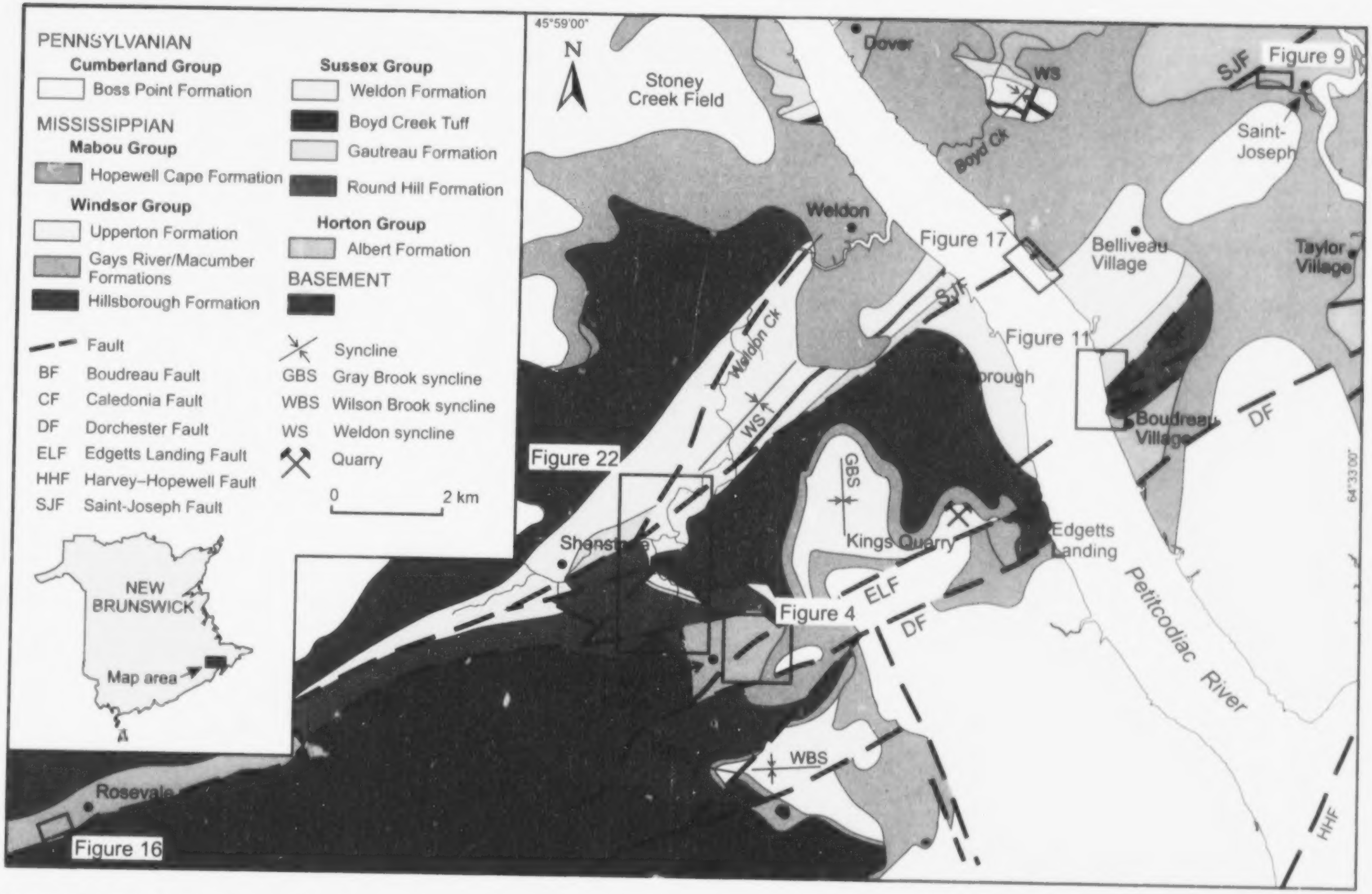
PENNSYLVANIAN
Cumberland Group
Boss Point Formation
MISSISSIPPIAN
Mabou Group
Hopewell Cape Formation
Windsor Group
Upperton Formation
Gays River/Macumber Formations
Hillsborough Formation
Sussex Group
Weldon Formation
Boyd Creek Tuff
Gautreau Formation
Round Hill Formation
Horton Group
Albert Formation
BASEMENT
Fault
BF Boudreau Fault
CF Caledonia Fault
DF Dorchester Fault
ELF Edgetts Landing Fault
HHF Harvey–Hopewell Fault
SJF Saint-Joseph Fault
Syncline
GBS Gray Brook syncline
WBS Wilson Brook syncline
WS Weldon syncline
Quarry
0
2 km
NEW BRUNSWICK
Map area
45°59'00"
N
Stoney Creek Field
Dover
WS
Boyd Ck
Weldon
Weldon Ck
WS
Figure 22
Shenstone
Figure 17
SJF
Figure 11
Hillsborough
GBS
Kings Quarry
Edgetts Landing
ELF
DF
Figure 4
WBS
Rosevale
Figure 16
Belliveau Village
Boudreau Village
DF
Petitcodiac River
SJF
Figure 9
Saint-Joseph
Taylor Village
64°33'00"
HHF

Figure 2. Geological map of the Rosevale–Hillsborough–Saint-Joseph area, southeastern New Brunswick (after St. Peter and Johnson 1997, 2004 revision; St. Peter 2004). Map area is outlined on Figure 1.

succession between (and including) Tournaisian oil shales of the Albert Formation and the uppermost Tournaisian–lowermost Visean conglomerate of the Hillsborough Formation. The transects also expose several major regional faults, namely, the Saint-Joseph Fault and several of its splays, the Caledonia Fault, the Edgetts Landing Fault, and the Dorchester Fault (Fig. 1, 2).

STRATIGRAPHY

Pre-Carboniferous rocks in the study area consist of Precambrian to lower Devonian, low- to high-grade metamorphic rocks, and related intrusions, hereafter termed "basement" (Fig. 1, 2). The Tournaisian and lower Visean rocks comprise the Horton, Sussex, and Windsor groups (Fig. 1–3), which lie in fault-bounded subbasins between blocks of the pre-Carboniferous rocks. Visean and younger Carboniferous units (Mabou and Cumberland groups) overlie rocks of the Horton, Sussex, and Windsor groups and in places overstep them to lie directly on the basement. In the study area (Fig. 1, 2), Visean and older rocks constitute the southeasternmost part of the Moncton Subbasin where it impinges on the Caledonia Uplift.

Horton Group

The oldest sedimentary rocks in the Moncton Subbasin belong to the Upper Devonian–Lower Carboniferous Horton Group, which is composed of the Memramcook Formation (not present in the study area) and the overlying Albert Formation (Fig. 3). In the absence of the Memramcook Formation, the Albert Formation locally lies directly on basement. Albert rocks comprise a succession of lacustrine oil shale and dolomitic shale interlayered with sandstone, limestone, and conglomerate (Norman 1941; Gussow 1953; Greiner 1962; Carter and Pickerill 1985a, b; St. Peter 1992).

Sussex Group

The Sussex Group (formerly "Moncton Group") lies unconformably above the Albert Formation (St. Peter and Johnson 1997, 2004 revision; St. Peter 2002, 2004 revision). It comprises coarse- and fine-grained lithofacies of the Weldon Formation, as described by Wright (1922), Norman (1941), and Gussow (1953); and fine-grained, grey clastic rocks, sulphates, and rock salt of the Gautreau Formation, as described by Norman (1932), Gussow (1953), Greiner (1962), and St. Peter (1992).

McLeod (1980) formally divided the Weldon Formation of Gussow (1953) and earlier workers into a lower, coarse-grained unit, which he called the Round Hill Formation, and a gradationally overlying unit, for which he retained the name Weldon Formation. McLeod's (1980) definitions of the Weldon and Round Hill formations are used here. The Round Hill Formation consists of grey-green and red-brown polymictic conglomerate and/or sedimentary breccia, lithic sandstone, and minor red and lesser grey mudrock. Northeast of its type area, the Round Hill Formation laterally gives way to the Gautreau Formation.

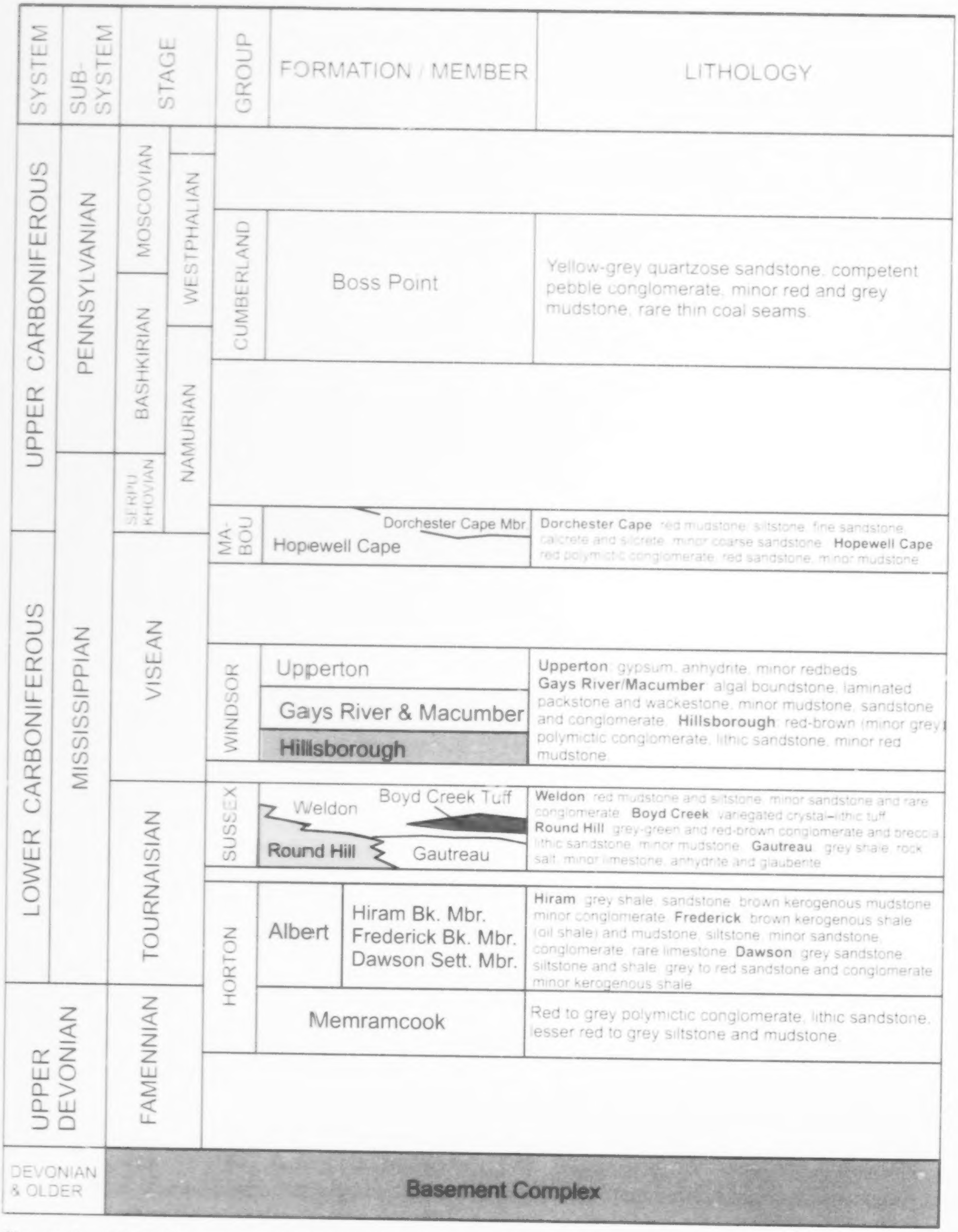

SYSTEM	SUB-SYSTEM	STAGE		GROUP	FORMATION / MEMBER	LITHOLOGY
UPPER CARBONIFEROUS	PENNSYLVANIAN	MOSCOVIAN	WESTPHALIAN			
		BASHKIRIAN		CUMBERLAND	Boss Point	Yellow-grey quartzose sandstone, competent pebble conglomerate, minor red and grey mudstone, rare thin coal seams.
			NAMURIAN			
	MISSISSIPPIAN	SERPUKHOVIAN		MABOU	Dorchester Cape Mbr. Hopewell Cape	**Dorchester Cape**: red mudstone/ siltstone, fine sandstone, calcrete and silcrete, minor coarse sandstone. **Hopewell Cape**: red polymictic conglomerate, red sandstone, minor mudstone
LOWER CARBONIFEROUS		VISEAN				
				WINDSOR	Upperton Gays River & Macumber **Hillsborough**	**Upperton**: gypsum, anhydrite, minor redbeds. **Gays River/Macumber**: algal boundstone, laminated packstone and wackestone, minor mudstone, sandstone and conglomerate. **Hillsborough**: red-brown (minor grey) polymictic conglomerate, lithic sandstone, minor red mudstone.
		TOURNAISIAN		SUSSEX	Weldon Boyd Creek Tuff **Round Hill** Gautreau	**Weldon**: red mudstone and siltstone, minor sandstone and rare conglomerate. **Boyd Creek**: variegated crystal–lithic tuff. **Round Hill**: grey-green and red-brown conglomerate and breccia, lithic sandstone, minor mudstone. **Gautreau**: grey shale, rock salt, minor limestone, anhydrite and glauberite.
				HORTON	Albert: Hiram Bk. Mbr. Frederick Bk. Mbr. Dawson Sett. Mbr.	**Hiram**: grey shale, sandstone, brown kerogenous mudstone, minor conglomerate. **Frederick**: brown kerogenous shale (oil shale) and mudstone, siltstone, minor sandstone, conglomerate, rare limestone. **Dawson**: grey sandstone, siltstone and shale, grey to red sandstone and conglomerate, minor kerogenous shale.
UPPER DEVONIAN		FAMENNIAN			Memramcook	Red to grey polymictic conglomerate, lithic sandstone, lesser red to grey siltstone and mudstone.
DEVONIAN & OLDER	**Basement Complex**					

Figure 3. Table of formations for the southeastern part of the Moncton Subbasin. Colours used here are cross-referenced to the legend on Figure 2.

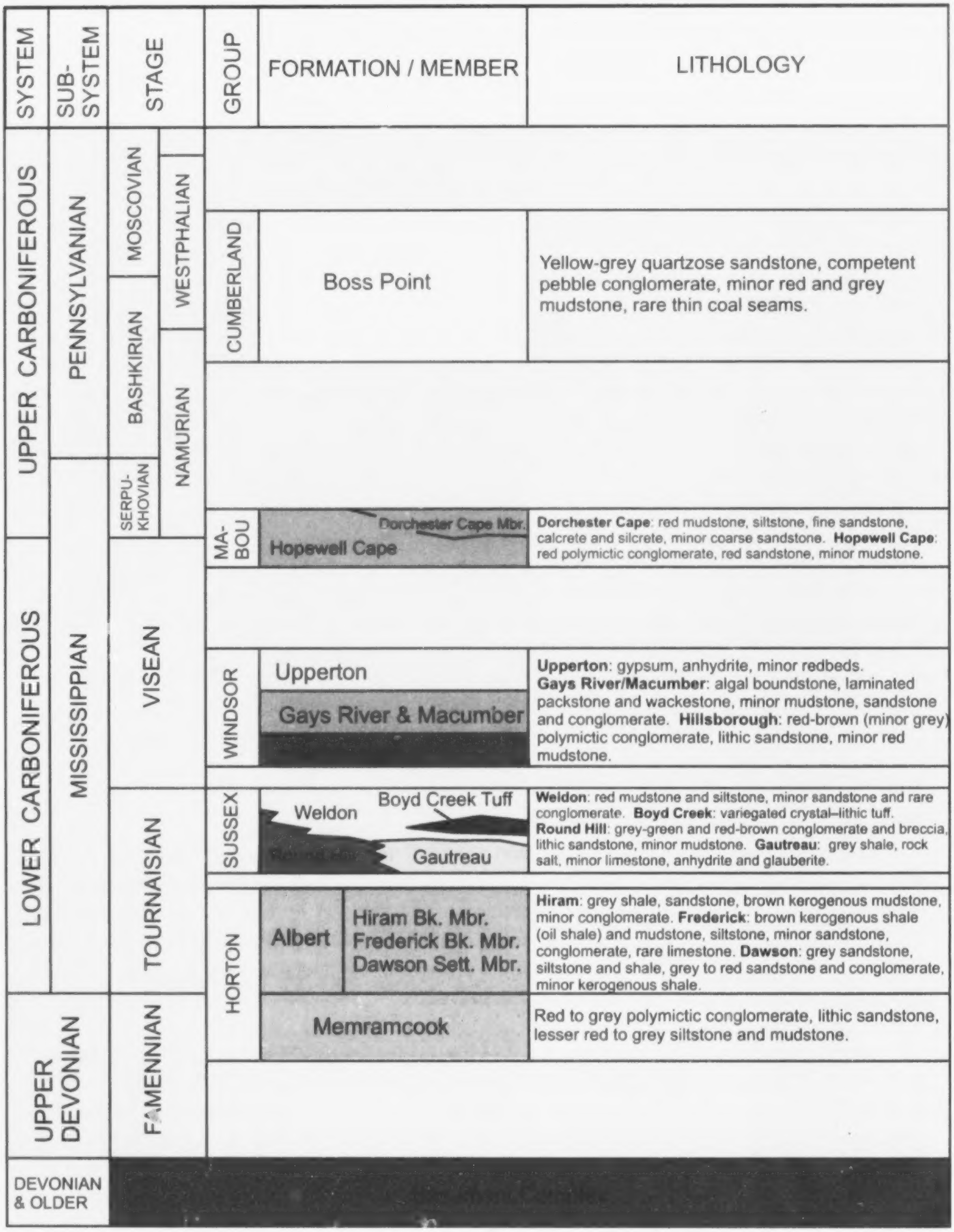

SYSTEM	SUB-SYSTEM	STAGE	STAGE	GROUP	FORMATION / MEMBER	LITHOLOGY
UPPER CARBONIFEROUS	PENNSYLVANIAN	MOSCOVIAN	WESTPHALIAN			
		BASHKIRIAN		CUMBERLAND	Boss Point	Yellow-grey quartzose sandstone, competent pebble conglomerate, minor red and grey mudstone, rare thin coal seams.
			NAMURIAN			
	MISSISSIPPIAN	SERPU-KHOVIAN		MA-BOU	Dorchester Cape Mbr. Hopewell Cape	**Dorchester Cape**: red mudstone, siltstone, fine sandstone, calcrete and silcrete, minor coarse sandstone. **Hopewell Cape**: red polymictic conglomerate, red sandstone, minor mudstone.
LOWER CARBONIFEROUS		VISEAN				
				WINDSOR	Upperton Gays River & Macumber [illegible]	**Upperton**: gypsum, anhydrite, minor redbeds. **Gays River/Macumber**: algal boundstone, laminated packstone and wackestone, minor mudstone, sandstone and conglomerate. **Hillsborough**: red-brown (minor grey) polymictic conglomerate, lithic sandstone, minor red mudstone.
		TOURNAISIAN		SUSSEX	Weldon Boyd Creek Tuff [illegible] Gautreau	**Weldon**: red mudstone and siltstone, minor sandstone and rare conglomerate. **Boyd Creek**: variegated crystal–lithic tuff. **Round Hill**: grey-green and red-brown conglomerate and breccia, lithic sandstone, minor mudstone. **Gautreau**: grey shale, rock salt, minor limestone, anhydrite and glauberite.
				HORTON	Albert: Hiram Bk. Mbr. Frederick Bk. Mbr. Dawson Sett. Mbr.	**Hiram**: grey shale, sandstone, brown kerogenous mudstone, minor conglomerate. **Frederick**: brown kerogenous shale (oil shale) and mudstone, siltstone, minor sandstone, conglomerate, rare limestone. **Dawson**: grey sandstone, siltstone and shale, grey to red sandstone and conglomerate, minor kerogenous shale.
UPPER DEVONIAN		FAMENNIAN			Memramcook	Red to grey polymictic conglomerate, lithic sandstone, lesser red to grey siltstone and mudstone.
DEVONIAN & OLDER					[illegible]	

Figure 3. Table of formations for the southeastern part of the Moncton Subbasin. Colours used here are cross-referenced to the legend on Figure 2.

The Weldon Formation conformably overlies the Gautreau and Round Hill formations; it comprises massive red mudrock, minor beds of sandstone, and rare polymictic conglomerate.

The Gautreau Formation consists of grey shale, muddy limestone, rock salt, minor anhydrite, and glauberite; it occurs mainly in the subsurface adjacent to the Petitcodiac River and north of the Saint-Joseph Fault (Fig. 2). Earlier publications (Norman 1941; Gussow 1953; Greiner 1962; McLeod 1980; St. Peter 1992) assigned the Gautreau Formation to the upper part of the Albert Formation on the basis of borehole data: all boreholes intersecting the formational boundary showed grey shale and evaporites of the Gautreau Formation overlying grey and brown kerogenous shale and sandstone of the Albert Formation. Yet Gautreau shale, unlike Albert shale, is never kerogenous. As well, two-dimensional seismic reflection profiles along the west side of the Petitcodiac River show a subtle angular discordance between the Albert Formation and overlying Gautreau Formation (St. Peter, unpublished data). Consequently, the Gautreau Formation is interpreted as being analogous to the Round Hill Formation, in that it discordantly overlies the Albert Formation and is gradationally succeeded by redbeds of the Weldon Formation.

The Sussex Group in the study area contains a thin unit (less than 30 m) of felsic tuff within the Weldon Formation. The tuff is exposed along Steeves Creek north of Hillsborough and along tributaries of Boyd Creek on the east side of the Petitcodiac River. Shroder (1963) selected the Boyd Creek occurrence as the type section, and St. Peter (1992) designated the unit as the Boyd Creek Tuff. This crystal–lithic–vitric tuff ranges from purple to grey to cream. It contains locally abundant, accidental volcanic clasts, rare quartz and feldspar phenocrysts, and rare glass shards.

A 7 m thick felsite body can be seen in the conglomerate of the Round Hill Formation on Peck Creek (McLeod 1980; St. Peter and Johnson 1997, 2004 revision). The felsite occurs in part as a highly deformed “dyke” and in part as irregular masses up to 1.5 m long and 40 cm thick. It may be genetically related to the Boyd Creek Tuff; if so, a time correlation could be inferred between the proximal Round Hill Formation and distal Weldon Formation.

Windsor Group

An angular unconformity separates the Sussex Group from the overlying Visean Windsor Group (Fig. 3). The Sussex Group consists (from oldest to youngest unit) of the Hillsborough, Gays River/Macumber, and Upperton formations (Fig. 3).

The Hillsborough Formation comprises a succession of red-brown conglomerate and coarse sandstone, and minor red mudrock (Wright 1922; Norman 1941; Gussow 1953; McLeod 1980). Regionally, the Hillsborough Formation is conformably succeeded by marine limestone of the Gays River Formation or its lateral equivalent, the Macumber

Formation (Wright 1922; Gussow 1953; McCutcheon 1981; St. Peter 1992). In the south limb of the Wilson Brook syncline (Fig. 2), limestone comprising algal boundstone, minor wackestone, and packstone of the Gays River Formation rests on crystalline basement (McCutcheon 1981). Elsewhere in the study area, the Macumber Formation is represented by grey to black laminated wackestone and packstone, and minor beds of calcareous sandstone and conglomerate. The Gays River and Macumber formations are succeeded by the Upperton Formation, which consists primarily of gypsum in surface exposures and anhydrite in the subsurface.

Mabou and Cumberland Groups

The Hopewell Cape Formation of the Mabou Group (St. Peter and Johnson 1997, 2004 revision) unconformably overlies the Windsor Group and older rocks (Fig. 3). The formation is a few tens of metres thick and is late Visean–Namurian (Serpukovian). It consists predominantly of red polymictic conglomerate and lithic sandstone, and minor mudrock (St. Peter and Johnson 1997, 2004 revision).

The Cumberland Group unconformably oversteps the Mabou Group and older Carboniferous formations and is the youngest sequence in the study area. It is represented by the late Namurian–nearly Westphalian (Bashkirian) Boss Point Formation, a widespread unit of distally derived, fluvial, plant-bearing, quartz-pebble conglomerate; grey crossbedded sandstone; rippled grey and red sandstone and siltstone; grey and red mudrock; and rare, thin coal seams (Browne 1991; St. Peter and Johnson 1997, 2004 revision).

DEFORMATION IN THE HORTON AND SUSSEX GROUPS

The following descriptions identify structures by letter and subscript: "F" for fold generation, "S" for foliation, and "L" for lineations, as recommended by standard texts such as Hobbs et al. (1976). Number subscripts are used where correlations can be made from one area to another. Thus, F_1 and F_2 represent folds with a clear, superimposed geometry, and S_1 and S_2 designate foliations related to the respective fold generations. S_0 is used here to represent bedding. Letter subscripts S_a and S_b indicate fold generations or foliations that are locally significant: that is, ones for which a local crosscutting sequence has been established, but for which no correlation can be shown beyond that location. Lineations commonly have a subscript and superscript. L^0_1, for instance, indicates an intersection lineation created by S_0 (bedding) and S_1.

Deformation in the Horton Group

Four traverses were used to produce a detailed structural analysis of rock deformation in the Horton Group. Three of the traverses were chosen because their continuous exposure enabled geometry to be constrained over several scales and because their sections have been extensively described in pre-existing literature. These traverses are located as follows.

1. The Frederick Brook–Albert Mines test pit area (Fig. 4 on Fig. 2) is one of the best exposed locations for the Frederick Brook Formation.

2. The Le Blanc Creek section near Saint-Joseph (Fig. 9 on Fig. 2) contains several hundred metres of semicontinuous section.

3. The Boudreau Village coastal section (Fig. 11 on Fig. 2) is heavily faulted but meets the necessary criteria of scale and exposure continuity.

The fourth traverse occurs in the Rosevale–Shenstone area along Stuart Mountain Road (Fig. 16 on Fig. 2). Its sections have limited outcrop exposure and are less extensively described in the literature, but they are included here because of their continuity with Caledonia basement rocks. These Precambrian units are not exposed in the other traverses.

Frederick Brook–Albert Mines Area

The test pit area beside Frederick Brook at Albert Mines provides enough exposure to allow compilation of a bedding trend-surface lithological and structural map (Fig. 4). Frederick Brook is the type locality for the Frederick Brook Member of the Albert Formation (Greiner 1962; St. Peter 1988; Wilson 2002). The member comprises kerogenous paper shale, silty shale, and dolomitic shale. It lies in faulted contact with crystalline basement to the west, the Round Hill Formation to the north and northwest, and the Hillsborough Formation to the south (St. Peter and Johnson 1997, 2004 revision). To the southeast, the Albert Formation is unconformably overlain by the Mabou Group (Fig. 2).

Three phases of tectonic folding can be seen in the Frederick Brook area (Fig. 4, 5). The earliest, F_1 phase is represented by tight to isoclinal folds of indeterminate plunge and trend (Fig. 4). The folds have produced overturned bedding, and their axial planes are broadly parallel to bedding (Fig. 6a, b). Folds wavelengths are between 10 and 50 m long and have amplitudes of about 100 m. Two complete closures can be demonstrated, and two more are inferred. F_1 folds occur in the main test pit and adjacent areas of Frederick Brook (Fig. 4, 7a, b). There, they have rotated large, soft-sediment slumps that formed along the boundary between the predominantly paper shale and dolomitic silty shale. Distinguishing individual folds as either F_1 or pre-F_1 structures can be difficult. The best criterion is how single folds relate to a large-scale fold pattern. The cross-section through the Frederick Brook–Albert Mines area (Fig. 5) illustrates one of these integrated patterns that define the large-scale F_1 folds.

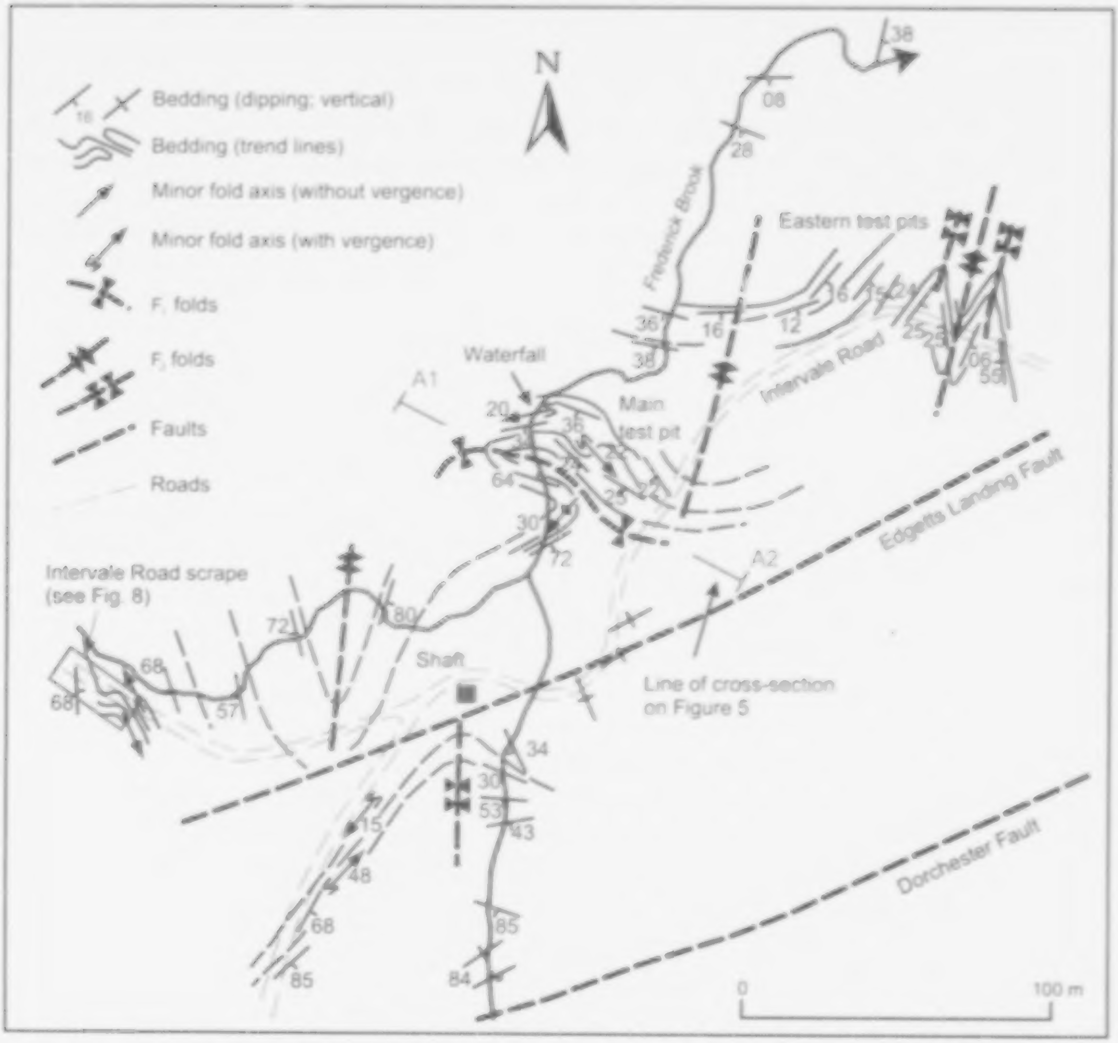
N
Bedding (dipping; vertical)
Bedding (trend lines)
Minor fold axis (without vergence)
Minor fold axis (with vergence)
F1 folds
F2 folds
Faults
Roads
Frederick Brook
Eastern test pits
Waterfall
Main test pit
Intervale Road
A1
A2
Edgetts Landing Fault
Intervale Road scrape (see Fig. 8)
Shaft
Line of cross-section on Figure 5
Dorchester Fault
0
100 m

Figure 4. Geological map of the Frederick Brook–Albert Mines area west of Albert Mines, showing the bedding trend-surface and other structural features. Map contains information from the present study, McLeod (1980), Wilson (2002), and unpublished data from D. Gemmell of Three-D Geoconsultants Ltd. Map area is outlined on Figure 2.

The second phase of folding (F_2) produced upright, open to tight anticlines and synclines (Fig. 4). The folds have nearly vertical axial planes, and their axes plunge southwest–south-southwest by 20° to 45° (Fig. 6b), refolding the F_1 structures. F_2 folds are best exposed in the western part of the eastern test pits, where they have produced a repetitive pattern resembling the letters "W" and "M." A similar pattern appears on a smaller scale in shale exposed in a roadbed and ditch along the Intervale Road west of the mine shaft (Fig. 8).

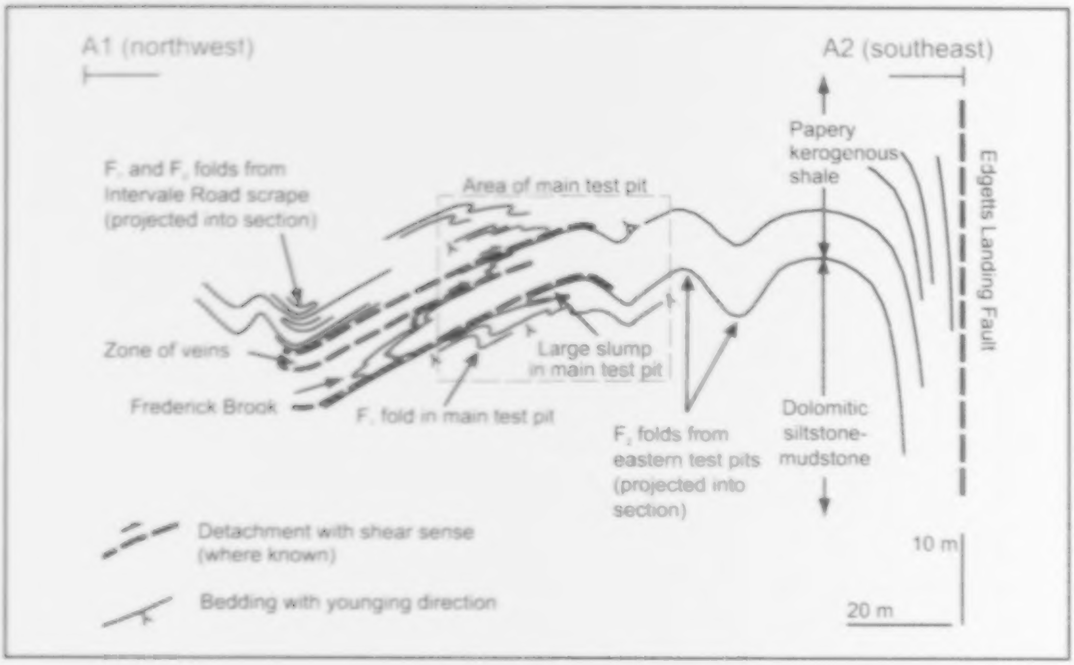
A1 (northwest)
A2 (southeast)
Papery kerogenous shale
F_1 and F_2 folds from Intervale Road scrape (projected into section)
Area of main test pit
Edgetts Landing Fault
Zone of veins
Large slump in main test pit
Frederick Brook
F_1 fold in main test pit
F_2 folds from eastern test pits (projected into section)
Dolomitic siltstone-mudstone
Detachment with shear sense (where known)
Bedding with younging direction
10 m
20 m

Figure 5. Composite structural section (A1–A2) of the Frederick Brook–Albert Mines area, looking southwest. Area of the section is marked on Figure 4. Plane of profile lies approximately perpendicular to the F_2 fold axes. Way-up (younging) indicators located between the detachments indicate a lack of reversal across the zone of veins.

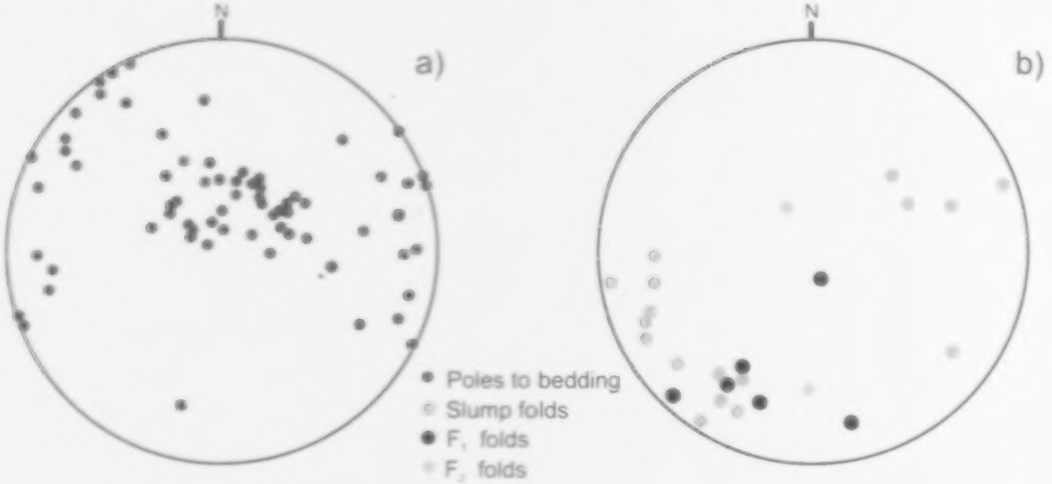

Figure 6. Equal area, lower hemisphere projections of a) poles to bedding and b) poles to fold axes from test pits and outcrops in the Frederick Brook–Albert Mines area.

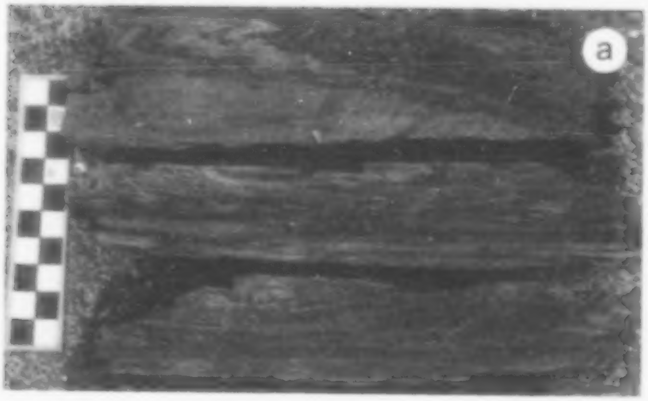

Figure 7. a) Deformation structures in the Fredericton Brook–Albert Mines area, showing soft-sediment folds in dolomitic siltstone from the eastern test pits (on Fig. 4). Scale bar is in centimetres.

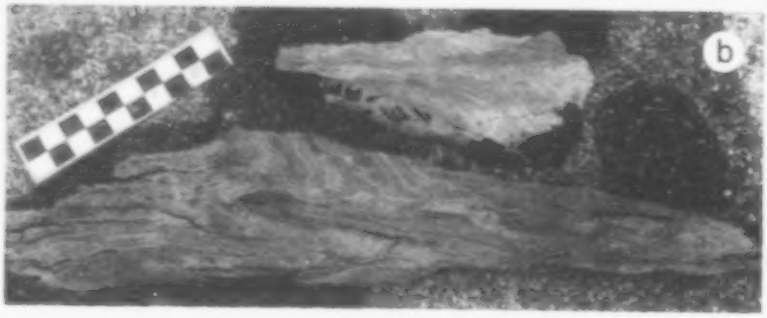

Figure 7. b) Deformation structures in the Fredericton Brook–Albert Mines area, showing F_1 folds in papery oil shale from the Frederick Brook waterfall (on Fig. 4). In the lower sample, crenulation cleavage with kerogen in the septae is developed in the fold closure, on the axial plane. Scale bar is in centimetres.

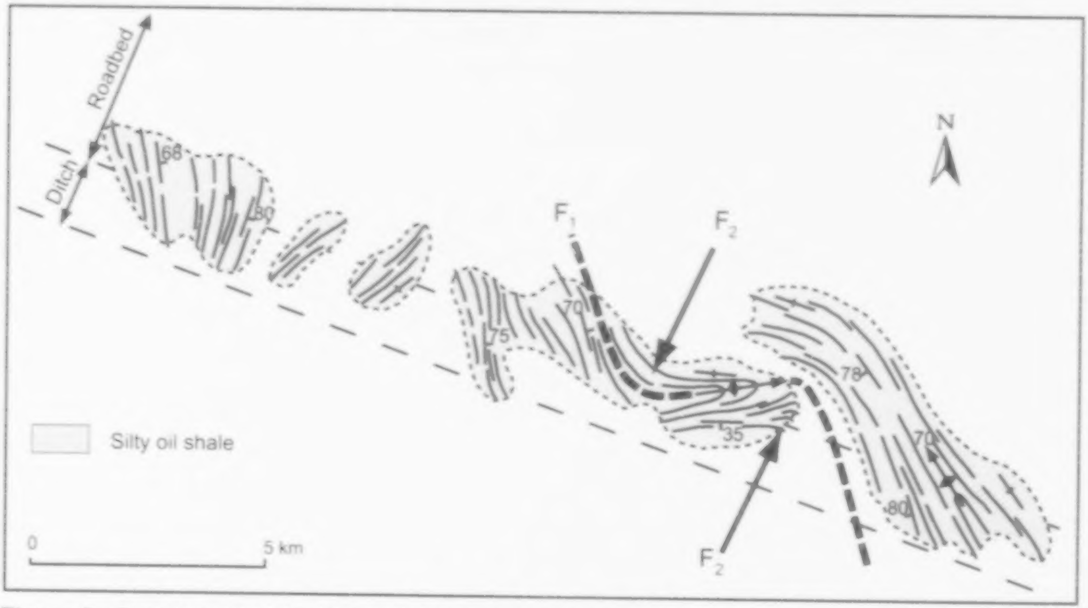

Figure 8. Sketch map of the Intervale Road scrape (on Fig. 4) in the Frederick Brook–Albert Mines area, showing structures (F_1 and F_2 overprint) exposed in silty oil shale of the Albert Formation.

The third phase of folding (F_3) has rotated bedding into a vertical attitude along the trace of the Edgetts Landing Fault (Fig. 4, 5), which hosts the albertite vein (Alcock 1948). F_3 folds are visible east of the mine shaft (Fig. 4) along the Intervale Road. Fold axes (probably F_1) are also rotated into steep orientations aligned in the same plane as the fault. Shale immediately northeast of the shaft contains box folds that developed in vertical or near-vertical bedding that strikes west-southwest. This geometry is consistent with the rotation of F_1 and F_2 folds, along with bedding, into the plane of the Edgetts Landing Fault. A similar rotation past the vertical can be seen along the southern tributary of Frederick Brook (Fig. 4) in outcrops near the Dorchester Fault (St. Peter and Johnson 1997, 2004 revision; Wilson 2002).

Sedimentary rocks near the test pits (Fig. 4), especially the dolomitic shale and siltstone, contain minor fold structures and deformed veins that cannot always be correlated to the three phases of folding just defined. Below the waterfall at Frederick Brook, for example, complex minor folds occur in the paper shale and dolomitic shale layers (Fig. 7b). An overall sense of vergence can be determined, although the symmetry of some minor folds is ambiguous. Over a distance of 50 m along the brook below the waterfall, these minor folds display a consistent vergence with an isoclinal F_1 fold, as indicated by bedding trend-surfaces mapped at the test pit and brook. Typically, these minor folds show considerable evidence of layer-slip in the more attenuated limbs (Fig. 5).

Apart from the above-named location, sites containing examples of both pre-F_2 and, evidently, pre-F_1 minor folds show no discernable pattern. The folds typically display a similar sense of shear (or vergence) in a given rock layer but demonstrate no consistent shape or symmetry across different layers that would link their vergence to large-scale structures (Fig. 5, 7a). Nor is there anything but the most local indication of way-up changes across fold axial planes, despite the fact that the folds have isoclinal to tight profiles. The existence of complementary fold vergences in different sets of these structures thus is largely absent because the lower inverted limb generally is sheared out.

These early structures may contain kerogenous material that defines cleavage septa and may have axial planar fabrics that crenulate bedding (Fig. 7b). However, they are still interpreted as soft-sediment slump folds such as those documented in paper shale and dolomitic shale from the Albert Formation between Norton and Sussex (Fig. 1) in the southwestern Moncton Subbasin (Wilson et al. 2004).

Arrays of deformed veins occur in the paper shale and, to a lesser extent, in the dolomitic shale of the main test pit (Fig. 5). Typically they consist of calcite- and calcite–siderite-bearing veins that lie parallel to bedding. Beefsteak textures (mineral fibres perpendicular to vein margins) are common. Complex growth patterns suggest either that deformation occurred from slip parallel to bedding, punctuated by several phases of fibre growth, or that fibre growth occurred during deformation (Durney and Ramsay 1973;

Ramsay and Huber 1983; cf. Williams and Urai 1989). Examples of these veins appear at several levels in the test pit area and along Frederick Brook.

One notable vein complex occurs along a limb of the F_1 fold that closes from the northwest end of the test pit near the Frederick Brook waterfall (Fig. 5). The veins are present in paper shale at a horizon located 2 m above the sharp transition from dolomitic shale. The veins appear to represent a larger scale example of the bedding-parallel detachments seen throughout the Frederick Brook area. The fact that beefsteak calcite veins occur at this detachment and also along a thrust in mudrock of the Weldon Formation at Peck Creek (described below) suggests that such vein complexes can be used to identify detachment zones (Fitches et al. 1986). It admittedly is simplistic to use only fibres to track deformation without knowing the primary geometry (Williams and Urai 1989). Nonetheless, the overall morphology of deformed veins can offer a reliable sense of shear.

Attempts to determine the asymmetry of F_1 fold structures and related detachments around Frederick Brook are complicated by the later F_2 and F_3 structures. Enough primary geometry remains, however, to estimate that the main F_1 structure and its detachment underwent an asymmetrical top-to-the-south movement, assuming a 30° or greater margin of error. The thrust structure thus seems to have shifted with its top into the south-to-southwest sector. A more precise determination cannot be made with the existing data set.

Le Blanc Creek Section

The Le Blanc Creek section is located in the eastern part of the study area (Fig. 9 on Fig. 2). At least three sets of folds occur in paper shale and dolomitic shale of the Albert Formation at Le Blanc Creek, especially just north of the headpond above the dam and along a small track to the east (Fig. 9).

The earliest folds are stratabound features on the scale of individual outcrops. The orientations of their axes and axial planes are inconsistent, even within a single outcrop (Fig. 10a). As such, they resemble the soft-sediment slump structures in the Frederick Brook area (previous section) and in the Albert Formation of similar facies near Sussex (Wilson et al. 2004).

These earliest structures are deformed by a second set of structures (F_1) that range in scale from folds of the same magnitude as the slump folds (Fig. 10b, c) to structures that display an asymmetric box profile characterized by a wavelength and amplitude of up to 5 m. The best example of the latter type is exposed along the track 50 m northeast of the Le Blanc Creek dam (Fig. 10d). Folds in that locale have strongly curvilinear hinge lines and highly varied amplitudes along the hinge. In some instances, the hinge lines are less than 5 m long, fading into the bedding at each end of the fold (Fig. 10b, c). Fold profiles are strongly asymmetrical, and axial planes curve into bedding planes of the dolomitic shale.

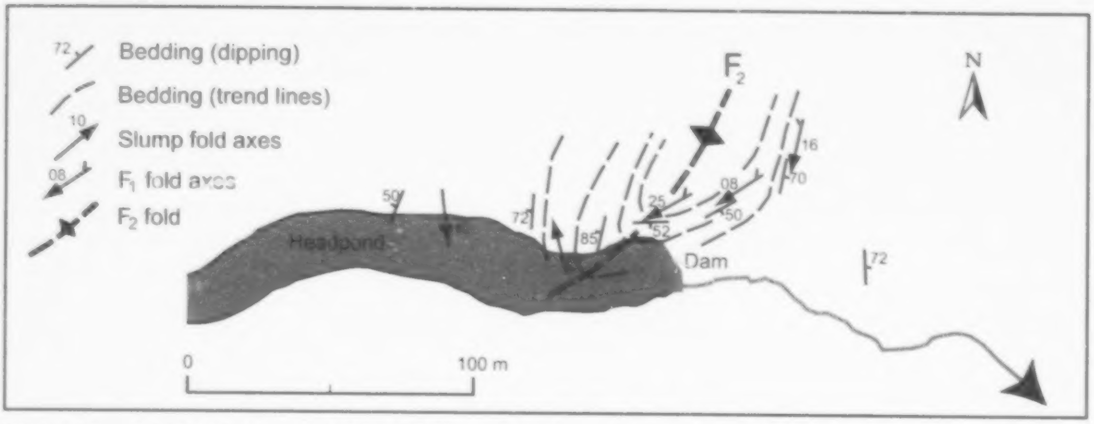
72
Bedding (dipping)
Bedding (trend lines)
10
Slump fold axes
08
F_1 fold axes
F_2 fold
F_2
N
50
72
85
25
52
08
50
16
70
Headpond
Dam
72
0
100 m

Figure 9. Geological map of the Le Blanc Creek area near Saint-Joseph, showing the bedding trend-surface. Map area is outlined on Figure 2.

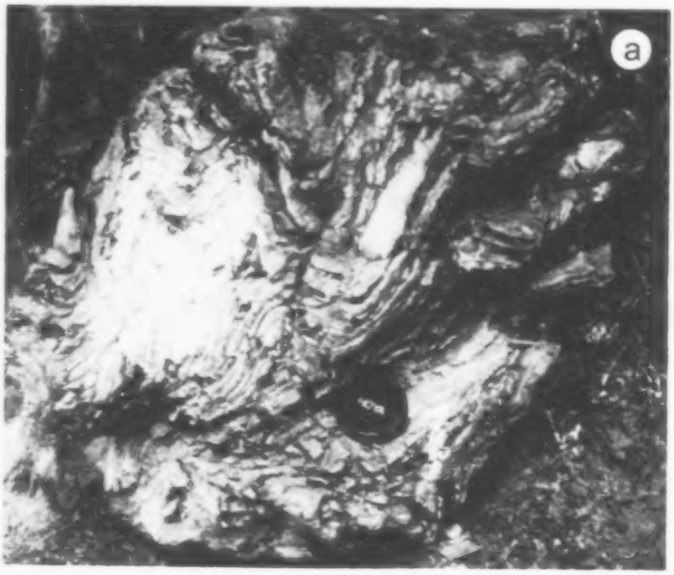

Figure 10. a) Bedrock structures from the Le Blanc Creek section near Saint-Joseph, showing a probable soft-sediment fold in papery oil shale. Lens cap is 55 mm.

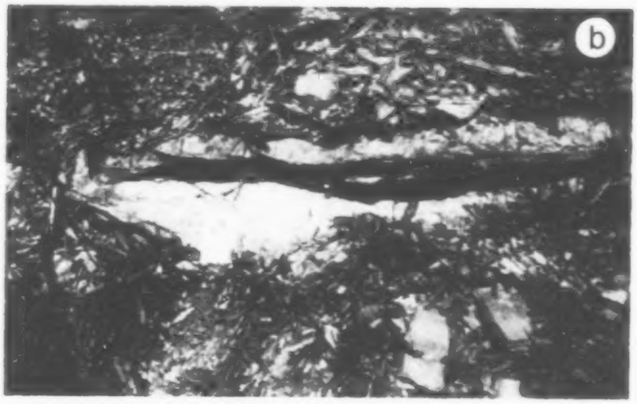

Figure 10. b) Bedrock structures from the Le Blanc Creek section near Saint-Joseph. Shows F_1 fold with a curvilinear hinge that dies out into the bedding plane at either end of this outcrop. Notebook is 18 cm long.

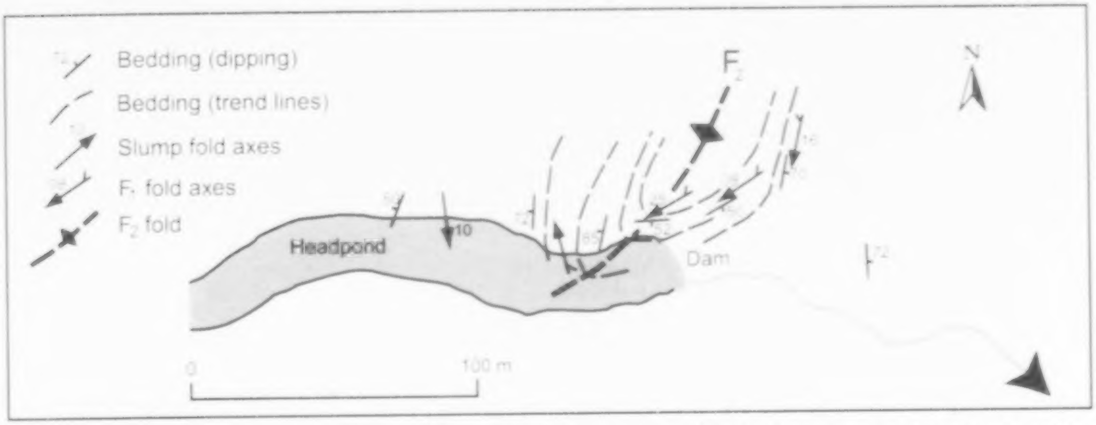
Bedding (dipping)
Bedding (trend lines)
Slump fold axes
F_1 fold axes
F_2 fold
F_2
N
Headpond
Dam
10
12
65
52
16
72
0
100 m

Figure 9. Geological map of the Le Blanc Creek area near Saint-Joseph, showing the bedding trend-surface. Map area is outlined on Figure 2.

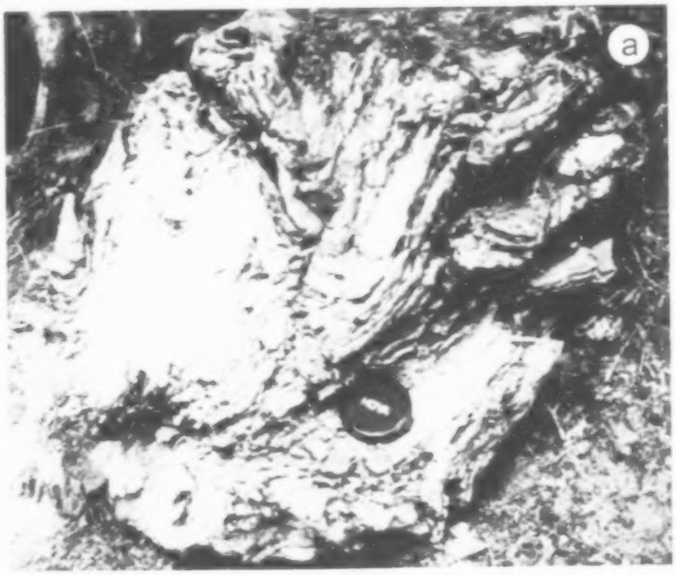

Figure 10. a) Bedrock structures from the Le Blanc Creek section near Saint-Joseph, showing a probable soft-sediment fold in papery oil shale. Lens cap is 55 mm.

Figure 10. b) Bedrock structures from the Le Blanc Creek section near Saint-Joseph. Shows F_1 fold with a curvilinear hinge that dies out into the bedding plane at either end of this outcrop. Notebook is 18 cm long.

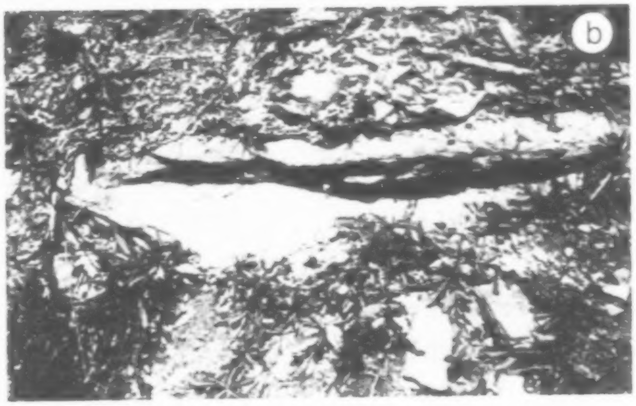

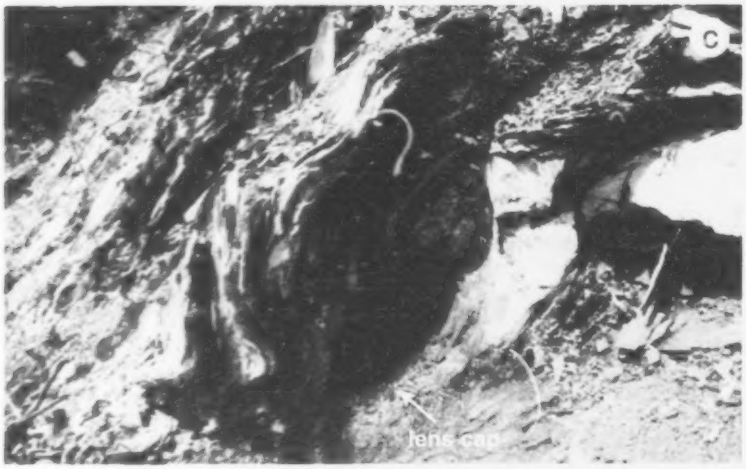

Figure 10. c) Bedrock structures from the Le Blanc Creek section near Saint-Joseph. Shows cross-section of an F_1 fold with a curvilinear hinge. Fold hinge does not continue here to any depth. Bedding plane folded in the foreground is planar 50 cm back, visible behind the fold. Lens cap is 55 mm.

Figure 10. d) Bedrock structures from the Le Blanc Creek section near Saint-Joseph. Shows a large-scale F_1 fold with a symmetrical box profile from a roadcut on the track 50 m northeast of the dam. Box closure is around the hammer. Shear sense is bedding parallel (near vertical here) with the right side down. Hammer is 55 cm long.

The F_2 folds at Le Blanc Creek are large, tight to open structures. They were mapped on the basis of variations in younging direction and strike declination (Fig. 9). Axes plunge 40° to 60° southwest. F_1 folds located on limbs of the F_2 folds show a scatter pattern consistent with rotation of a single set around the steeply plunging F_2 fold axes. When F_1 elements are rotated back to their original orientation, the asymmetry of the folds and other markers indicate a single sense of vergence related to bedding-parallel displacement. Kinematic indicators of this F_1-related, bedding-parallel deformation show a movement of top-to-the-south or -south-southwest.

Boudreau Village Section

The Boudreau Village section (Fig. 11 on Fig. 2) lies immediately north of Boudreau Village on the east shore of the Petitcodiac River, running south from Boudreau Creek for about 800 m (Fig. 11a, b). The exposure occurs along cliffs and tidal flats and is continuous for almost the entire section. Rocks are divided into five fault-defined panels (Fig. 11a, b), described here from north to south.

1. Panel 1 comprises mudrock, siltstone, and claystone, and interfingered fine- to coarse-grained sandstone. The rocks are predominantly red but include layers of minor greenish sandstone, siltstone, and claystone. The colour reflects the oxidation state of iron. The greenish rocks contain abundant pyrite, and the medium- to coarse-grained rocks are commonly saturated with bitumen. The mudrock features dessication cracks, salt pseudomorphs, rain pits, and syneresis cracks.

   McLeod (1980) included these rocks in the Albert Formation. Their affinities with rocks of the Sussex Group prompted their reassignment (Wilson 2002) to the Weldon Formation. In fact, they resemble the dessicated and evaporitic rocks of the Gautreau Formation more closely than the dominantly red mudrock of the Weldon Formation, and so are assigned here to the Gautreau Formation. The overall structure is an open, upright anticline plunging steeply southwest. Deformed mudcracks, some of which define box folds, occur at the south end of the panel and indicate bedding-parallel slip.

2. Panel 2 contains rocks assigned to the Albert Formation, namely grey to green shale interfingered with greyish to greenish-grey, medium- to coarse-grained sandstone. The shale is only rarely kerogenous, but some sandstone is hydrocarbon bearing. The rocks are more obviously deformed than those in the Gautreau Formation farther north. Bedding is contorted into a series of tight anticlines and synclines and plunges steeply southwest. Where outcrop is visible in three dimensions, as along the beach, the folds display evidence of curvilinear hinge lines. The interpretation of this geometry is supported by the distribution of axes to minor folds (Fig. 12a).

3. Rocks in Panel 3, assigned to the Round Hill Formation, are composed mainly of red, coarse-grained to gritty, feldspathic to arkosic sandstone that contains lenses of pebble conglomerate. Shale forms a minor part of the assemblage. Structures here, as in Panel 2, are dominated by tight folds with broken hinges. Fold axes generally plunge steeply southwest, shallowly southwest, or shallowly east-northeast.

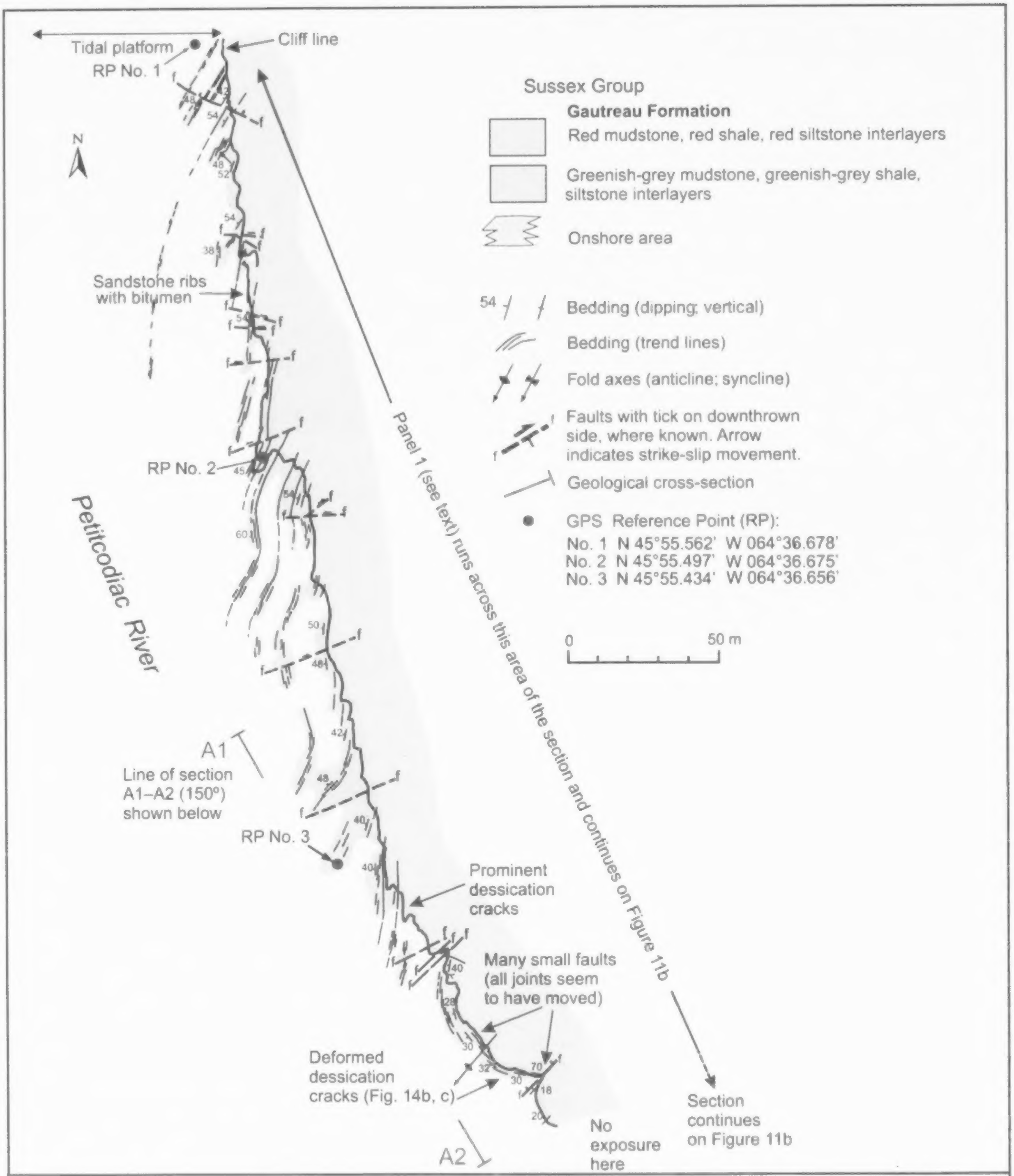
Tidal platform
Cliff line
RP No. 1
N
Sussex Group
Gautreau Formation
Red mudstone, red shale, red siltstone interlayers
Greenish-grey mudstone, greenish-grey shale, siltstone interlayers
Onshore area
54
Bedding (dipping; vertical)
Bedding (trend lines)
Fold axes (anticline; syncline)
Faults with tick on downthrown side, where known. Arrow indicates strike-slip movement.
f
Geological cross-section
GPS Reference Point (RP):
No. 1 N 45°55.562' W 064°36.678'
No. 2 N 45°55.497' W 064°36.675'
No. 3 N 45°55.434' W 064°36.656'
0
50 m
Sandstone ribs with bitumen
RP No. 2
Petitcodiac River
Panel 1 (see text) runs across this area of the section and continues on Figure 11b
A1
Line of section A1–A2 (150°) shown below
RP No. 3
Prominent dessication cracks
Many small faults (all joints seem to have moved)
Deformed dessication cracks (Fig. 14b, c)
No exposure here
Section continues on Figure 11b
A2
48
54
52
38
45
60
50
48
42
40
28
30
32
70
18
20

Figure 11. a) Geological map of the cliff and tidal platform in the Boudreau Village section. Map area (outlined on Fig. 2) covers the northern part of the section and continues on Figure 11b. Cross-section A1–A2 also continues on Figure 11b.

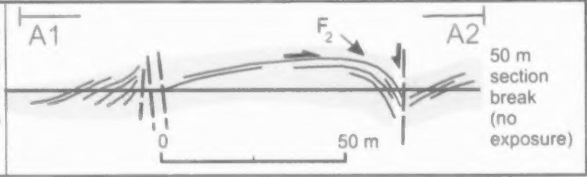
A1
F_2
A2
0
50 m
50 m section break (no exposure)

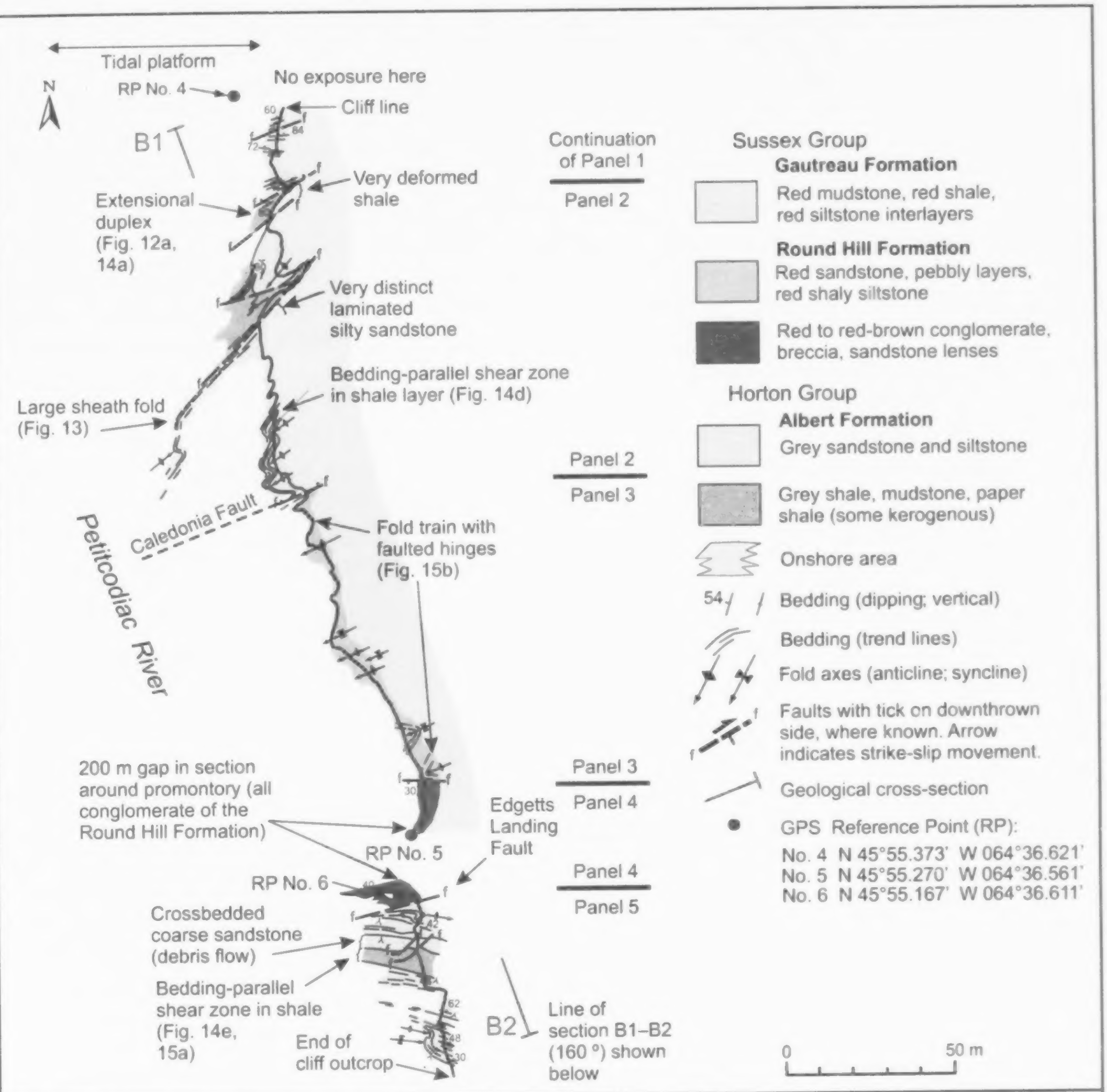
Tidal platform
N
RP No. 4
No exposure here
Cliff line
60
84
72
B1
Extensional duplex (Fig. 12a, 14a)
Very deformed shale
Very distinct laminated silty sandstone
Bedding-parallel shear zone in shale layer (Fig. 14d)
Large sheath fold (Fig. 13)
Caledonia Fault
Petitcodiac River
Fold train with faulted hinges (Fig. 15b)
200 m gap in section around promontory (all conglomerate of the Round Hill Formation)
30
RP No. 5
RP No. 6
40
Edgetts Landing Fault
Crossbedded coarse sandstone (debris flow)
Bedding-parallel shear zone in shale (Fig. 14e, 15a)
42
62
48
30
End of cliff outcrop
B2
Line of section B1–B2 (160 °) shown below
Continuation of Panel 1
Panel 2
Panel 2
Panel 3
Panel 3
Panel 4
Panel 4
Panel 5
Sussex Group
Gautreau Formation
Red mudstone, red shale, red siltstone interlayers
Round Hill Formation
Red sandstone, pebbly layers, red shaly siltstone
Red to red-brown conglomerate, breccia, sandstone lenses
Horton Group
Albert Formation
Grey sandstone and siltstone
Grey shale, mudstone, paper shale (some kerogenous)
Onshore area
54
Bedding (dipping; vertical)
Bedding (trend lines)
Fold axes (anticline; syncline)
Faults with tick on downthrown side, where known. Arrow indicates strike-slip movement.
Geological cross-section
GPS Reference Point (RP):
No. 4 N 45°55.373' W 064°36.621'
No. 5 N 45°55.270' W 064°36.561'
No. 6 N 45°55.167' W 064°36.611'
0
50 m

Figure 11. b) Geological map of the cliff and tidal platform in the Boudreau Village section. Map area (outlined on Fig. 2) shows the southern part of the section, continuing from Figure 11b. Cross-section B1–B2 on Figure 11b (below) continues from cross-section A1–A2 on Figure 11a. See text for explanation of panels.

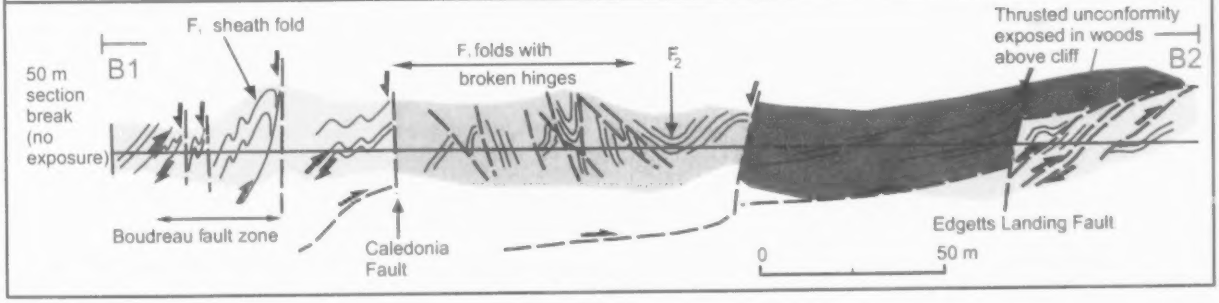
F1 sheath fold
B1
50 m section break (no exposure)
F1 folds with broken hinges
F2
Thrusted unconformity exposed in woods above cliff
B2
Boudreau fault zone
Caledonia Fault
Edgetts Landing Fault
0
50 m

4. Rocks in Panel 4 are also assigned to the Round Hill Formation. They occur near the southern end of the section, where they form a large promontory of red, matrix-supported conglomerate (and/or sedimentary breccia) and minor sandy interlayers. The matrix is clay-rich, feldspathic sandstone. Conglomerate clasts include abundant mafic volcanic debris, fine-grained metabasite, granite, felsite, and gneiss. Folds are not evident where bedding can be determined. However, a clast-orientation fabric is visible where the conglomerate contains abundant tabular clasts. The fabric lies parallel, and slightly oblique, to bedding. Slickensides also indicate some layer-parallel slip, but the clast-shape fabric appears to consist of clast imbrication enhanced by a tectonic fabric.

5. Panel 5, south of the promontory, comprises a succession of grey shale, grey to green or brown siltstone, and fine- to medium-grained sandstone. The rocks are assigned to the Albert Formation, although they lack kerogenous shale. Deformation is evident in large-scale box folds and in bedding-parallel deformation features such as box folds and extensional duplex structures that are confined to specific shale units.

The Boudreau Village section contains substantial evidence of bedding-parallel movement in the Albert Formation (Panels 2 and 5), such as where shale is interbedded with siltstone and sandstone 150 m north, and 100 m south, of the promontory (Fig. 11b). Two phases of folding are evident: F_1, related to bedding-parallel movement, and F_2 overprinting the earlier feature (Fig. 12a, b). Later, localized deformation is associated with faults.

North of the promontory (Panel 2), a large-scale F_1 fold with an acutely curvilinear hinge occurs in sandstone layers that transect both the cliff and beach (Fig. 11b, 13). In the cliff, the fold plunges 20° north-northeast. Farther west across the tidal flats, the plunge gradually shifts to southwest, steepens through the vertical, and then plunges east again at 70°. Shale on both sides of the sandstone unit contains sandstone ribs with minor folds. Axes of these folds display a similar attitudinal shift and more fully define the range of plunges (Fig. 12, 13). When considered together, the major and minor folds represent a large-scale sheath fold whose axial plane is bedding parallel, and whose antiformal closure is south-southeast (Fig. 13).

Several shaly units north and south of this large-scale F_1 fold contain extensional duplex structures (Fig. 14a) as well as minor folds that conform to geometry of the large-scale sheath fold. F_1 folds in the sheared shale units display box geometries consistent with bedding-parallel shortening (Fig. 14b–d). The folds and extensional features reflect the same kinematic asymmetry, indicating a bedding-parallel displacement along shale units with a top-to-the-south or -south-southeast movement. This segment of the section (Fig. 11b: cross-section B1–B2) is dominated by late faults and has been termed the

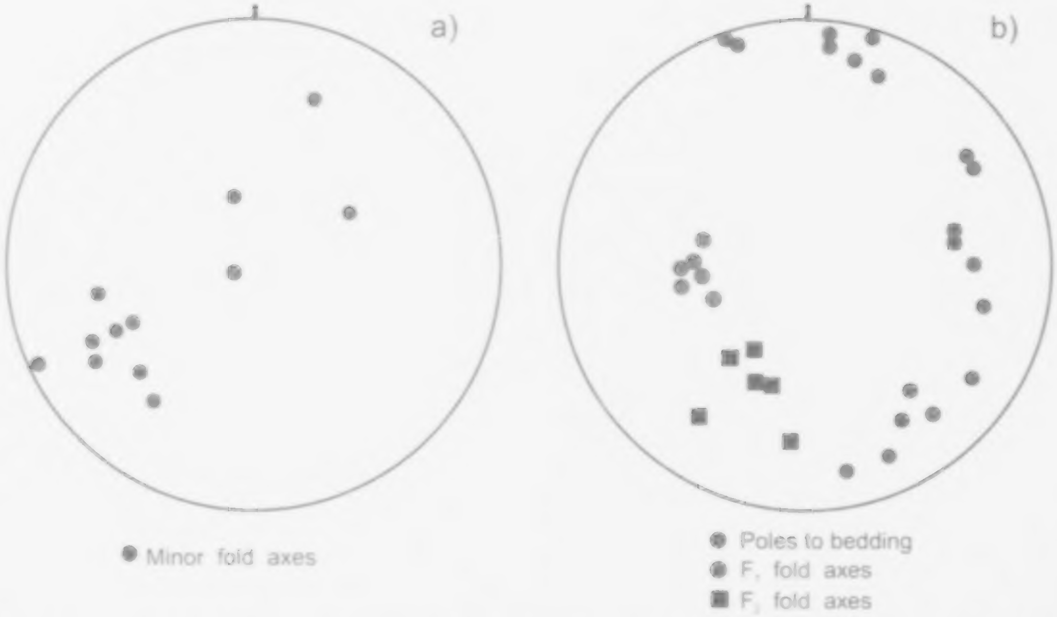

Figure 12. Equal area, lower hemisphere projections for bedding and fold axes in the Boudreau Village section. a) Poles to minor fold axes in the Boudreau fault zone (Fig. 11b: cross-section B1–B2), including the large sheath fold (Fig. 13, 14a). b) Poles to bedding and to F_1 and F_2 fold axes.

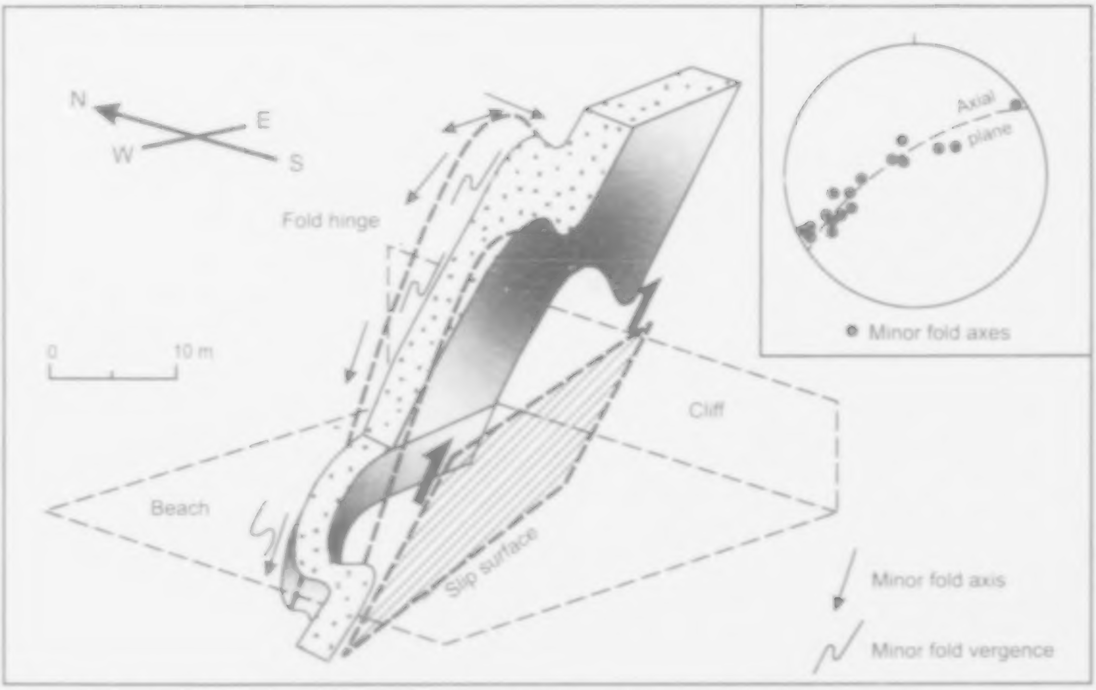
N
E
W
S
Fold hinge
0
10 m
Cliff
Beach
Slip surface
Axial plane
Minor fold axes
Minor fold axis
Minor fold vergence

Figure 13. Block diagram of the large sheath fold (marked on Fig. 11b) in the Albert Formation north of the promontory in the Boudreau Village section, looking northeast. Diagram shows the relationship of minor fold axes and shear sense. Inset shows minor fold axes associated with the sheath fold (compare with Fig. 12).

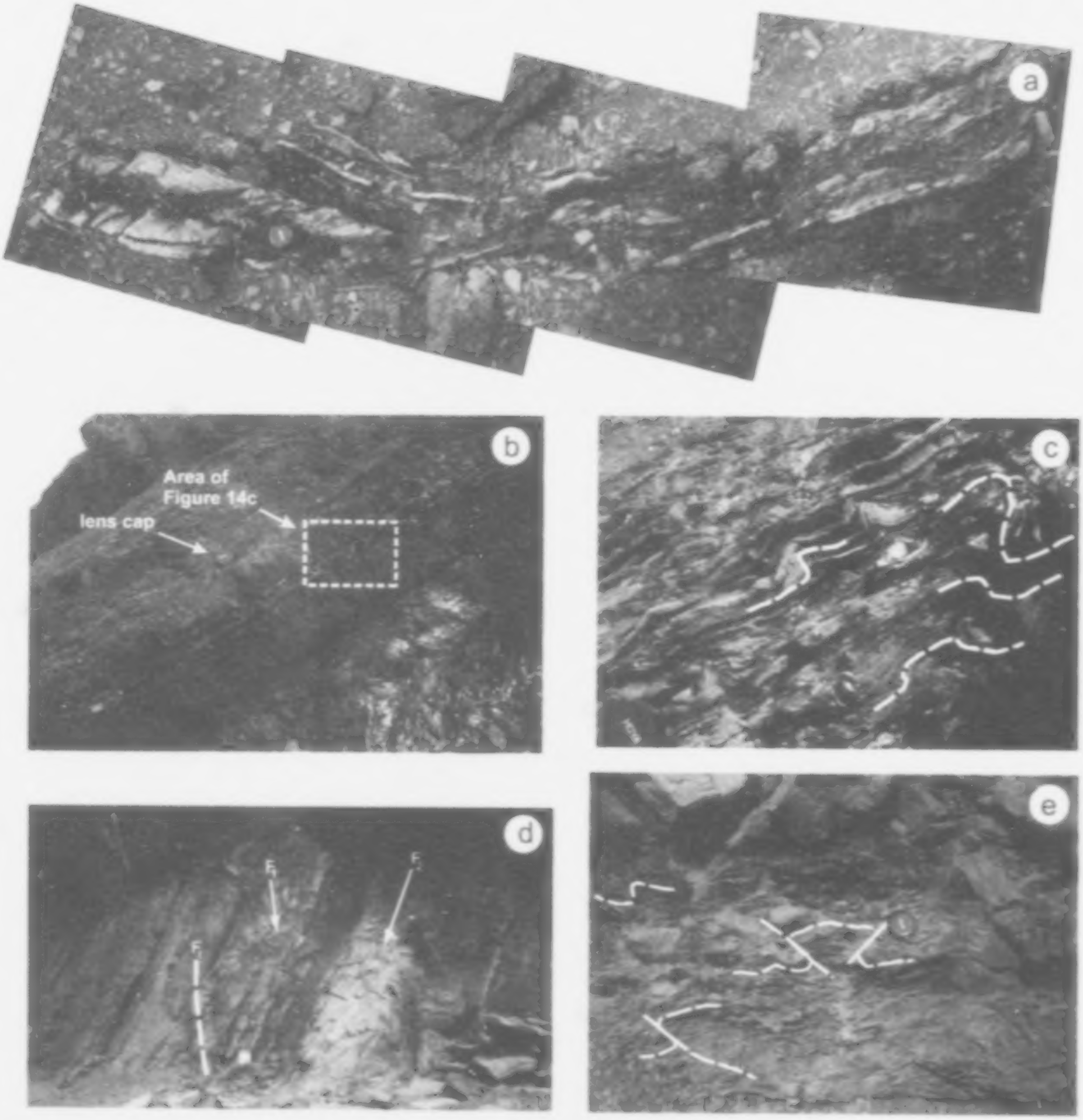

Figure 14. Bedrock structures in the Boudreau Village section (locations marked on Fig. 11a, b). a) Extensional duplex in sandstone ribs in sheared shale from the bedding-parallel shear zone within the Boudreau fault zone. Shear sense is top-to-right. Lens cap is 55 mm. b) Red mudrock of the Gautreau Formation showing preserved, deformed dessication cracks. Bedding-parallel shear sense is top-to-left. Lens cap is 55 mm. c) Detail from Figure 14b, showing profile of the box folds in deformed dessication cracks. Lens cap is 55 mm. d) Bedding-parallel shear zone in the folded shale between sandstone units of the Albert Formation immediately north of the faulted contact with the Round Hill Formation. Large F_1 anticline adjacent to the shear zone (shown by red arrows) plunges steeply toward the camera. Field assistant for scale. e) Profile of box folds in the bedding-parallel shear zone south of the promontory. Lens cap is 55 mm.

"Boudreau fault zone" by Wilson (2005). However, the late faulting clearly overprints the complex fold structures, and the sheath folds and related bedding-parallel features belong to a much earlier phase of deformation.

South of the promontory (Panel 5), similar shear zones appear in two shaly units (Fig. 11b, 14e). The attitudes of minor folds (F_1) and extensional duplexes are consistent with a movement of top-to-the-south or -south-southeast. Also present here are two unusual, rootless folds (Fig. 15a). They occur immediately south of the promontory on either side of a highly sheared 2 m thick shale unit. The first structure is a box-like antiform. Its axial plane appears to root into a sheared shale unit, as does a set of curvilinear fractures that radiate through the fold profile. The second structure occurs just south of the antiform. It is a topless synform, apparently truncated above by planar bedding along another thin but highly sheared shale unit (Fig. 15a). These two structures are interpreted to represent a hanging-wall antiform and a footwall synform related to detachment in the shear zone represented by the intervening 2 m thick shale. This is the only documented example in the study area of a bedding-parallel structure cutting upsection. Notably, the structure occurs toward the south, which is consistent with other kinematic indicators of early deformation associated with F_1 folds.

Tens of metres inland, rocks of the Round Hill Formation overlie this part of the Albert Formation. The contact between the Round Hill and Albert formations is not exposed but does not appear to be significantly offset. This is problematic, in that it is unclear how the shear zones in the underlying Albert Formation, just described, exit the sections updip. The preferred interpretation is that the contact here represents a roof thrust (Fig. 11b: cross-section B1–B2). The fold-and-thrust geometry extends north of the promontory to where broken-hinge F_1 folds in the Round Hill Formation (Fig. 15b) likely have thrusts above and below them that have since been faulted out. Only two F_1 fold closures are visible, but others can be deduced from changes in the younging direction. The structure here suggests the existence of a train of folds with broken-out hinges due to tightening (cf. Ramsay 1974). These thrust faults appear to continue into the bedding-parallel shear zones of Panel 5, although the geometry is heavily modified by later folding (F_2) and faulting, as seen in the Boudreau fault zone (Wilson 2005).

F_2 folds also occur in the Albert Formation in cliffs north of the Caledonia Fault (Fig. 11b). The folds affect the sheared shale layers and rotate structural elements that are related to F_1 folds. The second-generation, refolded F_1 structures (Fig. 14d) plunge steeply southwest (Fig. 11b, 12b) and are rare. They appear related to a set of analogous folds located just south of the Caledonia Fault in red sandstone and grainstone of the Round Hill Formation. The overprinting relationship at this site, however, cannot be clearly demonstrated (Fig. 15b).

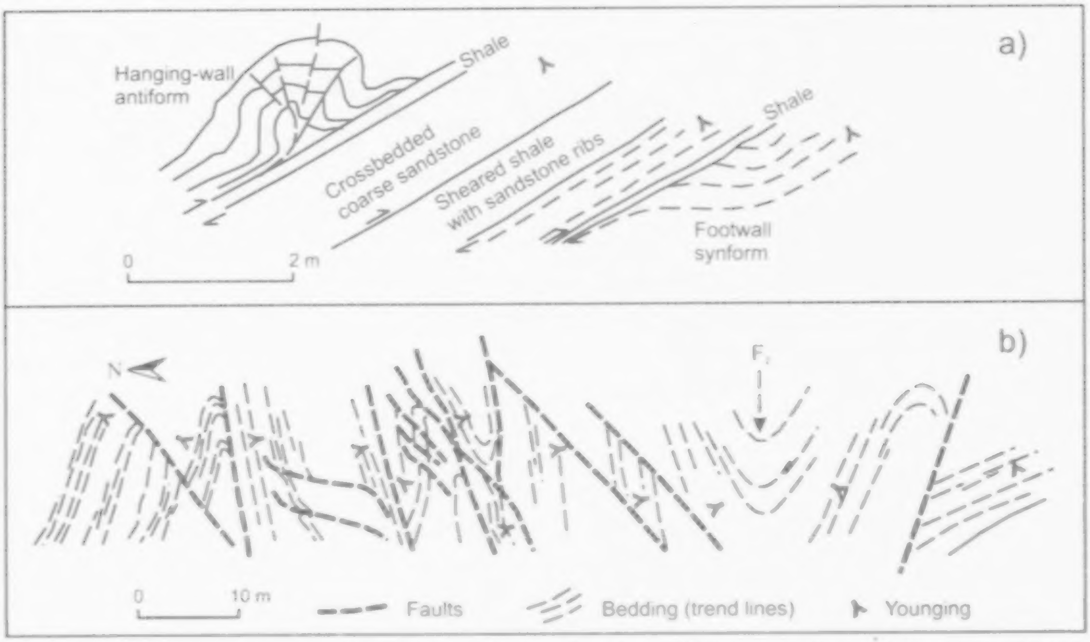

Figure 15. Cross-sections of structures in the Boudreau Village section. a) Cross-section in sandstone and shale of the Albert Formation south of the promontory (Fig. 11b). Shows interpretation of the bedding-parallel shear zones and the rootless and truncated folds. b) Cross-section in sandstone of the Round Hill Formation north of the promontory. Unlabelled folds are F_1.

Rosevale–Shenstone Area

Several creek and roadbed sections between Rosevale and Shenstone skim the northern edge of the pre-Carboniferous Caledonia basement block and its contact with the Albert Formation (Fig. 2). The section described here occurs along on Stuart Mountain Road near Rosevale (Fig. 16 on Fig. 2). It comprises highly contorted kerogenous shale and siltstone to fine-grained sandstone in faulted contact with banded gneiss of the Caledonia basement. Two phases of folding are present, as is localized brecciation of siltstone and fine-grained sandstone.

The Stuart Mountain section reveals a fold interference pattern produced by two generations of folds (Fig. 16a, b). The F_1 structures are uncommon and occur as isolated, tight to isoclinal folds in kerogenous shaly siltstone. Their scarcity makes it difficult to obtain a precise orientation; asymmetry, however, seems consistent with bedding-parallel deformation featuring a top-to-the-south movement. The F_1 folds are interbedded with kerogenous and non-kerogenous siltstone–sandstone, in which sandstone beds define the open F_2 folds. The F_2 folds trend west-southwest and plunge 5° to 25° (Fig. 16b).

At the top of the Stuart Mountain Road section, Caledonia basement rocks appear to overlie rocks of the Albert Formation that outcrop in a creek south of the section (St. Peter, pers. comm. 2005). The basement material most likely represents a fault-bounded sliver of older material within the Albert Formation. Exposure along the creek or Stuart Mountain Road is insufficient to better determine the significance of this basement sliver other than to note its probable allochthonous nature.

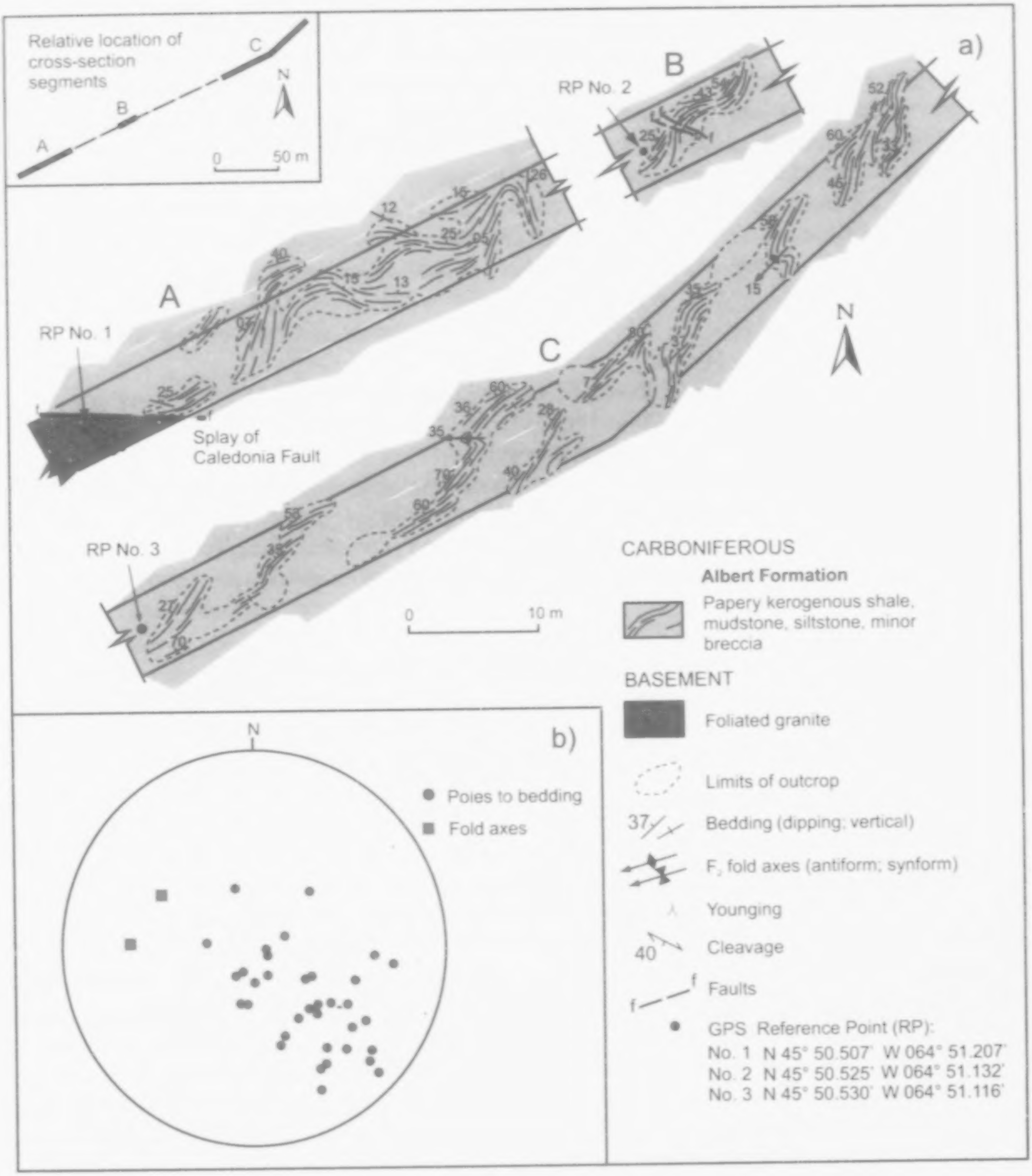

a)
Relative location of cross-section segments
A
B
C
N
0
50 m
RP No. 1
RP No. 2
RP No. 3
Splay of Caledonia Fault
0
10 m
CARBONIFEROUS
Albert Formation
Papery kerogenous shale, mudstone, siltstone, minor breccia
BASEMENT
Foliated granite
Limits of outcrop
Bedding (dipping; vertical)
F₂ fold axes (antiform; synform)
Younging
Cleavage
Faults
GPS Reference Point (RP):
No. 1 N 45° 50.507' W 064° 51.207'
No. 2 N 45° 50.525' W 064° 51.132'
No. 3 N 45° 50.530' W 064° 51.116'
b)
Poles to bedding
Fold axes

Figure 16. a) Detailed map of structures exposed in silty shale and fine-grained sandstone of the Albert Formation in the Peck Creek–Weldon Creek section. Map area is outlined on Figure 2. The Albert Formation lies in faulted contact here with the Caledonia basement along a splay of the Caledonia Fault. b) Poles to bedding and F_2 fold axes at the Peck Creek–Weldon Creek locality.

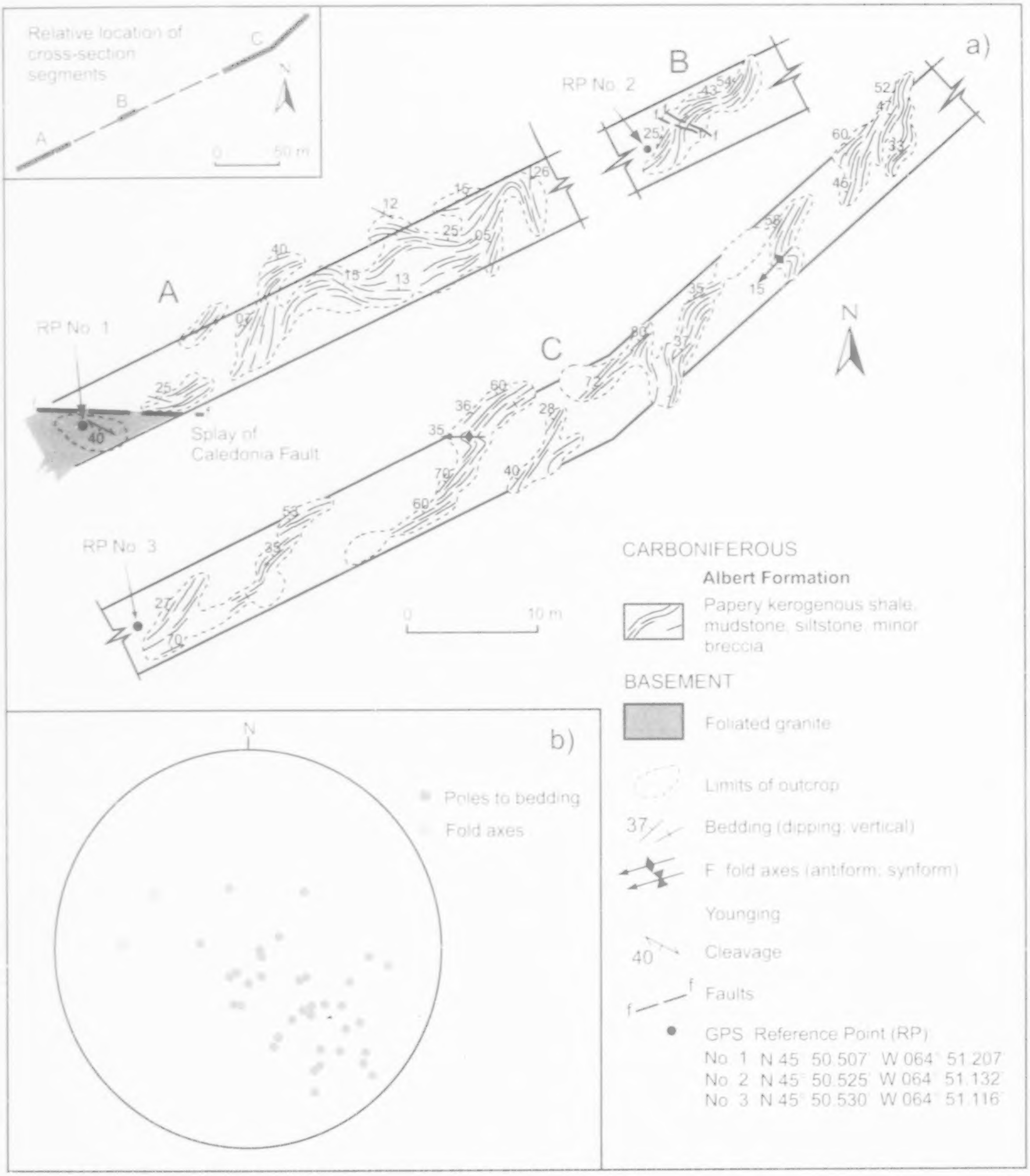
Relative location of cross-section segments
A
B
C
N
0
50 m
a)
B
RP No. 2
A
RP No. 1
Splay of Caledonia Fault
C
RP No. 3
N
0
10 m
b)
N
Poles to bedding
Fold axes
CARBONIFEROUS
Albert Formation
Papery kerogenous shale, mudstone, siltstone, minor breccia
BASEMENT
Foliated granite
Limits of outcrop
Bedding (dipping; vertical)
F fold axes (antiform; synform)
Younging
Cleavage
Faults
GPS Reference Point (RP)
No. 1 N 45° 50.507′ W 064° 51.207′
No. 2 N 45° 50.525′ W 064° 51.132′
No. 3 N 45° 50.530′ W 064° 51.116′

Figure 16. a) Detailed map of structures exposed in silty shale and fine-grained sandstone of the Albert Formation in the Peck Creek–Weldon Creek section. Map area is outlined on Figure 2. The Albert Formation lies in faulted contact here with the Caledonia basement along a splay of the Caledonia Fault. b) Poles to bedding and F fold axes at the Peck Creek–Weldon Creek locality.

Deformation in the Sussex Group

The three traverses used to produce a detailed structural analysis of rock deformation in the Sussex Group were chosen for their continuous, large-scale exposure, demonstrated relationship to other units, and coverage in existing literature. The traverses comprise the Boudreau Village section (Fig. 11 on Fig. 2) described above, which also includes rocks of the Sussex Group; the Belliveau Village traverse (Fig. 17 on Fig. 2), which provides a continuous section through the Weldon Formation and exposes the Gautreau Formation north of the Saint-Joseph Fault; and the Peck Creek–Weldon Creek section (Fig. 22 on Fig. 2), which constitutes the type locality for the Weldon and Round Hill formations.

Boudreau Village Section

Deformation in redbeds of the Sussex Group (Gautreau and Round Hill formations) in the Boudreau Village section (Fig. 11a) is limited to two parts of the section. One part (Panel 1 on Fig. 11a, b) consists of red and green mudrock and sandstone of the Gautreau Formation that form the northern 200 m of the section beside the faulted contact with the underlying Albert Formation. The other, more southerly, part (Panel 3 on Fig. 11b) comprises red sandstone and grainstone of the Round Hill Formation and occurs in a 150 m long section immediately north of the promontory.

In the northern part (Panel 1), deformation in the Gautreau Formation is restricted to particular horizons and is not a penetrative or pervasive feature. It is especially conspicuous in mudrock units and appears as deformation of the mudcracks and mudflakes (Fig. 14b, c). In most instances, the mudcracks have a distinct obliquity or asymmetry in cross-section and are always sheared in the same direction, consistent with a top-to-the-south movement. The mudflakes locally are folded; these folds show a distinctly asymmetric box profile that, again, is consistent with a top-to-the-south sense of bedding-parallel motion (Fig. 14b, c).

In the southern part (Panel 3), deformation in sandstone and grainstone of the Round Hill Formation is on a larger scale. The units have thin, shaly partings and are distorted into a set of open to tight folds with wavelengths in the order of 10 m and comparable amplitudes (Fig. 15b). The folds are rarely intact, and the hinges are typically disrupted by faults that die into bedding. The hinge-breaking faults have senses of motion consistent with bedding-parallel slip on their respective fold limbs. The geometry here is entirely consistent with the layers having been deformed into a series of chevron-type folds, where strain was taken up largely by layer-parallel slip until the fold-interlimb angle reached a critical value. Once this angle was exceeded, hinge break-out along discrete fault planes accommodated further increments of strain (Ramsay 1974; Tanner 1989).

Given the degree of fold disruption and extent of layer offset by hinge-breaking faults, it is difficult to attribute any overall sense of asymmetry to the package. However, these folds are overprinted by a second fold generation that plunges steeply and consistently to the southwest, as do the F_2 folds noted earlier in the adjacent Albert Formation (Fig. 11b, 13). This suggests that the disrupted fold set is an F_1 feature related to the bedding-parallel deformation described in the older Albert Formation rocks. The geometry and kinematics of these F_1 folds do not independently confirm the kinematics of a bedding-parallel deformation, but they are consistent with the top-to-the-south asymmetry already defined. Their presence and the overprinting of F_2 folds also demonstrate that the bedding-parallel deformation related to the F_1 folds affected rocks of the Sussex Group. The deformation style in coarse sedimentary rocks of the Round Hill Formation differs from that in the Albert Formation farther north (Panel 2), a consequence of rheological differences and competency contrast.

Some parts of the Round Hill conglomerate forming the promontory (Fig. 11b) are dominated by tabular clasts that exhibit an imbrication. Not all imbrication is depositional. Minor strain-related veins occur in the extensional sector around some clasts, and a faint fabric is evident in others. The fact that fabric is always parallel to bedding and shows no evident obliquity indicates tectonic enhancement of a depositional imbrication. The significance of this fabric becomes apparent only when the rocks are compared with other, more deformed, conglomerate of the Round Hill Formation farther west in the Peck Creek–Weldon Creek sections (described below).

Belliveau Village Section

A continuous section of the Sussex Group is exposed in cliffs along the Petitcodiac River south of Belliveau Creek (Fig. 17a–c). The creek marks the trace of the Saint-Joseph Fault (Fig. 1, 2, 17a). For present purposes, the Belliveau Village section is divided into three areas: north of Belliveau Creek (Fig. 17a); south of Belliveau Creek but north of the promontory (Fig. 17a, b); and south of the promontory (Fig. 17b). Sandstone layers are more common north of the promontory. South of the promontory, toward the south end, the section is dominated by a thick red mudrock sequence with rare sandstone beds. This sequence extends south beyond the map area to the Belliveau Village wharf.

North of Belliveau Creek and the trace of the Saint-Joseph Fault, the geology is highly complex. A breccia body occurs just north of the creek, where minor folds exhibit a vergence reversal across a breccia mass (Fig. 18a). The relationship of breccia to folding is unclear. However, the breccia mass appears to have a tabular shape that, like the fold axes, trends northeast. The fold vergence is consistent with the breccia being the remains of a diapiric evaporite body removed by solution collapse as the mass rose into the freshwater zone. In core from boreholes located 3 to 5 km farther west and northwest, rocks of the Gautreau Formation include evaporites containing halite and glauberite (St. Peter 1992). These data further support an interpretation that the breccia is a solution-collapse feature.

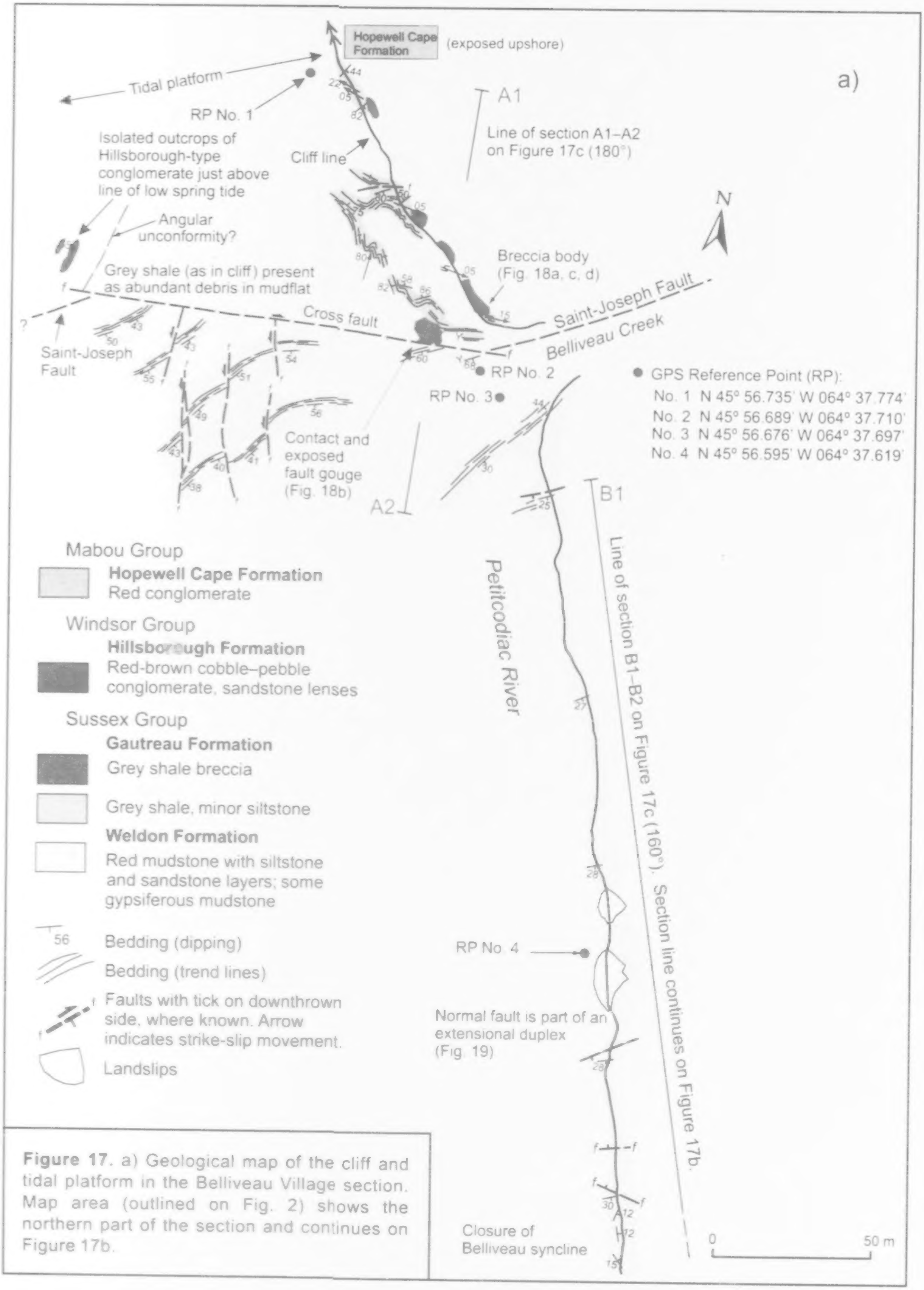
Hopewell Cape Formation
(exposed upshore)
a)
Tidal platform
RP No. 1
A1
Line of section A1–A2 on Figure 17c (180°)
Isolated outcrops of Hillsborough-type conglomerate just above line of low spring tide
Cliff line
N
Angular unconformity?
Grey shale (as in cliff) present as abundant debris in mudflat
Breccia body (Fig. 18a, c, d)
Saint-Joseph Fault
Cross fault
Belliveau Creek
?
Saint-Joseph Fault
RP No. 2
RP No. 3
● GPS Reference Point (RP):
No. 1 N 45° 56.735' W 064° 37.774'
No. 2 N 45° 56.689' W 064° 37.710'
No. 3 N 45° 56.676' W 064° 37.697'
No. 4 N 45° 56.595' W 064° 37.619'
Contact and exposed fault gouge (Fig. 18b)
A2
B1
Petitcodiac River
Line of section B1–B2 on Figure 17c (160°). Section line continues on Figure 17b.
Mabou Group
Hopewell Cape Formation
Red conglomerate
Windsor Group
Hillsborough Formation
Red-brown cobble–pebble conglomerate, sandstone lenses
Sussex Group
Gautreau Formation
Grey shale breccia
Grey shale, minor siltstone
Weldon Formation
Red mudstone with siltstone and sandstone layers; some gypsiferous mudstone
56 Bedding (dipping)
Bedding (trend lines)
Faults with tick on downthrown side, where known. Arrow indicates strike-slip movement.
Landslips
RP No. 4
Normal fault is part of an extensional duplex (Fig. 19)
Closure of Belliveau syncline
0
50 m

Figure 17. a) Geological map of the cliff and tidal platform in the Belliveau Village section. Map area (outlined on Fig. 2) shows the northern part of the section and continues on Figure 17b.

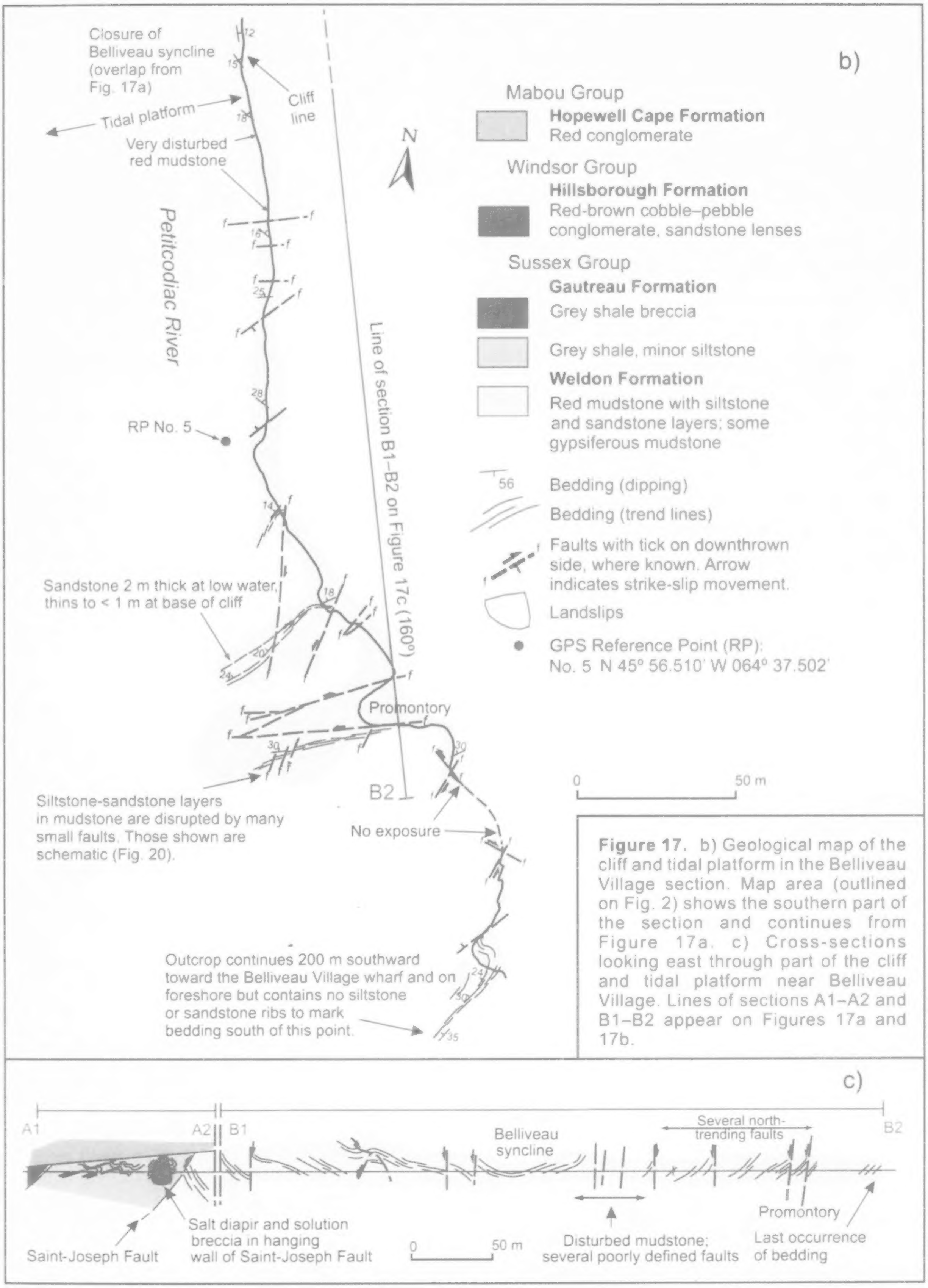
b)
Closure of Belliveau syncline (overlap from Fig. 17a)
Cliff line
Tidal platform
Very disturbed red mudstone
Petitcodiac River
RP No. 5
Line of section B1–B2 on Figure 17c (160°)
N
Sandstone 2 m thick at low water, thins to < 1 m at base of cliff
Promontory
Siltstone-sandstone layers in mudstone are disrupted by many small faults. Those shown are schematic (Fig. 20).
B2
No exposure
Outcrop continues 200 m southward toward the Belliveau Village wharf and on foreshore but contains no siltstone or sandstone ribs to mark bedding south of this point.
12
15
18
16
25
28
14
18
20
24
30
30
24
30
35
f
0
50 m
Mabou Group
Hopewell Cape Formation
Red conglomerate
Windsor Group
Hillsborough Formation
Red-brown cobble–pebble conglomerate, sandstone lenses
Sussex Group
Gautreau Formation
Grey shale breccia
Grey shale, minor siltstone
Weldon Formation
Red mudstone with siltstone and sandstone layers; some gypsiferous mudstone
56
Bedding (dipping)
Bedding (trend lines)
Faults with tick on downthrown side, where known. Arrow indicates strike-slip movement.
Landslips
GPS Reference Point (RP):
No. 5 N 45° 56.510' W 064° 37.502'
c)
A1
A2
B1
B2
Belliveau syncline
Several north-trending faults
Saint-Joseph Fault
Salt diapir and solution breccia in hanging wall of Saint-Joseph Fault
0
50 m
Disturbed mudstone; several poorly defined faults
Promontory
Last occurrence of bedding

Figure 17. b) Geological map of the cliff and tidal platform in the Belliveau Village section. Map area (outlined on Fig. 2) shows the southern part of the section and continues from Figure 17a. c) Cross-sections looking east through part of the cliff and tidal platform near Belliveau Village. Lines of sections A1–A2 and B1–B2 appear on Figures 17a and 17b.

A substantial, westward-trending cross fault occurs near the mouth of Belliveau Creek and appears to dextrally offset the Saint-Joseph Fault (Fig. 17a). Rocks immediately south of the cross fault consist of red mudrock and sandstone that correlate to, and appear continuous with, the Weldon Formation south of Belliveau Creek. In cliffs just north of the cross fault, in the hanging wall of the Saint-Joseph Fault (Wilson 2002), are grey shale, siltstone, and breccia assigned to the Gautreau Formation (Fig. 18b). The Gautreau rocks here are profoundly deformed. The folds are tight to isoclinal and upright to recumbent, and their limbs are broken along minor faults (Fig. 18c, d). The hinge lines are strongly curvilinear, probably because of refolding; the paucity of outcrop makes this interpretation equivocal, although the folds are geometrically consistent.

The contorted grey shale of the Gautreau Formation north of the cross fault is unconformably overlain by red sandstone and conglomerate assigned to the Hopewell Cape Formation of the Mabou Group. Slightly westward, at the northwestern end of the tidal platform (Fig. 17a), red-brown conglomerate assigned to the Hillsborough Formation overlies grey shale with an angular unconformity. This grey shale, like that north of the cross fault, is assigned to the Gautreau Formation. The location and bedding attitude of the Hillsborough conglomerate strongly indicate that it underlies the unconformity beneath the Mabou Group.

Timing of deformation in the Gautreau Formation is constrained by the Hopewell Cape conglomerate that unconformably overlies rocks of the Sussex Group in the cliff section (Fig. 17a). The angular unconformity intersects the cliff about 50 m north of the last outcrops of Gautreau Formation (just beyond the north end of Fig. 17a) and can be traced inland along the entire section (St. Peter and Johnson 1997, 2004 revision). The unconformity is not affected by folds seen in the Belliveau Village section and can be traced without offset across the Saint-Joseph Fault. The folds therefore must predate the angular unconformity at the base of the Mabou Group (Fig. 2, 3). If the isolated red conglomerate outcrops on the tidal platform are correctly interpreted as Hillsborough Formation (Fig. 17a), structures in the Gautreau Formation also could predate the Hillsborough Formation. On the other hand, bedding tilt of the latter formation implies movement of the Saint-Joseph Fault after deposition of the Hillsborough Formation and before that of the Mabou Group.

South of Belliveau Creek and the Saint-Joseph Fault, the Weldon Formation consists of interbedded red mudrock and sandstone, a succession that is punctuated by at least two thick intervals of red mudrock with sparse sandstone interbeds. The section here is dominated by a broad, open, upward-facing synform (possibly an F_1 structure) termed the Belliveau syncline. Its axis plunges shallowly (0° to 10°) west or southwest (Fig. 17a–c).

Smaller scale deformation south of Belliveau Creek is primarily fault-related and affected by complexities arising from rheological contrasts between mudrock and

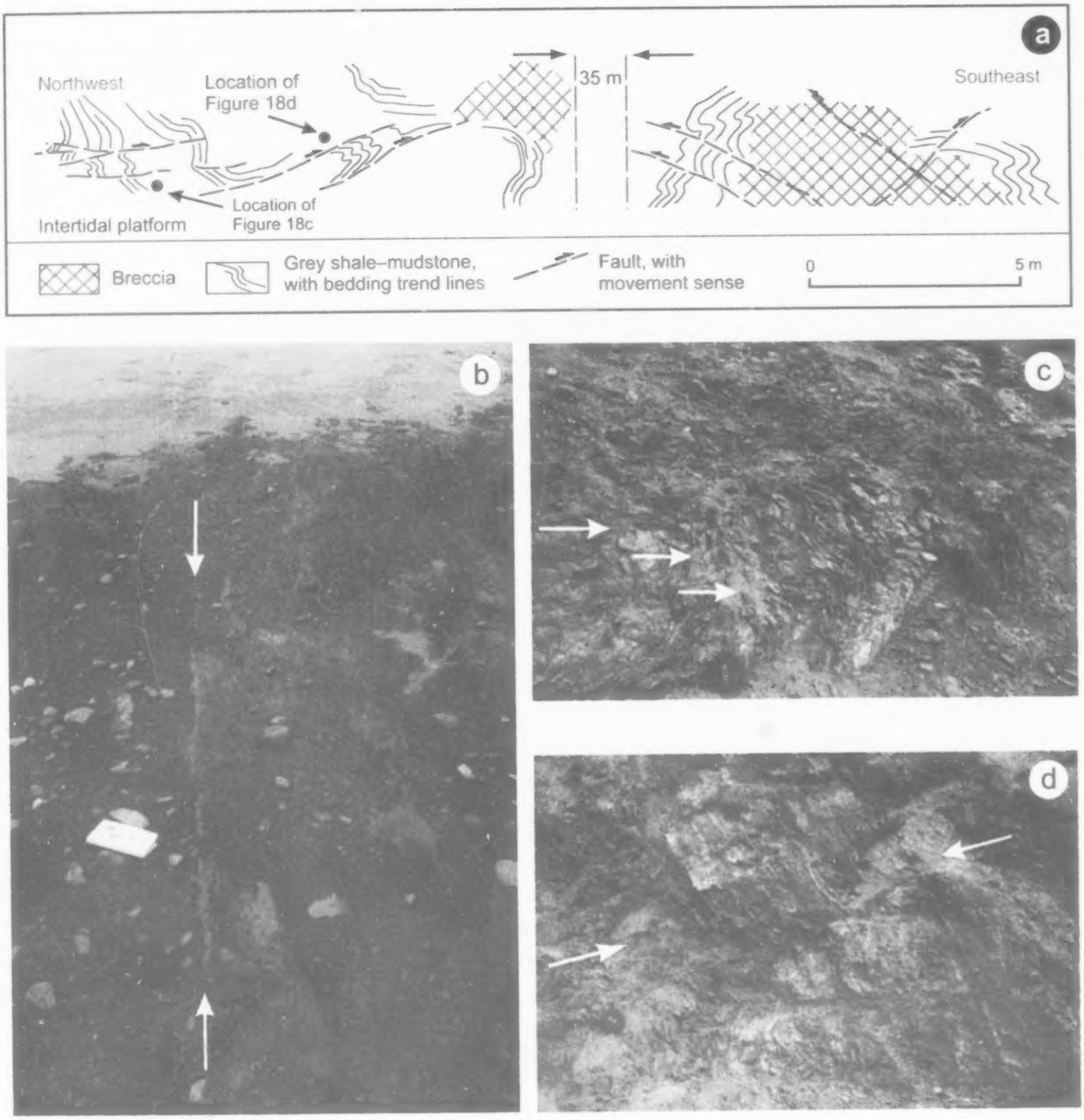
a
Northwest
Location of Figure 18d
35 m
Southeast
Intertidal platform
Location of Figure 18c
Breccia
Grey shale–mudstone, with bedding trend lines
Fault, with movement sense
0
5 m
b
c
d

Figure 18. Structures in the Gautreau Formation at the north end of the Belliveau Village section (Fig. 17a). a) Sketched section along cliffs through the Gautreau Formation showing relationship between breccia and minor folds. Section line is oblique to fold axes and strike, creating a horizontal exaggeration of the structures. b) Fault zone on the tidal platform separating red mudrock and sandstone of the Weldon Formation (left) from grey shale and breccia of the Gautreau Formation (right). Arrows mark the narrow gouge zone that represents the cross fault offsetting the trace of the Saint-Joseph Fault (Fig. 17a). View is looking west. Notebook is 18 cm long. c) Near-horizontal shear zones (arrows) disrupting steeply dipping beds in grey shale (photograph location marked on Fig. 18a). Lens cap is 55 mm. d) Shear plane (arrows) and folds in grey shale (photograph location marked on Fig. 18a). Lens cap is 55 mm.

sandstone. The deformation takes two forms: a fault-related extensional complex in the northern limb of the synform (Fig. 17a); and a complex deformation in the southern limb of the synform, south of the promontory (Fig. 17c).

The fault-related extensional complex consists of a set of high-angle faults that cut the sandstone–siltstone units and that are interconnected through broader shear zones in the intervening mudrock (Fig. 19). The structure is not as attenuated as it appears on the cliff (and in Fig. 19); rather, the cliff section is oblique to the high-angle faults in the sandstone, causing an exaggeration of the horizontal scale.

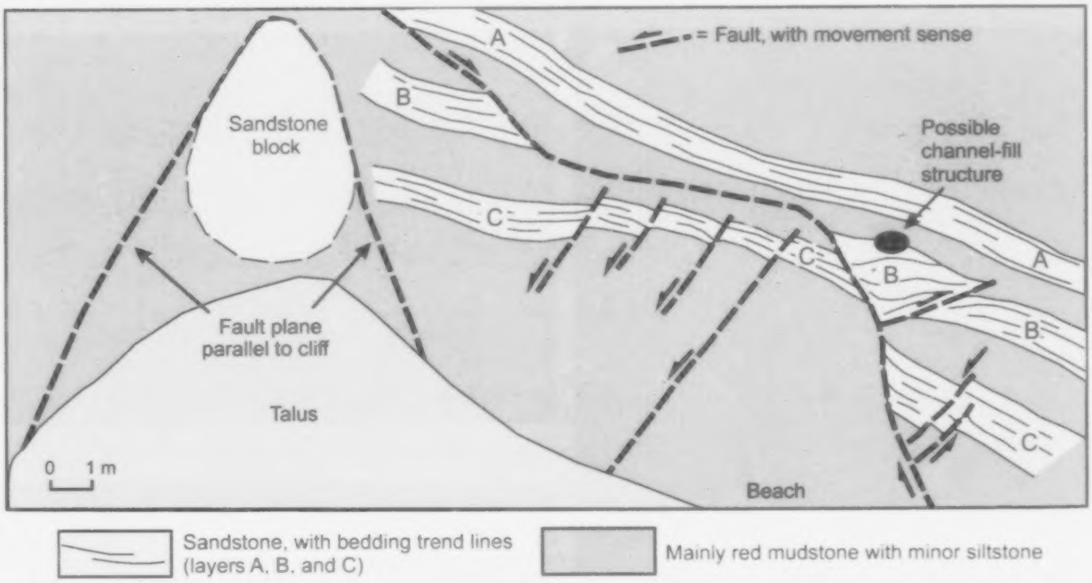
= Fault, with movement sense
A
B
Sandstone block
C
Possible channel-fill structure
C
B
A
B
Fault plane parallel to cliff
B
C
Talus
0 1 m
Beach
Sandstone, with bedding trend lines (layers A, B, and C)
Mainly red mudstone with minor siltstone

Figure 19. Structural features in the Weldon Formation, northern limb of the Belliveau syncline in the Belliveau Village section (see Fig. 17a for location). Diagram of the mudrock–sandstone outcrop shows extensional features associated with the curvilinear normal fault and its antithetic faults. The cliff section is oblique to high-angle faults in the sandstone, exaggerating the curvature of the main fault and the offset of sandstone layer B. The geometry of layer B and the disrupting faults is further complicated by the existence of a possible channel-fill structure in the hanging wall of the main fault (isolated by a small antithetic fault).

Deformation in the southern limb of the synform is extensive, especially in the thick, red mudrock sequence between the promontory and the Belliveau Village wharf where bedding is difficult to define. Deformation features consist of joints and fractures, of which at least six sets can be defined by crosscutting relationships, orientation, and movement sense. In places, the fractures are arranged geometrically (Fig. 20a, b) as cleavages to create a pencil structure (L^a_b). The cleavages invariably are early in the sequence (S_a and S_b) with intersection L^a_b (Fig. 20a, b). Green iron-reduction zones can be found associated with all later (later than S_b) fracture sets at one site or another (Fig. 20b–d), but do not appear with all sets in any one location. These later fractures show little consistency of

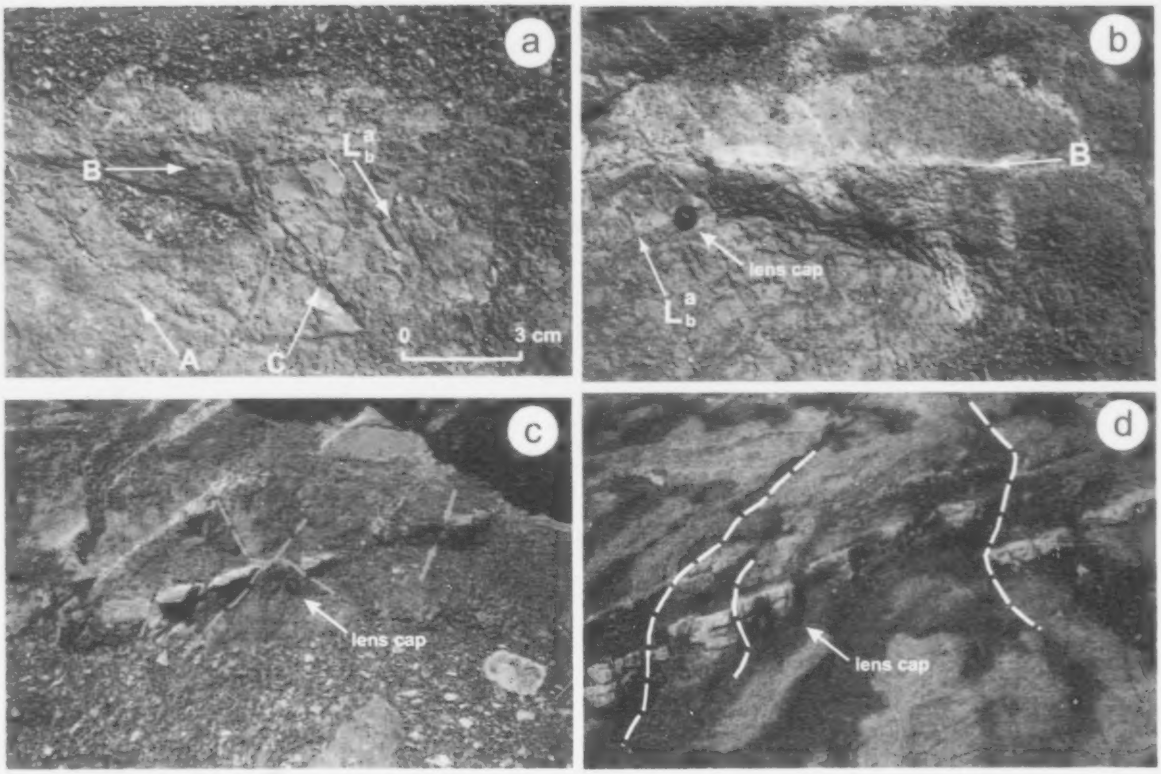

Figure 20. Structural features in the Weldon Formation, southern limb of the Belliveau syncline, in the Belliveau Village section (see Fig.17b for location). a) Features in mudrock. L^a_b is an intersection (pencil structure) of two early cleavages (S_a and S_b). A, B, and C mark later shear planes that disrupted and progressively obliterated the earlier features. The shear planes crosscut each other in alphabetic order. b) Pencil intersection structure L^a_b and shear plane B with prominent green iron-reduction zone in red mudrock along the later shear plane. Lens cap is 55 mm. c) Siltstone layer in red mudrock with three prominent, minor fault planes breaking up the bedding. Fault planes are shown as green dashed lines and green arrows. Red arrow marks a set of shear planes associated with the iron-reduction zone in red mudrock. Lens cap is 55 mm. d) Three sets of fractures disrupt an iron-reduced sandstone layer in red mudrock. Lens cap is 55 mm.

orientation (Fig. 21a, b). A few continuous sandstone layers occur around the promontory itself (Fig. 21c). Where sandstone layers are present and traceable for a few metres, three fracture sets consistently create extensional offsets. The fractures disrupt the sandstone layers and pencil structures, establishing an age relationship between fractures organized as a cleavage pair and those that extend the interbeds (Fig. 20a–c). It appears that sandstone interbeds in the southern limb of the synform underwent fracture-controlled extension after cleavages developed in the mudstone.

The kinematics and geometry of cleavages and fractures in the Belliveau Village section are unclear, but the timing relationship is important. The pencil structure L^a_b is always early. Its inconsistent orientation from one location to another is clearly disturbed; based on what admittedly is a small data set (Fig. 21d), it shows no obvious relationship to the synform. The fractures, shears, and joints (Fig. 21a, b) that display no evidence of movement have an ambiguous relationship to the synform. Those showing evidence of movement (Fig. 20c, d) are related to a prominent set of north–south faults situated on the tidal platform at the southern end of the promontory (Fig. 17b).

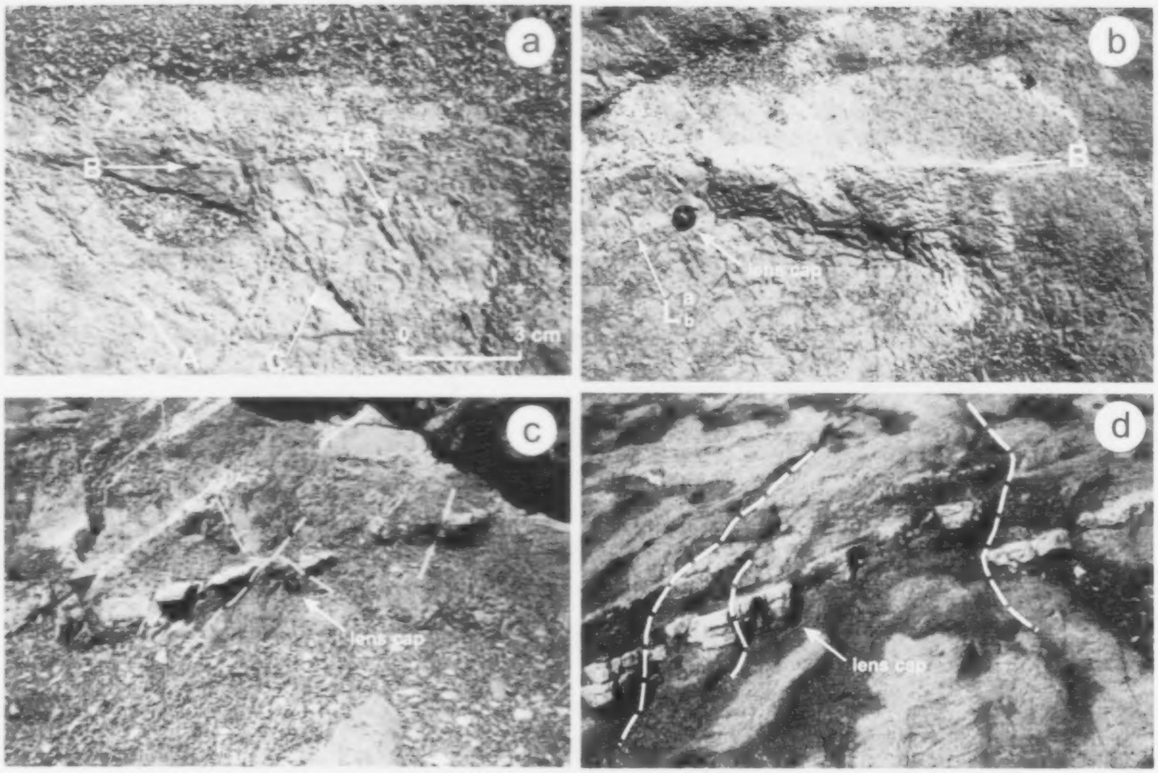

Figure 20. Structural features in the Weldon Formation, southern limb of the Belliveau syncline, in the Belliveau Village section (see Fig. 17b for location). a) Features in mudrock. L^a_b is an intersection (pencil structure) of two early cleavages (S_a and S_b). A, B, and C mark later shear planes that disrupted and progressively obliterated the earlier features. The shear planes crosscut each other in alphabetic order. b) Pencil intersection structure L^a_b and shear plane B with prominent green iron-reduction zone in red mudrock along the later shear plane. Lens cap is 55 mm. c) Siltstone layer in red mudrock with three prominent, minor fault planes breaking up the bedding. Fault planes are shown as green dashed lines and green arrows. Red arrow marks a set of shear planes associated with the iron-reduction zone in red mudrock. Lens cap is 55 mm. d) Three sets of fractures disrupt an iron-reduced sandstone layer in red mudrock. Lens cap is 55 mm.

orientation (Fig. 21a, b). A few continuous sandstone layers occur around the promontory itself (Fig. 21c). Where sandstone layers are present and traceable for a few metres, three fracture sets consistently create extensional offsets. The fractures disrupt the sandstone layers and pencil structures, establishing an age relationship between fractures organized as a cleavage pair and those that extend the interbeds (Fig. 20a–c). It appears that sandstone interbeds in the southern limb of the synform underwent fracture-controlled extension after cleavages developed in the mudstone.

The kinematics and geometry of cleavages and fractures in the Belliveau Village section are unclear, but the timing relationship is important. The pencil structure L^a_b is always early. Its inconsistent orientation from one location to another is clearly disturbed; based on what admittedly is a small data set (Fig. 21d), it shows no obvious relationship to the synform. The fractures, shears, and joints (Fig. 21a, b) that display no evidence of movement have an ambiguous relationship to the synform. Those showing evidence of movement (Fig. 20c, d) are related to a prominent set of north–south faults situated on the tidal platform at the southern end of the promontory (Fig. 17b).

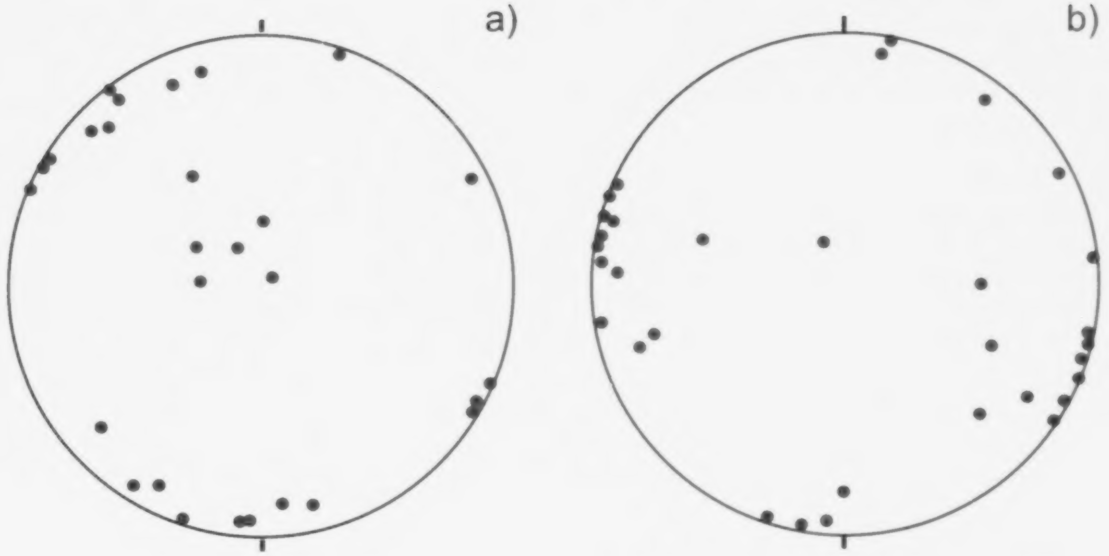

Poles to joints (n = 29)

Poles to minor faults and shears (n = 34)

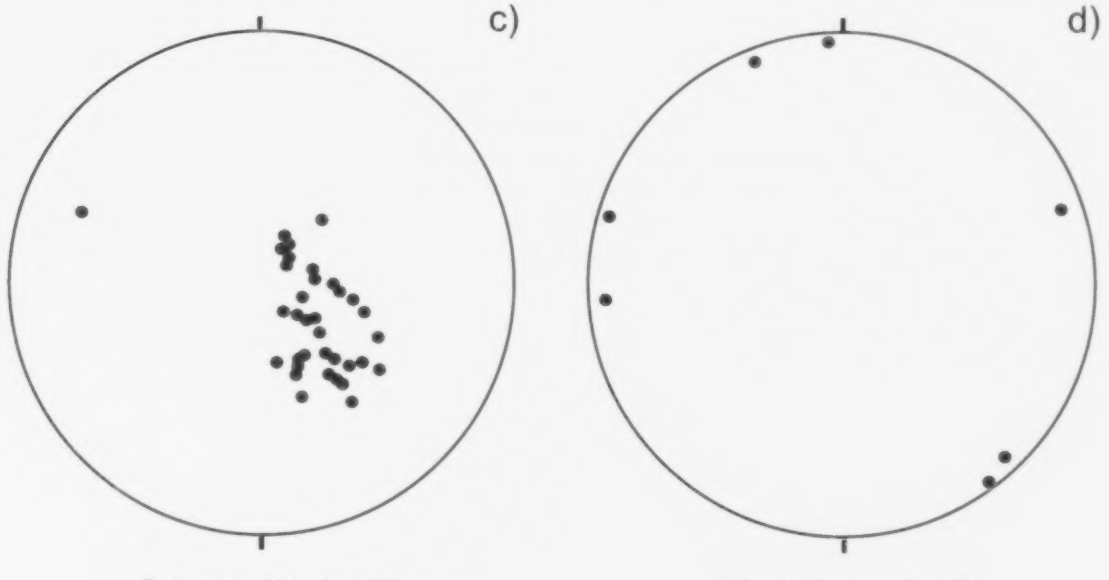

Poles to bedding (n = 36)

Poles to cleavage (n = 7)

Figure 21. Equal area, lower hemisphere projections of structural elements in the Belliveau Village section (Fig. 17a, b). a) Poles to joints, showing fractures that display no movement indicators. b) Poles to minor faults and sheared fractures. Note cluster trending north and near-vertical. c) Poles to bedding, showing geometry of the Belliveau syncline (Fig. 17c). There is a bias in data from the southern limb of the syncline. d) Poles to the cleavages noted as S_a and S_b in the caption for Figure 18a. Orientation is usually steeply dipping but varies between outcrops, indicating disruption by movement on later shears (as in Fig. 18b, c).

Peck Creek–Weldon Creek Section

The 2.5 km section along Weldon Creek and its tributary, Peck Creek, runs through type sections of the Weldon and Round Hill formations, exposing the relationship between the units (Fig. 22, 23). Part of the section was mapped by Wilson (2002), and the entire section was remapped by St. Peter (St. Peter 2004; St. Peter and Johnson 1997, 2004 revision).

Along Peck Creek, about 1 km from the creek mouth, olive-green to red-brown conglomerate of the Round Hill Formation is overlain by red and grey-green mudrock and sandstone assigned to the Gautreau Formation (Fig. 22, 23). The Round Hill Formation forms the high ground east and west of the creek in this area and also forms the conglomerate ridge east of the Intervale Road. Although not well exposed, Gautreau beds lie stratigraphically below red mudrock of the Weldon Formation and show a gradational contact with conglomerate of the Round Hill Formation.

About 500 m from the mouth of Peck Creek, on the west bank, is a felsite body (Fig. 22, 23) described by McLeod (1980) as a porphyritic felsic intrusion. It exhibits chilled margins and extensive auto-brecciation that mixes felsite with the conglomerate host rock. Much of the brecciation is likely primary but some may be tectonic, as the felsite is also deformed (Fig. 24a). In thin section, the felsite shows recrystallized quartz aggregates with a c-axis fabric, indicating deformation at elevated temperatures (Wilson 2005; pers. comm.). All these features are overprinted by a pervasive deformation fabric that gives much of the conglomerate a phyllitic appearance. Calcite- and quartz-filled veins are ubiquitous throughout the felsite.

The "cauliflower" margins on pillow-like structures in the felsite, and the mutual apophyses of felsite-in-host and host-in-felsite (Fig. 24a–c), are consistent with shallow intrusion of the felsite into wet, unconsolidated sediments (see Chapter 4 of Cas and Wright 1988). The felsite at Peck Creek, and the Boyd Creek Tuff (which lies north of the Saint-Joseph Fault in the Weldon Formation) are the only known Carboniferous igneous rocks in southeastern New Brunswick. If the interpretation offered here is correct — that is, if the felsite intruded wet (prelithified) Round Hill strata and is coeval with the Boyd Creek Tuff — then deformation evidently took place during deposition of the Weldon Formation.

The overall form of the felsite, shape-fabrics in some sheared felsite enclaves, and phyllitic fabric in the host rock, all imply a thrust fault immediately above the felsite body parallel to bedding of the Round Hill conglomerate. Vergence indicates a top-to-the-south or -southwest motion. The inferred structural setting confirms McLeod's (1980) interpretation and also appears related to the deformation observed farther north along Peck Creek.

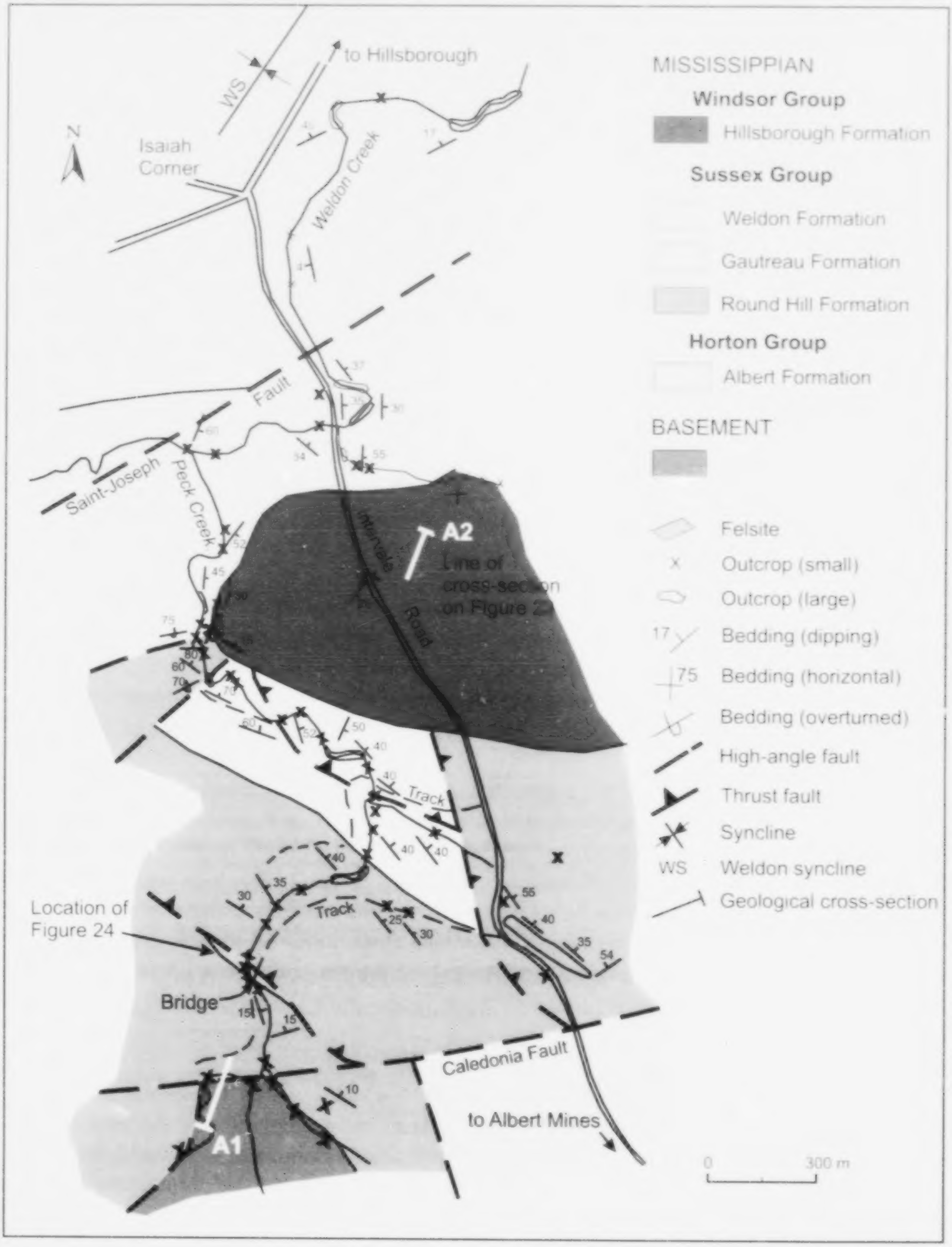
to Hillsborough
WS
N
Isaiah Corner
Weldon Creek
Fault
Saint-Joseph
Peck Creek
Intervale Road
A2
Line of cross-section on Figure 23
Track
Location of Figure 24
Bridge
Caledonia Fault
to Albert Mines
A1
0
300 m
MISSISSIPPIAN
Windsor Group
Hillsborough Formation
Sussex Group
Weldon Formation
Gautreau Formation
Round Hill Formation
Horton Group
Albert Formation
BASEMENT
Felsite
Outcrop (small)
Outcrop (large)
Bedding (dipping)
Bedding (horizontal)
Bedding (overturned)
High-angle fault
Thrust fault
Syncline
WS Weldon syncline
Geological cross-section

Figure 22. Geological map of the Peck Creek–Weldon Creek section immediately upstream from Weldon Creek (after St. Peter and Johnson 1997, 2004 revision). Map area is outlined on Figure 2.

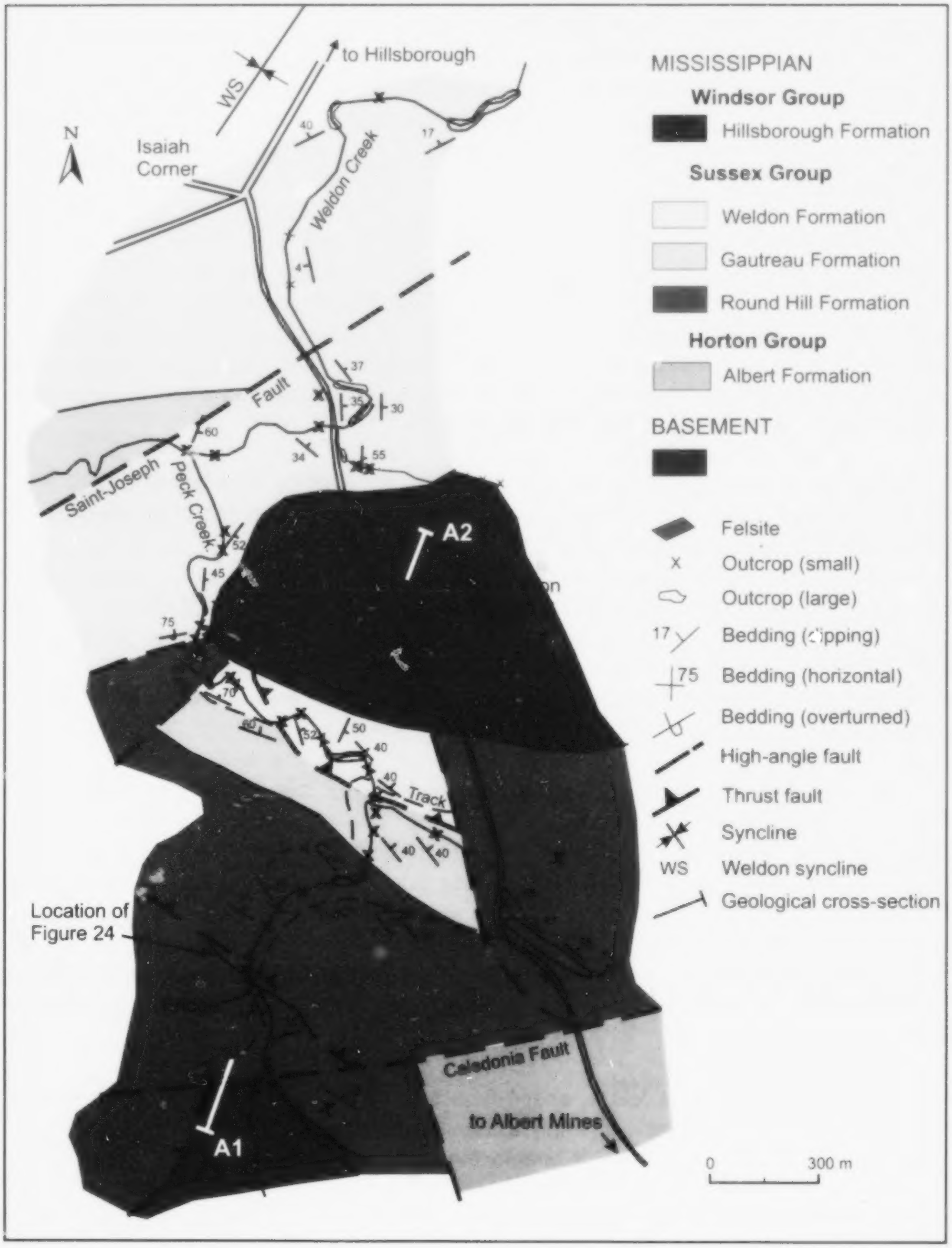
to Hillsborough
WS
N
Isaiah Corner
Weldon Creek
Fault
Saint-Joseph
Peck Creek
A2
A1
Track
Location of Figure 24
Caledonia Fault
to Albert Mines
0
300 m
MISSISSIPPIAN
Windsor Group
Hillsborough Formation
Sussex Group
Weldon Formation
Gautreau Formation
Round Hill Formation
Horton Group
Albert Formation
BASEMENT
Felsite
Outcrop (small)
Outcrop (large)
Bedding (dipping)
Bedding (horizontal)
Bedding (overturned)
High-angle fault
Thrust fault
Syncline
WS Weldon syncline
Geological cross-section

Figure 22. Geological map of the Peck Creek–Weldon Creek section immediately upstream from Weldon Creek (after St. Peter and Johnson 1997, 2004 revision). Map area is outlined on Figure 2.

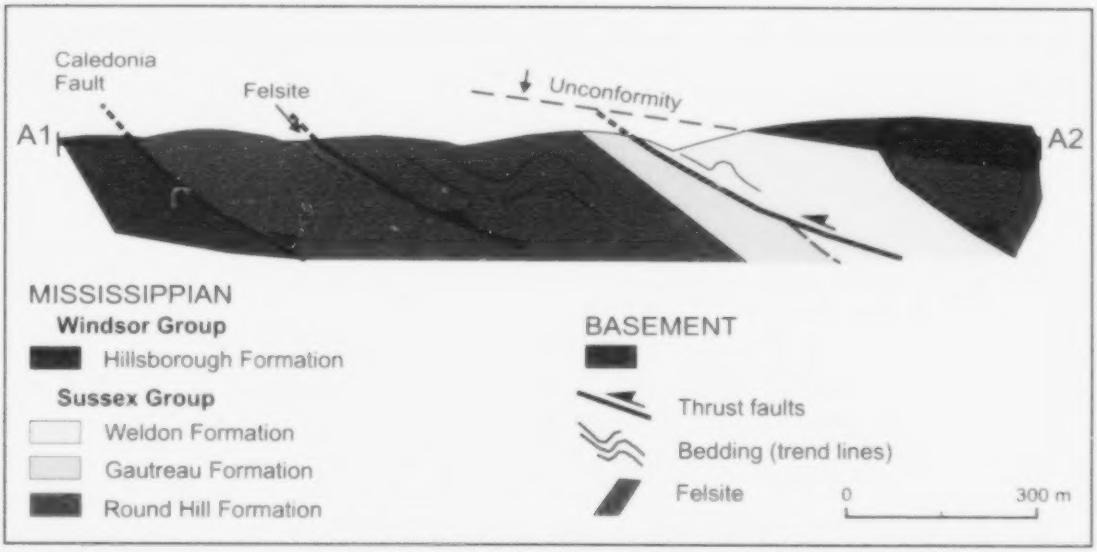
Caledonia Fault
Felsite
Unconformity
A1
A2
MISSISSIPPIAN
Windsor Group
Hillsborough Formation
Sussex Group
Weldon Formation
Gautreau Formation
Round Hill Formation
BASEMENT
Thrust faults
Bedding (trend lines)
Felsite
0
300 m

Figure 23. Composite geological cross-section for the Peck Creek–Weldon Creek section, showing unconformity at the base of the Hillsborough Formation (section line A1–A2 is marked on Fig. 22).

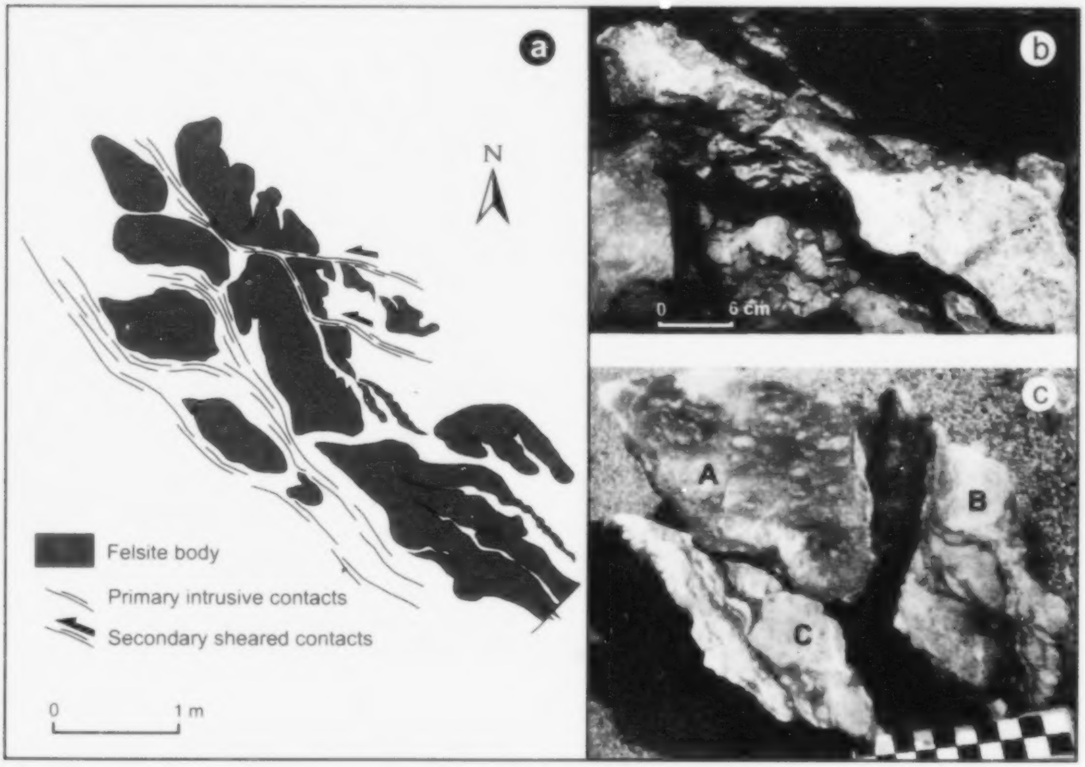
a
N
Felsite body
Primary intrusive contacts
Secondary sheared contacts
0
1 m
b
0
6 cm
c
A
B
C

Figure 24. a) Sketch of felsite body (see Fig. 22) at the Peck Creek–Weldon Creek section. Shows intrusive and sheared contacts between the felsite and its host conglomerate of the Round Hill Formation. b) Felsite veinlet with "cauliflower texture" along upper contact of the felsite with the sheared conglomerate. c) Slabs of felsite. Sample A shows mixed breccia of the felsite and phyllitic matrix with feldspar phenocrysts in both. Sample B shows veins of matrix in felsite, some with "cauliflower" textures along their contacts. Sample C shows veins and brecciated felsite. Scale is in centimetres.

Two antiform–synform pairs can be seen downstream of the felsite along Peck Creek (Fig. 22). A complex minor fold with an asymmetric box profile occurs in the intermediate limb of the larger fold pair, but its vergence is incongruent for a minor fold in this location. However, if the intermediate limb is restored to the horizontal, its vergence resembles that of the large-scale fold pair. This implies that both fold sets were produced by bedding-parallel slip, the minor fold set forming first. Moreover, the geometry implies that the strain rate exceeded the deformation accommodated by the minor fold, causing the entire bed to rotate as the major fold pair formed.

In the southern limb of the larger synform, small thrust faults ramp through the sandstone layers and root in the mudrock layers. Fault vergence is consistent with the overall kinematics of the fold pair described above. Thick beefsteak calcite veins occur extensively in mudrock in a zone 2 m thick, with individual veins reaching up to 25 cm thick (Fig. 25a–c). The zone shows internal folding and brecciation and marks a larger dislocation zone (Fig. 25c). Fold vergence has the same shear sense as the larger fold structures immediately north, implying that the antiform–synform pair is located in the hanging wall of a thrust contained within the mudrock unit.

A second, smaller antiform–synform pair occurs on the east bank of Peck Creek 100 m north of the felsite. Here, the north-dipping sandstone beds contain small thrust faults but no beefsteak calcite veins.

Farther down Peck Creek, the Round Hill conglomerate reappears as fault-bound panels exposed in the creek bed. Bedding is uniformly steep but dips north and south in juxtaposed panels. In one panel, bedding is overturned. No fold closures are preserved, but the changes of dip direction and younging indicate the presence of tight folds, with fold closures being broken out by small faults (Fig. 22, 23). The deformation style closely resembles that associated with F_1 folds in similar facies in the Boudreau Village section (Fig. 11b). The Peck Creek folds with their faulted-out hinges, for instance, trend west-southwest or southwest as do F_1 folds in the Boudreau Village section. The same trend occurs in the antiform–synform pairs just described, although they plunge shallowly east.

East of this part of Peck Creek, conglomerate of the Hillsborough Formation overlies rocks of the Sussex Group with angular unconformity (Fig. 22, 23). Neither the folds nor the faults described above can be traced through the unconformity, demonstrating that deformation predated the unconformity.

Immediately east of the Intervale Road bridge over Weldon Creek (Fig. 22), for about 1 km eastward along the creek, discontinuous outcrop exposes a thick, mudrock-dominated sequence with thin (generally less than 10 cm), minor sandstone interbeds. The mudrocks contain two strong, penetrative cleavages that form a pencil structure (Fig. 26a,

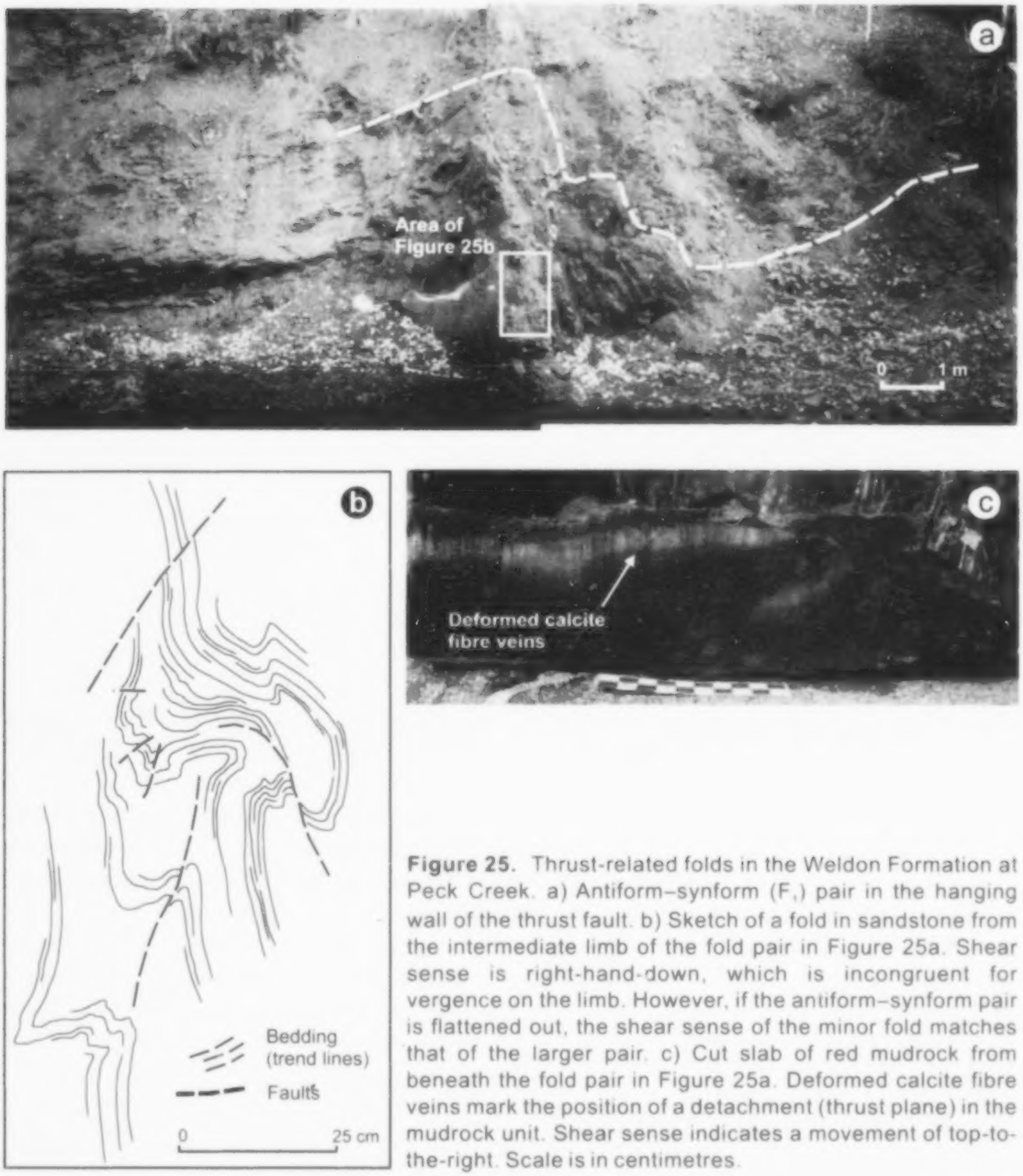

Figure 25. Thrust-related folds in the Weldon Formation at Peck Creek. a) Antiform–synform (F_1) pair in the hanging wall of the thrust fault. b) Sketch of a fold in sandstone from the intermediate limb of the fold pair in Figure 25a. Shear sense is right-hand-down, which is incongruent for vergence on the limb. However, if the antiform–synform pair is flattened out, the shear sense of the minor fold matches that of the larger pair. c) Cut slab of red mudrock from beneath the fold pair in Figure 25a. Deformed calcite fibre veins mark the position of a detachment (thrust plane) in the mudrock unit. Shear sense indicates a movement of top-to-the-right. Scale is in centimetres.

b). Both cleavages are spaced structures (0.5 to 1 cm thick lithons) that lie almost perpendicular to each other and near-perpendicular to bedding (Fig. 26b–d; 27a, b). Where thin sandstone layers are present, both cleavages pass through the layers with minor refraction, but neither shows evidence of slip disrupting the bedding (Fig. 26c, d).

The earlier cleavage (S_a) trends west–southwest and generally has blotchy, specular hematite, bluish vivianite on its septae, and a weakly developed slickenside lineation (L_s; Fig. 26a). The later cleavage (S_b) trends northwest; where present, it crosscuts S_a and

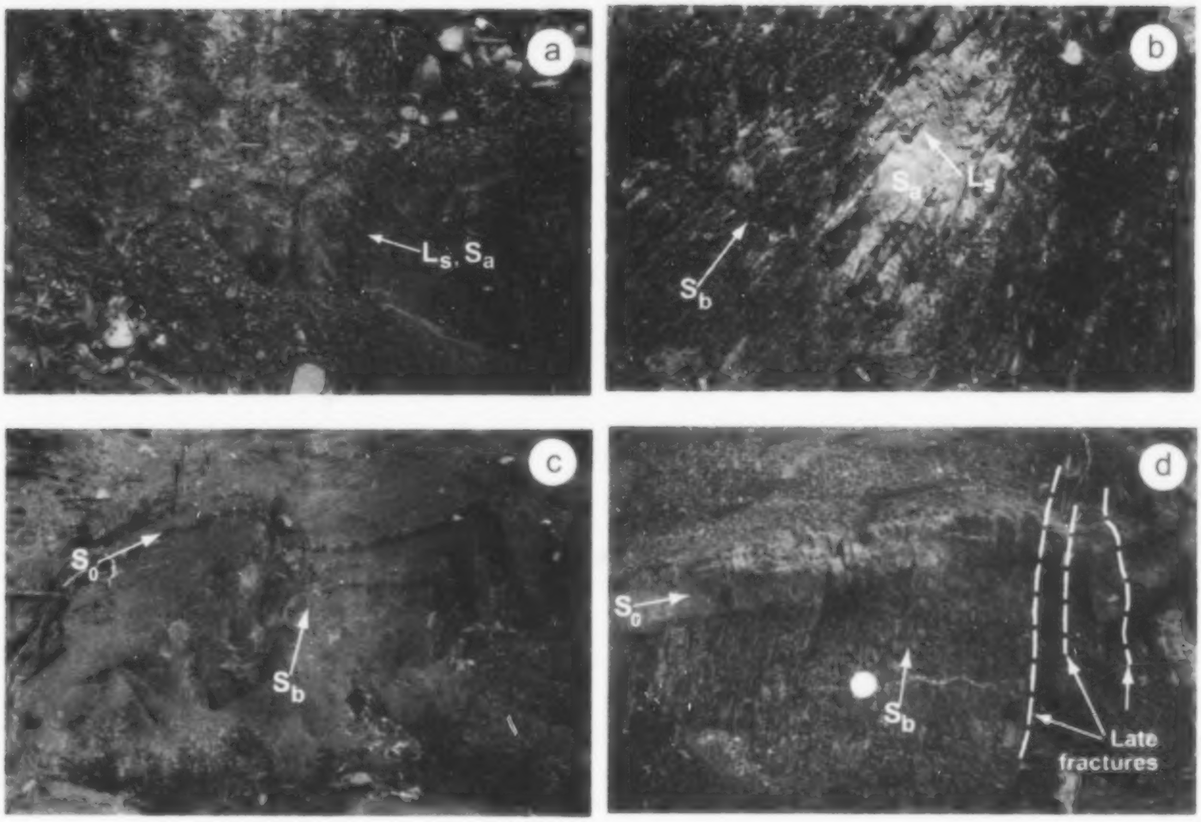

Figure 26. Cleavages in rocks of the Weldon Formation at Weldon Creek. a) S_a cleavage in mudrock with visible slickenside lineations (L_s). Specular hematite and vivianite are present on the S_a surface. Lens cap is 55 mm. b) Transposition of S_a into S_b leaving lithons of S_a and a distinctly curved L_s lineation. Lens cap is 55 mm. c) Outcrop view of S_b cleavage in mudrock cutting the bedding (S_0), as indicated by the sandstone layer. The apparent folds result from the cut effect on an irregular surface. Field assistant for scale. d) Detail from Figure 26c showing S_b cutting a sandstone bed without apparent offsets. One dollar coin is 2.7 mm.

transposes the earlier fabric (Fig. 26b). The transposition begins with a minor crenulation, giving a marked curvature to the S_a surfaces within S_b lithons. The curved S_a surfaces feature more distinctive specular hematite and better developed slickenside lineations (Fig. 26a, b). Within the more closely spaced S_b, the S_a septae become distinctly sigmoid and show no continuity across the septae (Fig. 26b). The sense of rotation in the sigmoid S_a septae is consistent. Despite their rotation, the slickenside lineations on S_a always lie close to the bedding plane in these outcrops. This orientation indicates that slip along S_b is bedding parallel and explains the lack of obvious disruption where S_b crosscuts the sandstone intervals (Fig. 26c, d; 27a, b). The only bedding offsets observed here occur where later fractures cross sandstone intervals. At least three sets of such fractures are apparent, and, in several cases, the fractures disrupt the S_b cleavage (Fig. 26d).

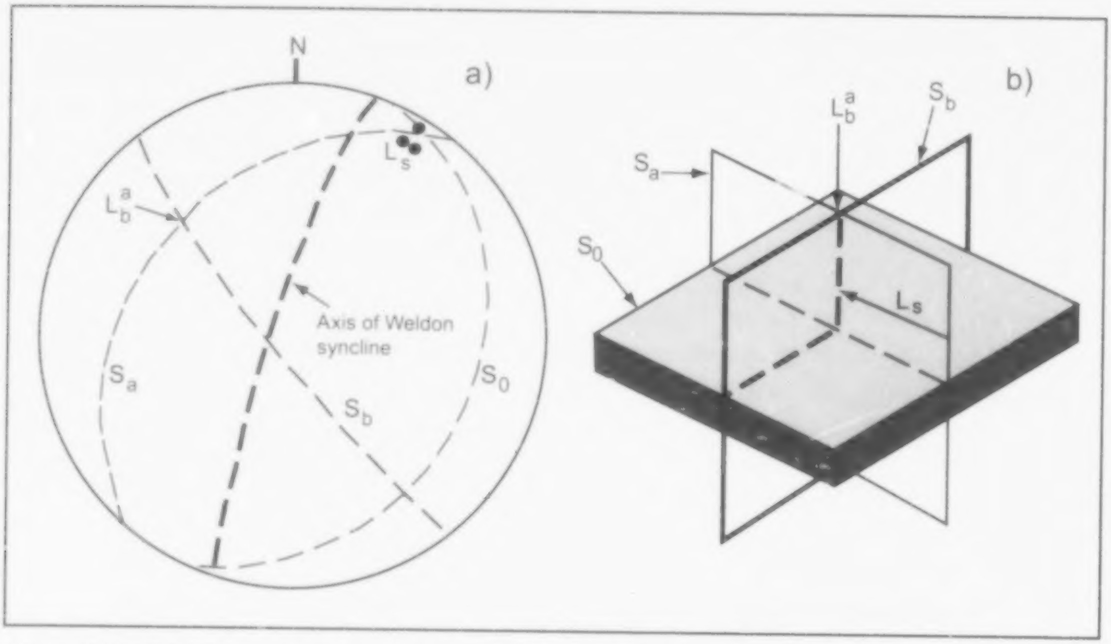

Figure 27. a) Structural features in mudrock of the Weldon Formation at Weldon Creek. Equal area, lower hemisphere projection shows bedding (S_0), the two cleavages (S_a and S_b), their intersection (L^a_b), and the slickenside lineations on S_a (L_s). b) Block diagram shows the bedding, cleavage, and lineation relations plotted on Figure 27a.

A broad, open synform termed the Weldon syncline (Fig. 2, 22) occurs at the northern edge of the Peck Creek–Weldon Creek section. McLeod (1980) and St. Peter and Johnston (1997, 2004 revision) interpreted the syncline as running north of the Saint-Joseph Fault; in fact, it forms a fold in the hanging wall of the fault.

SYNTHESIS OF DEFORMATION

Bedding-Parallel Deformation

Bedding-parallel deformation in rocks of both the Horton and Sussex groups is notably consistent in style and kinematics across the study area from Rosevale in the west to Saint-Joseph in the east. Where detachments have been identified and shear sense has been resolved, the detachments are low angle or bedding parallel with a top-to-the-south, -south-southwest or -south-southeast motion (Fig. 28).

Minor thrust faults occur wherever lithological contrasts facilitated their development. Small-scale thrust faults (noted earlier by such authors as Gussow 1953 and McLeod 1980) were observed during this study at three of the sections: Frederick Brook–Albert Mines, Boudreau Village, and Peck Creek–Weldon Creek. The larger scale Saint-Joseph, Dorchester (Wilson 2002), and Caledonia faults (Fig. 2, 28) may also have had an early thrust motion. Where overprinting relationships are clearly visible, this F_1 phase of deformation can be seen to succeed soft-sediment structures, as is well demonstrated at

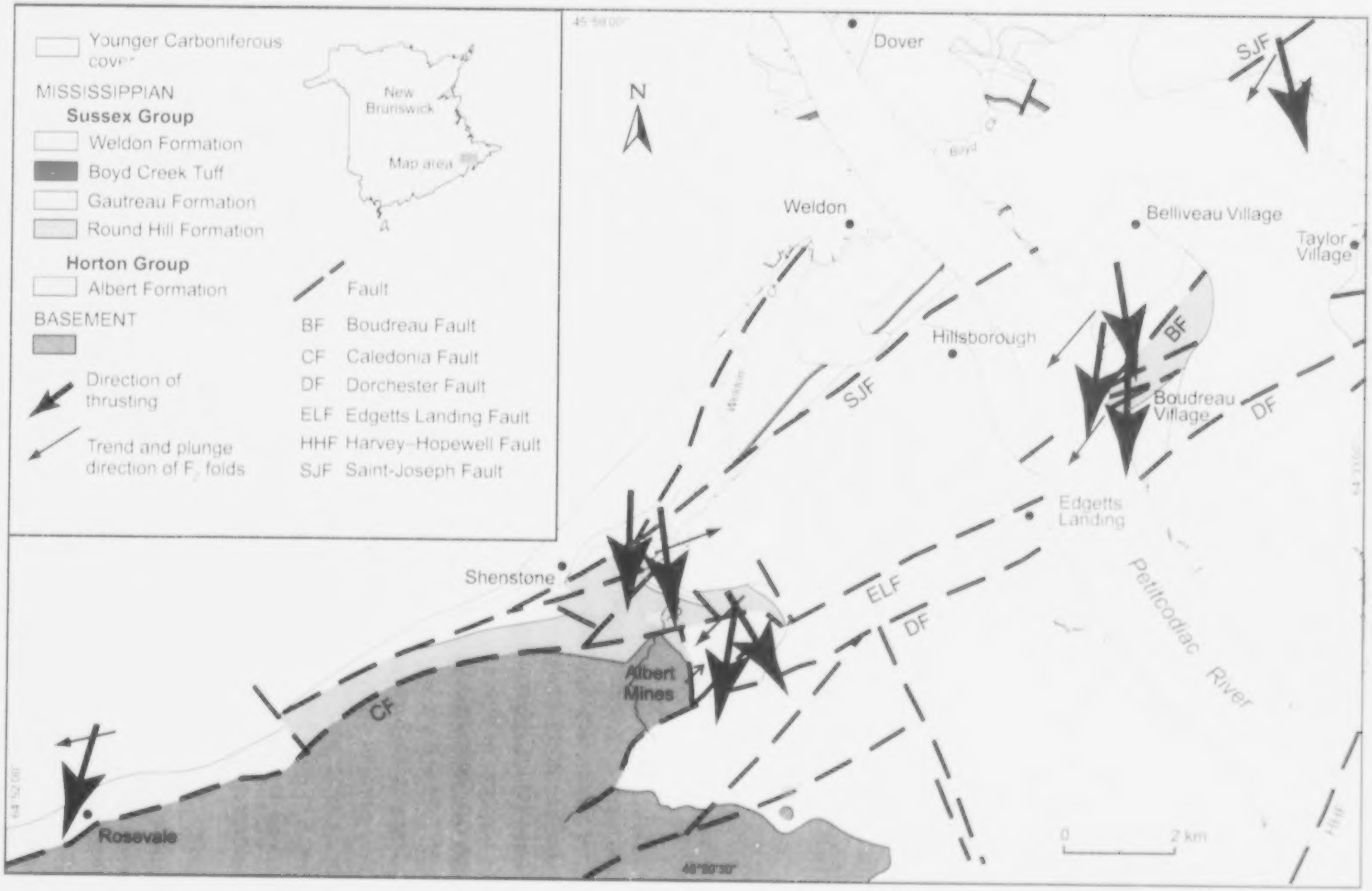
Younger Carboniferous cover
MISSISSIPPIAN
Sussex Group
Weldon Formation
Boyd Creek Tuff
Gautreau Formation
Round Hill Formation
Horton Group
Albert Formation
BASEMENT
Direction of thrusting
Trend and plunge direction of F_2 folds
Fault
BF Boudreau Fault
CF Caledonia Fault
DF Dorchester Fault
ELF Edgetts Landing Fault
HHF Harvey–Hopewell Fault
SJF Saint-Joseph Fault
New Brunswick
Map area
N
Dover
Weldon
Hillsborough
Belliveau Village
Taylor Village
Boudreau Village
Edgetts Landing
Shenstone
Albert Mines
Rosevale
Petitcodiac River
SJF
BF
DF
ELF
CF
HHF
0
2 km
45°50'30"

Figure 28. Map of the Rosevale–Hillsborough–Saint-Joseph area. Shows distribution of the Horton and Sussex groups, orientation of the F_2 fold axes, and derived sense of motion on the bedding-parallel shear zones and thrusts. All arrows give the top direction. The pattern suggests a north-northwest–south-southeast compression with a northwest–southeast element of transpression for the pre-Visean deformation.

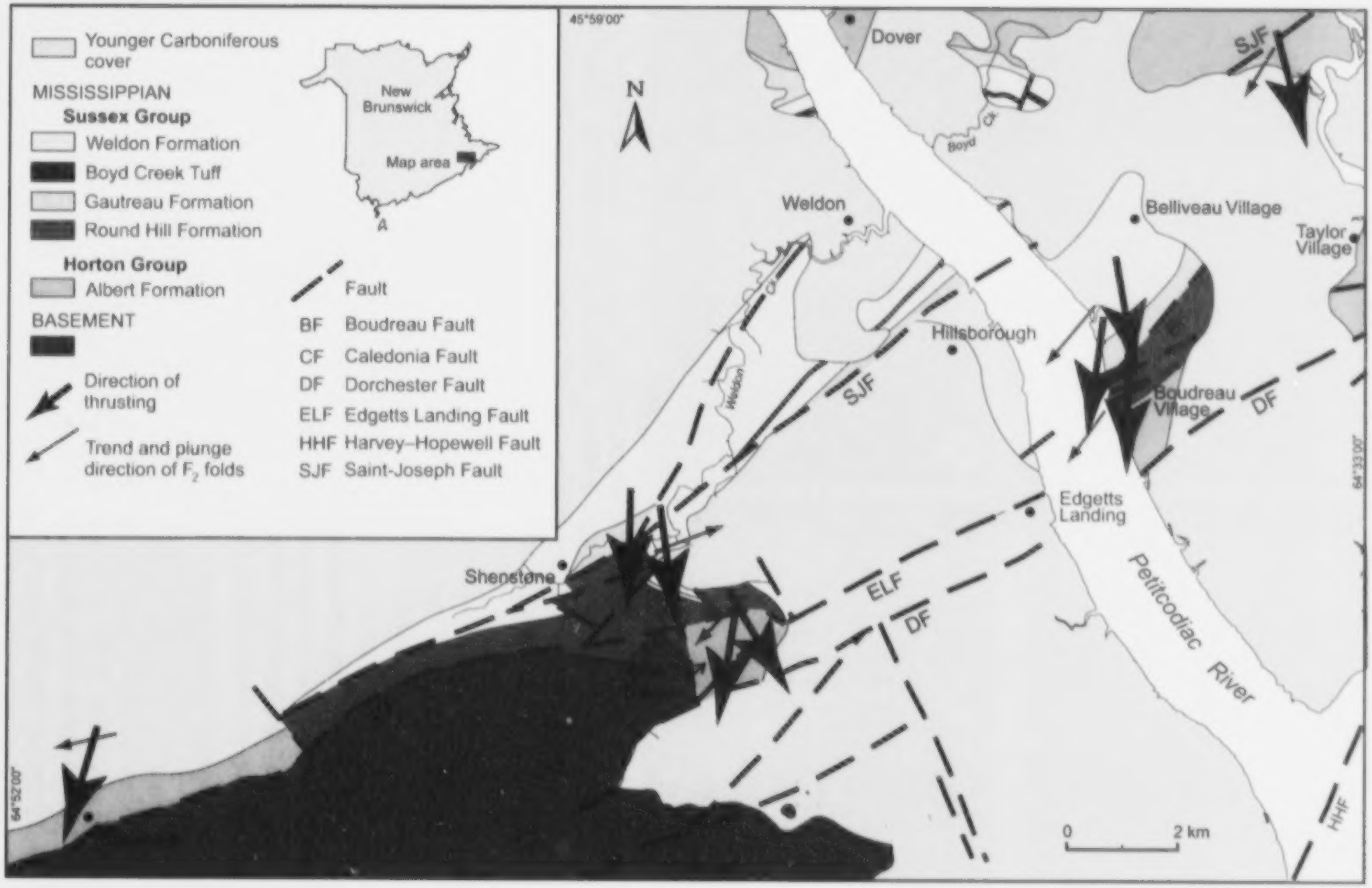
Younger Carboniferous cover
MISSISSIPPIAN
Sussex Group
Weldon Formation
Boyd Creek Tuff
Gautreau Formation
Round Hill Formation
Horton Group
Albert Formation
BASEMENT
Direction of thrusting
Trend and plunge direction of F_2 folds
Fault
BF Boudreau Fault
CF Caledonia Fault
DF Dorchester Fault
ELF Edgetts Landing Fault
HHF Harvey–Hopewell Fault
SJF Saint-Joseph Fault
New Brunswick
Map area
N
45°59'00"
64°33'00"
64°52'00"
Dover
Boyd Ck
Weldon
Weldon Ck
Belliveau Village
Taylor Village
Hillsborough
Boudreau Village
Edgetts Landing
Shenstone
Petitcodiac River
SJF
DF
ELF
HHF
0
2 km

Figure 28. Map of the Rosevale–Hillsborough–Saint-Joseph area. Shows distribution of the Horton and Sussex groups, orientation of the F_2 fold axes, and derived sense of motion on the bedding-parallel shear zones and thrusts. All arrows give the top direction. The pattern suggests a north-northwest–south-southeast compression with a northwest–southeast element of transpression for the pre-Visean deformation.

Le Blanc Creek and Frederick Brook. The bedding-parallel deformation is overprinted by a second set of folds (F_2) at Albert Mines, Boudreau Village, and Rosevale. The folds trend consistently southwest across the region, but their plunges vary considerably, ranging from steep at Boudreau Village to nearly horizontal at Rosevale (Fig. 28). This F_1–F_2 relationship is found in rocks of the Albert, Round Hill, and Weldon formations, suggesting that the entire F_1–F_2 deformation event took place in the Tournaisian, during or after deposition of the Sussex Group.

The Tournaisian deformation has a strikingly different signature in rocks of the Horton Group (Albert Formation) and the overlying Sussex Group (Round Hill, Weldon and Gautreau formations). Rocks higher in the section show successively weaker deformation. Detachments and associated folds and fabrics in the Sussex Group are confined largely to the Round Hill Formation or (in the Peck Creek and Boudreau Village sections) the lower Weldon Formation. Higher in these sections, detachments and tight folds apparently are absent; however, open folds such as the Belliveau and Weldon synclines are present, as are cleavages of ambiguous significance. The single instance of intense, complex deformation in these upper units occurs in an outcrop of Gautreau Formation at the north end of the Belliveau Village section (Fig. 17a). Otherwise, rocks of the upper Weldon and younger formations appear to have been carried relatively passively above a more strongly deformed zone situated lower in the stratigraphic section.

In the Belliveau Village section, two early cleavages (S_a and S_b) generated pencil structures (Fig. 21a, b, d), but their geometry has little consistency. In contrast, the S_a and S_b cleavages in the Peck Creek–Weldon Creek section have a consistent geometry and age relationship. The interpretation here is that cleavages developed very early, during the formation of mudrock, while bedding-parallel deformation was accommodated by bulk shortening of the mudrock layers before bedding began to rotate during folding. At Weldon Creek, both cleavages developed without substantial disruption of bedding. This occurred, despite the fact that S_b involved substantial transposition of the early S_a cleavage, because rotation took place in a plane parallel to bedding. Only when bedding began to rotate, and deformation was accommodated along distinct fractures, did the earlier formed cleavages become disrupted (Fig. 26d). The process proceeded further in the Belliveau Village section, where cleavages are preserved only as isolated relics in mudrock. Here, the evolution can be related to the southern limb of the large, open synform (the Belliveau syncline) in the cliff section (Fig. 17a–c).

In the Peck Creek–Weldon Creek section, no such relationship can be clearly demonstrated. McLeod (1980) traced a broad, open synform through the area (the Weldon syncline), but the well preserved cleavages seen here have no obvious geometric relationship to the axial plane of the structure. McLeod (1980) placed the Saint-Joseph Fault just north of the Peck Creek–Weldon Creek section (Fig. 22), and a southern splay of the fault immediately south of it. Although both cleavages occur in the footwall of these early structures, the geometry of the S_a and S_b cleavages, again, bears little obvious relationship to the presumed orientation of the faults. The preferred interpretation is that the cleavages are an expression of the bedding-parallel deformation affecting the Sussex Group. Nonetheless, cleavages in the Weldon Creek cliffs represent a transient feature of this evolution, one that originally was more widespread.

Timing of the deformation is well constrained. The folds and thrusts at Peck Creek are truncated by the angular unconformity (uppermost Tournaisian or lowermost Visean) beneath the Hillsborough Formation. Structures in the Belliveau Village section likewise are truncated by the angular unconformity beneath the Mabou Group. The Peck Creek relationship indicates that these structures were formed before deposition of the Windsor Group and probably are pre-Visean. A more precise dating hinges on interpretation of the felsite body at Peck Creek; if its correlation with the Boyd Creek Tuff proves correct, then the hot deformation of quartz aggregates in the intrusion implies that deformation took place during deposition of the upper part of the Weldon Formation.

The overall framework of this deformation event is constrained by its relationship to thrusting, especially southward-directed thrusting. The F_2 folds suggest transpression rather than simply a north–south shortening of the southern margin of the Moncton Subbasin, in that the shortening apparently involved a right-lateral strike-slip component. Significantly, this deformation shortened the section and thickened units in the Horton and Sussex groups against the Caledonia basement. The event appears to be one of several episodes of basin inversion recognized in the Moncton Subbasin by St. Peter (1992, 1993), Nickerson (1994), and Wilson (2005).

Faults and Their Relationship to Deformation

The major east-northeast-trending faults in the study area have been the subject of various interpretations over the years. Gussow (1953) described them as steeply inclined reverse faults that controlled the distribution of units thrusted south against the Caledonia basement. Webb (1963) proposed that thrusting represented a minor feature of fault reactivation and that the main phase of fault motion essentially was strike-slip. In fact, it is difficult to make any general statement regarding behaviour of the faults, as each structure is characterized by a distinctive history of repeated movements over time (St. Peter 1992, 1993).

St-Joseph Fault and Its Splays

The history of movement along the Saint-Joseph Fault (Fig. 2) is one of the best constrained in the study area. The earliest movement may be related to the late Tournaisian–pre-Visean episode of bedding-parallel deformation just described, during which the Saint-Joseph Fault originated as a large-scale thrust. The fault affects rocks of the Horton and Sussex groups but is truncated by the late Visean angular unconformity at the base of the Mabou Group east of the Petitcodiac River.

Based on seismic reflection profiles, Wilson (2002) interpreted the Saint-Joseph Fault as a shallowly north-dipping structure. The vergence of folding in cliffs in the northern part of the Belliveau Village section is consistent with this interpretation. An interpreted southern splay of the fault was shown by McLeod (1980) to account for a dip change between the Hillsborough Formation and overlying Macumber Formation in the Gray Brook syncline southwest of Hillsborough (Fig. 2). The present study found this relationship to be an angular unconformity, which implies that the southern splay predates the Windsor Group. However, the Saint-Joseph Fault cuts the Hillsborough Formation north of Gray Brook, indicating that the main fault, at least, moved after deposition of the Hillsborough Formation.

Edgetts Landing and Dorchester Faults

The Edgetts Landing Fault (Fig. 2, 11b) juxtaposes the Albert and Round Hill formations in the Boudreau Village section south of the promontory (St. Peter and Johnson 1997, 2004 revision; Wilson 2002). West of the Petitcodiac River, the fault is marked by the creek at Edgetts Landing and a deep gully south of Kings Quarry. From there, it can be traced westward through the albertite mine site (Fig. 4), after which it curves south to merge with the Dorchester Fault (McLeod 1980; St. Peter and Johnson 1997, 2004 revision).

The Dorchester Fault (Fig. 2) crosses the Petitcodiac River south of the Edgetts Landing Fault. West of there, it truncates outcrop of the Mabou Group (Hopewell Cape Formation). The Dorchester Fault shows a northward-dipping reflector in seismic profiles immediately east of the Petitcodiac River (Wilson 2002), which implies that it, like the Saint-Joseph Fault, originated as a thrust. Unlike the latter structure, however, the Dorchester Fault shows evidence of having moved after deposition of the Windsor Group. The movement affects not only the Hillsborough Formation but also the marine carbonate–evaporite succession in the upper Windsor Group (St. Peter 2001).

Evidence of the earliest movements on the Edgetts Landing and Dorchester faults can be seen near Albert Mines, where F_1 and F_2 structures are rotated into the fault traces. The faults dip vertically or steeply northward here, which implies that neither structure was involved in the pre-Visean deformation of the Horton and Sussex groups. Both faults displace rocks of the Mabou and Windsor groups, and the Edgetts Landing Fault offsets outcrop of the Cumberland Group on the ridge south of Kings Quarry (Fig. 2). Both faults thus were active long after movement ceased on the Saint-Joseph Fault and its splays. The complexity of this later movement can be seen in the ridge south of Kings Quarry. Here, the Edgetts Landing Fault offsets rocks of the Windsor Group with a downthrow of 60 to 75 m to the north and offsets the base of the Mabou Group (Hopewell Cape Formation) with a downthrow of 30 to 50 m to the south. These observations suggest that the Edgetts Landing Fault underwent repeated movements with a change of throw between deposition of the Mabou and Cumberland groups.

Caledonia Fault

The Caledonia Fault is well defined around Peck Creek in the western part of the study area (Fig. 2), where it forms part of the northern margin of the Caledonia basement. The fault terminates outcrop of the Round Hill Formation at the southern end of the conglomerate ridge east of the Intervale Road. Along Peck Creek itself, the main fault trace delineates the boundary between basement rocks and the Round Hill Formation (Fig. 22). Although the fault surface is not exposed, outcrops on the north bank of the creek and in the creek bed lie within metres of the contact and indicate a shallow to moderate northerly dip to the fault.

About 125 m east of this locality, an outcrop in the creek bed shows shears associated with early movement on the fault. The shears trend 120° and have a northeasterly dip of 25°. They are cut by later shears that trend 80° and have a northerly dip of 80°; the late shears reflect the present fault trace.

RELATIONSHIP OF DEFORMATION TO THE HYDROCARBON SYSTEM

The Albert Formation in the study area contains all the necessary elements of a petroleum system and has a long history of hydrocarbon exploration and production. Between 1911 and 1991, Albert sands in the Stoney Creek Field (Fig. 2) produced oil and gas (Foley 1989; St. Peter 2000; St. Peter and Spady 2003). Hydrocarbon exploration in the area was revitalized following construction of the Maritimes and Northeast Pipeline in 1999 and continues today.

Information derived from the present study has enabled some constraints to be placed on the formation of potential traps and the timing of petroleum migration. Source rocks of the petroleum system in the study area are believed to be the kerogenous (oil) shale and kerogenous mudrock of the Albert Formation (Chowdhury 1995; Chowdhury et al. 1991). Kerogen laminae are ubiquitous in the oil shale; some beds contain up to 27% total organic carbon (St. Peter and Spady 2003).

Extensive thermal maturation data exist for the Albert Formation in southeastern New Brunswick. Data include vitrinite reflectance, spore colour alteration indices, and Rock-eval Pyrolysis (Tmax) results for hundreds of outcrop and well samples (MacIntosh and St. Peter 2005). The data show that the organic-rich Albert beds in the study area matured to at least the oil window. Further evidence of this maturation level is demonstrated by the many surface showings of dead oil or bitumen (Martel 1985). The more deeply buried (greater than 2 km) beds west of Hillsborough (Fig. 2) lie within the dry gas zone (Chowdhury 1995).

Structural events that resulted in the formation, and possible subsequent breaching, of petroleum traps in the study area have been studied (Gussow 1953; Hea 1974; Foley

1989; St. Peter 1992; Chowdhury 1995; Wilson 2002) but never assessed in detail. The subject is beyond the mandate of the present study as well, but a few observations are warranted. The Stoney Creek Field, and its eastern extension near Dover and Taylor Village across the Petitcodiac River (Fig. 2), is a combined stratigraphic/structural trap (Henderson 1940; Foley 1989). The gas-leg at Stoney Creek occurs within a gently south-dipping homocline in the northern and western parts of the field. The oil-leg occurs within an anticlinal closure in the southeast part of the field. The anticline does not appear to include warped beds of the overlying Sussex Group, which have a fairly uniform east–west strike and southerly dip along the south flank of the field. By implication, the folding event that produced the anticlinal oil trap took place during deposition of the Horton Group before deposition of the Sussex Group.

Seismic reflection profiles and borehole records from sites between Albert Mines and Taylor Village (Lynch 1999; Wilson 2002) reveal an antiform in the Albert Formation that has an east-northeast-trending axis. The antiform lies unconformably below the north-dipping unconformity beneath the Sussex Group (Round Hill Formation) and was shaped during deposition of the Horton Group. In 2001 and 2002, Columbia Natural Resources Canada Limited undertook oil test production of the Stoney Creek Field, drilling four wells near the crest of the antiform in the Edgetts Landing and Taylor Village areas.

The timing of migration is estimated, partly on the basis of burial history charts, to be late Carboniferous (Chowdhury 1995) or even Permian (St. Peter 1997). Oil shows have been reported from all formations in the area up to and including the Boss Point Formation (Martel 1985; St. Peter and Johnson 1997, 2004 revision). During the present study, solid bitumen (albertite) veins and/or oil shows were observed in 1) most exposures of the Albert Formation, 2) beds of the Round Hill and Gautreau formations in the Boudreau Village section, 3) conglomerate of the Hillsborough Formation at Edgetts Landing, 4) carbonates and sulphates of the Windsor Group near Kings Quarry, and 5) conglomerate of the Hopewell Cape Formation overlying the Albert Formation at Albert Mines.

Hydrocarbon generation and migration likely did not take place during deposition of the Horton or Sussex groups or while deformation occurred during, or shortly after, their deposition. None of the albertite veins observed in beds of the Horton Group (Albert Formation) or Sussex Group, for instance, is crumpled by folds. Significantly, the beefsteak calcite veins that mark the detachment surface in the oil shale test pit at Albert Mines are bitumen-free; similar veins marking the thrust detachment at Peck Creek also contain no bitumen.

Evidence suggests that the Saint-Joseph Fault (Fig. 2) was dormant prior to deposition of the Hopewell Cape Formation (St. Peter and Johnson 1997, 2004 revision). Because faults that cut evaporites are known to seal quickly, the Saint-Joseph Fault and its splays most likely would not have provided pathways through the Gautreau evaporites when hydrocarbon migration occurred during the late Carboniferous. The possibility therefore exists that evaporites from the Gautreau Formation may have acted as a seal for oil or gas in the underlying Albert Formation. The potential relationship has not yet been assessed in the study area but could be significant. To date, no deep test holes have been drilled in sandstone of the Albert Formation below the Gautreau evaporites.

Faults that cut beds of the source rocks in the Albert Formation, that predate petroleum migration, and that did not become sealed, appear to have acted as upward migration pathways into younger strata. The albertite veins and oil shows in rocks of the Boss Point Formation are an example of such migration. Faults with late displacements such as the Edgetts Landing and Dorchester faults almost certainly would have breached charged traps in the underlying Albert Formation. Petroleum explorationists thus should assess in detail the movement history of faults situated near any potential hydrocarbon plays being evaluated.

CONCLUSIONS

Based on results of the present study and previous investigations, the relationship between deformation events and faults in the area bounded by Rosevale and Saint-Joseph in southeastern New Brunswick can be summarized as follows.

1. Rocks of the Horton and Sussex groups underwent a deformation episode characterized by predominantly bedding-parallel strain that produced folds (F_1) with box-like profiles and bedding-parallel shear zones whose vergence indicates movement along thrusts with a top-to-the-south (between south-southwest and south-southeast) motion. Trains of chevron-profiled folds developed locally and are marked by overtightening of closures and hinge collapse along minor faults. These features are overprinted by a related set of open to tight upright folds (F_2) that plunge consistently southwest. The plunge is steep around Saint-Joseph and Boudreau Village and more shallow farther west at Albert Mines and Rosevale. Overall kinematic analysis suggests that this southward shortening was accompanied by right-lateral movement along west-southwest-trending strike-slip structures. In the Peck Creek–Weldon Creek section, all these features are truncated by the angular unconformity that defines the base of the Hillsborough Formation. If the correlation of the felsite at Peck Creek with the Boyd Creek Tuff is valid, this deformation affected rocks of both the Horton and Sussex groups and occurred during deposition of the Weldon Formation. This is not the first study to imply the importance of thrusts in deformation of Carboniferous rocks in the Hillsborough region (cf. Gussow 1953). However, it is the first investigation able to delimit a thrust-related deformation event to a narrow age range, that being the late Tournaisian or earliest Visean. Even if the correlation of the felsite at Peck

Creek with the Boyd Creek Tuff is not confirmed, this deformation event still must predate deposition of the Hillsborough Formation.

2. Several of the large regional faults, specifically the Saint-Joseph, Caledonia and Dorchester faults, are candidates for having originated as thrusts during deformation that occurred before deposition of the Hillsborough Formation.

3. The Caledonia Fault has not affected rocks of the Windsor Group in the Gray Brook syncline and appears to be the only regional fault that became dormant after this earlier history of deformation.

4. The Edgetts Landing Fault seems not to have shared the early history of other regional faults, at least as a thrust fault (Wilson 2005). The first surface manifestation of the Edgetts Landing Fault in the Albert Mines area is the rotation of F_1 and F_2 folds and related features. Dip-slip movement along the fault occurred during at least two later events. Following deposition of the Windsor Group, carbonates of that group were downthrown to the north along the fault; sometime after that event, rocks of the Mabou and Cumberland groups were downthrown to the south across the same structure.

5. The Dorchester Fault has the longest and most complex movement history of all structures in the study area. Its early history appears to have been as a thrust fault related to F_1 and F_2 folding in the Horton and Sussex groups. In the upper reaches of Peck Creek, it is manifested as a reverse fault that brings rocks of the Caledonia basement over those of the Hillsborough Formation (McLeod 1980). Near Upper Dorchester, the fault juxtaposes the Windsor Group (Lime-kiln Brook Formation) with the Horton Group (Albert Formation) (St. Peter 2001). The Dorchester Fault also displaces rocks of the Cumberland Group (Boss Point Formation) between the Petitcodiac and Memramcook rivers (St. Peter and Johnson 1997, 2004 revision).

ACKNOWLEDGEMENTS

This study would not have been possible without the collaboration of several colleagues. Thanks are especially due to Les Fyffe, Director of the Geological Surveys Branch, New Brunswick Department of Natural Resources, for his support from the beginning. Paul Wilson and David Keighley with the Department of Geology, University of New Brunswick (UNB), have been a constant source of ideas and discussion both in the laboratory and in the field. Special thanks go to Perry Clark: a more enthusiastic and helpful field assistant could not have been wished for. Joseph C. White, Chair of the Department of Geology at UNB, offered personal support, departmental facilities, and discussions on the results of this study. Ancel Murphy and Calvin Nash, technicians in the

Department of Geology, provided their invaluable skills in preparing thin sections and rock slabs from some singularly intractable material. Don Gemmell of Three-D GeoConsultants Ltd., Fredericton, permitted free access to old files and records pertaining to the Albert Mines and Le Blanc Creek areas, and his help is gratefully acknowledged.

Steve McCutcheon with the Geological Surveys Branch of the New Brunswick Department of Natural Resources is thanked for editing our first draft and greatly improving the organization and brevity of the paper.

REFERENCES

Alcock, F.J. 1948. Exploration of oil shale in the Albert Mines area. *In* Summary of Investigations on New Brunswick Oil Shale. Canada Department of Mines and Resources; Mines, Forests and Scientific Services Branch, No. 825, pp. 11–18.

Browne, G.H. 1991. The sedimentology of the Boss Point Formation (Pennsylvanian), eastern New Brunswick and northern Nova Scotia. Unpublished Ph.D. thesis, University of Western Ontario, London, Ontario, Canada, 552 p.

Carter, D.C., and Pickerill, R.K. 1985a. Algal swamp, marginal and shallow evaporitic lacustrine lithofacies from the Late Devonian–Early Carboniferous Albert Formation, southeast New Brunswick, Canada. Maritime Sediments and Atlantic Geology, **21**: 69–86.

Carter, D.C., and Pickerill, R.K. 1985b. Lithostratigraphy of the Late Devonian–Early Carboniferous Horton Group of the Moncton Subbasin, southern New Brunswick. Maritime Sediments and Atlantic Geology, **21**: 11–24.

Cas, R.A.F., and Wright, J.V. 1988. Volcanic successions modern and ancient. Unwin Hyman, London, 528 p.

Chowdhury, A.H. 1995. Sedimentology, diagenesis and organic geochemistry of the Albert Formation, Moncton Subbasin, New Brunswick, Canada. Unpublished Ph.D. thesis, University of New Brunswick, Fredericton, New Brunswick, Canada, 249 p.

Chowdhury, A.H., Fowler, M.G., and Noble, J.P.A. 1991. Petroleum geochemistry and geology of the Albert Formation, Moncton Subbasin, New Brunswick, Canada. Bulletin of Canadian Petroleum Geology, **39**: 315–331.

Dawson, J.W. 1853. On the Albert Mine, Hillsborough, New Brunswick. Quarterly Journal of the Geological Society London, **9**: 107–114.

Durney, D.W., and Ramsay, J.G. 1973. Incremental strains measured by syntectonic crystal growth. *In* Gravity and Tectonics. *Edited by* K.A. de Jong and R. Scholten. Wiley, New York, pp. 67–96.

Fitches, W.R., Cave, R., Craig, J., and Maltman, A.J. 1986. Early veins as evidence of detachment in the lower Palaeozoic rocks of the Welsh basin. Journal of Structural Geology, **8**: 607–620.

Foley, S.L. 1989. Geology of the Stoney Creek oil and gas field, and its implications regarding the tectonic evolution of the eastern Moncton Subbasin, New Brunswick.

Department of Natural Resources and Energy; Minerals and Energy Division, Geoscience Report 89-1, 77 p.

Greiner, H.R. 1962. Facies and sedimentary environments of Albert shale, New Brunswick. American Association of Petroleum Geologists Bulletin, **46**: 219–234.

Gussow, W.C. 1953. Carboniferous stratigraphy and structural geology of New Brunswick, Canada. American Association of Petroleum Geologists Bulletin, **34**: 1713–1816.

Hea, S.P. 1974. Petroleum potential of the province of New Brunswick, Canada. Unpublished report, Weaver Oil and Gas Corporation, 51 p.

Henderson, J.A.L. 1940. The development of oil and gas in New Brunswick. Canadian Institute of Mining and Metallurgy, Transactions, **43**: 159–178.

Hobbs, B.E., Means, W.D., and Williams, P.F. 1976. An outline of structural geology. Wiley, New York, 571 p.

Lynch, G. 1999. Shell Canada Limited Albert oil shale: geological results from slim hole drilling program, November 15, 1998–99. Unpublished work report on Shell Canada Limited bituminous shale licences to search. Submitted to New Brunswick Department of Natural Resources and Energy; Minerals and Energy Division, 33 p.

MacIntosh, J.A., and St. Peter, C.J. 2005. Maritimes basin thermal maturation project: Carboniferous organic geochemical (NB_COG) database for New Brunswick. New Brunswick Department of Natural Resources; Minerals, Policy and Planning Division, Geological Surveys Branch, Open File Report 2005-5, 55 pp.

Martel, A.T. 1985. Reservoir characteristics of surface showings, Hillsborough (21 H/15) map-area. New Brunswick Department of Forests, Mines and Energy; Mineral Resources Division, Plate 86-83B.

McCutcheon, S.R. 1981. Stratigraphy and paleogeography of the Windsor Group in southern New Brunswick. New Brunswick Department of Natural Resources; Mineral Resources Branch, Open File Report 81-31, 210 p.

McLeod, M.J. 1980. Geology and mineral deposits of the Hillsborough area, map area V-22 and V-23 (parts of 21H/15E and 21H/15W). New Brunswick Department of Natural Resources; Mineral Resources Branch, Map Report 79-6, 35 p.

Nickerson, W.A. 1994. Geophysical constraints on the stratigraphy, structure and tectonic evolution of the Late Devonian/Carboniferous Moncton Subbasin, New Brunswick. Unpublished Ph.D thesis, Memorial University of Newfoundland, St. John's, Newfoundland, Canada, 340 p.

Norman, G.W.H. 1932. Stratigraphy of the Stoney Creek oil and gas field, New Brunswick. *In* Oil and Gas in Eastern Canada. Canada Department of Mines, Geological Survey, Economic Geology Series 9, pp.167–173.

Norman, G.W.H. 1941. Hillsborough map sheet, Albert and Westmorland counties, New Brunswick. Geological Survey of Canada, Map 647A (with marginal notes).

Ramsay, J.R. 1974. Development of chevron folds. Geological Society of America Bulletin, **85**: 1741–1754.

Ramsay, J.R., and Huber, M.I. 1983. The techniques of modern structural geology. Vol. I: strain analysis. Academic Press, London, 700 p.

St. Peter, C. 1988. Assessment of potential sites of recoverable oil shale in New Brunswick. Department of Natural Resources and Energy; Minerals and Energy Division, Geoscience Report 88-2, 70 p.

St. Peter, C. 1992. Lithologic facies, seismic facies, and strike-slip setting of the Lower Carboniferous alluvial/fluvial/lacustrine Albert Formation of New Brunswick. New Brunswick Department of Natural Resources and Energy; Mineral Resources Division, Geoscience Report 92-2, 145 p.

St. Peter, C. 1993. Maritimes Basin evolution: key geologic and seismic evidence from the Moncton Subbasin of New Brunswick. Atlantic Geology, **29**: 233–270.

St. Peter, C. 1997. The Carboniferous petroleum system of New Brunswick — a review (abstract). *In* Canadian Society of Petroleum Geologists–Society of Economic Paleontologists and Mineralogists, Joint Convention (June 1997, Calgary), Program with Abstracts (p. 22). *Compiled by* B. Beauchamp.

St. Peter, C. 2000. Oil shale and oil and natural gas in New Brunswick: historical and current industry-related activities. New Brunswick Department of Natural Resources and Energy; Minerals and Energy Division, Information Circular 2000-5, 14 p.

St. Peter, C. 2001. Petroleum geology in the Carboniferous of southeastern New Brunswick. *In* Guidebook to Field Trips in New Brunswick and Western Maine. *Edited by* R. Pickerill and D. Lentz. 93rd Annual Meeting New England Intercollegiate Geological Conference, Fredericton, New Brunswick, Trip A-4, 30 p.

St. Peter, C. 2002. Bedrock geology of the McCully natural gas field area, Moncton Subbasin (parts of 21 H/11, 12, 13, and 14), New Brunswick. New Brunswick Department of Natural Resources and Energy; Minerals and Energy Division, Plate 2002-33 (revised 2004).

St. Peter, C. 2004. Recent advances in understanding of Carboniferous stratigraphy in New Brunswick. *In* Exploration and Mining in New Brunswick. *Edited by* S.A.A Merlini. New Brunswick Department of Natural Resources; Minerals, Policy and Planning, Information Circular, Abstracts, pp. 47–48.

St. Peter, C., and Johnson, S.C. 1997. Carboniferous geology of the Hillsborough map area (NTS 21 H/15), Westmorland and Albert counties, New Brunswick. New Brunswick Department of Natural Resources and Energy; Minerals and Energy Division, Plate 97-8 (revised 2004).

St. Peter, C., and Spady, D. 2003. Gas find puts focus on New Brunswick. The American Oil & Gas Reporter, **46** (5): 55–63.

Shroder, J.F. 1963. Stratigraphy and tectonic history of the Moncton Group of nonmarine redbeds of New Brunswick, Canada. Unpublished M.Sc. thesis, University of Massachusetts, Amherst, Massachusetts, U.S.A., 83 p.

Tanner, P.W.G. 1989. The flexural-slip mechanism. Journal of Structural Geology, **11**: 635–655.

Webb, G.W. 1963. Occurrence and exploration significance of strike-slip faults in southern New Brunswick, Canada. American Association of Petroleum Geologists Bulletin, **47**: 1904–1927.

Williams, P.F., and Urai, J.L. 1989. Curved fibre veins: an alternative explanation. Tectonophysics, **158**: 311–333.

Wilson, P. 2002. Structural geology of the Albert Mines–Taylor Village area, southeastern New Brunswick. *In* Current Research 2001. *Edited by* B.M.W. Carroll. New Brunswick Department of Natural Resources and Energy; Minerals, Policy and Planning Division, Mineral Resource Report 2002-4, pp. 129–153.

Wilson, P. 2005. Stratigraphy, structural geology and tectonic history of the McCully area, southwestern Moncton Subbasin, southern New Brunswick. New Brunswick Department of Natural Resources; Minerals, Policy and Planning Division, Mineral Resource Report 2005-5, 104 p.

Wilson, P., White, J.C., Park, A.F., Keighley, D., and Gingras, M.K. 2004. Strain features and deformation mechanisms in synsedimentary high-strain zones. Geological Association of Canada, Annual Meeting Abstracts, 2004, p. 134.

Wright, W.J. 1922. Geology of the Moncton map-area. Canada Department of Mines, Geological Survey, Memoir No. 129, 69 p.

INFORMATION VALUES FOR TRACE ELEMENTS IN FIVE NEW BRUNSWICK TILL REFERENCE MATERIALS

ALLEN A. SEAMAN [1] AND G. REX BOLDON [1]

[1] Geological Surveys Branch, New Brunswick Department of Natural Resources,
P.O. Box 6000, Fredericton, New Brunswick, CANADA E3B 5H1 *(allen.seaman@gnb.ca)*

Seaman, A.A., and Boldon, G.R. 2005. Information values for trace elements in five New Brunswick till reference materials. *In* Geological Investigations in New Brunswick for 2004. *Edited by* G.L. Martin. New Brunswick Department of Natural Resources; Minerals, Policy and Planning Division, Mineral Resource Report 2005-1, pp. 99–126.

The New Brunswick Department of Natural Resources (NBDNR) has prepared five standard reference samples for use as laboratory checks in its ongoing till geochemistry program. They are designated as standards NB-CS1, NB-01, NB-02, NB-03, and NB-04. Values of NB-CS1 and NB-04 approximate the mean values for basal tills in west-central New Brunswick. NB-01 has extremely anomalous values for base and precious metals. NB-02 and NB-03 are characterized by elevated values for Au and associated elements.

The NBDNR has sufficient quantities of NB-CS1, NB-02, NB-03, and NB-04 to provide splits for prospectors and mining companies active in the province. Supplies of NB-01 are highly limited, however, and it is recommended that another standard be developed to represent anomalous base-metal values.

Le ministère des Ressources naturelles du Nouveau-Brunswick (MRNNB) a préparé cinq échantillons de référence standard qui seront utilisés comme échantillons témoins de laboratoire dans le cadre de son programme permanent d'étude géochimique des tills. Les échantillons sont désignés à titre de normes NB-CS1, NB-01, NB-02, NB-03 et NB-04. Les concentrations des échantillons NB-CS1 et NB-04 correspondent aux concentrations moyennes approximatives des tills de fond dans le centre-ouest du Nouveau-Brunswick. L'échantillon NB-01 présente des concentrations extrêmement anomales de métaux communs et de métaux précieux. Les échantillons NB-02 et NB-03 se caractérisent par des concentrations élevées d'Au et d'éléments connexes.

Le MRNNB dispose de quantités suffisantes d'échantillons NB-CS1, NB-02, NB-03 et NB-04 pour fournir des échantillons fractionnés aux prospecteurs et aux sociétés minières actives dans la province. Les réserves d'échantillons NB-01 sont toutefois très limitées; il est recommandé qu'on établisse une autre norme pour représenter les concentrations anomales de métaux communs.

INTRODUCTION

For many years, till samples sent by the New Brunswick Department of Natural Resources (NBDNR) to external laboratories for geochemical analysis were accompanied by splits of standard reference materials from the Geological Survey of Canada (GSC). The GSC standards included lake sediment and stream sediment standards LKSD-1, LKSD-2, LKSD-3, LKSD-4, STSD-1, STSD-2, STSD-3, and STSD-4 (Lynch 1990); and soil and till standards TILL-1, TILL-2, TILL-3, and TILL-4 (Lynch 1996). Because stocks for many of the GSC standards have gradually become depleted, the NBDNR decided in 2001 to develop its own reference materials to supplement the GSC standards. The NBDNR standards comprise one natural sample, designated as NB-CS1, and four manufactured mixtures, designated as NB-01, NB-02, NB-03, and NB-04.

During development of the GSC LKSD and STSD standards, Lynch (1990) specifically avoided using or incorporating reference samples that were highly anomalous in one or more elements. Concentration gradients were broadened for several elements during development of the TILL standards (Lynch 1996). When producing the NBDNR reference materials, it was decided to create standards that reflected as closely as possible the range of values for economically significant elements most likely to be encountered in New Brunswick till samples. Hence, several NBDNR standards were spiked to enhance concentration values for elements of economic interest.

This paper documents preparation of the five NBDNR standards and reports their current recommended values. Data for these standards were derived from only three laboratories; in the case of some elements or element extractions, analyses were obtained from a single laboratory. These considerations are partially ameliorated by the fact that analyses have been performed on multiple batches over several years. Nonetheless, the volume of data remains limited, especially for the most recently produced standards, NB-03 and NB-04. Hence, the values are reported here solely for information purposes.

SAMPLE COLLECTION AND STANDARD PREPARATION

Standard NB-CS1

Material for standard NB-CS1 originally was collected as part of a till sampling project in the Coldstream map area (NTS 21 J/06) in west-central New Brunswick (Seaman 2001). The sample site, CS-B10, is exposed in a large roadcut beside Highway 104 on the north side of Becaguimec Stream between the community of Coldstream and the Highway 570 intersection (Fig. 1). The site comprises a thick basal-till section underlying glaciofluvial sand and gravel.

In 2000, duplicate field samples were obtained from two levels in the section. Samples CS-B10-1 and CS-B10-2 were collected at 4.3 m and 3.2 m respectively above the base of

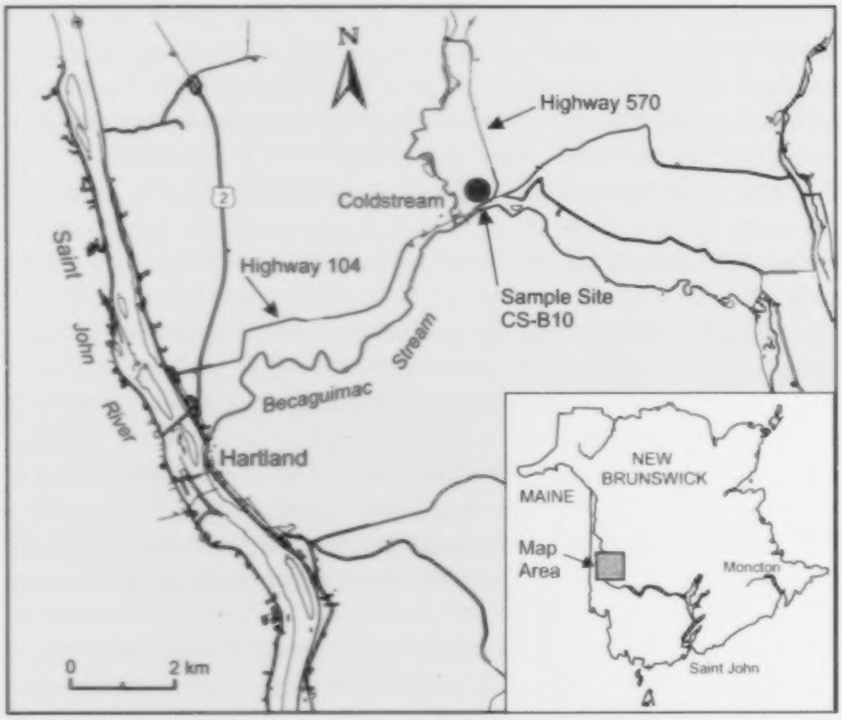

Figure 1. Location of sample site CS-B10, source of the original material for NBDNR standard reference material NB-CS1. The site corresponds to UTM Zone 19T, 618320 E, 5133160 N, NAD27.

the ditch. Analyses of the two samples yielded closely comparable values for most elements, indicating that similar material could be obtained from the site for future work (Seaman 2002). As an additional benefit, the material here is fairly fine grained. It contains only 20% to 30% gravel, and its matrix fraction comprises about 33% sand (Seaman 2001). Clay content is high, however, which causes some difficulty with disaggregation.

Archived material remaining from sample CS-B10-1 (Seaman 2002) was used to produce the initial NB-CS1 standard. The material underwent the typical till preparation method employed in the NBDNR geochemistry laboratory: it was dried and then passed through stainless steel sieves to obtain the silt-plus-clay (< 63 μm) fraction. Several kilograms of additional material collected from this site in 2002 were similarly processed.

Standards NB-01, NB-02, and NB-03

Standards NB-01, NB-02, and NB-03 were produced using material obtained primarily from NBDNR till geochemistry surveys conducted in southern, central, and northern New Brunswick. Individual till samples from these surveys were prepared as noted above for standard NB-CS1. Sufficient quantities of the silt-plus-clay fraction were removed from each sample for geochemical analysis and for archival purposes, in case future analytical work might be required. The surplus material was then used to prepare the three standards, as described below.

1. Most of standard NB-01 contains material from till sampling projects carried out during 2000 in NTS map areas 21 G/07 (Pronk et al. 2002); 21 J/06 (Seaman 2001); and 21 O/11 and 21 O/14 (Parkhill et al. 2002).

2. Standard NB-02 consists mainly of material from till sampling projects conducted during 2001 in NTS map areas 21 G/06 (Pronk et al. 2002); 21 J/06 (Seaman 2002); and 21 O/11, 21 O/12, 21 O/13, and 21 O/14 (Parkhill et al. 2002).

3. Standard NB-03 is composed mainly of material from till sampling projects carried out in 2002 in NTS map areas 21 G/03 (Pronk et al. 2003a); 21 G/10 (Pronk et al. 2003b); 21 J/06 and 21 J/07 (Seaman 2003); and 21 O/12 (Parkhill et al. 2002).

Standard NB-01 was spiked with surplus rock pulp from several mineral deposit studies. Standards NB-02 and NB-03 were mixed with miscellaneous surplus rock or mineral pulps from projects conducted by the NBDNR and University of New Brunswick. Several methods were used to homogenize the standard material; these included passing it repeatedly through sample splitters, stirring it with a paint mixer, and tumbling or rolling it in pails.

Standard NB-04

Standard NB-04 was manufactured using surplus, unprocessed material from the GSC till sampling program conducted in the Miramichi Highlands between 1985 and 1989 (Lamothe 1990a–c, 1992). The samples were processed and homogenized as noted above for the other standards. No supplementary material was added to standard NB-04; its values consequently represent the mean values for till deposits in the Miramichi Zone of central and northern New Brunswick.

CHARACTERIZATION OF REFERENCE MATERIALS

Analytical Procedures

The five NBDNR standards were developed specifically to use in the Department's ongoing till geochemistry program. Unlike the GSC standards, which were analyzed many times by more than 30 laboratories, the NBDNR standards have been analyzed by only three laboratories to date. These are Acme Analytical Laboratories Limited of Vancouver, British Columbia; Activation Laboratories Limited of Ancaster, Ontario; and Becquerel Laboratories Incorporated of Mississauga, Ontario. The three laboratories (hereafter referred to as Acme, Actlabs, and Becquerel) provided analyses that led to the establishment of provisional values for the GSC standards reported by Lynch (1990, 1996).

Acme performed analyses for the NBDNR using its "Ultratrace" Inductively Coupled Plasma–Mass Spectrometry (ICP–MS) procedure, catalogued by Acme (2005) as Group 1F-MS. The technique involves digesting a 15 or 30 g sample in aqua regia (concentrated hydrochloric and nitric acids) and analyzing the resulting solution using ICP–MS. This procedure has the advantage of providing low detection limits for Ag (2 ppb) and Au (0.2 ppb) but offers only partial digestion for many other elements. Acme analyzed all splits of the five standards for the basic suite of 37 elements, which consists of Au plus Ag, *Al*, As, *B*, *Ba*, Bi, *Ca*, Cd, Co, *Cr*, Cu, *Fe*, Ga, Hg, *K*, *La*, *Mg*, *Mn*, Mo, *Na*, *Ni*, *P*, Pb, *S*, Sb, *Sc*, Se, *Sr*, Te, *Th*, *Ti*, Tl, *U*, *V*, *W*, and Zn. As well, Acme analyzed several splits of NB-01, NB-02, NB-03, and NB-04 for the full suite of 53 elements, which includes all of the above plus *Be*, *Ce*, *Cs*, *Ge*, *Hf*, In, *Li*, *Nb*, *Pd*, *Pt*, *Rb*, Re, *Sn*, *Ta*, *Y*, and *Zr*. Elements shown here in italics represent those listed by Acme (2005) as having undergone only partial extraction.

Actlabs analyses provided NBDNR with "near-total" values for 54 elements in its "Au + 53" package, catalogued as Code 1H2 (Hg is catalogued separately as Code 1G; Actlabs 2005). Analyses were conducted using a variety of methods, described below.

1. Values for Au plus 34 other elements were obtained by using Instrumental Neutron Activation Analysis (INAA), which requires a sample weight of between 15 and 35 g. Values for some of these elements also were derived from other methods that offered lower detection limits. For typical New Brunswick till samples, the Actlabs INAA data provides usable values for the following elements: As, Au, Ba, Br, Ce, Co, Cr, Cs, Eu, Fe, Hf, La, Lu, Mo, Na, Nd, Rb, Sb, Sc, Sm, Ta, Tb, Th, U, W, and Yb.

2. Values for Ag, Al, Be, Ca, Cd, Cu, K, Mg, Mn, Mo, Ni, P, Pb, S, Sr, Ti, V, Y, and Zn were determined by using Inductively Coupled Plasma–Optical Emission Spectrometry (ICP–OES). The technique involves dissolving a 0.25 g sample in a four-acid solution of hydrochloric, nitric, perchloric, and hydrofluoric acids to provide a total or near-total digestion.

3. Values for Bi, Ge, In, Se, Sn, Te, and Tl were obtained by using ICP–MS on an aqua regia acid digest solution.

4. Hg values were determined by using Cold Vapour–Atomic Absorption Spectrometry (CV–AAS).

Actlabs (2005) considers its values obtained for Al, Sn, Tl, and Y to be only partial.

Duplicate splits of samples sent by NBDNR to Acme for "Ultratrace" ICP–MS analysis often are shipped as well to Becquerel for INAA testing using the company's geochemical exploration package (Becquerel 2005). The combined data from these two laboratories provide a suite of elements similar to that obtained from the Actlabs "Au + 53" package. Becquerel and Actlabs use comparable sample weights for their INAA procedure, and both laboratories follow a similar testing method. Their suite of elements, however, differs slightly in two regards. First, Becquerel reports values for Ti and Zr but not for Nd. Second, the erratic detection of Ni at levels below 100 ppm, as seen in the Actlabs INAA results, does not occur with Becquerel analyses. Becquerel Ni values are therefore usable and closely match results obtained by Actlabs using ICP–OES.

Data Analysis

A rigorous statistical analysis of the NBDNR reference materials was considered unwarranted, given the limited quantity of data available for each standard. Instead, data outliers were removed using the two-step trimming method described by Lynch (1990). The method involves calculating the mean and standard deviation of raw data for each element in a standard. In Step 1, all values lying above or below two standard deviations of the mean are trimmed from the data set; a second mean and standard deviation is then calculated from the remaining data. Step 2 duplicates Step 1 to calculate a third mean and standard deviation. Results of the third calculation define the recommended values for that element in the standard. According to Lynch (1990, p. 156), the "first step tended to remove extreme outliers; the second step produced a tighter data set."

The element Mo in standard NB-02 is used here to demonstrate the full two-step trimming process. The data set for Mo was obtained from 47 separate analyses of standard NB-02, including data generated through ICP–OES by Actlabs, ICP-MS by Acme, and INAA by both Actlabs and Becquerel. The raw mean value was 10.2 ppm and had a standard deviation of 42.9 ppm, calculated on the basis of n-1. The first trim removed an extremely high value of 298 ppm from the data set; the value likely resulted from a Mo-rich nugget within the sample split. The mean and standard deviation following the first trim were 4.0 ppm and 2.3 ppm, respectively. The second trim removed three moderately high values (9 to 13 ppm) from the data set. Based on the remaining 43 analyses, the resulting recommended value for Mo in standard NB-02 was 3.5 ppm with a standard deviation of 1.3 ppm.

When the indicated value of an element lay below the detection limit, the value was arbitrarily set at 50% of the detection limit — again, following the lead of Lynch (1990). Using the above example, two of the Mo readings in standard NB-02 occurred below the detection limit of 1 ppm. The value for these two analyses therefore was set at 0.5 ppm for calculation purposes. Lynch (1990, 1996) refers to such values as "qualified."

The mean and standard deviation were calculated to a level of precision one order of magnitude greater than that of the least accurate level of precision reported by the laboratories. For example, both Actlabs and Becquerel report Mo values to the 1 ppm level, whereas Acme reports Mo values to the 0.01 ppm level. The mean and standard deviation values for Mo therefore are reported to a precision of 0.1 ppm.

Results

The two-step trimming process was not required for all data during production of the NBDNR standards. Certain elements in some standards showed no outliers in the raw data; other elements needed only one trim to bring all values to within two standard deviations of the mean.

Table 1 (which appears with Tables 2 to 7 at the end of this paper) lists recommended near-total values for each element in the five NBDNR standards. Tables 2 to 6 show additional details for each standard, including the:

- partial extraction data obtained;
- sample standard deviations, based on n-1;
- number of analyses on which the mean and standard deviation were based;
- number of qualified values;
- number of outliers, if any, excluded from the data set during the trimming process; and
- analytical methods used to generate the data.

Where the calculated mean value following the second trim lay below the highest detection limit for that element, the mean value was shown (Tables 1 to 6) as being less than that detection limit (e.g. < 1) and given no standard deviation. Similarly, the partial extraction value for W in standard NB-03 is shown to be greater than 100 ppm.

Interlab Correlations

Near-total values provided by the three laboratories were comparable for most elements. Most major discrepancies related to elements such as Ag, Ta, and Tb that typically occur at levels approaching the lower limit of detection. However, several other systematic discrepancies were observed.

Sb values from Acme were consistently lower than those from Actlabs and Becquerel and so were not included in the near-total Sb values on Table 1. For the same reason, Acme Sb values were listed separately on Tables 2 to 6 from those provided by Actlabs and Becquerel. Acme Sb values for the GSC standards were also consistently lower than total values reported by Lynch (1990, 1996) but were comparable to partial extraction values for the lake and stream sediment standards reported by Lynch (1990). One possible explanation for the discrepancy is that Sb underwent some volatilization during sample dissolution. Acme (2005) reports this possibility for some of their other analytical methods that use the more aggressive, four-acid digest technique.

A large discrepancy exists between Actlabs and Acme results for Tl: Actlabs values are two to nine times higher than Acme values. Actlabs (2005) reports that its technique gives only partial extraction of Tl, whereas Acme (2005) states that its methodology allows for full Tl dissolution. Because Lynch (1990, 1996) did not provide Tl values for the GSC standards, this discrepancy cannot be explained and is simply reported here.

The Acme and Actlabs partial digestion values for Sn are closely comparable, but the Actlabs digestion technique for Al and Y is more thorough than that of Acme. Consequently, Actlabs values are two to five times higher for Al and are two to three times higher for Y. For comparison, the mean values of Al and Y obtained from Actlabs for the GSC standards range from 50% to 100% of the total values reported by Lynch (1990, 1996).

Homogeneity Testing

No formal homogeneity tests have been conducted on the five NBDNR standard reference samples. However, the standards have yielded similar analytical values each year since their development, which indicates an acceptable homogeneity. Moreover, homogeneity of the NBDNR standards appears to closely match that of the GSC standards: a comparison of standard deviations for both series shows the deviations to be of comparable magnitude for most elements (Table 7).

Notwithstanding the above, the NBDNR does not yet totally rely on these new standards. All sample batches are currently shipped with both GSC and NBDNR standards, allowing the GSC standards to serve as verifiers of the NBDNR materials.

Comparison of NBDNR Standards with Natural Basal Till Samples

Table 1 compares the five NBDNR standards with basal till samples collected in west-central New Brunswick between 1990 and 2004. Minimum and maximum values for the basal till samples were derived from 1803 samples, with the following exceptions.

1. For elements analyzed by ICP–OES (except base-metal elements), values were based on 1105 samples; base-metal values included analyses by AAS.

2. For elements analyzed by ICP–MS (except Sn), values were based on 759 samples; Sn values included analyses by a fusion-ICP procedure.

The mean and standard deviation for each element were calculated after using a one-step trim process to eliminate values that differed by more than four standard deviations from the mean of the raw data. Calculations were based on a reduced data set that used only one sample site per grid point. Potentially anomalous follow-up samples collected for analytical confirmation work were deleted from the data set to remove their elevating influence on the mean.

The following definitions are based on values obtained from one-step trimming of the reduced west-central New Brunswick data set:

- threshold anomalous: 2 to < 4 standard deviations above the mean;
- anomalous: 4 to < 8 standard deviations above the mean;
- very anomalous: 8 to < 16 standard deviations above the mean; and
- extremely anomalous: ≥ 16 standard deviations above the mean.

Standard NB-CS1

Standard NB-CS1 is anomalous in Ca, and threshold anomalous in Mn and Sr. Values for Hf and Se lie well below mean values, whereas values for Co, Mg, and Ni are elevated but subthreshold. Values for the remaining elements lie within one standard deviation of the mean.

Standard NB-01

Standard NB-01 is extremely anomalous in Ag, As, Au, Bi, Cd, Cu, Pb, Sb, and Zn; very anomalous in Hg, Mo, Se, and Te; and anomalous in Ba, Ca, Mn, Sr, and W. It represents the only NBDNR standard to contain In in values above the 0.2 ppm detection limit of Actlabs. Be, Co, Fe, and P are present at elevated but subthreshold levels. Near-total values for the remaining elements lie within one standard deviation of the mean. Partial extraction data indicate that this standard is also extremely anomalous in S and anomalous in Sn.

Standard NB-02

Standard NB-02 is extremely anomalous in W; anomalous in As, Ca, and Co; and threshold anomalous in Au, Sr, and Ta. Values for Cr, Hf, Ni, Ti, and V lie well below mean values, whereas values for Bi, K, Lu, Na, Pb, Rb, Tb, Yb, and Zn occur at elevated but subthreshold levels. Near-total values for the remaining elements lie within one standard deviation of the mean. Partial extraction data indicate that this standard is also threshold anomalous in S.

Standard NB-03

Standard NB-03 is extremely anomalous in W; very anomalous in Au; anomalous in Hg, Pb, and Sb; and threshold anomalous in As and Co. Cr, Eu, Fe, Hf, Nd, Sc, and V are present at levels well below the mean. K, Na, and Ta are present at elevated but subthreshold levels. Values for the remaining elements lie within one standard deviation of the mean.

Standard NB-04

Standard NB-04 differs from the other till reference materials in being a true average standard. It is devoid of anomalous element concentrations, and values for most elements lie within one standard deviation of the mean. The exceptions are Ca, Mg, Sr, Ti, and Zn, which occur at elevated but subthreshold levels; and Eu, Lu, Nd, and Se, which occur at low concentration levels.

CONCLUSIONS

The five till reference materials developed by the NBDNR have met the Department's need to supplement the dwindling stocks of GSC standards. Sufficient data now exist for standards NB-CS1, NB-01, and NB-02 to confidently use their recommended values for most elements. The data available for standards NB-03 and NB-04 are more limited but nonetheless are homogenous enough to serve as standards. Future analyses will refine the elemental values assigned to each standard and likely will improve confidence in them.

Values obtained for standards NB-CS1 and NB-04 closely approximate those of the average basal till from west-central New Brunswick. Standards NB-02 and NB-03 possess elevated Au, As, and W values and will serve as suitable reference checks for samples showing anomalous concentration levels of these elements. Standard NB-01 is a good check material for samples that contain extremely anomalous values of precious and base metals. Although the more extreme values in standard NB-01 are several times higher than the highest values from basal till samples just mentioned, it is reasonable to expect such values from samples obtained proximal to a mineral occurrence.

The NBDNR holds sufficient quantities of standards NB-CS1, NB-02, NB-03, and NB-04 to offer splits to prospectors and mining companies active in New Brunswick. Quantities of standard NB-01 are more limited, and splits of this standard will be available only for applications where samples are expected to contain extremely anomalous values of base or precious metals. It is recommended that another standard be developed to represent anomalous base-metal values. A proviso for obtaining standard splits will be to send the NBDNR a copy of all analytical results obtained for them, together with details concerning the analytical methodology used. New data thus obtained will be combined with the NBDNR data to refine elemental values for all five standards.

TABLES 1 TO 7

Table 1
Comparison of mean "near-total" values for NBDNR Standard reference materials with range of values obtained for basal till samples from west-central New Brunswick.

Table 2
Current recommended values for NBDNR standard reference material NB-CS1.

Table 3
Current recommended values for NBDNR standard reference material NB-01.

Table 4
Current recommended values for NBDNR standard reference material NB-02

Table 5
Current recommended values for NBDNR standard reference material NB-03.

Table 6
Current recommended values for NBDNR standard reference material NB-04.

Table 7
Comparison of standard deviation as percentage of mean value for GSC and NBDR standard reference material.

Table 1. Comparison of mean "near-total" values for NBDNR standard reference materials with range of values obtained for basal till samples from west-central New Brunswick.

	NBDNR Standards					**Basal Till Samples from West-Central New Brunswick**			
	NB-CS1	**NB-01**	**NB-02**	**NB-03**	**NB-04**	**Min.**	**Mean**	**S. Dev.**	**Max.**
Element									
Ag (ppm)	**< 0.4**	**19.8**	**0.35**	< 0.5	*< 0.4*	< 0.2	0.3	0.2	5.7
As (ppm)	**11.1**	**840.8**	**90.86**	63.42	15.63	< 0.5	17.96	17.35	1512.5
Au (ppb)	**1.3**	**89.1**	**9.6**	20.0	1.4	< 2	2.1	2.0	60
Ba (ppm)	508	1114	363	*357*	*383*	< 51	437	104	2800
Be (ppm)	1.7	4.9	4.1	*4.1*	*3.3*	< 1	2.7	1.7	16
Bi (ppm)	**0.21**	**66.53**	**2.63**	1.53	*0.94*	< 0.1	0.84	1.06	16.4
Br (ppm)	< 0.5	7.21	1.81	*4.41*	*7.98*	< 0.5	7.52	7.71	113
Ca (%)	2.0	1.6	2.1	*0.664*	*0.920*	< 0.01	0.395	0.295	2.56
Cd (ppm)	**< 0.3**	**30.2**	**0.31**	< 0.3	*< 0.3*	< 0.3	0.31	0.19	3.2
Ce (ppm)	76.1	78.7	81.4	*75.3*	*76.2*	30	96.4	22.7	870
Co (ppm)	**20.8**	**21.7**	**36.8**	33.7	14.0	3	14.9	5.0	59
Cr (ppm)	120	87.8	52.8	*61.9*	*87.5*	9	99.5	26.2	394
Cs (ppm)	5.2	6.3	6.9	*6.0*	*5.4*	2	6.2	3.5	147
Cu (ppm)	**29.7**	**1095.8**	**30.3**	23.8	*34.5*	3	26.0	11.5	401
Eu (ppm)	1.7	1.5	1.2	*1.0*	*1.0*	< 0.2	1.5	0.3	5.1
Fe (%)	4.24	5.32	2.99	*2.81*	*3.78*	1.37	3.73	0.84	11.15
Ga (ppm)	5.87	5.79	4.69	*4.69*	*6.75*	-	-	-	-
Ge (ppm)	0.50	0.16	0.30	0.15	*0.27*	< 0.1	0.47	0.30	1.8
Hf (ppm)	7.2	8.3	5.4	*4.9*	*8.0*	4	10.5	2.5	31
Hg (ppb)	**35.3**	**354.9**	**25.3**	228.8	*36.4*	< 5	39.7	26.6	374
In (ppm)	< 0.2	1.37	< 0.2	< 0.2	*< 0.1*	-	-	-	-
K (%)	2.149	1.599	2.872	*2.756*	*2.510*	0.46	2.105	0.537	5.43
La (ppm)	38.3	37.6	38.0	*39.8*	*40.6*	12	45.2	9.7	150
Lu (ppm)	0.45	0.51	0.90	*0.51*	*0.32*	0.13	0.63	0.19	2.85
Mg (%)	1.477	1.201	1.044	*0.771*	*1.503*	0.19	1.105	0.337	2.48
Mn (ppm)	1576.1	2842.5	612.0	*535.1*	*891.0*	65	740.2	366.4	7797

Table 1 *(cont'd)*. Comparison of mean "near-total" values for NBDNR standard reference materials with range of values obtained for basal till samples from west-central New Brunswick.

	NBDNR Standards					Basal Till Samples from West-Central New Brunswick			
	NB-CS1	NB-01	NB-02	NB-03	NB-04	Min.	Mean	S. Dev.	Max.
Element									
Mo (ppm)	**< 1**	**20.5**	**3.5**	1.7	0.9	< 1	1.7	1.9	31
Na (%)	1.19	1.27	1.995	*1.717*	*1.450*	0.02	1.360	0.348	2.75
Nd (ppm)	32.4	28.0	28.0	*25.3*	*24.3*	< 6	35.4	9.3	110
Ni (ppm)	65.1	42.4	20.7	*36.3*	*53.0*	6	45.7	16.0	174
P (%)	0.0650	0.0871	0.0560	*0.0422*	*0.0650*	0.008	0.0584	0.0227	0.301
Pb (ppm)	**15.7**	**2590.7**	**34.3**	67.2	*27.7*	4	20.7	10.0	587
Rb (ppm)	96.3	89.4	180	*157*	*100*	< 6	113	54	558
Sb (ppm)	0.99	61.97	1.73	*4.88*	*0.95*	< 0.1	1.21	0.81	100
Sc (ppm)	15.8	12.6	13.4	*9.91*	*13.1*	3.9	14.2	3.1	34.4
Se (ppm)	**0.24**	**3.22**	**0.33**	0.55	*0.22*	< 0.1	0.57	0.25	10.4
Sm (ppm)	6.37	6.28	7.83	*6.66*	*6.15*	2.2	7.03	1.80	20.5
Sr (ppm)	137.4	195.8	132.1	*96.4*	*103.3*	18	80.3	22.6	182
Ta (ppm)	0.81	0.63	3.9	*2.52*	*0.98*	< 0.5	1.22	0.96	10.4
Tb (ppm)	0.79	0.61	1.56	*0.95*	*0.73*	< 0.5	0.88	0.46	3.8
Te (ppm)	< 0.1	**0.80**	**< 0.1**	< 0.1	*< 0.1*	< 0.1	0.12	0.08	1.6
Th (ppm)	9.9	12.0	18.52	*18.06*	*13.63*	6.8	15.27	6.51	100
Ti (ppm)	0.510	0.489	0.377	*0.424*	*0.652*	0.13	0.503	0.121	1.23
U (ppm)	2.26	3.86	7.16	*5.49*	*4.22*	< 0.5	4.35	2.85	77
V (ppm)	102.7	86.9	63.9	*68.7*	*117.3*	22	96.1	23.8	295
W (ppm)	< 1	9.6	301.2	*220.5*	*2.6*	< 1	1.3	2.0	75
Yb (ppm)	3.1	3.5	5.6	*4.0*	*3.1*	0.8	4.2	1.3	19.3
Zn (ppm)	**71.7**	**3447**	**86.3**	60.7	*89.6*	16	66.5	18.5	1126
Zr (ppm)	*282*	291	*278*	*387*	*310*	-	-	-	-

Underlined italic font indicates < 5 separate analyses. *Italic font* indicates 5–9 separate analyses.

Normal font indicates 10–24 separate analyses. **Bold font** indicates ≥ 25 separate analyses.

Table 2. Current recommended values for NBDNR standard reference material NB-CS1.

	Recommended Values for Standard NB-CS1					**Analytical Methods Used**			
	Mean	**S.D.**	**n**	**Qualified**	**Outliers**	**ICP-MS**	**ICP-OES**	**INAA**	**Other**
Element									
Ag (ppb)	29.4	2.3	14	1	1	X			
Ag (ppm)	0.36	0.19	12	5	0		X		
Al (%)	*2.023*	*0.139*	*15*	*0*	*0*	*X*			
Al (%)	*5.952*	*1.686*	*12*	*0*	*0*		*X*		
As (ppm)	11.1	2.4	31	0	2	X		X	
Au (ppb)	1.3	1.0	30	10	3	X		X	
B (ppm)	*3.2*	*0.7*	*15*	*0*	*0*	*X*			
Ba (ppm)	*109.49*	*9.90*	*14*	*0*	*1*	*X*			
Ba (ppm)	508	54	15	0	3			X	
Be (ppm)	1.7	0.8	12	3	0		X		
Bi (ppm)	0.21	0.08	25	0	2	X			
Br (ppm)	< 0.5	-	18	17				X	
Ca (%)	*1.819*	*0.110*	*14*	*0*	*1*	*X*			
Ca (%)	2.0	0.2	18	3	5		X	X	
Cd (ppm)	0.054	0.017	15	0	0	X			
Cd (ppm)	< 0.3	-	12	10			X		
Ce (ppm)	76.1	6.1	17	0	1			X	
Co (ppm)	20.8	1.8	30	0	3	X		X	
Cr (ppm)	*44.99*	*2.99*	*15*	*0*	*0*	*X*			
Cr (ppm)	120	10	16	0	2			X	
Cs (ppm)	5.2	0.6	18	0	0			X	
Cu (ppm)	29.7	1.4	25	0	2	X	X		
Eu (ppm)	1.7	0.3	17	1	1			X	
Fe (%)	*3.581*	*0.107*	*14*	*0*	*1*	*X*			
Fe (%)	4.24	0.28	15	0	3			X	
Ga (ppm)	5.87	0.37	15	0	0	X			
Ge (ppm)	0.50	0.28	12	2	0	X			
Hf (ppm)	7.2	0.8	17	0	1			X	
Hg (ppb)	35.3	6.6	26	0	0	X			CV-AAS
In (ppm)	< 0.2	-	12	12		X			
K (%)	*0.209*	*0.041*	*15*	*0*	*0*	*X*			
K (%)	2.149	0.223	11	0	1		X		
La (ppm)	*26.73*	*0.81*	*13*	*0*	*2*	*X*			
La (ppm)	38.3	2.6	17	0	1			X	
Lu (ppm)	0.45	0.09	18	0	0			X	
Mg (%)	*1.089*	*0.039*	*13*	*0*	*2*	*X*			
Mg (%)	1.477	0.077	11	0	1		X		
Mn (ppm)	*1646.4*	*71.9*	*14*	*0*	*1*	*X*			
Mn (ppm)	1576.1	112.8	11	0	1		X		
Mo (ppm)	0.385	0.024	15	0	0	X			

Table 2 *(cont'd)*. Current recommended values for NBDNR standard reference material NB-CS1.

	Recommended Values for Standard NB-CS1					Analytical Methods Used			
	Mean	S.D.	n	Qualified	Outliers	ICP-MS	ICP-OES	INAA	Other
Element									
Mo (ppm)	< 1	-	30	19			X	X	
Na (%)	*0.0073*	*0.001*	*14*	*0*	*1*	*X*			
Na (%)	1.19	0.13	18	0	0			X	
Nd (ppm)	32.4	3.9	10	0	1			X	
Ni (ppm)	*60.74*	*3.83*	*15*	*0*	*0*	*X*			
Ni (ppm)	65.1	2.8	17	0	2		X	X	
P (%)	*0.0603*	*0.0024*	*15*	*0*	*0*	*X*			
P (%)	0.0650	0.0079	12	0	0		X		
Pb (ppm)	15.7	2.8	24	0	3	X	X		
Rb (ppm)	96.3	15.6	16	0	2			X	
S (%)	*0.016*	*0.008*	*26*	*4*	*1*	*X*	*X*		
Sb (ppm)	0.449	0.062	15	0	0	X			
Sb (ppm)	0.99	0.12	15	0	3			X	
Sc (ppm)	*4.71*	*0.72*	*15*	*0*	*0*	*X*			
Sc (ppm)	15.8	1.2	17	0	1			X	
Se (ppm)	0.24	0.16	24	2	3	X			
Sm (ppm)	6.37	0.31	15	0	3			X	
Sn (ppm)	*< 1*	*-*	*12*	*6*		*X*			
Sr (ppm)	*83.16*	*4.75*	*14*	*0*	*1*	*X*			
Sr (ppm)	137.4	23.8	12	0	0		X		
Ta (ppm)	0.81	0.55	17	7	1			X	
Tb (ppm)	0.79	0.35	18	5	0			X	
Te (ppm)	< 0.1	-	27	8		X			
Th (ppm)	*6.53*	*0.4*	*15*	*0*	*0*	*X*			
Th (ppm)	9.9	0.7	17	0	1			X	
Ti (%)	*0.0266*	*0.0060*	*15*	*0*	*0*	*X*			
Ti (ppm)	0.510	0.036	11	0	2		X	X	
Tl (ppm)	*0.57*	*0.05*	*11*	*0*	*1*	*X*			
Tl (ppm)	0.065	0.005	13	0	2	X			
U (ppm)	*0.52*	*0.09*	*15*	*0*	*0*	*X*			
U (ppm)	2.26	0.29	17	0	1			X	
V (ppm)	*34.7*	*1.7*	*15*	*0*	*0*	*X*			
V (ppm)	102.7	3.8	11	0	1		X		
W (ppm)	*< 0.1*	*-*	*15*	*13*		*X*			
W (ppm)	< 1	-	18	13				X	
Y (ppm)	*24.7*	*3.0*	*10*	*0*	*2*		*X*		
Yb (ppm)	3.1	0.6	18	0	0			X	
Zn (ppm)	71.7	7.4	25	0	2	X	X		
Zn (ppm)	< 100	-	18	7				X	
Zr (ppm)	282	25	6	1	1			X	

Italic font indicates partial extraction data.

Table 3. Current recommended values for NBDNR standard reference material NB-01.

	Recommended Values for Standard NB-01					Analytical Methods Used			
	Mean	S.D.	n	Qualified	Outliers	ICP-MS	ICP-OES	INAA	Other
Element									
Ag (ppb)	19700	2300	46	1	6	X	X	X	
Ag (ppm)	19.7	2.3	46	1	6	X	X	X	
Al (%)	*1.873*	*0.052*	*18*	*0*	*0*	*X*			
Al (%)	*5.008*	*1.193*	*12*	*0*	*1*		*X*		
As (ppm)	840.8	33.9	37	0	3	X		X	
Au (ppb)	89.1	14.6	36	0	4	X		X	
B (ppm)	*1.9*	*0.8*	*17*	*1*	*1*	*X*			
Ba (ppm)	*109.61*	*29.55*	*18*	*0*	*0*	*X*			
Ba (ppm)	1114	137	19	0	3			X	
Be (ppm)	*1.03*	*0.15*	*3*	*0*	*0*	*X*			
Be (ppm)	4.9	0.7	12	0	1		X		
Bi (ppm)	66.53	2.85	27	0	4	X			
Br (ppm)	7.21	1.51	21	1	1			X	
Ca (%)	*1.229*	*0.018*	*15*	*0*	*3*	*X*			
Ca (%)	1.6	0.6	22	5	1		X	X	
Cd (ppm)	30.2	3.3	36	1	5	X	X	X	
Ce (ppm)	*39.90*	*2.43*	*3*	*0*	*0*	*X*			
Ce (ppm)	78.7	5.5	20	0	2			X	
Co (ppm)	21.7	1.1	40	0	1	X	X	X	
Cr (ppm)	*39.16*	*1.78*	*18*	*0*	*0*	*X*			
Cr (ppm)	87.8	13.1	22	0	0			X	
Cs (ppm)	*3.723*	*0.150*	*3*	*0*	*0*	*X*			
Cs (ppm)	6.3	0.7	22	0	0			X	
Cu (ppm)	1095.8	56.1	27	0	4	X	X		
Eu (ppm)	1.5	0.3	18	1	4			X	
Fe (%)	*4.236*	*0.110*	*18*	*0*	*0*	*X*			
Fe (%)	5.32	0.28	19	0	3			X	
Ga (ppm)	5.79	0.15	17	0	1	X			
Ge (ppm)	0.16	0.06	16	2	0	X			
Hf (ppm)	*0.080*	*0.010*	*3*	*0*	*0*	*X*			
Hf (ppm)	8.3	0.7	20	0	2			X	
Hg (ppb)	354.9	18.8	28	0	3	X			CV-AAS
In (ppm)	1.37	0.07	13	0	3	X			
K (%)	*0.132*	*0.007*	*18*	*0*	*0*	*X*			
K (%)	1.599	0.246	13	0	0		X		
La (ppm)	*15.72*	*1.07*	*18*	*0*	*0*	*X*			
La (ppm)	37.6	2.4	22	0	0			X	
Li (ppm)	*26.33*	*0.40*	*3*	*0*	*0*	*X*			
Lu (ppm)	0.51	0.06	17	0	5			X	
Mg (%)	*0.843*	*0.032*	*18*	*0*	*0*	*X*			
Mg (%)	1.201	0.158	13	0	0		X		
Mn (ppm)	*2202.7*	*43.6*	*16*	*0*	*2*	*X*			
Mn (ppm)	2842.5	194.9	11	0	2		X		
Mo (ppm)	20.5	2.1	49	0	3	X	X	X	
Na (%)	*0.0166*	*0.0014*	*18*	*0*	*0*	*X*			

Table 3 *(cont'd)*. Current recommended values for NBDNR standard reference material NB-01.

	Recommended Values for Standard NB-01					Analytical Methods Used			
	Mean	**S.D.**	**n**	**Qualified**	**Outliers**	**ICP-MS**	**ICP-OES**	**INAA**	**Other**
Element									
Na (%)	1.27	0.07	20	0	2			X	
Nb (ppm)	*0.890*	*0.070*	*3*	*0*	*0*	*X*			
Nd (ppm)	28.0	2.6	11	0	1			X	
Ni (ppm)	*37.63*	*1.42*	*18*	*0*	*0*	*X*			
Ni (ppm)	42.4	4.9	23	0	0		X	X	
P (%)	*0.0841*	*0.0030*	*17*	*0*	*1*	*X*			
P (%)	0.0871	0.0148	13	0	0		X		
Pb (ppm)	2590.7	114.2	28	0	3	X	X		
Pd (ppb)	*< 10*	*-*	*3*	*3*		*X*			
Pt (ppb)	*< 2*	*-*	*3*	*3*		*X*			
Rb (ppm)	*18.20*	*1.21*	*3*	*0*	*0*	*X*			
Rb (ppm)	89.4	12.2	19	0	3			X	
Re (ppb)	*2.0*	*0.0*	*3*	*0*	*0*	*X*			
S (%)	*1.298*	*0.127*	*27*	*0*	*4*	*X*	*X*		
Sb (ppm)	49.296	3.226	16	0	2	X			
Sb (ppm)	61.97	3.02	20	0	2			X	
Sc (ppm)	*3.58*	*0.37*	*18*	*0*	*0*	*X*			
Sc (ppm)	12.6	0.5	20	0	2			X	
Se (ppm)	3.22	0.37	26	3	5	X			
Sm (ppm)	6.28	0.49	22	0	0			X	
Sn (ppm)	*8.4*	*0.9*	*15*	*0*	*1*	*X*			
Sr (ppm)	*106.78*	*2.86*	*17*	*0*	*1*	*X*			
Sr (ppm)	195.8	26.0	13	0	0		X		
Ta (ppm)	*< 0.05*	*-*	*3*	*3*		*X*			
Ta (ppm)	0.63	0.46	21	12	1			X	
Tb (ppm)	0.61	0.36	22	10	0			X	
Te (ppm)	0.80	0.07	28	0	3	X			
Th (ppm)	*6.08*	*0.36*	*18*	*0*	*0*	*X*			
Th (ppm)	12.0	1.1	21	0	1			X	
Ti (%)	*0.0581*	*0.0046*	*17*	*0*	*1*	*X*			
Ti (ppm)	0.489	0.062	16	0	1		X	X	
Tl (ppm)	*1.05*	*0.08*	*11*	*2*	*2*	*X*			
Tl (ppm)	0.362	0.024	18	0	0	X			
U (ppm)	*1.62*	*0.07*	*18*	*0*	*0*	*X*			
U (ppm)	3.86	0.48	20	0	2			X	
V (ppm)	*41.4*	*1.4*	*18*	*0*	*0*	*X*			
V (ppm)	86.9	5.0	12	0	1		X		
W (ppm)	*5.14*	*0.29*	*18*	*0*	*0*	*X*			
W (ppm)	9.6	1.0	20	2	2			X	
Y (ppm)	*9.587*	*0.407*	*3*	*0*	*0*	*X*			
Y (ppm)	*23.5*	*3.2*	*12*	*0*	*1*		*X*		
Yb (ppm)	3.5	0.9	21	0	1			X	
Zn (ppm)	3447	174	45	0	7	X	X	X	
Zr (ppm)	*5.27*	*0.35*	*3*	*0*	*0*	*X*			
Zr (ppm)	291	144	10	3	0			X	

Italic font indicates partial extraction data.

Table 4. Current recommended values for NBDHR standard reference material NB-02.

	Recommended Values for Standard NB-02					Analytical Methods Used			
	Mean	**S.D.**	**n**	**Qualified**	**Outliers**	**ICP-MS**	**ICP-OES**	**INAA**	**Other**
Element									
Ag (ppb)	350	100	25	2	4	X	X		
Ag (ppm)	0.35	0.10	25	2	4	X	X		
Al (%)	*1.184*	*0.024*	*16*	*0*	*2*	*X*			
Al (%)	*5.966*	*2.518*	*11*	*0*	*0*		*X*		
As (ppm)	90.86	7.95	36	0	1	X		X	
Au (ppb)	9.6	1.7	31	3	6	X		X	
B (ppm)	*1.5*	*0.6*	*16*	*1*	*2*	*X*			
Ba (ppm)	*33.12*	*2.28*	*17*	*0*	*1*	*X*			
Ba (ppm)	363	63	18	0	1			X	
Be (ppm)	*1.27*	*0.06*	*3*	*0*	*0*	*X*			
Be (ppm)	4.1	0.5	9	0	2		X		
Bi (ppm)	2.63	0.40	27	0	2	X			
Br (ppm)	1.81	1.39	19	7	0			X	
Ca (%)	*1.153*	*0.036*	*17*	*0*	*1*	*X*			
Ca (%)	2.1	0.2	16	1	3		X	X	
Cd (ppm)	0.31	0.09	26	4	3	X	X		
Ce (ppm)	*58.90*	*0.46*	*3*	*0*	*0*	*X*			
Ce (ppm)	81.4	7.9	18	0	1			X	
Co (ppm)	36.8	2.3	35	0	4	X	X	X	
Cr (ppm)	*19.05*	*0.97*	*16*	*0*	*2*	*X*			
Cr (ppm)	52.8	10.4	18	1	1			X	
Cs (ppm)	*2.847*	*0.072*	*3*	*0*	*0*	*X*			
Cs (ppm)	6.9	0.5	17	0	2			X	
Cu (ppm)	30.3	1.1	25	0	4	X	X		
Eu (ppm)	1.2	0.5	19	2	0			X	
Fe (%)	*2.002*	*0.077*	*17*	*0*	*1*	*X*			
Fe (%)	2.99	0.29	19	0	0			X	
Ga (ppm)	4.69	0.20	17	0	1	X			
Ge (ppm)	0.30	0.25	14	2	0	X			
Hf (ppm)	*0.450*	*0.053*	*3*	*0*	*0*	*X*			
Hf (ppm)	5.4	3.0	16	4	3			X	
Hg (ppb)	25.3	17.7	26	4	3	X			CV-AAS
In (ppm)	< 0.2	-	14	11		X			
K (%)	*0.176*	*0.01*	*16*	*0*	*2*	*X*			
K (%)	2.872	0.347	11	0	0		X		
La (ppm)	*28.36*	*1.03*	*16*	*0*	*2*	*X*			
La (ppm)	38.0	2.4	19	0	0			X	
Li (ppm)	*26.30*	1.49	3	0	0	*X*			
Lu (ppm)	0.90	0.26	19	0	0			X	
Mg (%)	*0.558*	*0.010*	*16*	*0*	*2*	*X*			
Mg (%)	1.044	0.217	11	0	0		X		
Mn (ppm)	*369.7*	*16.5*	*17*	*0*	*1*	*X*			
Mn (ppm)	612.0	30.5	10	0	1		X		
Mo (ppm)	3.5	1.3	43	2	4	X	X	X	
Na (%)	*0.0370*	*0*	*15*	*0*	*3*	*X*			
Na (%)	1.995	0.102	19	0	0			X	
Nb (ppm)	*2.113*	*0.133*	*3*	*0*	*0*	*X*			

Table 4 *(cont'd)*. Current recommended values for NBDHR standard reference material NB-02.

	Recommended Values for Standard NB-02					Analytical Methods Used			
	Mean	S.D.	n	Qualified	Outliers	ICP-MS	ICP-OES	INAA	Other
Element									
Nd (ppm)	28.0	4.6	11	0	0			X	
Ni (ppm)	*14.48*	*0.78*	*17*	*0*	*1*	*X*			
Ni (ppm)	20.7	2.3	16	0	3		X	X	
P (%)	*0.0485*	*0*	*16*	*0*	*2*	*X*			
P (%)	0.0560	0.0060	10	0	1		X		
Pb (ppm)	34.3	4.1	26	0	3	X	X		
Pd (ppb)	*< 10*	*-*	*3*	*3*		*X*			
Pt (ppb)	*< 2*	*-*	*3*	*3*		*X*			
Rb (ppm)	*21.43*	*0.90*	*3*	*0*	*0*	*X*			
Rb (ppm)	180	25	17	0	2			X	
Re (ppb)	*2.0*	*0.0*	*3*	*0*	*0*	*X*			
S (%)	*0.041*	*0.019*	*28*	*1*	*1*	*X*	*X*		
Sb (ppm)	0.631	0.043	17	0	1	X			
Sb (ppm)	1.73	0.11	17	0	2			X	
Sc (ppm)	*3.46*	*0.36*	*18*	*0*	*0*	*X*			
Sc (ppm)	13.4	0.6	17	0	2			X	
Se (ppm)	0.33	0.25	25	4	4	X			
Sm (ppm)	7.83	0.79	19	0	0			X	
Sn (ppm)	*3.3*	*0.7*	*14*	*0*	*0*	*X*			
Sn (ppm)	145	81	8	3	0			X	
Sr (ppm)	*29.94*	*1.21*	*16*	*0*	*2*	*X*			
Sr (ppm)	132.1	15.6	11	0	0		X		
Ta (ppm)	*< 0.05*	*-*	*3*	*3*		*X*			
Ta (ppm)	3.90	0.50	17	0	2			X	
Tb (ppm)	1.56	0.17	17	2	2			X	
Te (ppm)	< 0.1	-	29	16		X			
Th (ppm)	*15.22*	*0.93*	*17*	*0*	*1*	*X*			
Th (ppm)	18.52	1.66	18	0	1			X	
Ti (%)	*0.0793*	*0*	*17*	*0*	*1*	*X*			
Ti (ppm)	0.377	0.094	15	0	0		X	X	
Tl (ppm)	*1.09*	*0.04*	*9*	*0*	*2*	*X*			
Tl (ppm)	0.119	0.011	17	0	1	X			
U (ppm)	*4.33*	*0.18*	*16*	*0*	*2*	*X*			
U (ppm)	7.16	0.67	17	0	2			X	
V (ppm)	*30.6*	*1.0*	*16*	*0*	*2*	*X*			
V (ppm)	63.9	7.6	11	0	0		X		
W (ppm)	*260.74*	*36.99*	*11*	*0*	*0*	*X*			
W (ppm)	301.2	42.1	19	0	0			X	
Y (ppm)	*22.393*	*0.943*	*3*	*0*	*0*	*X*			
Y (ppm)	*47.7*	*16.1*	*11*	*0*	*0*		*X*		
Yb (ppm)	5.6	0.7	17	0	2			X	
Zn (ppm)	86.3	9.6	27	0	2	X	X		
Zn (ppm)	118	46	18	4	0			X	

Italic font indicates partial extraction data.

Table 5. Current recommended values for NBDNR standard reference material NB-03.

	Recommended Values for Standard NB-03					**Analytical Methods Used**			
	Mean	**S.D.**	**n**	**Qualified**	**Outliers**	**ICP-MS**	**ICP-OES**	**INAA**	**Other**
Element									
Ag (ppb)	169.4	12.2	9	0	0	X			
Ag (ppm)	0.41	0.15	5	1	0		X		
Al (%)	*1.547*	*0.084*	*9*	*0*	*0*	*X*			
Al (%)	*3.621*	*1.156*	*5*	*0*	*0*		*X*		
As (ppm)	63.42	5.60	15	0	2	X		X	
Au (ppb)	20.0	6.0	15	0	2	X		X	
B (ppm)	*1.2*	*0.7*	*9*	*3*	*0*	*X*			
Ba (ppm)	*42.16*	*3.99*	*9*	*0*	*0*	*X*			
Ba (ppm)	357	77	8	0	0			X	
Be (ppm)	*1.19*	*0.20*	*7*	*0*	*0*	*X*			
Be (ppm)	4.1	0.5	5	0	0		X		
Bi (ppm)	1.53	0.16	14	0	0	X			
Br (ppm)	4.41	0.54	8	0	0			X	
Ca (%)	*0.222*	*0.008*	*9*	*0*	*0*	*X*			
Ca (%)	0.664	0.190	5	0	0		X		
Cd (ppm)	0.099	0.011	9	0	0	X			
Cd (ppm)	<0.3	-	5	2			X		
Ce (ppm)	*67.30*	*3.87*	*7*	*0*	*0*	*X*			
Ce (ppm)	75.3	10.9	8	0	0			X	
Co (ppm)	33.7	2.6	17	0	0	X		X	
Cr (ppm)	*23.98*	*2.05*	*9*	*0*	*0*	*X*			
Cr (ppm)	61.9	18.7	8	0	0			X	
Cs (ppm)	*2.619*	*0.102*	*7*	*0*	*0*	*X*			
Cs (ppm)	6.0	0.04	7	0	1			X	
Cu (ppm)	23.8	2.0	14	0	0	X	X		
Eu (ppm)	1.0	0.3	8	1	0			X	
Fe (%)	*2.433*	*0.090*	*9*	*0*	*0*	*X*			
Fe (%)	2.81	0.17	8	0	0			X	
Ga (ppm)	4.69	0.39	9	0	0	X			
Ge (ppm)	0.15	0.15	12	7	0	X			
Hf (ppm)	*0.159*	*0.037*	*7*	*0*	*0*	*X*			
Hf (ppm)	4.9	4.0	8	3	0			X	
Hg (ppb)	228.8	47.3	14	0	0	X			CV-AAS
In (ppm)	<0.2	-	12	5		X			
K (%)	*0.128*	*0.013*	*9*	*0*	*0*	*X*			
K (%)	2.756	0.118	5	0	0		X		
La (ppm)	*31.21*	*2.39*	*9*	*0*	*0*	*X*			
La (ppm)	39.8	0.5	6	0	2			X	
Li (ppm)	*31.44*	*2.18*	*7*	*0*	*0*	*X*			
Lu (ppm)	0.51	0.25	8	1	0			X	
Mg (%)	*0.508*	*0.018*	*9*	*0*	*0*	*X*			
Mg (%)	0.771	0.092	5	0	0		X		
Mn (ppm)	*376.8*	*11.9*	*9*	*0*	*0*	*X*			
Mn (ppm)	535.1	51.9	5	0	0		X		
Mo (ppm)	1.7	0.4	16	2	3	X	X	X	
Na (%)	*0.0193*	*0*	*8*	*0*	*1*	*X*			

Table 5 (*cont'd*). Current recommended values for NBDNR standard reference material NB-03.

	Recommended Values for Standard NB-03					Analytical Methods Used			
	Mean	**S.D.**	**n**	**Qualified**	**Outliers**	**ICP-MS**	**ICP-OES**	**INAA**	**Other**
Element									
Na (%)	1.717	0.110	8	0	0			X	
Nb (ppm)	*2.649*	*0.187*	*7*	*0*	*0*	*X*			
Nd (ppm)	25.3	1.6	5	0	0			X	
Ni (ppm)	*26.79*	*1.72*	*9*	*0*	*0*	*X*			
Ni (ppm)	36.3	2.2	8	0	0		X	X	
P (%)	*0.0331*	*0.002*	*9*	*0*	*0*	*X*			
P (%)	0.0422	0.005	5	0	0		X		
Pb (ppm)	67.2	6.6	12	0	2	X	X		
Pd (ppb)	*< 10*	*-*	*7*	*7*		*X*			
Pt (ppb)	*< 2*	*-*	*7*	*7*		*X*			
Rb (ppm)	*17.61*	*1.04*	*7*	*0*	*0*	*X*			
Rb (ppm)	157	34	8	0	0			X	
Re (ppb)	*1.6*	*0.9*	*7*	*1*	*0*	*X*			
S (%)	*0.016*	*0.009*	*13*	*2*	*1*	*X*	*X*		
Sb (ppm)	2.871	0.326	9	0	0	X			
Sb (ppm)	4.88	0.68	8	0	0			X	
Sc (ppm)	*3.22*	*0.32*	*9*	*0*	*0*	*X*			
Sc (ppm)	9.91	1.33	8	0	0			X	
Se (ppm)	0.55	0.33	12	3	2	X			
Sm (ppm)	6.66	1.35	8	0	0			X	
Sn (ppm)	*1.8*	*0.2*	*12*	*0*	*0*	*X*			
Sr (ppm)	*8.72*	*0.54*	*9*	*0*	*0*	*X*			
Sr (ppm)	96.4	16.4	5	0	0		X		
Ta (ppm)	*< 0.05*	*-*	*7*	*7*		*X*			
Ta (ppm)	2.52	0.68	8	0	0			X	
Tb (ppm)	0.95	0.59	8	2	0			X	
Te (ppm)	< 0.1	-	14	1		X			
Th (ppm)	*14.11*	*1.17*	*9*	*0*	*0*	*X*			
Th (ppm)	18.06	3.08	8	0	0			X	
Ti (%)	*0.0380*	*0.004*	*9*	*0*	*0*	*X*			
Ti (ppm)	0.424	0.033	8	0	0		X	X	
Tl (ppm)	*1.09*	*0.07*	*5*	*0*	*0*	*X*			
Tl (ppm)	0.131	0.014	9	0	0	X			
U (ppm)	*3.63*	*0.33*	*9*	*0*	*0*	*X*			
U (ppm)	5.49	0.89	8	0	0			X	
V (ppm)	*25.6*	*0.9*	*9*	*0*	*0*	*X*			
V (ppm)	68.7	6.0	5	0	0		X		
W (ppm)	*> 100*	*-*	*9*	*9*		*X*			
W (ppm)	220.5	27.0	8	0	0			X	
Y (ppm)	*17.391*	*0.922*	*7*	*0*	*0*	*X*			
Y (ppm)	*30.0*	*9.5*	*5*	*0*	*0*		*X*		
Yb (ppm)	4.0	1.3	8	0	0			X	
Zn (ppm)	60.7	7.5	14	0	0	X	X		
Zn (ppm)	108	40	5	1	0			X	
Zr (ppm)	*7.91*	*0.46*	*7*	*0*	*0*	*X*			
Zr (ppm)	387	255	3	1	0			X	

Italic font indicates partial extraction data.

Table 6. Current recommended values for NBDNR standard reference material NB-04.

	Recommended Values for Standard NB-04					**Analytical Methods Used**			
	Mean	**S.D.**	**n**	**Qualified**	**Outliers**	**ICP-MS**	**ICP-OES**	**INAA**	**Other**
Element									
Ag (ppb)	53.0	0.8	4	0	0	X			
Ag (ppm)	0.32	0.18	3	1	0		X		
Al (%)	*2.365*	*0.054*	*4*	*0*	*0*	*X*			
Al (%)	*4.967*	*0.090*	*3*	*0*	*0*		*X*		
As (ppm)	15.63	1.50	10	0	0	X		X	
Au (ppb)	1.4	0.5	9	4	1	X		X	
B (ppm)	*1.8*	*1.0*	*4*	*0*	*0*	*X*			
Ba (ppm)	*64.58*	*1.68*	*4*	*0*	*0*	*X*			
Ba (ppm)	383	33	6	0	0			X	
Be (ppm)	*0.93*	0.19	4	0	0	*X*			
Be (ppm)	3.3	0.6	3	0	0		X		
Bi (ppm)	0.94	0.07	7	0	0	X			
Br (ppm)	7.98	0.88	6	0	0			X	
Ca (%)	*0.133*	*0.005*	*4*	*0*	*0*	*X*			
Ca (%)	0.920	0.046	3	0	0		X		
Cd (ppm)	0.165	0.013	4	0	0	X			
Cd (ppm)	<0.3	-	3	3			X		
Ce (ppm)	*68.75*	*2.18*	*4*	*0*	*0*	*X*			
Ce (ppm)	76.2	9.7	6	0	0			X	
Co (ppm)	14.0	1.0	10	0	0	X		X	
Cr (ppm)	*47.00*	*3.04*	*4*	*0*	*0*	*X*			
Cr (ppm)	87.5	13.1	6	0	0			X	
Cs (ppm)	*2.868*	*0.094*	*4*	*0*	*0*	*X*			
Cs (ppm)	5.4	0.8	6	0	0			X	
Cu (ppm)	34.5	2.3	7	0	0	X	X		
Eu (ppm)	1.0	0.0	5	0	1			X	
Fe (%)	*3.155*	*0.062*	*4*	*0*	*0*	*X*			
Fe (%)	3.78	0.13	6	0	0			X	
Ga (ppm)	6.75	0.13	4	0	0	X			
Ge (ppm)	0.27	0.28	7	2	0	X			
Hf (ppm)	*0.143*	*0.010*	*4*	*0*	*0*	*X*			
Hf (ppm)	8.0	2.3	6	0	0			X	
Hg (ppb)	36.4	4.9	7	0	0	X			CV-AAS
In (ppm)	<0.1	-	7	3		X			
K (%)	*0.153*	*0.015*	*4*	*0*	*0*	*X*			
K (%)	2.510	0.053	3	0	0		X		
La (ppm)	*32.38*	*0.71*	*4*	*0*	*0*	*X*			
La (ppm)	40.6	2.8	6	0	0			X	
Li (ppm)	*25.98*	*1.20*	*4*	*0*	*0*	*X*			
Lu (ppm)	0.32	0.18	6	2	0			X	
Mg (%)	*0.883*	*0.025*	*4*	*0*	*0*	*X*			
Mg (%)	1.503	0.040	3	0	0		X		
Mn (ppm)	*584.5*	*12.2*	*4*	*0*	*0*	*X*			
Mn (ppm)	891.0	16.1	3	0	0		X		
Mo (ppm)	0.9	0.6	10	3	0	X	X	X	
Na (%)	*0.0063*	*0.0005*	*4*	*0*	*0*	*X*			
Na (%)	1.450	0.160	6	0	0			X	

Table 6 *(cont'd).* Current recommended values for NBDNR standard reference material NB-04.

	Recommended Values for Standard NB-04					Analytical Methods Used			
	Mean	S.D.	n	Qualified	Outliers	ICP-MS	ICP-OES	INAA	Other
Element									
Nb (ppm)	*1.288*	*0.092*	*4*	*0*	*0*	*X*			
Nd (ppm)	24.3	1.2	3	0	0			X	
Ni (ppm)	*39.03*	*0.44*	*4*	*0*	*0*	*X*			
Ni (ppm)	53.0	4.3	6	0	0		X	X	
P (%)	*0.0508*	*0.0028*	*4*	*0*	*0*	*X*			
P (%)	0.0650	0.0020	3	0	0		X		
Pb (ppm)	27.7	2.1	7	0	0	X	X		
Pd (ppb)	*<10*	-	*4*	*4*		*X*			
Pt (ppb)	*<2*	-	*4*	*4*		*X*			
Rb (ppm)	*20.33*	*0.66*	*4*	*0*	*0*	*X*			
Rb (ppm)	100	15	6	0	0			X	
Re (ppb)	*<1*	-	*4*	*4*		*X*			
S (%)	*0.016*	*0.013*	*7*	*4*	*0*	*X*	*X*		
Sb (ppm)	0.478	0.021	4	0	0	X			
Sb (ppm)	0.95	0.14	6	0	0			X	
Sc (ppm)	*4.48*	*0.30*	*4*	*0*	*0*	*X*			
Sc (ppm)	13.1	1.9	6	0	0			X	
Se (ppm)	0.22	0.17	7	3	0	X			
Sm (ppm)	6.15	1.05	6	0	0			X	
Sn (ppm)	*2.2*	*0.4*	*6*	*0*	*1*	*X*			
Sr (ppm)	*7.58*	*0.42*	*4*	*0*	*0*	*X*			
Sr (ppm)	130.3	2.5	3	0	0		X		
Ta (ppm)	*< 0.05*	-	*4*	*4*		*X*			
Ta (ppm)	0.98	0.65	6	2	0			X	
Tb (ppm)	0.73	0.39	6	2	0			X	
Te (ppm)	< 0.1	-	7	3		X			
Th (ppm)	*11.08*	*0.43*	*4*	*0*	*0*	*X*			
Th (ppm)	13.63	2.27	6	0	0			X	
Ti (%)	*0.0998*	*0.0046*	*4*	*0*	*0*	*X*			
Ti (ppm)	0.652	0.077	6	0	0		X	X	
Tl (ppm)	*0.70*	*0.00*	*3*	*0*	*0*	*X*			
Tl (ppm)	0.155	0.006	4	0	0	X			
U (ppm)	*2.30*	*0.08*	*4*	*0*	*0*	*X*			
U (ppm)	4.22	0.39	6	0	0			X	
V (ppm)	*49.3*	*1.5*	*4*	*0*	*0*	*X*			
V (ppm)	117.3	6.8	3	0	0		X		
W (ppm)	*0.55*	*0.06*	*4*	*0*	*0*	*X*			
W (ppm)	2.6	1.2	6	1	0			X	
Y (ppm)	*13.145*	*0.321*	*4*	*0*	*0*	*X*			
Y (ppm)	*34.7*	*2.1*	*3*	*0*	*0*		*X*		
Yb (ppm)	3.1	0.1	5	1	1			X	
Zn (ppm)	89.6	12.3	7	0	0	X	X		
Zn (ppm)	173	45	3	0	0			X	
Zr (ppm)	*7.18*	0.33	4	0	0	*X*			
Zr (ppm)	310	205	3	1	0			X	

Italic font indicates partial extraction data.

Table 7. Comparison of standard deviation as percentage of mean value for GSC and NBDNR standard reference material. (NBDNR values were derived from the two-step trimming process.)

	GSC Standards			NBDNR Standard Reference Material				
	Min.	**Mean.**	**Max.**	**NB-CS1**	**NB-01**	**NB-02**	**NB-03**	**NB-04**
Element								
Ag	4.1	21.2	50.0	7.8	11.5	28.6	7.2	1.5
Al (ICP-MS)	-	*n/a*	-	*6.9*	*2.8*	*2.0*	*5.4*	*2.3*
Al (ICP-OES)	0.6	2.3	6.7	*28.3*	*23.8*	*42.2*	*31.9*	*1.8*
As	4.6	6.7	9.1	21.6	4.0	8.7	8.8	9.6
Au	30.8	62.9	100.0	76.9	16.4	17.7	30.0	35.7
B	3.1	7.2	10.1	*21.9*	*42.1*	*40.0*	*58.3*	*55.6*
Ba	*4.7*	*6.2*	*7.4*	*9.0*	*27.0*	*6.9*	*9.5*	*2.6*
Ba	7.4	9.5	16.7	10.6	12.3	17.4	21.6	8.6
Be	-	*n/a*	-	*n/a*	*14.6*	*4.7*	*16.8*	*20.4*
Be	3.0	16.9	37.5	47.1	14.3	12.2	12.2	18.2
Bi	7.5	7.5	7.5	38.1	4.3	15.2	10.5	7.4
Br	6.2	10.9	25.0	<	20.9	76.8	12.2	11.0
Ca	-	*n/a*	-	*6.0*	*1.5*	*3.1*	*3.6*	*3.8*
Ca	3.6	6.0	10.3	10.0	37.5	9.5	28.6	5.0
Cd	*20.0*	*36.2*	*66.7*	31.5	10.8	29.0	11.1	7.9
Ce	-	*n/a*	-	*n/a*	*6.1*	*0.8*	*5.8*	*3.2*
Ce	6.8	9.8	12.7	8.0	7.0	9.7	14.5	12.7
Co	5.9	10.3	25.0	8.7	5.1	6.3	7.7	7.1
Cr	*7.5*	*12.4*	*20.0*	*6.6*	*4.5*	*5.1*	*8.5*	*6.5*
Cr	9.2	12.8	18.9	8.5	14.9	19.7	30.2	15.0
Cs	-	*n/a*	-	*n/a*	*4.0*	*2.5*	*3.9*	*3.3*
Cs	8.3	23.7	80.0	11.5	11.1	7.2	0.0	14.8
Cu	6.7	10.8	22.7	4.7	5.1	3.6	8.4	6.7
Eu	10.5	29.4	50.0	14.4	20.0	41.5	31.3	0.0
Fe	*2.9*	*8.2*	*16.7*	*3.0*	*2.6*	*3.8*	*3.7*	*2.0*
Fe	3.6	6.1	10.6	6.6	5.3	9.7	6.0	3.4
Ga	-	n/a	-	6.3	2.6	4.3	8.3	1.9
Ge	-	n/a	-	56.0	37.5	83.3	100.0	103.7
Hf	-	*n/a*	-	*n/a*	*12.5*	*11.8*	*23.3*	*7.0*
Hf	7.7	15.4	25.0	11.1	8.4	55.6	81.6	28.8
Hg	*7.8*	*14.1*	*30.8*	18.7	5.3	70.0	20.7	13.5
In	-	n/a	-	<	5.1	<	<	<
K	-	*n/a*	-	*19.6*	*5.3*	*5.1*	*10.2*	*9.8*
K	1.5	4.1	7.4	10.4	15.4	12.1	4.3	2.1
La	-	*n/a*	-	*3.0*	*6.8*	*3.6*	*7.7*	*2.2*
La	5.8	9.2	12.5	6.8	6.4	6.3	1.3	6.9
Li	6.7	11.7	28.6	*n/a*	*1.5*	*5.7*	*6.9*	*4.6*
Lu	12.5	27.4	57.1	20.0	11.8	28.9	48.8	56.3
Mg	-	*n/a*	-	*3.6*	*3.8*	*1.8*	*3.5*	*2.8*
Mg	2.6	4.8	7.9	5.2	13.2	20.8	11.9	2.7
Mn	*5.3*	*12.0*	*18.9*	*4.4*	*2.0*	*4.5*	*3.2*	*2.1*
Mn	3.6	5.8	7.7	7.2	6.9	5.0	9.7	1.8
Mo	12.5	27.9	50.0	6.2	10.2	37.1	23.5	3.1
Na	-	*n/a*	-	*9.6*	*8.4*	*3.8*	*3.6*	*7.9*
Na	1.9	3.5	8.0	10.9	5.5	5.1	6.4	11.0

Table 7 *(cont'd)*. Comparison of standard deviation as percentage of mean value for the GSC and NBDNR standard reference material. (NBDNR values were derived from the two-step trimming process.)

	GSC Standards			**NBDNR Standard Reference Material**				
	Min.	**Mean.**	**Max.**	**NB-CS1**	**NB-01**	**NB-02**	**NB-03**	**NB-04**
Element								
Nb	10.0	37.7	114.3	*n/a*	*7.9*	*6.3*	*7.1*	*7.1*
Nd	6.2	9.1	15.0	12.0	9.3	16.4	6.3	4.9
Ni	*8.5*	*11.4*	*16.7*	*6.3*	*3.8*	*5.4*	*6.4*	*1.1*
Ni	9.4	15.9	20.8	4.3	11.6	11.1	6.1	8.1
P	-	*n/a*	-	*4.0*	*3.6*	*3.7*	*6.3*	*5.5*
P	2.5	6.5	10.7	12.2	17.0	10.7	10.7	3.1
Pb	6.1	9.7	18.8	17.8	4.4	12.0	9.8	7.6
Pd	-	*n/a*	-	<	<	<	<	<
Pt	-	*n/a*	-	<	<	<	<	<
Rb	-	*n/a*	-	*n/a*	*6.6*	*4.2*	*5.9*	*3.2*
Rb	8.4	16.5	35.7	16.2	13.6	13.9	21.6	15.5
Re	-	*n/a*	-	*n/a*	*0.0*	*0.0*	*56.3*	<
S	8.3	20.7	33.3	*50.0*	*9.8*	*46.3*	*56.3*	*81.3*
Sb (ICP-OES)	5.9	9.0	12.5	12.1	4.9	6.4	13.9	14.7
Sb (ICP-MS)	*33.3*	*47.2*	*69.4*	13.8	6.5	6.8	11.4	4.4
Sc	-	*n/a*	-	*15.3*	*10.3*	*10.4*	*9.9*	*6.7*
Sc	8.3	14.0	22.2	7.6	4.0	4.5	13.4	14.5
Se	-	n/a	-	66.7	11.5	75.8	60.0	77.3
Sm	6.6	10.1	18.0	4.9	7.8	10.1	20.3	17.1
Sn	20.0	37.1	66.7	<	*10.7*	*21.2*	*11.1*	*16.2*
Sr	-	*n/a*	-	*5.7*	*26.5*	*4.0*	*6.2*	*5.5*
Sr	3.4	16.3	34.5	17.3	13.3	11.8	17.0	1.9
Ta	-	*n/a*	-	*n/a*	<	<	<	<
Ta	10.0	14.7	30.0	67.9	73.0	12.8	27.0	66.3
Tb	10.0	23.0	58.3	44.3	59.0	10.9	62.1	53.4
Te	-	n/a	-	75.0	8.8	<	<	<
Th	-	*n/a*	-	*6.1*	*5.9*	*6.1*	*8.3*	*3.9*
Th	6.1	9.4	13.7	7.1	9.2	9.0	17.1	16.9
Ti	-	*n/a*	-	*22.6*	*7.9*	*5.7*	*9.5*	*4.6*
Ti	2.7	8.0	20.7	7.1	12.7	24.9	7.8	11.8
Tl	-	*n/a*	-	*8.8*	*7.6*	*3.7*	*3.7*	*0.0*
Tl	-	n/a	-	7.7	6.6	9.2	10.7	3.9
U	-	*n/a*	-	*17.3*	*4.3*	*4.2*	*9.1*	*3.5*
U	5.4	9.8	16.7	12.8	12.4	9.4	16.2	9.2
V	*10.5*	*21.7*	*37.3*	*4.9*	*3.4*	*3.3*	*3.5*	*3.0*
V	9.4	11.5	16.3	3.7	5.8	11.9	8.7	5.8
W	-	*n/a*	-	<	*5.6*	*14.2*	>	*10.9*
W	11.8	20.1	28.6	<	10.4	14.0	12.2	46.2
Y	-	*n/a*	-	*n/a*	*4.2*	*4.2*	*5.3*	*2.4*
Y	9.1	24.0	47.4	12.1	13.6	33.8	31.7	6.1
Yb	10.0	14.8	23.1	19.4	25.5	12.5	32.5	3.2
Zn	6.2	9.0	11.2	10.3	5.0	11.1	12.4	13.7
Zr	-	*n/a*	-	*n/a*	*6.6*	*6.4*	*5.8*	*4.6*
Zr	4.9	10.8	16.2	8.8	49.5	47.1	65.9	66.1

Italic font indicates partial extraction data. < = below detection limit > = above detection limit

ACKNOWLEDGEMENTS

Jillian Craig checked the values in Tables 1 to 6 against values in the original data files from which they were derived. This report was improved by the constructive criticisms of Steve McCutcheon, P.Geo., and Toon Pronk, P.Geo., of the Geological Surveys Branch, New Brunswick Department of Natural Resources.

REFERENCES

Acme 2005. Acme in 2005. Acme Analytical Laboratories Ltd. URL http://www.acmelab.com/temp/200541020401/2005_Price_Brochure_V2_page_size.pdf {May 2005}.

Actlabs 2005. Actlabs schedule of services. Activation Laboratories Ltd. URL http://www.actlabs.com/docs/Schedule%20of%20Services.pdf {May 2005}.

Becquerel 2005. Geochemical exploration. Becquerel Laboratories Inc. URL http://www.becquerellabs.com/Geochemical%20Soils.html {May 2005}.

Lamothe, M. 1990a. Till geochemistry over the northern Miramichi Zone and vicinity, New Brunswick. Geological Survey of Canada, Open File 2236, 88 p.

Lamothe, M. 1990b. Till geochemistry over the central Miramichi Zone and vicinity, New Brunswick. Geological Survey of Canada, Open File 2237, 106 p.

Lamothe, M. 1990c. Till geochemistry over the southern Miramichi Zone and vicinity, New Brunswick. Geological Survey of Canada, Open File 2238, 62 p.

Lamothe, M. 1992. Pleistocene stratigraphy and till geochemistry of the Miramichi Zone, New Brunswick. Geological Survey of Canada, Bulletin 433, 58 p.

Lynch, J. 1990. Provisional elemental values for eight new geochemical lake sediment and stream sediment reference materials, LKSD-1, LKSD-2, LKSD-3, LKSD-4, STSD-1, STSD-2, STSD-3, and STSD-4. Geostandards Newsletter, **14**: 153–167.

Lynch, J. 1996. Provisional elemental values for four new geochemical soil and till reference materials, TILL-1, TILL-2, TILL-3 and TILL-4. Geostandards Newsletter, **20**: 277–287.

Parkhill, M.A., Doucet, D., and Arseneau, P. 2002. Quaternary geology and till geochemistry of northwestern New Brunswick. *In* Abstracts, 2002: 27th Annual Review of Activities. *Edited by* B.M.W. Carroll. New Brunswick Department of Natural Resources and Energy; Minerals, Policy and Planning Division, Information Circular 2002-1, p. 45.

Pronk, A.G., Boldon, G.R., and Allard, S. 2002. Till geochemistry and field data of the Rollingdam (NTS 21 G/06) and McDougall Lake (NTS 21 G/07) map areas, southwestern New Brunswick. New Brunswick Department of Natural Resources and Energy; Minerals, Policy and Planning Division, Open File 2002-4, 68 p.

Pronk, A.G., Allard, S., and Boldon, G.R. 2003a. Till geochemistry of the St. Stephen (NTS 21 G/03) map area, Charlotte County, New Brunswick. New Brunswick Department of Natural Resources; Minerals, Policy and Planning Division, Open File 2003-12, 48 p.

Pronk, A.G., Allard, S., and Boldon, G.R. 2003b. Till geochemistry of the Fredericton Junction (NTS 21 G/10) map area, York and Sunbury counties, New Brunswick. New Brunswick Department of Natural Resources; Minerals, Policy and Planning Division, Open File 2003-13, 58 p.

Seaman, A.A. 2001. Preliminary report — till geochemistry of part of the west half of the Coldstream (NTS 21 J/06) map area, Carleton and York counties, New Brunswick. New Brunswick Department of Natural Resources and Energy; Minerals and Energy Division, Open File 2001-2, 51 p.

Seaman, A.A. 2002. Till geochemistry of the central and eastern parts of the Coldstream (NTS 21 J/06) map area, York and Carleton counties, New Brunswick. New Brunswick Department of Natural Resources and Energy; Minerals, Policy and Planning Division, Open File 2002-5, 80 p.

Seaman, A.A. 2003. Follow-up till geochemistry, Coldstream (NTS 21 J/06) map area and part of the adjacent Napadogan (NTS 21 J/07) map area, York and Carleton counties, New Brunswick. New Brunswick Department of Natural Resources; Minerals, Policy and Planning Division, Open File 2003-11, 103 p.

GILMOUR BROOK SOUTH BASE-METAL OCCURRENCE, BATHURST MINING CAMP, NORTHERN NEW BRUNSWICK

JAMES A. WALKER [1]

[1] Geological Surveys Branch, New Brunswick Department of Natural Resources,
P.O. Box 50, Bathurst, New Brunswick, CANADA E2A 3Z1 (*jim.walker@gnb.ca*)

Walker, J.A. 2005. Gilmour Brook South base-metal occurrence, Bathurst Mining Camp, northern New Brunswick. *In* Geological Investigations in New Brunswick for 2004. *Edited by* G.L. Martin. New Brunswick Department of Natural Resources; Minerals, Policy and Planning Division, Mineral Resource Report 2005-01, pp. 127–166.

Drilling in the Gilmour Brook area, located in the southeastern Bathurst Mining Camp, northern New Brunswick, has intersected a continuous stratigraphic section through the Tetagouche Group and into the underlying Miramichi Group. The Miramichi Group consists of interlayered black shale and grey, locally feldspar-rich wacke of the Patrick Brook Formation. The Tetagouche Group contains four formations. In ascending order, these are 1) the Nepisiguit Falls Formation, which comprises two facies: fine-grained volcaniclastic rocks and minor felsic flows of the Little Falls Member; and coarse-grained crystal-rich tuffs of the Grand Falls Member, 2) the Flat Landing Brook Formation, a thick sequence of grey to black, aphyric to sparsely feldspar-phyric rhyolites, 3) the Little River Formation, which comprises interbedded mafic volcanic and sedimentary rocks, and 4) the Tomogonops Formation, composed of interbedded calcareous shale and wacke.

The Gilmour Brook South base-metal occurrence is hosted by a stratigraphic section similar to that of the "Brunswick Horizon." Sulphide mineralization is commonly present as semi-massive to massive occurrences within, or at the top of, the Grand Falls Member of the Nepisiguit Falls Formation. The stratiform Pb–Zn mineralization has been intersected intermittently over a strike of 1400 m and to vertical depths of 700 m. Unlike the Brunswick deposits located farther north, the Gilmour Brook South occurrence shows little evidence of a laterally extensive exhalite, as it lacks an Algoma-type iron formation. The absence of this iron formation suggests either that deposition of the host sequence occurred under persistent anoxic conditions or that a high sedimentation rate and rapid burial may have prevented development of an iron-rich exhalite.

Des travaux de forage dans le secteur du ruisseau Gilmour, situé dans le sud-est du Camp minier de Bathurst, dans le Nord du Nouveau-Brunswick, ont entrecoupé une section stratigraphique continue à travers le groupe de Tetagouche et à l'intérieur du groupe sous-jacent de Miramichi. Le groupe de Miramichi à la base de la section est constitué de schiste noir interstratifé et de wacke localement cristallin, gris, de la Formation de Patrick Brook. Le groupe sus- de Tetagouche comporte quatre formations.

Celles-ci comprennent, dans un ordre ascendant 1) la Formation de Nepisiguit Falls, qui présente deux faciès : des roches volcanoclastiques à grains fins et une quantité restreinte de coulées felsiques du membre des chutes Little; et des tufs cristallins grossiers du membre des chutes Grand, 2) la Formation de Flat Landing Brook, une séquence épaisse de rhyolites aphyriques à rarement porphyrofeldspathiques grises à noires, 3) la Formation de Little River, qui se compose de roches sédimentaires et volcanomafiques interlitées, et 4) la Formation de Tomogonops, composée de wacke et de schiste calcareux interlités.

La venue de métaux communs du ruisseau Gilmour Sud est incluse dans une section stratigraphique similaire à celle de l'horizon Brunswick. Une minéralisation de sulfures est communément présente sous forme de venues semi-massives à massives à l'intérieur ou au sommet du membre des chutes Grand de la Formation de Nepisiguit Falls. On a recoupé la minéralisation de Pb–Zn stratiforme par intermittence le long d'un axe de 1 400 mètres et à des profondeurs verticales de 700 mètres. Contrairement aux gîtes Brunswick au nord, la venue du ruisseau Gilmour Sud présente peu d'indices d'exhalite latéralement étendue, car elle est dépourvue d'une formation ferrifère de type Algoma. L'absence de cette formation de fer laisse supposer que la sédimentation de la séquence hôte est survenue dans des conditions anoxiques persistantes ou qu'un taux de sédimentation prononcé pourrait avoir empêché le développement d'exhalite sédimentaire riche en fer.

INTRODUCTION

The Gilmour Brook South base-metal sulphide occurrence (New Brunswick Department of Natural Resources Mineral Occurrence Database Unique Reference Number (URN) 1394) lies in the southeastern part of the Bathurst Mining Camp (BMC), approximately 20 km south-southeast of the Brunswick No. 12 deposit, and 36 km south-southwest of the City of Bathurst (Fig. 1). The Pb–Zn mineralization at Gilmour Brook South is positioned at the same stratigraphic level as the Brunswick No. 6 and No. 12 deposits, at the top of the Nepisiguit Falls Formation (Fig. 2) in what is termed the "Brunswick Horizon;" the horizon contains the largest tonnage of economic sulphide mineralization in the BMC (Goodfellow and McCutcheon 2003).

The first exploration work at Gilmour Brook South was carried out by Key Anacon Mines Ltd. to investigate coincident north–south-trending magnetic and EM anomalies. Follow-up trenching uncovered 2.5 m of massive sulphides (Key Anacon Mines Ltd. 1977). After this initial discovery, no significant work took place in the area until Noranda Exploration Ltd. conducted ground geophysical surveys (Fig. 3) and a 40-hole diamond program (Banville 2001).

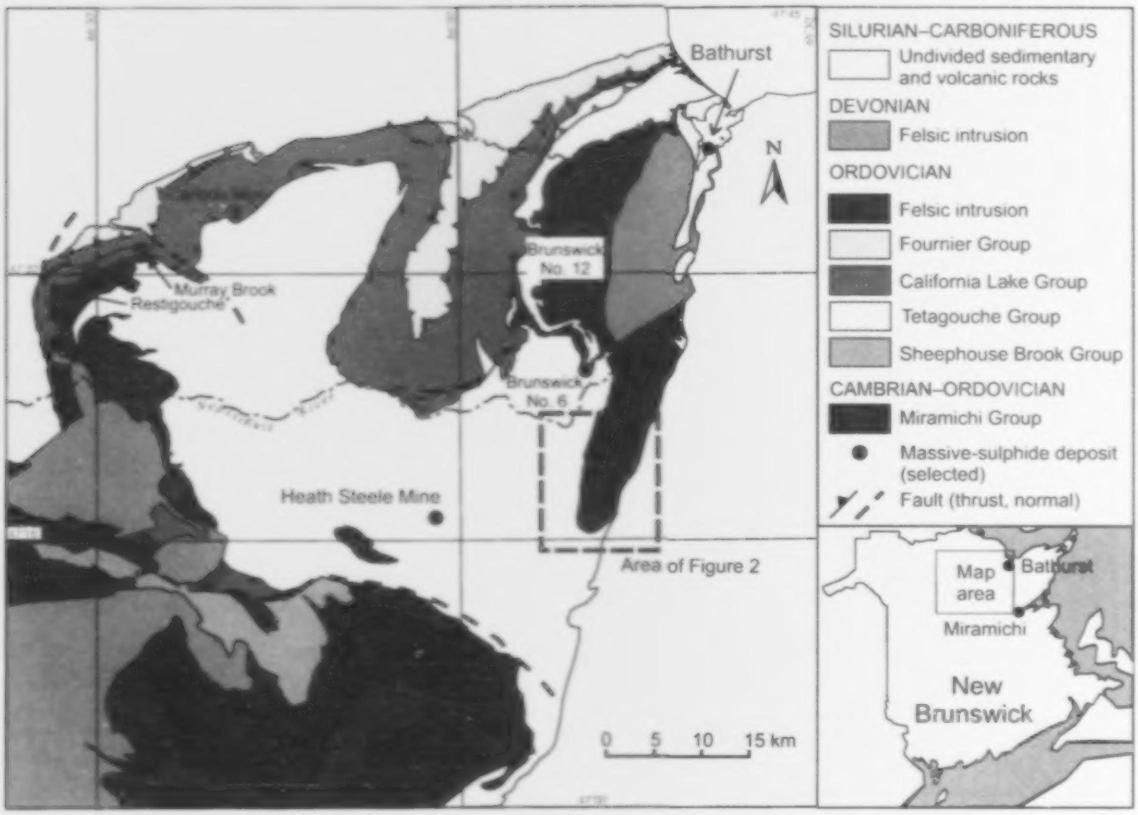
Bathurst
N
Brunswick No. 12
Murray Brook
Restigouche
Brunswick No. 6
Heath Steele Mine
Area of Figure 2
0 5 10 15 km
SILURIAN–CARBONIFEROUS
Undivided sedimentary and volcanic rocks
DEVONIAN
Felsic intrusion
ORDOVICIAN
Felsic intrusion
Fournier Group
California Lake Group
Tetagouche Group
Sheephouse Brook Group
CAMBRIAN–ORDOVICIAN
Miramichi Group
Massive-sulphide deposit (selected)
Fault (thrust, normal)
Map area
Bathurst
Miramichi
New Brunswick

Figure 1. Geology of the Bathurst Mining Camp, modified after van Staal et al. (2002). The Gilmour Brook area is outlined here in red (see Fig. 2).

This report is part of an ongoing assessment of New Brunswick's mineral deposits by the New Brunswick Department of Natural Resources. The work aims to establish the position of significant base-metal occurrences within the currently recognized stratigraphic framework of the BMC. The immediate objective of the current investigation is to document the size and extent of the known sulphide resource at Gilmour Brook South and to determine the chemical effects of hydrothermal activity (if any) associated with the mineralization process.

REGIONAL GEOLOGY

The BMC is underlain by polydeformed Early–Middle Ordovician bimodal volcanic and sedimentary rocks deposited in the Tetagouche–Exploits back-arc basin on the southeastern margin of the Iapetus Ocean. The back-arc basin formed landward of the Popelogan–Victoria Arc (van Staal et al. 2003) on a thick, Cambrian–Early Ordovician sedimentary sequence bordering the Avalonian continental margin (van Staal and Fyffe 1991).

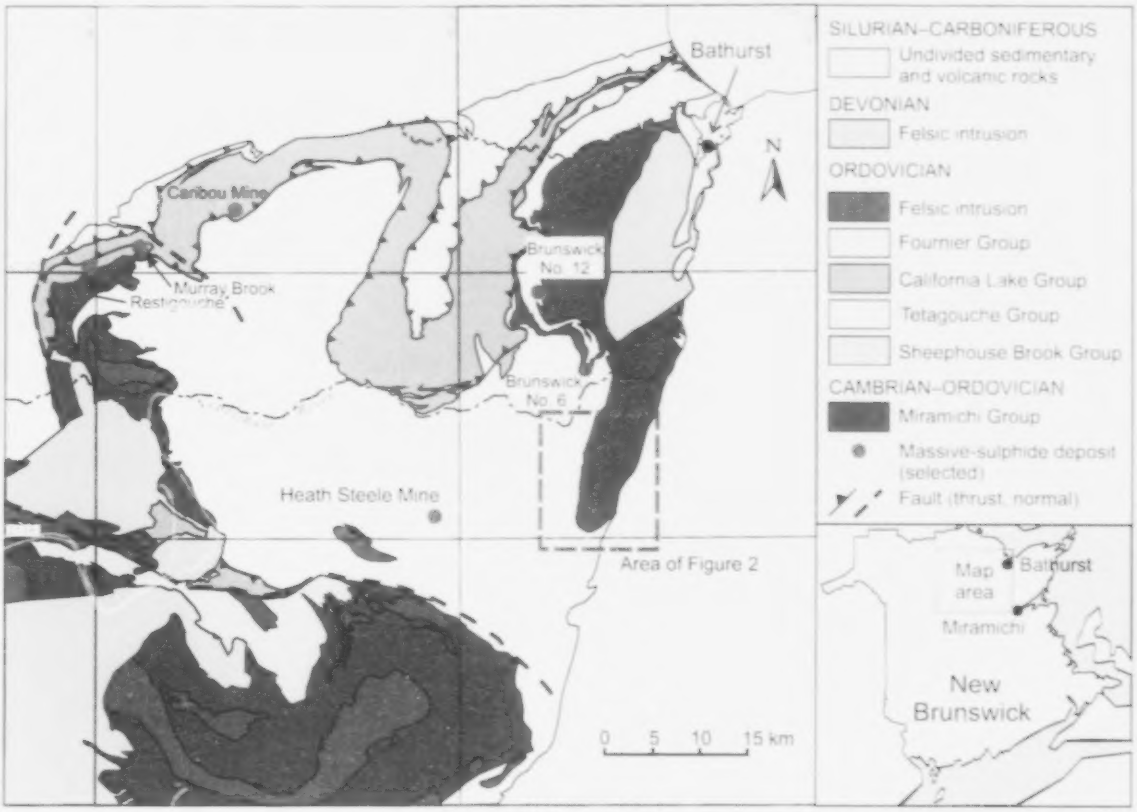
Bathurst
Caribou Mine
Murray Brook
Restigouche
Brunswick No. 12
Brunswick No. 6
Heath Steele Mine
Area of Figure 2
N
0 5 10 15 km
SILURIAN–CARBONIFEROUS
Undivided sedimentary and volcanic rocks
DEVONIAN
Felsic intrusion
ORDOVICIAN
Felsic intrusion
Fournier Group
California Lake Group
Tetagouche Group
Sheephouse Brook Group
CAMBRIAN–ORDOVICIAN
Miramichi Group
Massive-sulphide deposit (selected)
Fault (thrust, normal)
Map area
Bathurst
Miramichi
New Brunswick

Figure 1. Geology of the Bathurst Mining Camp, modified after van Staal et al. (2002). The Gilmour Brook area is outlined here in red (see Fig. 2).

This report is part of an ongoing assessment of New Brunswick's mineral deposits by the New Brunswick Department of Natural Resources. The work aims to establish the position of significant base-metal occurrences within the currently recognized stratigraphic framework of the BMC. The immediate objective of the current investigation is to document the size and extent of the known sulphide resource at Gilmour Brook South and to determine the chemical effects of hydrothermal activity (if any) associated with the mineralization process.

REGIONAL GEOLOGY

The BMC is underlain by polydeformed Early–Middle Ordovician bimodal volcanic and sedimentary rocks deposited in the Tetagouche–Exploits back-arc basin on the southeastern margin of the Iapetus Ocean. The back-arc basin formed landward of the Popelogan–Victoria Arc (van Staal et al. 2003) on a thick, Cambrian–Early Ordovician sedimentary sequence bordering the Avalonian continental margin (van Staal and Fyffe 1991).

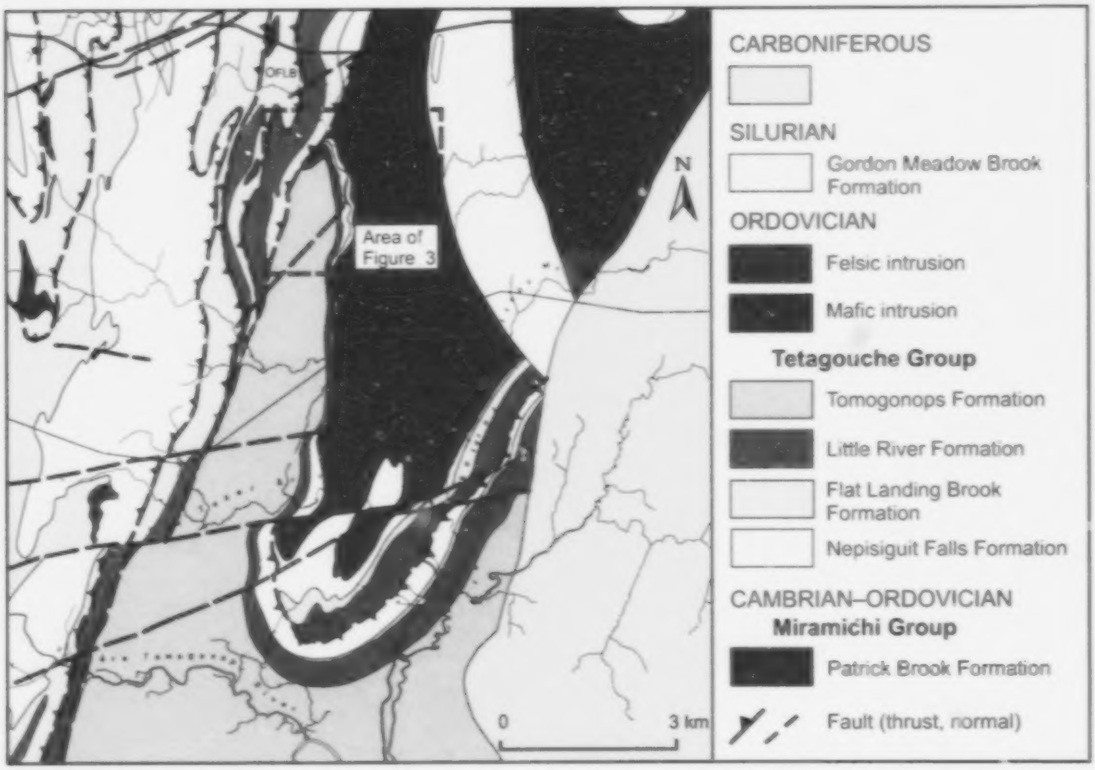
OFLB
Area of Figure 3
N
0
3 km
CARBONIFEROUS
SILURIAN
Gordon Meadow Brook Formation
ORDOVICIAN
Felsic intrusion
Mafic intrusion
Tetagouche Group
Tomogonops Formation
Little River Formation
Flat Landing Brook Formation
Nepisiguit Falls Formation
CAMBRIAN–ORDOVICIAN
Miramichi Group
Patrick Brook Formation
Fault (thrust, normal)

Figure 2. Geology of the Gilmour Brook area, modified after van Staal et al. (2002). Map location is outlined on Figure 1.

Rocks of the BMC were dismembered, deformed, and juxtaposed in an accretionary prism during the Late Ordovician–Early Silurian closure of the Tetagouche–Exploits back-arc basin (van Staal 1994). Deformation related to this subduction event is complex, and at least five generations of folding have been distinguished (van Staal 1994; McCutcheon and Walker 2001). Four major thrust nappes have been recognized in the BMC. Each nappe contains a distinctive internal stratigraphy and features numerous stratigraphic cut-outs and repetitions related to subsidiary thrust faults.

As currently understood, the regional stratigraphy comprises five major sequences. In ascending order, these are the Miramichi, Sheephouse Brook, Tetagouche, California Lake, and Fournier groups (Fig. 1) that collectively make up the Bathurst Supergroup (see Wilson et al. 1998; Thomas et al. 2000; and van Staal et al. 2003 for detailed descriptions). The Miramichi Group consists of quartzose turbidites that form the substratum to the back-arc volcanic pile. The Tetagouche, Sheephouse Brook, and California Lake groups contain distinctive mafic and felsic volcanic sequences that were formed in different parts of the back-arc basin. The Fournier Group contains mafic volcanic rocks and gabbroic rocks that represent remnants of back-arc oceanic crust.

A total of 46 known volcanogenic massive-sulphide deposits occur in the BMC and are spatially associated with felsic volcanic rocks. Nine deposits have reached either

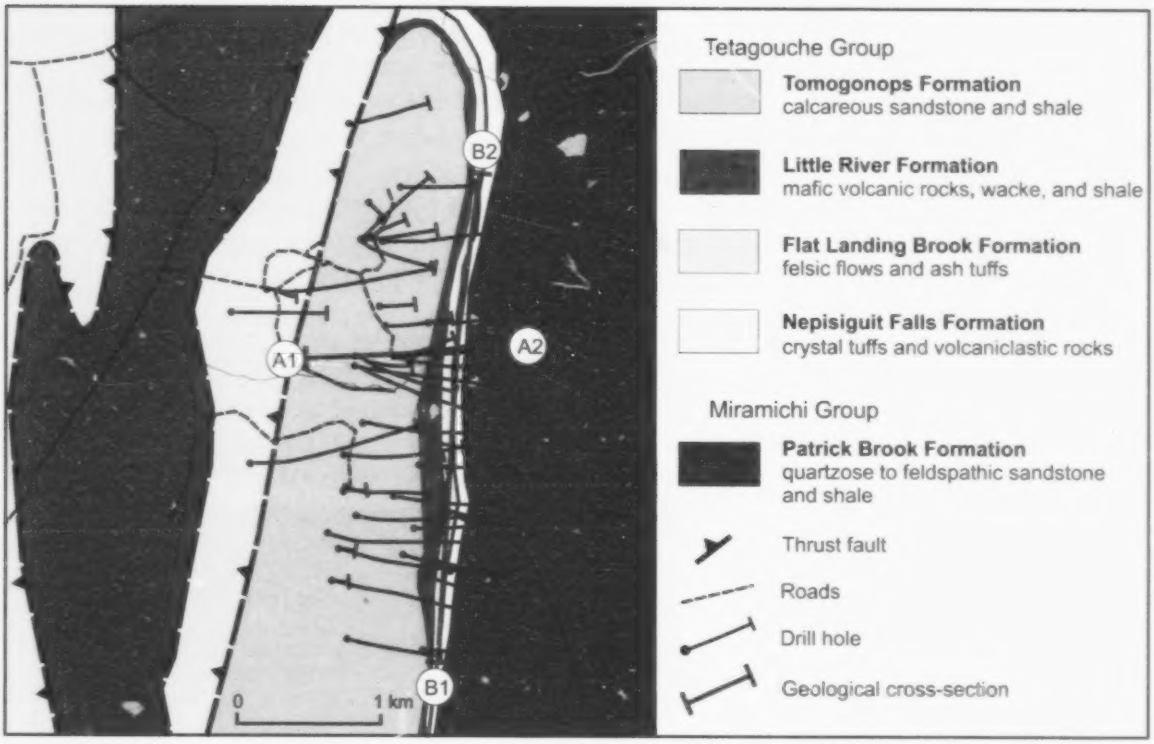
B2
A1
A2
B1
0
1 km
Tetagouche Group
Tomogonops Formation
calcareous sandstone and shale
Little River Formation
mafic volcanic rocks, wacke, and shale
Flat Landing Brook Formation
felsic flows and ash tuffs
Nepisiguit Falls Formation
crystal tuffs and volcaniclastic rocks
Miramichi Group
Patrick Brook Formation
quartzose to feldspathic sandstone and shale
Thrust fault
Roads
Drill hole
Geological cross-section

Figure 3. Detailed geology of the Gilmour Brook area, marking the position of the drill hole collars (map location is outlined on Fig. 2). Cross-section A1–A2 through the Gilmour Brook South sulphide occurrence is shown on Figure 8; longitudinal section B1–B2 is shown on Figure 13.

production or an advanced stage of pre-production development. The most notable of these is the currently producing Brunswick Mine or Brunswick No. 12 deposit (Fig. 1), which contained a pre-mining resource of 229 Mt of massive sulphides (Goodfellow and McCutcheon 2003).

Felsic volcanic rocks of the Tetagouche Group host 32 of the 46 deposits in the BMC. Of these, 24 occur within the Nepisiguit Falls Formation in the lower part of the stratigraphic section; the remaining eight occur within the overlying Flat Landing Brook Formation (McCutcheon et al. 2001). Chemically precipitated iron formation overlies, and is laterally continuous with, many of the deposits hosted by the Nepisiguit Falls Formation, whereas iron formation is absent to poorly developed within deposits of the Flat Landing Brook Formation. Mafic volcanic rocks of the Little River Formation and overlying wacke and shale of the Tomogonops Formation form the upper part of the Tetagouche Group.

STRATIGRAPHIC SETTING OF HOST ROCKS

Drill core from the Gilmour Brook South occurrence provides a complete stratigraphic record through the Ordovician volcanic sequence in the southeastern part of the BMC. The section begins with the Patrick Brook Formation of the Miramichi Group (Fig. 2, 3), then

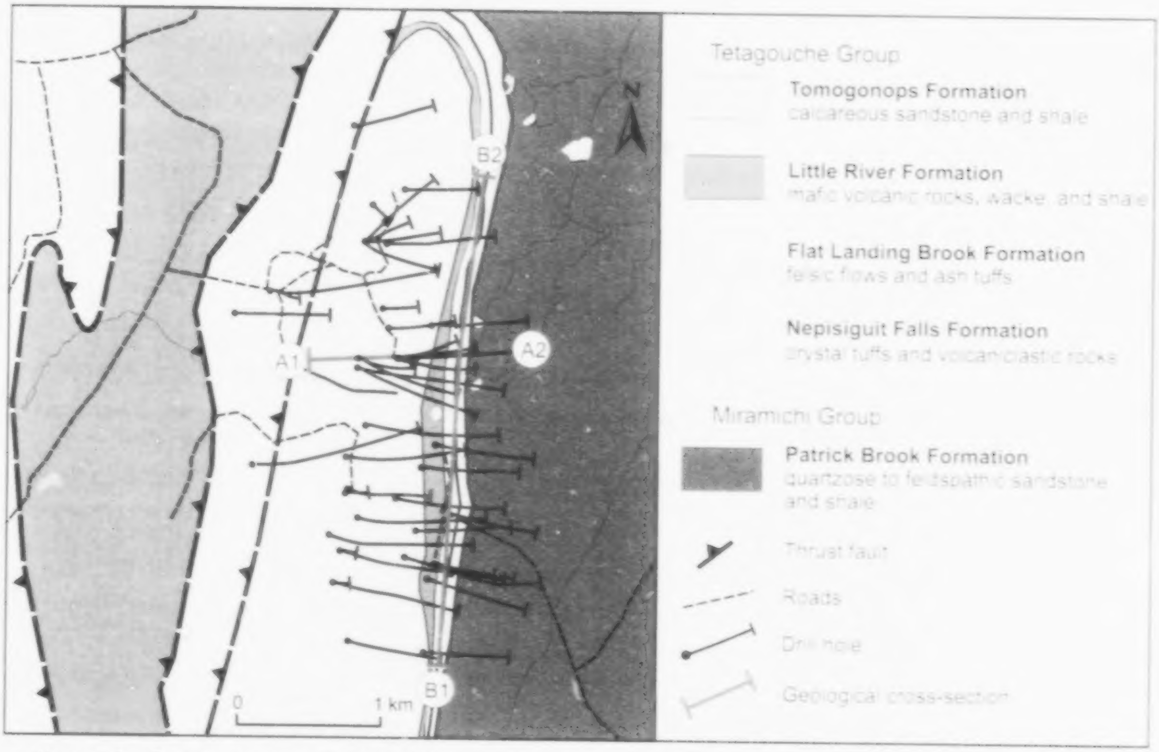
B2
N
A1
A2
B1
0
1 km
Tetagouche Group
Tomogonops Formation
calcareous sandstone and shale
Little River Formation
mafic volcanic rocks, wacke, and shale
Flat Landing Brook Formation
felsic flows and ash tuffs
Nepisiguit Falls Formation
crystal tuffs and volcaniclastic rocks
Miramichi Group
Patrick Brook Formation
quartzose to feldspathic sandstone and shale
Thrust fault
Roads
Drill hole
Geological cross-section

Figure 3. Detailed geology of the Gilmour Brook area, marking the position of the drill hole collars (map location is outlined on Fig. 2). Cross-section A1–A2 through the Gilmour Brook South sulphide occurrence, is shown on Figure 8; longitudinal section B1–B2 is shown on Figure 13.

production or an advanced stage of pre-production development. The most notable of these is the currently producing Brunswick Mine or Brunswick No. 12 deposit (Fig. 1), which contained a pre-mining resource of 229 Mt of massive sulphides (Goodfellow and McCutcheon 2003).

Felsic volcanic rocks of the Tetagouche Group host 32 of the 46 deposits in the BMC. Of these, 24 occur within the Nepisiguit Falls Formation in the lower part of the stratigraphic section; the remaining eight occur within the overlying Flat Landing Brook Formation (McCutcheon et al. 2001). Chemically precipitated iron formation overlies, and is laterally continuous with, many of the deposits hosted by the Nepisiguit Falls Formation, whereas iron formation is absent to poorly developed within deposits of the Flat Landing Brook Formation. Mafic volcanic rocks of the Little River Formation and overlying wacke and shale of the Tomogonops Formation form the upper part of the Tetagouche Group.

STRATIGRAPHIC SETTING OF HOST ROCKS

Drill core from the Gilmour Brook South occurrence provides a complete stratigraphic record through the Ordovician volcanic sequence in the southeastern part of the BMC. The section begins with the Patrick Brook Formation of the Miramichi Group (Fig. 2, 3), then passes conformably upward into the Nepisiguit Falls, Flat Landing Brook, Little River, and Tomogonops formations of the Tetagouche Group.

Patrick Brook Formation

The Patrick Brook Formation in the Gilmour Brook area consists of light grey sandstone and interbedded black (locally graphitic) shale. The sandstone beds are up to 1 m thick and generally have a quartzose composition. Feldspar clasts are less abundant than in the type section at the confluence of Patrick Brook and the Tetagouche River but constitute up to 20% of the detritus in some core intervals. Shale beds average less than 10 cm in thickness. The sandstone-to-shale ratio varies considerably throughout the unit. In DDH GS-30, for example, the top of the unit contains approximately 50% black shale in intervals up to 1 m thick, but, with depth, the shale becomes subordinate to sandstone (Fig. 4a, b).

Nepisiguit Falls Formation

In the area of Brunswick Mines, the Nepisiguit Falls Formation has been divided into two facies: the Little Falls and Grand Falls members. The Little Falls Member consists

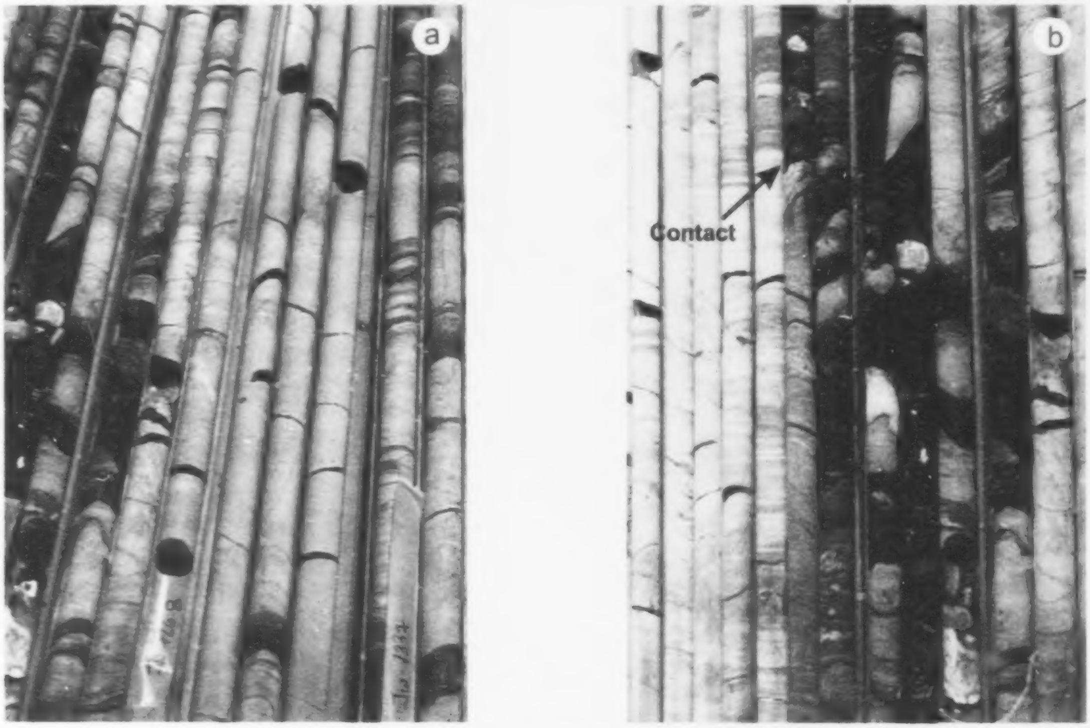

Figure 4. Rock types and contact relationships in the Patrick Brook Formation (Miramichi Group) in the Gilmour Brook area. a) Interbedded sandstone and subordinate black (locally graphitic) shale; DDH GS-28 from 720 to 730 m. b) Upper contact of the Patrick Brook Formation with fine-grained rocks of the Nepisiguit Falls Formation. Note that shale increases toward the top of the Patrick Brook Formation. In both figures, stratigraphic top is to the lower left. The diameter of the drill core in these figures, as well as in Figures 5, 6, 7, and 11, is approximately 4.5 cm.

largely of fine-grained, volcaniclastic rocks (Langton and McCutcheon 1993) that are interpreted to represent vent-distal tuffs and reworked tuffs (Rogers et al. 2003a). The Grand Falls Member consists mainly of coarse-grained quartz–feldspar crystal tuffs (Langton and McCutcheon 1993) that are interpreted to represent vent-proximal pyroclastic deposits and/or synvolcanic hypabyssal intrusions (Rogers et al. 2003a). In some districts of the BMC such as the Heath Steele area (Lentz and Wilson 1997), volcaniclastic rocks of the Little Falls Member lie at the base of the section and are gradational upward into the Grand Falls Member; in other locations, such as the Flat Landing Brook area, their order is reversed (Walker and Lentz, in press).

Both volcanic facies of the Nepisiguit Falls Formation can be recognized in the Gilmour Brook area. At the base of the formation, the fine-grained volcaniclastic facies typical of the Little Falls Member is usually, but not always, dominant and locally contains thin, crystal-rich lenses (Fig. 5a, b). Toward the top of the formation, the crystal-rich facies of the Grand Falls Member becomes more prevalent (Fig. 5c, d), although it remains

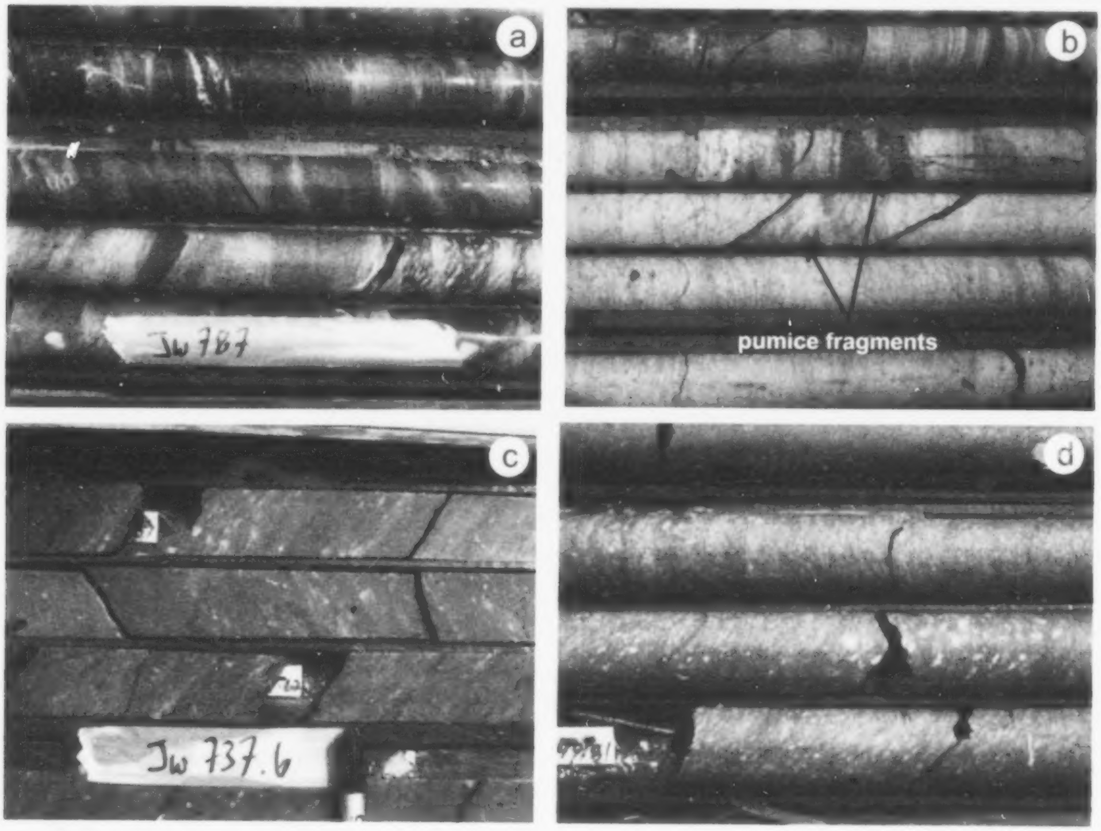

Figure 5. Variation in rock types of the Nepisiguit Falls Formation in the Gilmour Brook area. a) Basal part of the Nepisiguit Falls Formation, showing fine-grained volcaniclastic rocks of the Little Falls Member containing a thin (< 15 cm), crystal-rich lens within a few metres of the contact with the underlying Patrick Brook Formation (DDH GS-28 at 787 m). b) Crystal-bearing pumice clasts within fine-grained volcaniclastic rocks of the Little Falls Member (DDH GS-30 at 647 m). c) Quartz–feldspar crystal tuff of the Grand Falls Member interlayered with ash tuff of the Little Falls Member (DDH GS-28 at 737.6 m). d) Quartz–feldspar crystal tuff of the Grand Falls Member.

volumetrically subordinate to the fine-grained facies. Aphyric felsic flows are locally interlayered with volcaniclastic rocks of the Little Falls Member below the mineralized horizon in DDH GS-37. In DDH GS-30, the Little Falls and Grand Falls members are 29 m and 41 m thick respectively, for a total thickness of 70 m. In other drill hole intersections, the two members can reach a total thickness of 120 m.

Crystal-rich pumice clasts (Fig. 5b) that formed during explosive volcanic activity are present in rocks of the Little Falls Member and could imply a primary pyroclastic origin for the unit. However, the limited number of pumice fragments, the dominantly fine-grained nature of the rocks, and the presence of narrow (10 to 30 cm) lenses of crystal-rich (winnowed) material all suggest that the unit more likely has volcaniclastic origin. No definitive pyroclastic rocks exist in the Gilmour Brook area. The most likely source of the pumice fragments lies northward along strike in the Brunswick No. 6 area (Fig. 1), where the Grand Falls and Little Falls members are 250 m and 400 m thick respectively, giving a total thickness of 650 m for the Nepisiguit Falls Formation (Rogers et al. 2003a).

The relationship between the two tuffaceous facies in the Gilmour Brook area implies that at least two eruptive events are recorded in the Nepisiguit Falls Formation. The first event generated fine-grained ash tuffs and reworked tuffs typical of the Little Falls Member; these materials probably were deposited some distance from the vent. The second event produced both a fine-grained and a coarse-grained facies, the latter being more typical of the vent-proximal Grand Falls Member.

The contact between the Nepisiguit Falls Formation and the overlying Flat Landing Brook Formation is variable in nature. In some drill core, aphyric rhyolite or ash tuff of the Flat Landing Brook Formation lie in sharp conformable contact with ash tuff or crystal tuff of the Nepisiguit Falls Formation. In other core (such as DDH GS-30), black shale and fine-grained sandstone mark the boundary between the two units. Several core samples show the massive sulphides as being conformable on, and/or gradational into, the underlying Nepisiguit Falls Formation.

Flat Landing Brook Formation

The Flat Landing Brook Formation (Fig. 6a–f) consists of light grey to black aphyric rhyolite and minor pyroclastic rocks. Less commonly, the rhyolite contains small (< 2 mm), scattered feldspar phenocrysts. Devitrification textures such as spherulites occur locally (Fig. 6a), as do amygdaloidal textures. Primary fragmental textures interpreted to represent carapace breccias or sole breccias have also been recognized in some locales (Fig. 6b, c).

Thin units of ash tuff, lapilli tuff (dominated by lithic fragments), and minor volcaniclastic rocks are locally interlayered with the rhyolite. Fine-grained ash tuff occurs throughout the section, but in some drill holes it is especially prevalent at the base of the

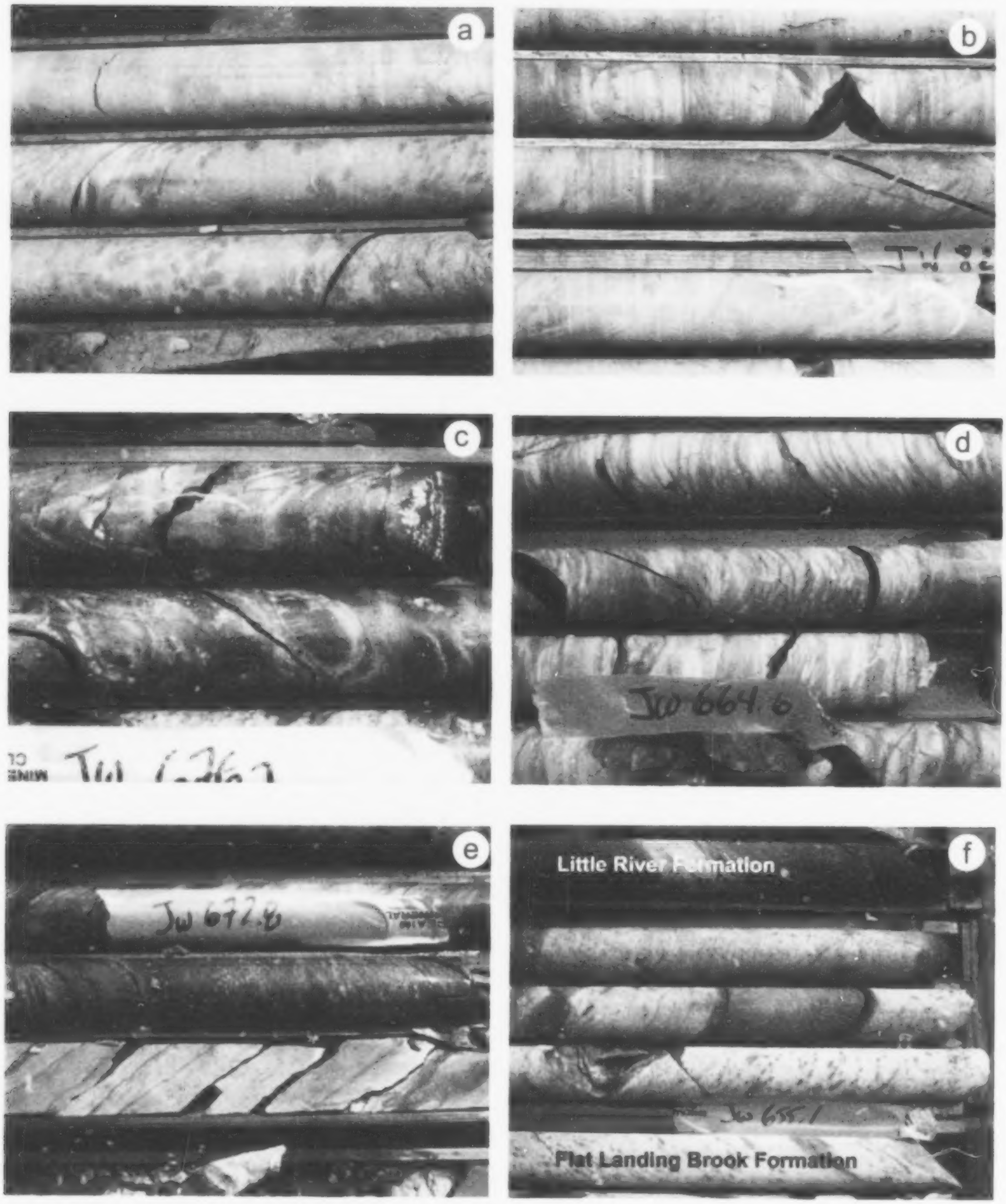
a
b
c
d
Jw 664.6
e
Jw 672.8
f
Little River Formation
Jw 655.1
Flat Landing Brook Formation

Figure 6. Rocks of the Flat Landing Brook Formation in the Gilmour Brook area. a) Black spherulitic rhyolite (DDH GS-37b at 787 m). b) Fragmental textures in black rhyolite (DDH GS-37b at 820 m). c) Rhyolitic sole breccia (DDH GS-28 at 676 m). d) Grey felsic ash tuff (DDH GS-28 at 664.6 m). e) Lens of quartz–feldspar-crystal-rich volcaniclastic rock within ash tuff in the hanging wall (DDH GS-28 at 672.8 m). f) Interbedded felsic ash tuff and black shale at the transitional upper contact of the Flat Landing Brook Formation with the Little River Formation (DDH GS-28 at 655.1 m).

Flat Landing Brook Formation (Fig. 6d). In places, thin (~ 20 cm) layers of quartz–feldspar-crystal-rich (> 20%) material are interlayered with the ash tuffs (Fig. 6e).

Thin, pyrite-bearing ash tuff horizons at the top of the Flat Landing Brook Formation are interlayered with, and gradational into, shale and/or basalt of the overlying Little River Formation (Fig. 6f). This transitional boundary marks the change from felsic-dominated to mafic-dominated volcanism recognized throughout the BMC (van Staal et al. 2003a).

Little River Formation

The Little River Formation in the Gilmour Brook area comprises black shale and subordinate medium grey wacke in its lower part (Fig. 7a) and is composed mainly of mafic volcanic rocks in its upper part (Fig. 7b). The entire unit at surface likely does not exceed a thickness of 75 m; at depth, however, some drill holes have intersected up to 200 m of the formation. The mafic volcanic rocks are easily recognized in core samples by their green colour and their local carbonate- and magnetite-rich zones (Fig. 7b). Mafic rocks of the formation occur in the northern part of the Gilmour Brook area, are completely absent in the southern part, and then reappear at the nose of an antiform farther south (Fig. 2, 3).

Tomogonops Formation

The Tomogonops Formation consists of thin-bedded, buff calcareous sandstone interlayered with grey-green, locally calcareous siltstone (Fig. 7c). Wacke layers with individual grains up to 3 mm in diameter are locally common. Graphitic shale lenses are abundant in the lower part of the section but are absent in the upper part, suggesting a gradational, sedimentological relationship with shales of the underlying Little River Formation. For the purpose of this paper, the base of the Tomogonops Formation is defined as the lower contact of the first calcareous sedimentary layer.

The original thickness of the Tomogonops Formation is unknown, as its strata are truncated by a thrust fault to the west and buried by Carboniferous rocks to the east (Fig. 2, 3). Nonetheless, the exposed thickness is at least 700 m and may be as great as 1.5 km.

STRUCTURAL GEOLOGY

On the basis of stratigraphic evidence, the structural block hosting the Gilmour Brook South occurrence is interpreted to be a south-closing anticline (Fig. 3). The stratiform mineralization lies on the western limb of the structure and dips moderately (approximately 45°) west, although areas of more steeply inclined (≤ 70°) stratigraphy can be observed (Fig. 8). The Tomogonops Formation at the top of the sequence has yielded primary sedimentary structures including graded beds and fine-grained to coarse-grained contacts consistent with a westward-younging, right-way-up sequence. This gross distribution of the

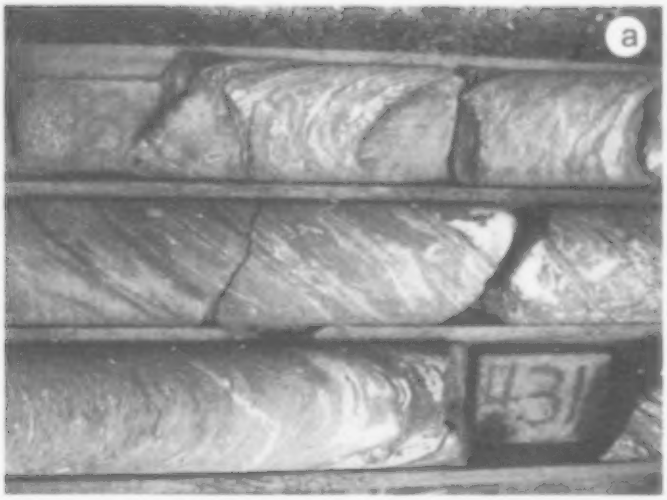

Figure 7. a) Sedimentary rocks of the Little River Formation in the Gilmour Brook area.

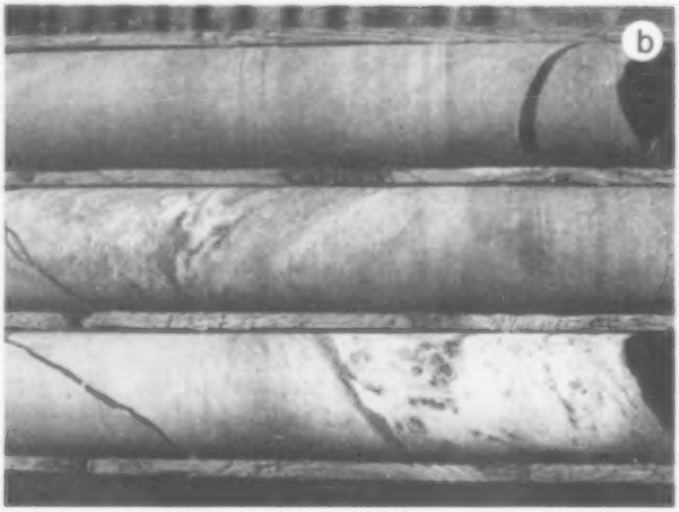

Figure 7. b) Mafic volcanic rocks of the Little River Formation in the Gilmour Brook area.

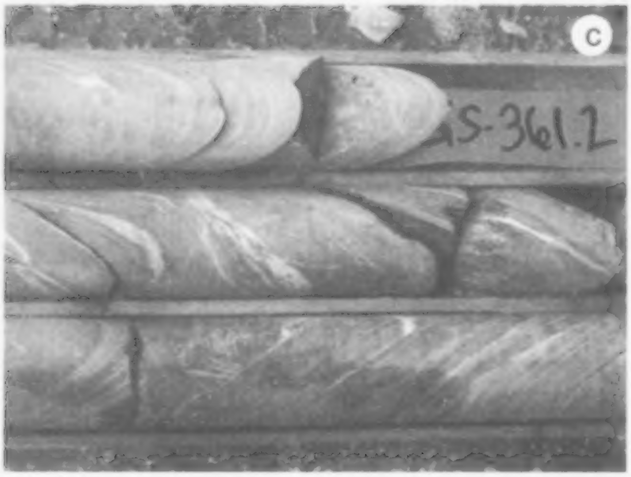

Figure 7. c) Sedimentary rocks of the Tomogonops Formation in the Gilmour Brook area.

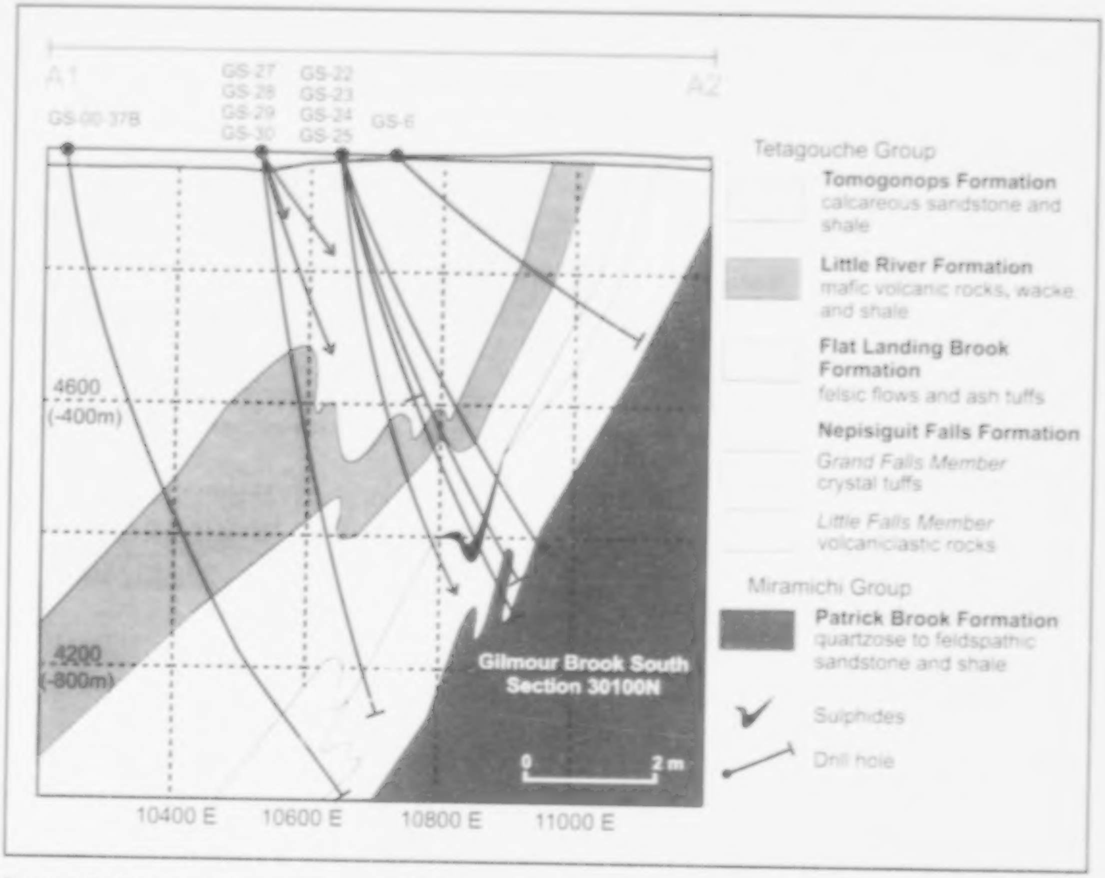
A1
A2
GS-00-37B
GS-27
GS-28
GS-29
GS-30
GS-22
GS-23
GS-24
GS-25
GS-6
4600
(-400m)
4200
(-800m)
Gilmour Brook South
Section 30100N
0
2 m
10400 E
10600 E
10800 E
11000 E
Tetagouche Group
Tomogonops Formation
calcareous sandstone and shale
Little River Formation
mafic volcanic rocks, wacke and shale
Flat Landing Brook Formation
felsic flows and ash tuffs
Nepisiguit Falls Formation
Grand Falls Member
crystal tuffs
Little Falls Member
volcaniclastic rocks
Miramichi Group
Patrick Brook Formation
quartzose to feldspathic sandstone and shale
Sulphides
Drill hole

Figure 8. Geological cross-section A1–A2 through the Gilmour Brook South occurrence. Line of section is marked on Figure 3.

Tetagouche Group, characterized by felsic volcanic rocks at the base transitioning into mafic volcanic rocks and then sedimentary rocks, is consistent with the stratigraphy of the Tetagouche Group recognized elsewhere. It also supports the interpretation of a westward-younging sequence (van Staal and Fyffe 1991; van Staal et al. 2003).

The Gilmour Brook area, like the entire BMC, has undergone polyphase deformation. However, evidence that appears elsewhere to distinguish folding events in the BMC is rarely, if ever, recognized in any one outcrop or in drill core in the study area. In most drill core examined during this project, the dominant structural fabric lies at a high angle to the core axis and is interpreted to represent a combination of S and S, whereas a later, less well developed fabric is oriented roughly parallel to the core axis and is interpreted to be axial planar to F folds. Given that the deformational event D is primarily a layer-parallel thrusting with abundant sheath fold development, and that D consists of upright to vertical isoclinal folds (van Staal 1985, 1994), the associated S and S fabrics tend to be subparallel everywhere except in hinge regions of the F folds. Consequently, definitive S and S cleavage relationship are rarely seen. Instead, the most prevalent cleavage is an S–S composite cleavage.

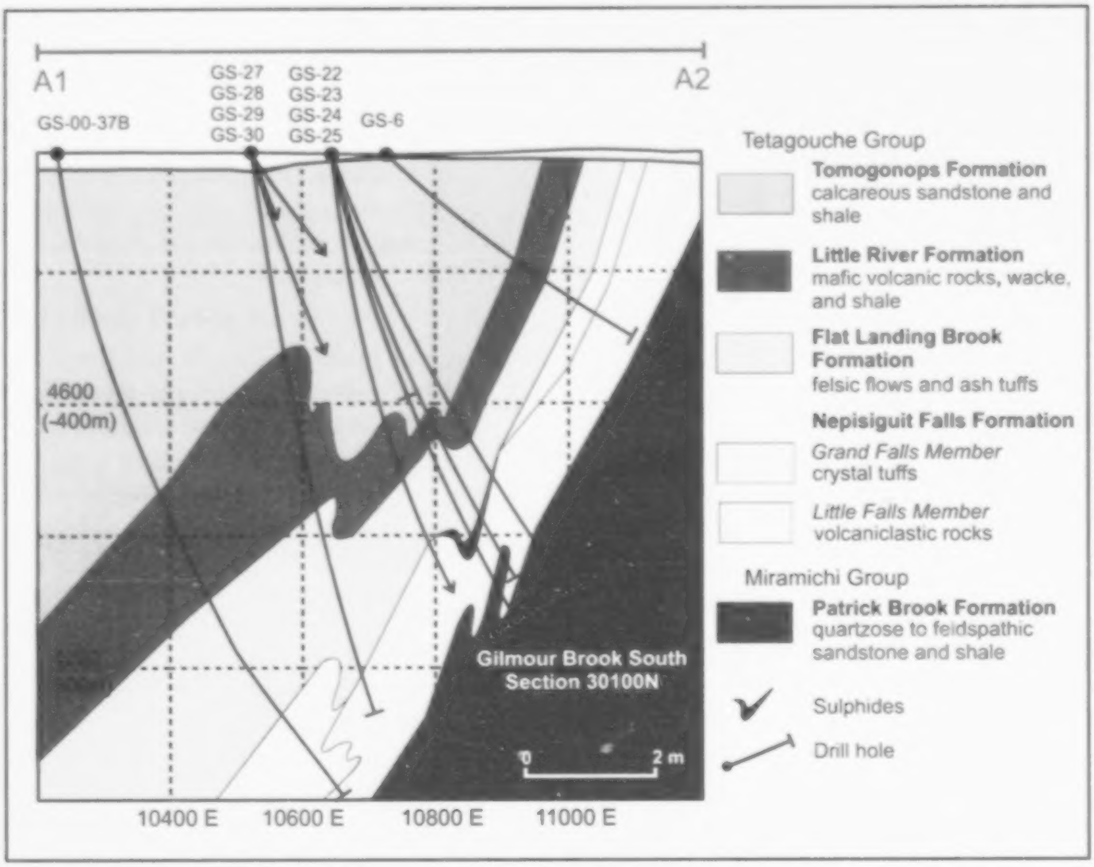
A1
A2
GS-00-37B
GS-27
GS-28
GS-29
GS-30
GS-22
GS-23
GS-24
GS-25
GS-6
4600
(-400m)
Gilmour Brook South
Section 30100N
0
2 m
10400 E
10600 E
10800 E
11000 E
Tetagouche Group
Tomogonops Formation
calcareous sandstone and shale
Little River Formation
mafic volcanic rocks, wacke, and shale
Flat Landing Brook Formation
felsic flows and ash tuffs
Nepisiguit Falls Formation
Grand Falls Member
crystal tuffs
Little Falls Member
volcaniclastic rocks
Miramichi Group
Patrick Brook Formation
quartzose to feldspathic sandstone and shale
Sulphides
Drill hole

Figure 8. Geological cross-section A1–A2 through the Gilmour Brook South occurrence. Line of section is marked on Figure 3.

Tetagouche Group, characterized by felsic volcanic rocks at the base transitioning into mafic volcanic rocks and then sedimentary rocks, is consistent with the stratigraphy of the Tetagouche Group recognized elsewhere. It also supports the interpretation of a westward-younging sequence (van Staal and Fyffe 1991; van Staal et al. 2003).

The Gilmour Brook area, like the entire BMC, has undergone polyphase deformation. However, evidence that appears elsewhere to distinguish folding events in the BMC is rarely, if ever, recognized in any one outcrop or in drill core in the study area. In most drill core examined during this project, the dominant structural fabric lies at a high angle to the core axis and is interpreted to represent a combination of S_0 and S_1, whereas a later, less well developed fabric is oriented roughly parallel to the core axis and is interpreted to be axial planar to F_2 folds. Given that the deformational event D_1 is primarily a layer-parallel thrusting with abundant sheath fold development, and that D_2 consists of upright to vertical isoclinal folds (van Staal 1985, 1994), the associated S_1 and S_2 fabrics tend to be subparallel everywhere except in hinge regions of the F_2 folds. Consequently, definitive S_1 and S_2 cleavage relationship are rarely seen. Instead, the most prevalent cleavage is an S_1–S_2 composite cleavage.

Mapping by van Staal et al. (2003) shows a thrust separating the Tetagouche and Miramichi groups in the Gilmour Brook area. The present study found no evidence of this structure within the drilling area. However, a thrust at a lower stratigraphic level, within the Miramichi Group, cannot be ruled out. Minor, late-stage brittle faults may have acted to interleave units locally, as evidenced in DDH GS-28, where a thin slice of rocks from the Miramichi Group is juxtaposed against fine-grained rocks from the Nepisiguit Falls Formation. Massive sulphides above and below this block may represent the same horizon that was offset along normal to oblique-slip faults lying at a high angle to the stratigraphy (Fig. 3).

LITHOGEOCHEMISTRY

A total of 53 samples were collected from unaltered host rocks and hydrothermally altered zones at Gilmour Brook South. Samples were analyzed to determine the chemical affinity of the various rock types and to document effects of hydrothermal alteration (if any) on the host units. A total of 33 samples of felsic volcanic rocks were collected from the Gilmour Brook South drill core: 14 from the Nepisiguit Falls Formation and 19 from the Flat Landing Brook Formation. Four samples of mafic volcanic rocks were collected from the Little River Formation. As well, 16 sedimentary rock samples were collected: six from the Patrick Brook Formation (Miramichi Group), four from the Little River Formation, and six from the Tomogonops Formation (both of the Tetagouche Group).

Felsic Volcanic Rocks

Volcanic rocks are typically classified using major element variables such as SiO_2, Na_2O, and K_2O. Two of the most commonly used discrimination diagrams are the K_2O vs SiO_2 and the $Na_2O + K_2O$ vs SiO_2 diagrams developed by Le Maitre et al. (1989).

On the $Na_2O + K_2O$ vs SiO_2 diagram (Fig. 9a), most felsic volcanic samples from the Gilmour Brook South occurrence appear to have normal $Na_2O + K_2O$ contents and plot in the rhyolite and dacite fields. However, Tables 1 to 4 (included with Tables 5 to 7 at the end of this paper) show that the Na_2O content of the rocks is low and that the $Na_2O + K_2O$ content is mainly a function of anomalously high K_2O (Fig. 9b). Depletion of Na_2O and enrichment of K_2O are well documented in the BMC and are attributed to interaction of seawater with heated volcanic rocks at the time of deposition or shortly thereafter (Lentz 1996). Trace-element ratios are more reliable for protolith determination in rocks that have undergone hydrothermal alteration and/or greenschist-grade metamorphism (Lentz 1996).

Felsic volcanic rocks at Gilmour Brook South can be divided into four populations, based upon their distribution on a Zr/TiO_2 vs Nb/Y discrimination diagram. The crystal-rich tuff of the Grand Falls Member and aphyric flows interlayered with the Little Falls Member, both of the Nepisiguit Falls Formation, cluster tightly in the lower part of the rhyodacite/dacite field (Fig. 9c). In contrast, felsic flows of the Flat Landing Brook

Formation tend to cluster in the rhyolite field (Fig. 9d). The fine-grained volcaniclastic rocks (Little Falls Member) of the Nepisiguit Falls Formation appear to have alkaline affinities, displaying a high Nb/Y, and plot in the trachyandesite field (Fig. 9c). Composition of the ash tuff of the Flat Landing Brook Formation is spread between the andesite and rhyolite fields (Fig. 9d). This scatter in fine-grained samples is likely attributable to varying degrees of terrigenous sedimentary input into the volcaniclastic rocks rather than to differences in primary magmatic composition of the source rocks. Alternatively, the lower Y values could have resulted from incomplete digestion of resistant phases such as the Y-bearing mineral monazite during sample preparation for chemical analysis; this could account for the higher than normal Nb–Y ratios.

Trace-element analysis shows that, at Gilmour Brook South, the boundary between the Nepisiguit Falls and Flat Landing Brook formations cannot be absolutely defined on the basis of chemistry, as some volcaniclastic rocks at the boundary are macroscopically indistinguishable and have overlapping chemistries. Moreover, black rhyolite that occurs in the hanging wall immediately above the sulphide-bearing horizon has a Zr–TiO_2 ratio similar to that of crystal tuffs from the Nepisiguit Falls Formation (Fig. 9c, d). Aphyric rhyolite flows with chemical similarities to the Nepisiguit Falls Formation have not been previously recognized within the BMC. However, in the Gilmour Brook area, as elsewhere in the BMC, volcanic rocks of the Nepisiguit Falls Formation generally have a lower Zr–TiO_2 ratio than do rocks of the Flat Landing Brook Formation.

Mafic Volcanic Rocks

Volcanic samples from the Little River Formation (Table 5) plot in the basanite and trachyandesite fields on the $Na_2O + K_2O$ vs SiO_2 diagram (Fig. 9a) and in the alkalic basalt field on the Zr/TiO_2 vs Nb/Y diagram (Fig. 9d). Their chemistry is similar to that of the Brunswick Mines Member of the Little River Formation in the hanging wall of the Brunswick No. 12 deposit (van Staal et al. 1991, 2003; Rogers and van Staal 2003).

Sedimentary Rocks

Major-element chemistry of sedimentary rocks from the Gilmour Brook area (Tables 4 to 7) can be used to distinguish rocks deposited before or during felsic volcanism from those deposited during later, mafic volcanism (Rogers et al. 2003b). Samples from the Patrick Brook Formation of the Miramichi Group plot in the "felsic volcanic" field on an MgO vs Cr discrimination diagram (Fig. 10a), which is consistent with having received input from a felsic volcanic source, probably the Popelogan–Victoria Arc (Rogers et al. 2003a). Most samples collected from the Little River and Tomogonops formations of the Tetagouche Group fall in the "mafic volcanic" field, meaning that material for the sedimentary rocks was sourced from dominantly mafic volcanic (ophiolitic) terranes. On the other hand, one sedimentary sample from the Little River Formation and two sedimentary samples from the Tomogonops Formation plot in the "felsic volcanic" field.

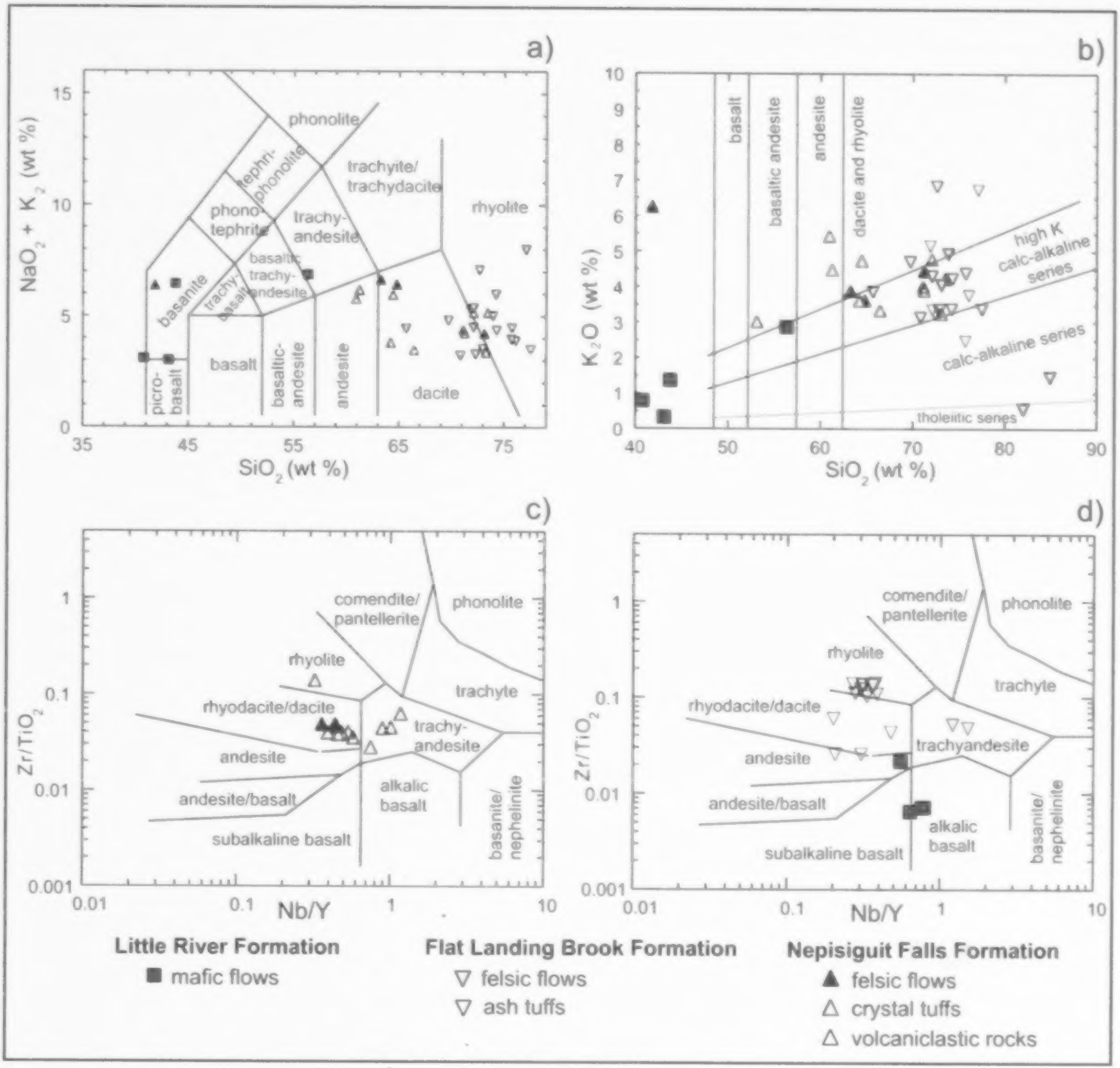

Figure 9. Lithogeochemical variation diagrams for volcanic rocks at Gilmour Brook South. a) Na$_2$O + K$_2$O vs SiO$_2$ diagram. b) K$_2$O vs SiO$_2$ diagram. c) Zr/TiO$_2$ vs Nb/Y diagram for footwall. d) Zr/TiO$_2$ vs Nb/Y diagram for hanging wall. Fields for Figures 9a and 9b are from Le Maitre et al. (1989). Fields for Figures 9c and 9d are from Winchester and Floyd (1977).

Trace-element chemistry can also be used to distinguish the source of sedimentary rocks in the BMC. On the V–Zr/2–Ni ternary diagram (Fig. 10b), shale samples from the Patrick Brook Formation lie above a line from the V apex to Zr/2 = 60%, whereas those from the Little River (with one exception) and Tomogonops formations lie below this line. Similarly, on the Zr/Cr vs V/Nb diagram (Fig. 10c), shales from the Miramichi and Tetagouche groups are divided by a line of slope (m) = 0.17; shale from the Patrick Brook Formation (Miramichi Group) has a higher Zr/Cr, whereas shale from the Little River and

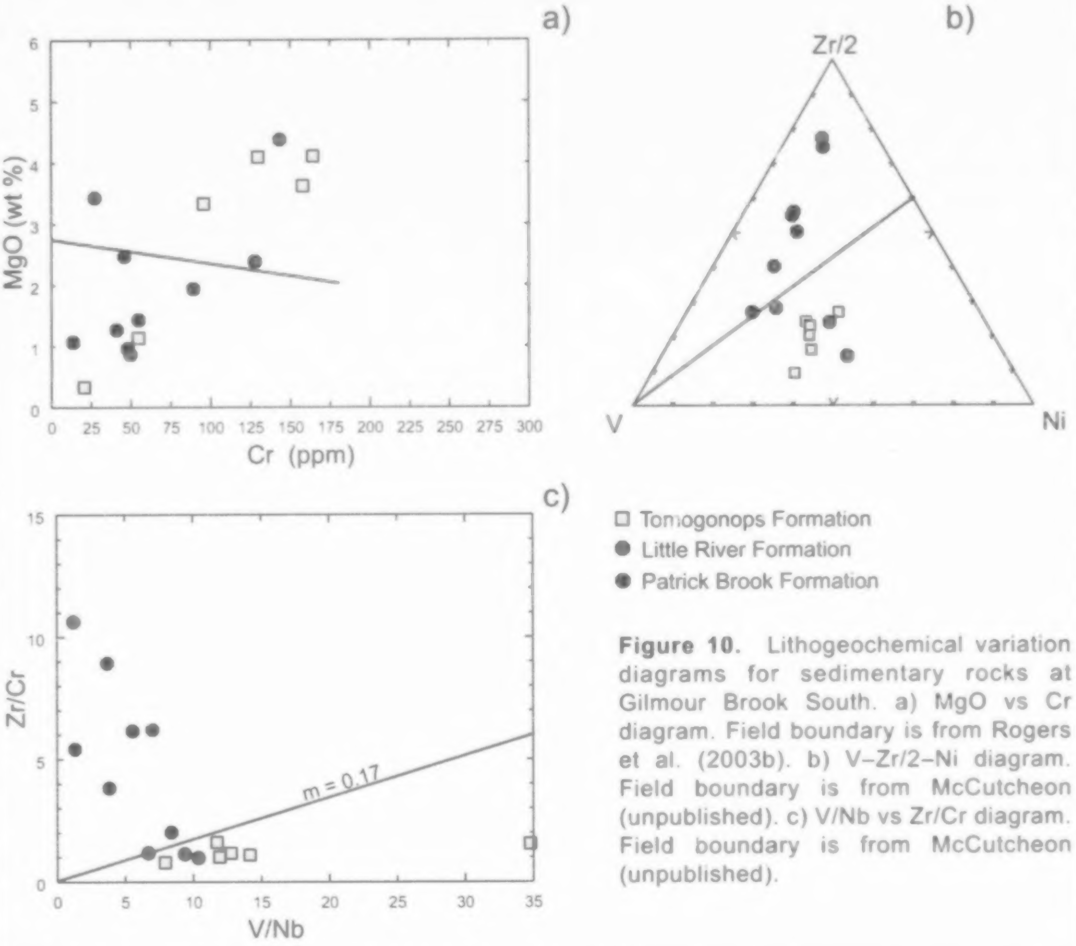

Figure 10. Lithogeochemical variation diagrams for sedimentary rocks at Gilmour Brook South. a) MgO vs Cr diagram. Field boundary is from Rogers et al. (2003b). b) V–Zr/2–Ni diagram. Field boundary is from McCutcheon (unpublished). c) V/Nb vs Zr/Cr diagram. Field boundary is from McCutcheon (unpublished).

Tomogonops formations (Tetagouche Group) has a higher V/Nb. The chemistry of the younger sedimentary rocks (the Little River and Tomogonops formations) reflects a mafic-dominated source that most likely was the obducted ophiolitic rocks bordering the Tetagouche–Exploits back-arc basin (Rogers et al. 2003a).

GILMOUR BROOK SOUTH MINERALIZATION

The stratigraphic position of the Gilmour Brook South occurrence is similar to that of the "Brunswick Horizon" mineralization, in that the occurrence's stratiform massive-sulphide lenses are situated along the boundary between the Nepisiguit Falls and Flat Landing Brook formations of the Tetagouche Group (Fig. 2). Unlike the Brunswick No. 6 and No. 12 deposits farther north, the occurrence has no well developed oxide facies iron formation. The mineralized horizon at Gilmour Brook South is intermittent over a strike of 1400 m and has been intersected to a vertical depth of 700 m (Fig. 8).

Because the massive sulphides at Gilmour Brook South are extensively recrystallized, it is impossible to determine if the mineral layering was originally primary (Fig. 11a). The massive lenses locally contain narrow zones (20 to 50 cm wide) of brecciated sulphide fragments in a sulphide matrix (Fig. 11b). However, it is unclear whether this texture is in part primary or is purely an effect of metamorphism. Local sphalerite and pyrite stringers that intersect the dominant fabric at a moderate angle suggest that the sulphides underwent at least some postdepositional to syntectonic remobilization.

The footwall of the sulphide lenses is generally in gradational contact and locally in sharp contact with crystal-rich rocks (Grand Falls Member) or crystal-poor rocks (Little Falls Member) of the Nepisiguit Falls Formation (Fig. 11c, d). Some drill core shows

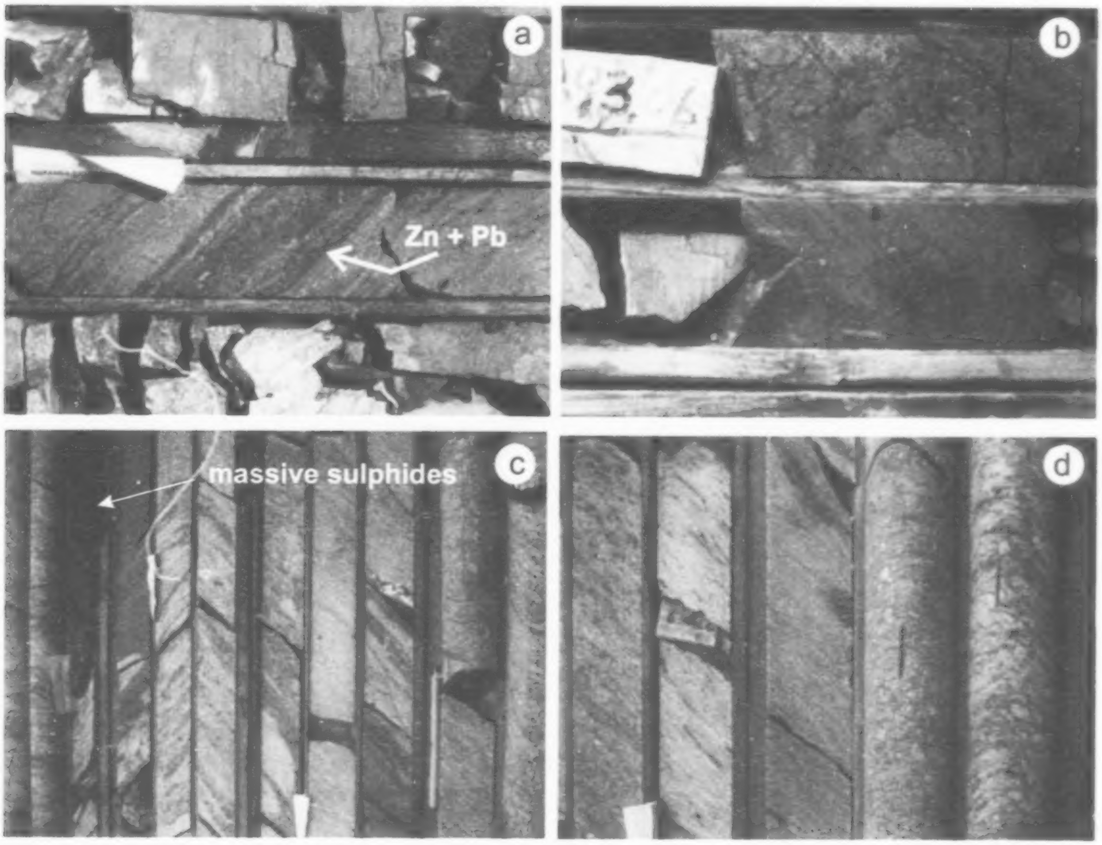

Figure 11. Massive-sulphide textures at Gilmour Brook South. a) Massive sulphides (dominantly pyrite) with a zone of high-grade sphalerite and galena (DDH GS-38 at 767 m). b) Pyrite breccia zone consisting of large, massive pyrite fragments in a recrystallized pyrite matrix (DDH GS-41 at 893.6 m). c) Massive sulphides in sharp contact (left side of photograph) with felsic volcanic fragmental rocks of the Flat Landing Brook Formation in the hanging wall; sulphides in the footwall consist of stringers and disseminations in crystal–lithic rocks of the Nepisiguit Falls Formation (DDH GS-29 at 774 m). d) Disseminated sulphides in the Nepisiguit Falls Formation in the footwall (DDH GS-29 at 782 m).

evidence of sulphide replacing the matrix of the crystal tuffs: DDH GS-31, for example, contains several narrow (< 50 cm) pulses of sulphide mineralization separated by chloritic zones that contain variable amounts of disseminated to patchy pyrite (Fig. 11d). At least some parts of the deposit appear to have been formed by subsurface replacement of the more permeable horizons, as seen in DDH GS-31, where the matrix of a quartz-crystal tuff is replaced by sulphides (Fig. 11e). In other locations, only discordant sulphide stringers occur in the footwall.

The hanging wall contact of the sulphide lenses with ash tuff, rhyolite, or lithic tuff of the Flat Landing Brook Formation invariably is sharp (Fig. 11c, f); locally, the upper contact of the sulphide lenses shows evidence of folding (Fig. 11f). Several drill logs report "chert" in the hanging wall contact with massive sulphides, but this material most likely is ash tuff or fine-grained hyaloclastite of the overlying Flat Landing Brook Formation.

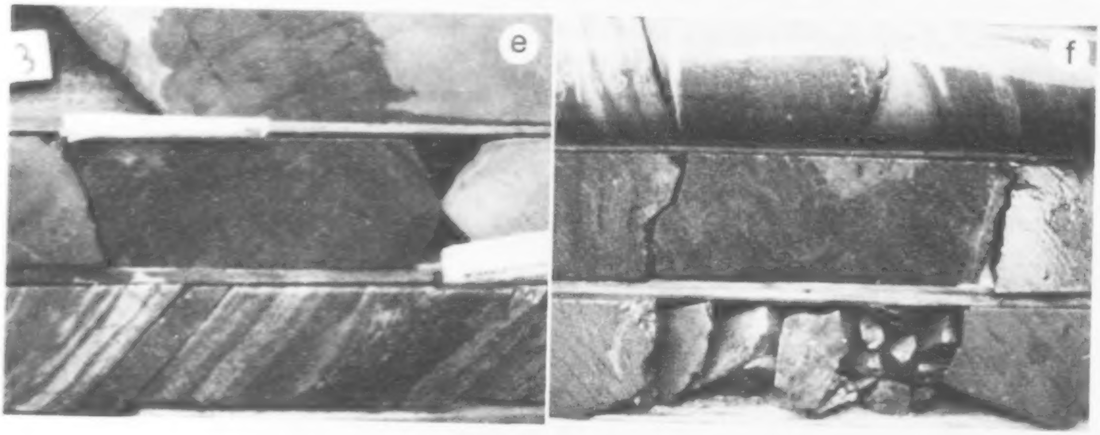

Figure 11 *(cont'd).* Massive-sulphide textures at Gilmour Brook South. e) Disseminated sulphides in chloritized quartz-crystal tuff of the Nepisiguit Falls Formation (DDH GS-31 at approximately 573 m). f) Felsic volcanic rocks (fragmental textures) of the Flat Landing Brook Formation in the hanging wall adjacent to the massive sulphides. The top of the sulphide lens is folded and contains sphalerite and galena; the lower part of the lens is massive pyrite (DDH GS-41 at 891.6 m).

The majority of base-metal assays (n=944) from the Gilmour Brook South occurrence plot in the Pb–Zn field on a Pb–Cu–Zn ternary diagram (Fig. 12). The average Zn–Pb ratio is 2.44, typical of deposits in the BMC and indeed of many felsic, volcanic-hosted deposits worldwide (Franklin et al. 1981). The average Cu–Pb–Zn ratio is 1:2.5:6.1 with an average Ag content of 7.6 g/t. The small number of samples clustered around the Cu apex (assays of 0.13% Cu over 28 m from DDH GS-38) may represent vent-proximal Cu-enriched mineralization. The most economically significant intersection at Gilmour Brook South came from DDH GS-22 and assayed 0.19% Cu, 1.02% Pb, 9.61% Zn, and 32.3 g/t Ag over 7.98 m (Noranda, unpublished data). Some narrower, high-grade zones have also been found. DDH GS-14, for instance, intersected 7.63% Pb and 13.57% Zn over 2.89 m.

Contours have been plotted to show the thickness of massive sulphides and the Pb + Zn assay data along a longitudinal section at Gilmour Brook South (Fig. 13). Sulphides

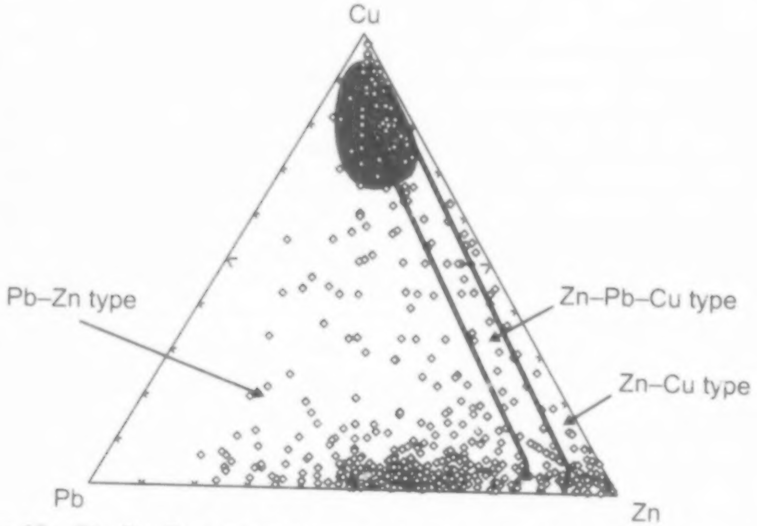

Figure 12. Pb–Cu–Zn ternary diagram showing assay data (n = 944) from the Gilmour Brook South occurrence. The blue shaded area highlights samples from DDH GS-38. Fields boundaries are from Franklin et al. (1981).

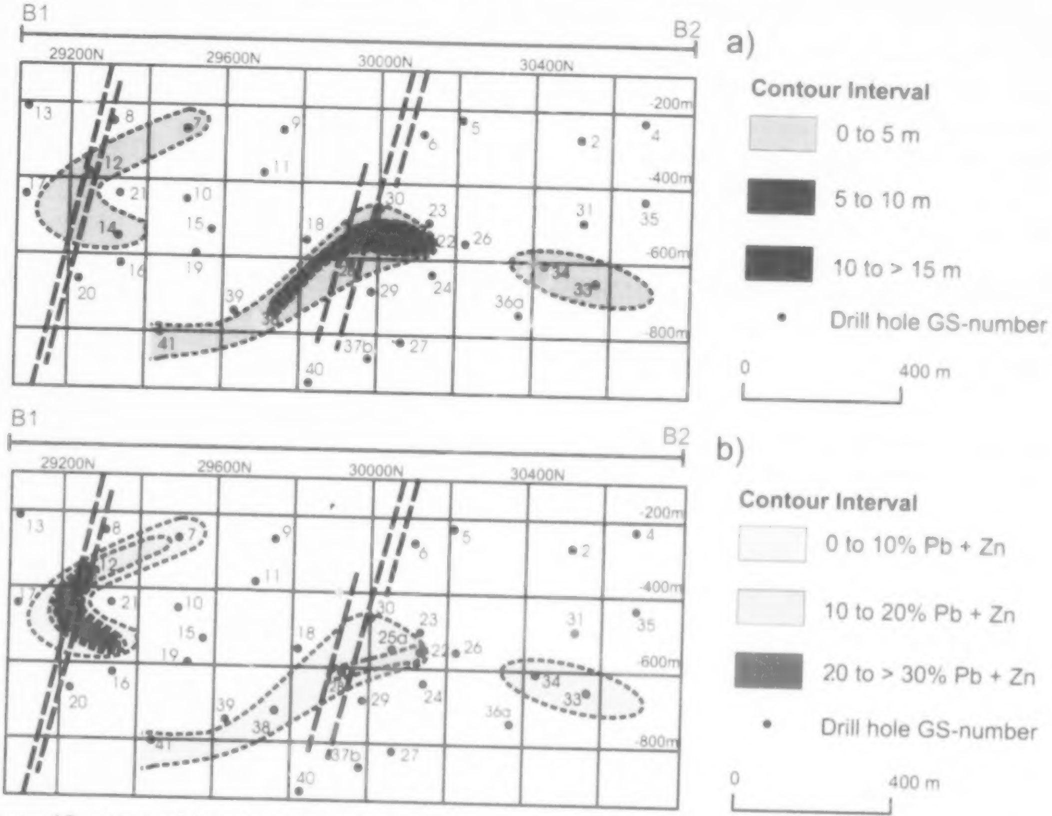
B1
B2
a)
29200N
29600N
30000N
30400N
-200m
-400m
-600m
-800m
Contour Interval
0 to 5 m
5 to 10 m
10 to > 15 m
Drill hole GS-number
0
400 m
B1
B2
b)
Contour Interval
0 to 10% Pb + Zn
10 to 20% Pb + Zn
20 to > 30% Pb + Zn
Drill hole GS-number
0
400 m

Figure 13. Line of longitudinal section B1–B2 (marked on Fig. 3) for the Gilmour Brook South occurrence. a) Thickness of massive sulphides; contours at 5 m intervals. b) Pb + Zn in wt %; contours at 10% intervals. Dashed lines represent brittle faults too small to show on Figure 3.

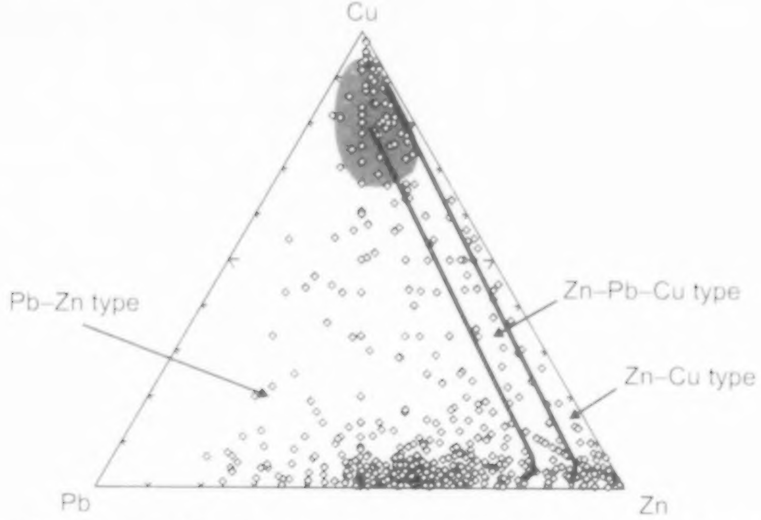

Figure 12. Pb–Cu–Zn ternary diagram showing assay data (n = 944) from the Gilmour Brook South occurrence. The blue shaded area highlights samples from DDH GS-38. Fields boundaries are from Franklin et al. (1981).

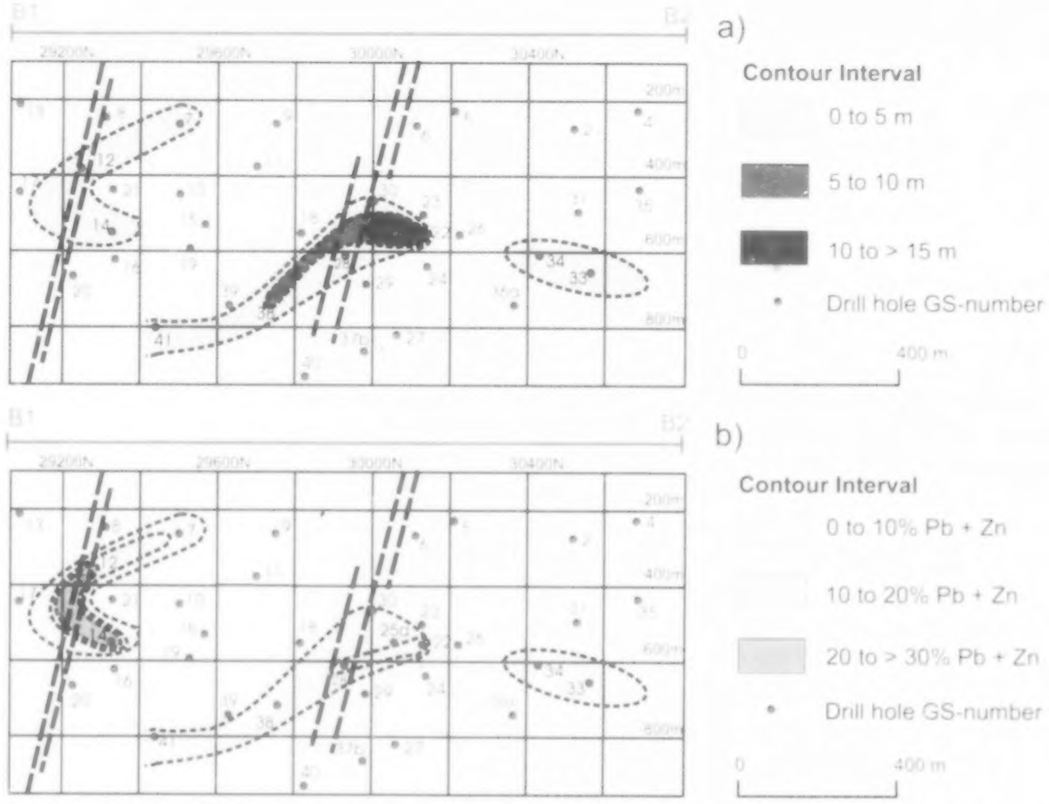
B1
B2
29200N
29600N
30000N
30400N
200m
400m
600m
800m
a)
Contour Interval
0 to 5 m
5 to 10 m
10 to > 15 m
Drill hole GS-number
0
400 m
b)
Contour Interval
0 to 10% Pb + Zn
10 to 20% Pb + Zn
20 to > 30% Pb + Zn
Drill hole GS-number
0
400 m

Figure 13. Line of longitudinal section B1–B2 (marked on Fig. 3) for the Gilmour Brook South occurrence. a) Thickness of massive sulphides; contours at 5 m intervals. b) Pb + Zn in wt %; contours at 10% intervals. Dashed lines represent brittle faults too small to show on Figure 3.

vary from being dominant in pyrite–pyrrhotite–chalcopyrite, as in DDH GS-25a and DDH GS-38, to being dominant in pyrite–sphalerite–galena, as in DDH GS-7, DDH GS-12, and DDH GS-14 (Fig. 13). Sections with higher Cu and abundant pyrrhotite are interpreted to represent a more vent-proximal facies, whereas Zn–Pb-rich zones are interpreted to represent concordant stratiform mineralization. In some cross-sections, chalcopyrite and pyrrhotite appear to increase toward the east (footwall) side of the sulphide horizon. This poorly developed zoning supports a westward-younging direction, as similar relationships are seen in other stratiform sulphide deposits throughout the BMC and elsewhere (Franklin et al. 1981).

The Gilmour Brook South occurrence appears to be divisible into at least two lenses, albeit on the basis of information from fairly wide-spaced drill holes. To the south is a shallow lens that has thin (about 3.5 m thick) but very high-grade (8% to 29% Pb + Zn) accumulations of massive sulphides; this lens appears to be drilled off in both directions along strike and downdip (Fig. 13). The second, deeper lens apparently tops at 215 m below surface and consists of thicker (1 to 15.7 m) sulphide accumulations. The average grade in the deep lens is lower than that in the shallow lens but is quite variable, ranging from less than 2% to 19% Pb + Zn. Interestingly, the four thickest sulphide intersections in the deep lens (those with more than 4 m of massive sulphides) define a zone that is at least 700 m long. Although the shallow part of this lens in the vicinity of DDH GS-22 and DDH GS-25a seems to have been drilled off, the extension that rakes to the south is open downdip and downplunge. To the south, around DDH GS-41 (Fig. 13), sulphides were intersected at 680 m below surface; however, it is unclear whether this represents the downdip extension of the thick lens.

The structural model of the Brunswick No. 12 deposit (van Staal 1985) identifies refolded F_1 folds (F_2 fold noses) as a possible target for additional tonnage at depth. Drilling results (Hussey 1992) confirmed this hypothesis at the No. 12 deposit, although the intersected sulphides were not economic. This model potentially could apply to the Gilmour Brook South mineralization, as the upper and lower sulphide lenses may occur on opposite limbs of an F_1 fold whose nose lies to the south and at depth.

HYDROTHERMAL ALTERATION

Hydrothermal alteration at the Gilmour Brook South occurrence is divided into proximal chlorite and quartz, and distal sericite. Footwall alteration is variously developed and is dominated by sericite alteration with subordinate chlorite alteration. The most intense footwall alteration is spatially related to sulphide veins and presumably reflects alteration adjacent to a feeder conduit, as described in many VMS systems (Franklin et al. 1981).

Chemical data from sedimentary rocks of the Gilmour Brook area (Table 4 to 7) have been plotted on discrimination diagrams to determine the amount of hydrothermal input into these rocks. None of the samples appears to have a significant hydrothermal component according to the Fe–Al–Mn diagram (Fig. 14a) or the Fe/Ti vs Al/(Al + Fe + Mn) diagram (Fig. 14b). The absence of a recognizable hydrothermal component in these rocks could be explained in several ways: 1) mineralizing fluids were focused along permeable horizons within the volcanic pile and precipitated sulphides below the rock water interface, 2) the exhalitive chemical signature was masked and/or diluted by regular sedimentation, and 3) rapid burial by felsic volcanic rocks may have smothered the hydrothermal cell before an exhalite (other than massive sulphides) could form.

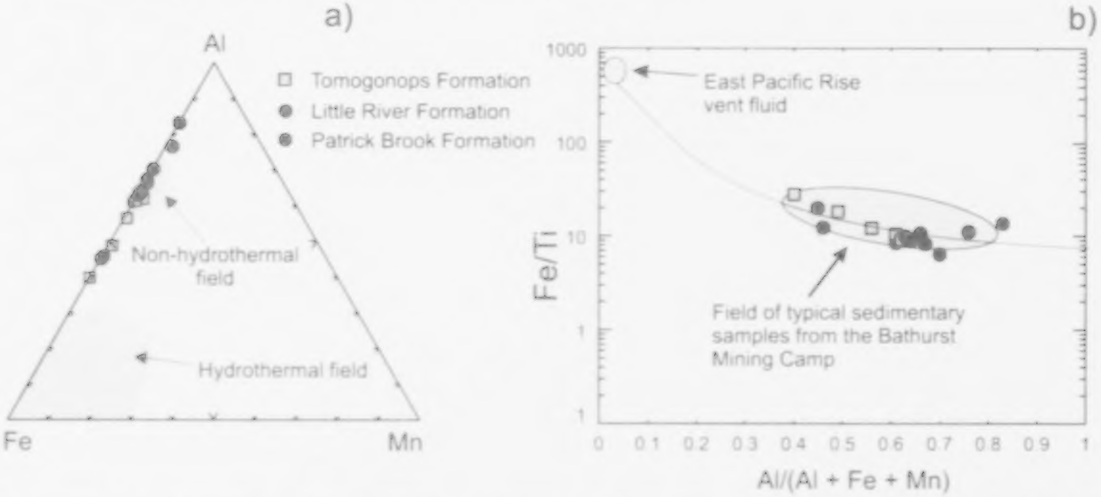

Figure 14. Lithogeochemical variation diagrams for sedimentary rocks at Gilmour Brook South. a) Fe–Al–Mn ternary diagram. b) Fe/Ti vs Al/(Al + Fe + Mn) diagram. Field boundaries in both figures are from Boström (1973).

DISCUSSION AND CONCLUSIONS

The Gilmour Brook area is unique in the BMC. It is the only known location to feature a complete section through the Miramichi Group and the overlying Tetagouche Group. As well, the relatively thin accumulation of felsic volcanic (150 to 400 m) and mafic volcanic (0 to 160 m) rocks suggests that, from a paleogeographic standpoint, this area probably was peripheral to major volcanic centres that presumably were located along the axis of the Tetagouche–Exploits back-arc basin.

The type section for the Nepisiguit Falls Formation is up to 650 m thick; it contains a lower massive (tuff lava) facies approximately 250 m thick, and an upper volcaniclastic facies approximately 400 m thick. In the Gilmour Brook area, the formation is much thinner, ranging from approximately 70 to 120 m thick. This thinner sequence, coupled with the absence of a massive facies, suggests that the Gilmour Brook area was probably distal to the vent from which the Nepisiguit Falls lavas were erupted. The fact that the

Nepisiguit Falls Formation is dominated by fine-grained, volcaniclastic rocks at the base of the sequence and coarse-grained, crystal-rich rocks at the top suggests that the formation in this area records at least two pulses of felsic volcanism.

Throughout the BMC, the Grand Falls Member is characterized by the absence of primary volcanic textures such as breccias or hyaloclastite aprons. This is attributed to the presumed mode of emplacement, which is interpreted to be as shallow sills, dykes, cryptodomes, and minor flows. However, the low aspect ratio indicated by the present distribution of the Grand Falls Member in the Gilmour Brook area suggests that the unit's crystal tuffs and related volcaniclastic rocks are of subaqueous pyroclastic origin. The polyphase deformation and greenschist-grade metamorphism in the BMC would all but preclude the preservation of primary pyroclastic textures except within rocks in low-strain areas. In contrast, the Little Falls Member is interpreted to have formed entirely from deposition as reworked tuffs of the Grand Falls Member and is characterized by bedded deposits that have undergone varying degrees of crystal sorting, winnowing, and grading.

The Gilmour Brook South base-metal occurrence comprises a small stratiform sulphide accumulation. Like other deposits of the "Brunswick Horizon", it is situated on the boundary between crystal tuffs and associated volcaniclastic rocks of the Nepisiguit Falls Formation, and the aphyric to sparsely feldspar-phyric lavas of the Flat Landing Brook Formation. Unlike other deposits of the "Brunswick Horizon," it lacks evidence of a laterally continuous Algoma-type iron formation. In this, the Gilmour Brook South occurrence more closely resembles the stratigraphic section at the Key Anacon deposit, where an Algoma-type iron formation is also lacking (Lentz 1995). At Key Anacon, however, the Little River Formation lies directly on the sulphide-bearing horizon at the top of the Nepisiguit Falls Formation, whereas at Gilmour Brook South, rhyolite of the Flat Landing Brook Formation overlies the massive-sulphide horizon.

The absence of iron formation at Gilmour Brook South suggests that deposition of the host sequence took place under persistent anoxic conditions. Alternatively, rapid sedimentation and burial by stratigraphically higher units may have prevented oxidation of the sulphide body and the development of an iron-rich sedimentary exhalitive.

TABLES 1 TO 7

Table 1
Lithogeochemical data from crystal tuff of the Grand Falls Member and felsic flows of the Little Falls Member, Nepisiguit Falls Formation, Gilmour Brook area, Bathurst Mining Camp.

Table 2
Lithogeochemical data from volcaniclastic rocks of the Little Falls Member, Nepisiguit Falls Formation, Gilmour Brook area, Bathurst Mining Camp.

Table 3
Lithogeochemical data from rhyolite and tuff samples of the Flat Landing Brook Member, Gilmour Brook area, Bathurst Mining Camp.

Table 4
Lithogeochemical data from tuffaceous sedimentary samples of the Flat Landing Brook Member, Nepisiguit Falls Formation, Gilmour Brook area, Bathurst Mining Camp.

Table 5
Lithogeochemical data from the Little River Formation, Gilmour Brook area, Bathurst Mining Camp.

Table 6
Lithogeochemical data from the Patrick Brook Formation, Gilmour Brook area, Bathurst Mining Camp.

Table 7
Lithogeochemical data from the Tomogonops Formation, Gilmour Brook area, Bathurst Mining Camp.

Table 1. Lithogeochemical data from crystal tuff of the Grand Falls Member and felsic flows of the Little Falls Member, Nepisiguit Falls Formation, Gilmour Brook South area, Bathurst Mining Camp *(table continues on next page).*

Sample	GS-28 -737.6	GS-28 -748.5	GS-28 -771	GS37B -1011.5	GS37B -1017.3	GS-25A -649.2	GS-39A -845.5
Laboratory	Actlabs	Actlabs	Actlabs	Actlab	Actlabs	ACME	ACME
Rock Type	QAS with sulphides	QAS	QFAS	amygdaloidal rhyolite	amygdaloidal rhyolite altered	QAS	QAS
SiO_2	60.94	64.45	73.53	41.82	64.8	64.22	61.25
Al_2O_3	17.08	15.98	12.93	16.39	13.14	12.92	16.81
Fe_2O_3	8.58	5.53	2.23	18.03	7.63	10.63	6.41
MnO	0.036	0.04	0.039	0.221	0.305	0.03	0.11
MgO	0.9	0.8	1.27	4.14	3.33	0.58	3.04
CaO	0.36	0.2	0.57	0.37	0.4	0.15	0.98
Na_2O	0.34	1.22	0.9	0.12	2.83	0.2	1.69
K_2O	5.43	4.74	4.24	6.25	3.62	3.61	4.48
TiO_2	0.837	0.847	0.632	1.007	0.858	0.72	0.83
P_2O_5	0.16	0.07	0.19	0.13	0.25	0.09	0.18
LOI wt %	4.07	5.17	2.27	10.1	1.7	6.6	4
TOTAL wt %	98.74	99.03	98.8	98.59	98.86	99.81	99.88
TOT/C wt %	-	-	-	-	-	0.05	0.05
S	4.46	4.83	0.34	12.41	0.81	6.52	2.26
Ag	7.3	3.5	-0.3	13.0	0.7	0.1	0.1
As	5	76	1	511	9	79.9	3.7
Au	4	17	4	59	2	15	0.25
Ba	838	1650	541	3290	1260	497	817
Be	3	3	3	3	2	-	-
Bi	0.5	1.4	2.8	97.0	-0.1	27.2	0.3
Br	-0.5	-0.5	-0.5	-0.5	-0.5	-	-
Cd	4.1	0.7	1.0	19.4	1.6	0.05	1.1
Co	17.3	14.5	7.3	23.9	9.1	77.1	11.3
Cr	46	123	29.6	1.2	-0.5	34.2	41.1
Cs	4.2	2.5	4.7	4.3	5.5	6.8	3.4
Cu	113	19	12	106	3	339.8	21.9
Ga	28	26	21	14	22	21.6	26
Ge	0.7	0.6	0.9	1.0	0.7	-	-
Hf	9.2	10.0	6.9	12.9	11.7	8.2	9.7
Hg	-1	-1	-1	1	-1	0.03	0.005
In	0.5	-0.1	-0.1	0.7	-0.1	-	-
Ir	-2	-3	-2	-1	-1	-	-
Mo	3	6	-2	-2	-2	2.9	2.1
Na	0.22	0.92	0.62	0.08	2.51	-	-
Nb	18.9	19.3	15.7	24.9	22.7	13.9	17.1
Ni	16.7	17.2	13.4	1.2	1.1	17.4	15.6
Pb	1755	41	39	27605	50	32.7	19.2
Rb	259	205	230	172	122	172.3	181.4

Sample	GS-28 -737.6	GS-28 -748.5	GS-28 -771	GS37B -1011.5	GS37B -1017.3	GS-25A -649.2	GS-39A -845.5
Laboratory	Actlabs	Actlabs	Actlabs	Actlab	Actlabs	ACME	ACME
Rock Type	QAS with sulphides	QAS	QFAS	amygdaloidal rhyolite	amygdaloidal rhyolite altered	QAS	QAS
Sb	12.8	12.9	0.7	16.9	2.2	10.5	0.4
Sc	15.8	16.4	6.7	24.2	23.3	5	15
Se	-0.5	-0.5	-0.5	7.7	-0.5	-	-
Sn	5.6	4.5	2.0	16.0	3.3	4	0.5
Sr	26	62	31	31	60	20.1	44.9
Ta	1.30	1.33	1.06	1.71	1.47	0.8	0.8
Th	19.4	20.9	14.9	15.7	15.0	17.7	22.3
Tl	3.92	2.67	3.13	0.82	2.81	2.5	0.1
U	3.20	2.75	3.30	4.15	3.85	2.3	3.4
V	65	66	39	42	39	58	74
W	9	8	2	11	2	15.9	3.7
Y	42	40	34	69	52	26	43.4
Zn	1960.6	25.8	76.0	17231	117	31	512
Zr	320	342	242	494.6	412.2	290.8	329
La	66.3	69.2	47.9	69.0	50.4	52.7	59.8
Ce	141	146	103	152	109	108.3	119.3
Pr	15.9	16.3	11.7	18.0	12.3	12.13	13.58
Nd	59.8	62.4	43.5	70.6	48.4	49.8	57
Sm	12.56	12.71	9.45	15.68	10.92	9.7	10.9
Eu	2.53	1.78	1.36	2.37	2.43	1.96	1.58
Gd	10.78	10.85	8.17	13.96	10.47	7.82	9.53
Tb	1.66	1.65	1.34	2.33	1.79	0.9	1.32
Dy	8.71	8.63	7.15	13.2	10.6	4.65	7.81
Ho	1.66	1.62	1.35	2.67	2.11	0.96	1.55
Er	4.81	4.77	3.98	8.17	6.51	2.23	3.81
Tm	0.662	0.680	0.549	1.17	0.964	0.31	0.67
Yb	3.92	4.29	3.19	6.99	6.06	2.2	3.85
Lu	0.617	0.661	0.491	1.04	0.894	0.31	0.52
La_n/Lu_n	1.137	1.109	1.033	0.703	0.597	1.801	1.218
Tot REE	331.1	341.4	243.4	377.1	272.6	254.0	291.2

1. Major oxides in wt %.
2. All trace elements in ppm except S (wt %), Au (ppb), and Hg (ppb).
3. Values preceded by a negative sign are below detection limits.
4. QAS = quartz-crystal-rich; QFAS = quartz–feldspar-crystal-rich.

Table 2. Lithogeochemical data from volcaniclastic rocks of the Little Falls Member, Nepisiguit Falls Formation, Gilmour Brook South area, Bathurst Mining Camp *(table continues on next page)*.

Sample	GS-28 -715.8	GS-28 -787	GS-25A -665.8	GS-25A -675.2	GS-39A -959	GS-39A -986
Laboratory	Actlabs	Actlabs	ACME	ACME	ACME	ACME
Rock Type	ash-siltstone	ash tuff	chloritic ash tuff	ash tuff	ash tuff	ash tuff (sed?)
SiO_2	73.09	72.07	66.45	71.22	73.11	83.92
Al_2O_3	12.6	13.48	14.76	13.52	12.73	5.98
Fe_2O_3	3.63	3.83	8.46	5.61	5.39	4.71
MnO	0.11	0.038	0.12	0.04	0.01	0.06
MgO	3.13	1.7	2.25	1.01	0.36	1.05
CaO	0.03	0.3	0.33	0.39	0.56	0.14
Na_2O	0.13	0.39	0.13	0.35	0.19	0.06
K_2O	3.25	4.79	3.34	3.91	4.06	1.07
TiO_2	0.237	0.505	0.41	0.15	0.06	0.68
P_2O_5	0.04	0.1	0.24	0.25	0.38	0.11
LOI wt %	2.91	2.53	3.3	3.4	3	2
TOTAL wt %	99.16	99.72	99.85	99.89	99.88	99.8
TOT/C wt %	-	-	0.01	0.05	0.01	0.01
S	0.34	0.77	0.41	1.72	2.3	0.45
Ag	0.8	0.3	0.05	0.1	0.1	0.05
As	-1	2	4	11.8	0.25	5
Au	-2	-2	1.6	0.8	3.4	3.1
Ba	443	265	520	325	276	124
Be	3	2	-	-	-	-
Bi	5.4	5.2	0.7	5	2.8	0.4
Br	-0.5	-0.5	-	-	-	-
Cd	0.6	0.9	0.05	0.05	0.05	0.05
Co	1.7	9.1	10.7	1.2	60.4	4.8
Cr	49	133	27.4	27.4	6.8	3.4
Cs	3.2	5.6	4.3	5.9	4.3	1.5
Cu	1	22	48.9	101.8	301.6	39.8
Ga	24	20	22.8	23.6	20.1	9.9
Ge	1.1	1.4	-	-	-	-
Hf	9.9	5.8	4.4	3	1.9	18.6
In	0.3	-0.1	-	-	-	-
Ir	-2	-2	-	-	-	-
Mo	-2	-2	4.3	0.4	0.6	1.2
Na	0.08	0.25	-	-	-	-
Nb	15.9	13.8	17.2	16.7	16.2	12
Ni	-1.0	14.5	13.3	4.8	2.1	8.1
Pb	16	32	1.3	7.2	4.3	3.2
Rb	191	269	196.4	251.5	204.7	57.1
Sb	0.8	1.1	1.9	0.7	0.2	0.1

Sample	GS-28 -715.8	GS-28 -787	GS-25A -665.8	GS-25A -675.2	GS-39A -959	GS-39A -986
Laboratory	Actlabs	Actlabs	ACME	ACME	ACME	ACME
Rock Type	ash-siltstone	ash tuff	chloritic ash tuff	ash tuff	ash tuff	ash tuff (sed?)
Sc	12.5	7.6	7	3	2	8
Se	-0.5	-0.5	-	-	-	-
Sn	4.3	1.7	4	6	9	6
Sr	11	26	14.1	19.4	16.2	7.9
Ta	1.11	1.20	2.3	2	2.1	0.5
Th	15.4	11.5	8.2	6	1.8	11.4
Tl	3.36	2.54	0.2	0.2	0.1	0.05
U	4.51	3.74	6.9	7.4	10.7	2.3
V	-5	39	48	12	2.5	32
W	2	5	5.8	3.7	3.8	4.3
Y	49	24	23	16.5	13.8	35.4
Zn	72.2	75.3	42	18	20	36
Zr	332	179	114.6	68.4	37.7	630.3
La	38.9	32.0	23.3	10.9	4.1	36.5
Ce	83.7	68.9	49.1	24.1	9.2	83.4
Pr	9.33	7.58	5.51	2.65	1.18	9.14
Nd	35.1	28.5	22.9	10.3	5.3	36.8
Sm	7.67	6.08	5.4	3.2	2.3	8.1
Eu	1.01	0.87	1.39	0.6	0.43	1.3
Gd	7.65	5.13	4.99	3.57	2.86	6.55
Tb	1.52	0.89	0.69	0.58	0.52	0.95
Dy	9.56	4.92	4.33	3.11	2.95	5.83
Ho	2.02	0.95	0.7	0.47	0.43	1.28
Er	6.20	2.81	1.81	0.94	0.86	3.21
Tm	0.950	0.423	0.31	0.16	0.13	0.54
Yb	5.63	2.50	1.72	0.84	0.76	3.65
Lu	0.864	0.373	0.27	0.12	0.07	0.51
La_n/Lu_n	0.477	0.910	0.914	0.962	0.620	0.758
Tot REE	210.1	162.0	122.4	61.5	31.1	197.8

Major oxides in wt %.
All trace elements in ppm except S (wt %) and Au (ppb).
Values preceded by a negative sign are below detection limits.

Table 3. Lithogeochemical data from rhyolite and tuff samples of the Flat Landing Brook Formation, Gilmour Brook South area, Bathurst Mining Camp (*table continues on next page).*

Sample	GS-25A -588	GS-25A -629.3	GS-38 -926	GS-28 -676	GS-28 -695.3	GS37B -0752	GS37B -0776	GS37B -0787.2	GS37B -0879.3	GS37B -0888.6
Laboratory	ACME	ACME	ACME	Actlabs	Actlabs	Actlabs	Actlabs	Actlabs	Actlabs	Actlabs
Rock Type	felsic tuff	felsic tuff	felsic tuff	rhyolite (chloritic)	rhyolite (chloritic)	feldspar phyric rhyolite	feldspar phyric rhyolite	black rhyolite	black amygdaloidal rhyolite	black rhyolite
SiO_2	71.9	72.44	74.22	84.92	72.09	72.11	75.71	82.02	73.86	77.1
Al_2O_3	14.17	9.7	14.46	5.62	14.6	13.65	11.68	8.95	12.59	11.27
Fe_2O_3	2.81	7.29	1.23	3.85	2.87	2.93	2.77	1.86	2.8	2.18
MnO	0.04	0.01	0.02	0.044	0.058	0.042	0.037	0.02	0.018	0.018
MgO	1.69	0.52	0.82	1.64	1.22	1.35	2.73	1.32	3.28	0.16
CaO	0.32	0.12	0.45	0.05	0.59	1.73	0.53	0.44	0.15	0.29
Na_2O	0.09	0.1	2.6	0.08	0.19	2.01	1.48	3.59	0.1	1.26
K_2O	5.16	3.24	3.38	1.46	4.31	3.36	2.48	0.55	4.94	6.74
TiO_2	0.24	0.36	0.12	0.108	0.137	0.302	0.24	0.172	0.256	0.24
P_2O_5	0.16	0.07	0.31	0.03	0.29	0.07	0.06	0.06	0.08	0.08
LOI wt.%	3	5.4	2.4	2.06	3.06	1.99	2.42	0.97	2.11	0.62
TOTAL wt.%	99.7	99.3	100.03	99.84	99.42	99.55	100.1	99.92	100.18	99.95
TOT/C	0.02	0.05	0.05	-	-	-	-	-	-	-
S	1	5.45	0.19	0.88	1.14	0.13	0.01	0.02	0.01	0.06
Ag	0.05	1.3	0.05	0.4	-0.3	-0.3	0.4	-0.3	0.6	0.4
As	2.1	138	0.25	2	2	-1	1	-1	2	15
Au	2.1	24.9	0.25	-2	-2	-2	5	-2	5	-1
Ba	1026	398	177	284	463	538	639	135	261	497
Be	-	-	-	2	2	4	4	2	3	2
Bi	0.1	0.1	0.3	2.4	7.4	4.1	2.7	3.3	12.5	0.7
Br	-	-	-	-0.5	-0.5	-0.5	-0.5	-0.5	-0.5	-0.5
Cd	3.1	9.9	0.05	0.6	0.6	1.0	0.7	0.5	0.8	0.4
Co	5.7	3.2	1.2	1.2	1.6	2.4	1.7	1.3	2.2	2
Cr	3.4	6.8	13.7	140	12.1	-0.8	35.2	-0.7	32.8	8.8
Cs	3.6	2.3	4.8	1.4	4.5	6.4	3.7	0.8	9.5	1.2
Cu	53.8	73.6	7.2	15	24	8	5	9	3	13
Ga	19.5	12.3	23.2	10	29	27	17	10	20	15
Ge	-	-	-	0.9	1.4	1.5	1.5	1.0	1.5	1.0
Hf	4.8	2.9	2.2	4.7	3.0	10.7	8.6	6.1	9.2	8.1
Hg	0.01	0.21	0.005	-1	-1	-1	-1	-1	-1	-1
In	-	-	-	-0.1	0.1	-0.1	-0.1	-0.1	-0.1	-0.1
Ir	-	-	-	-2	-2	-2	-1	-3	-4	2
Mo	0.6	3.1	0.8	2	-2	3	-2	3	4	-2
Na	-	-	-	0.06	0.13	1.49	1.13	2.74	0.06	1.13
Nb	9.9	4.8	18	7.1	18.1	21.9	13.9	11.1	14.2	14.6
Ni	13.7	1.5	2.4	1.7	5.2	3.1	1.5	1.9	1.1	2.8
Pb	7.5	87.4	4	20	29	21	8	16	36	24
Rb	230.5	139.9	198.1	75	279	154	136	24	232	118
Sb	0.2	15	0.05	0.7	2.6	0.4	0.3	0.3	0.6	0.4
Sc	3	10	3	5.1	4.2	9.7	8.4	5.8	9.3	8.4

Sample	GS-25A -588	GS-25A -629.3	GS-38 -926	GS-28 -676	GS-28 -695.3	GS37B -0752	GS37B -0776	GS37B -0787.2	GS37B -0879.3	GS37B -0888.6
Laboratory	ACME	ACME	ACME	Actlabs	Actlabs	Actlabs	Actlabs	Actlabs	Actlabs	Actlabs
Rock Type	felsic tuff	felsic tuff	felsic tuff	rhyolite (chloritic)	rhyolite (chloritic)	feldspar phyric rhyolite	feldspar phyric rhyolite	black rhyolite	black amygdaloidal rhyolite	black rhyolite
Se	-	-	-	-0.5	1.7	3.2	-0.5	-0.5	-0.5	-0.5
Sn	3	0.5	5	2.5	10.6	5.4	5.3	1.3	3.7	3.8
Sr	19.3	12.3	33.4	11	32	129	80	106	12	79
Ta	0.9	0.1	1.7	0.48	2.39	1.58	1.20	0.83	1.12	1.16
Th	12.7	4.6	3.9	7.28	3.54	22.3	17.9	12.7	17.0	17.4
Tl	0.2	2	0.1	2.90	7.07	1.90	1.78	0.37	2.67	1.89
U	7	2.1	9	2.04	7.75	5.08	4.53	3.30	4.90	3.81
V	13	15	8	-5	6	-5	-5	-5	-5	-5
W	3.6	4	4	1	3	-1	-1	-1	-1	5
Y	49.4	23.3	15	19	12	57	50	34	46	44
Zn	1348	5460	12	63.7	62.0	79.7	68.7	43.9	75.7	67.3
Zr	144.6	92.5	62.7	153	66	331	268	197	314	249
La	20.3	19.1	9.9	23.9	9.23	66.7	52.1	51.5	53.5	43.5
Ce	46.7	40.4	21.7	49.2	20.5	136	108	99.6	113	92.9
Pr	5.47	4.54	2.42	5.43	2.37	15.1	12.0	10.7	12.5	10.3
Nd	21.2	20.2	9.5	20.1	10.3	56.7	44.9	39.7	47.6	38.9
Sm	5.8	4.5	3.4	4.26	3.06	12.28	9.73	7.64	10.26	8.58
Eu	1.01	1.93	0.28	0.78	0.59	1.61	0.80	1.03	1.13	0.98
Gd	6.48	3.9	3.73	3.81	3.05	10.93	8.96	6.54	9.47	8.07
Tb	1.2	0.56	0.6	0.66	0.55	1.93	1.60	1.08	1.59	1.46
Dy	7.84	3.79	3.03	3.89	2.97	10.8	9.42	6.39	8.71	8.59
Ho	1.68	0.76	0.46	0.84	0.46	2.28	1.94	1.33	1.75	1.71
Er	4.28	2.33	0.97	2.62	1.15	7.24	6.06	4.13	5.42	5.36
Tm	0.7	0.35	0.16	0.409	0.144	1.08	0.899	0.634	0.805	0.823
Yb	4.39	2.42	0.72	2.51	0.84	6.43	5.37	3.83	4.86	4.89
Lu	0.63	0.42	0.09	0.410	0.121	0.962	0.806	0.581	0.745	0.732
La_n/Lu_n	0.341	0.482	1.165	0.616	0.811	0.734	0.684	0.938	0.761	0.630
Tot REE	127.7	105.2	57.0	118.7	55.3	330.0	262.5	234.7	271.4	226.8

Major oxides in wt %.
All trace elements in ppm except S (wt %), Au (ppb), and Hg (ppb).
Values preceded by a negative sign are below detection limits.

Table 4. Lithogeochemical data from tuffaceous sedimentary samples of the Flat Landing Brook Formation, Gilmour Brook area, Bathurst Mining Camp *(table continues on next page)*.

Sample	GS-28 -655.1	GS-28 -664.6	GS-28 -681	GS-28 -683.7	GS37B -0925.7	GS37B -0948.4	GS37B -0998	GS-25A -580
Laboratory	Actlabs	Actlabs	Actlabs	Actlabs	Actlabs	Actlabs	Actlabs	ACME
Rock Type	ash tuff/ sed	chloritic ash <1% pyrite	sericite altered ash tuff	chloritic ash tuff	felsic tuff/ sed	felsic tuff/ sed	grey tuff/ sed	felsic tuff
SiO_2	74.29	70.84	77.51	72.91	72.63	69.72	75.74	76.08
Al_2O_3	12.75	12.39	10.52	12.41	13.36	14.17	11.36	11.01
Fe_2O_3	3.65	5.29	3.91	3.9	2.95	2.55	3.48	4.12
MnO	0.028	0.096	0.01	0.089	0.113	0.116	0.335	0.03
MgO	0.96	3.63	0.47	2.75	0.91	5.42	1.96	0.93
CaO	0.05	0.06	0.06	0.02	0.4	0.05	0.12	0.25
Na_2O	0.12	0.09	0.13	0.12	0.24	0.09	0.09	0.12
K_2O	4.24	3.15	3.38	3.37	6.84	4.71	4.39	3.77
TiO_2	0.24	0.242	0.205	0.23	0.273	0.209	0.227	0.47
P_2O_5	0.04	0.04	-0.01	0.04	0.06	0.04	0.05	0.09
LOI wt %	2.51	3.1	2.43	2.96	1.79	3.1	2.16	2.7
TOTAL wt %	98.88	98.91	98.62	98.81	99.56	100.2	99.9	99.72
TOT/C wt %	-	-	-	-	-	-	-	0.01
S	1.61	0.38	2.36	0.89	0.37	0.33	1.23	1.75
Ag	0.9	0.7	2.2	2.8	0.9	0.8	1.1	0.2
As	3	7	1	48	-1	-1	53	3.1
Au	3	3	5	-2	-1	-1	1	1.8
Ba	1780	570	734	751	651	462	1610	1293
Be	4	3	3	4	4	4	3	-
Bi	1.0	1.9	2.6	44.5	7.5	4.7	3.6	0.4
Br	-0.5	-0.5	-0.5	-0.5	-0.5	-0.5	-0.5	-
Cd	8.5	1.0	10.6	5.9	0.7	0.8	0.9	2.5
Co	2.6	2.7	1.4	1.8	1.5	2.3	4.1	5.7
Cr	56	-0.5	-0.9	46.8	56.4	-0.5	20.2	34.2
Cs	1.8	3.2	2.0	2.8	3.8	3.6	2.5	1.9
Cu	225	9	195	12	13	2	4	28.5
Ga	25	23	13	23	20	19	15	15
Ge	0.8	1.4	0.7	1.2	1.7	0.6	1.0	-
Hf	9.6	9.5	8.2	9.6	11.0	9.2	8.2	3.5
Hg	-1	-1	-1	-1	-1	-1	-1	0.03
In	0.1	0.1	0.2	0.2	-0.1	-0.1	-0.1	-
Ir	-2	-1	-2	-2	-4	-4	2	-
Mo	23	-2	5	4	-2	-2	-2	4
Na	0.08	0.14	0.09	0.08	0.2	0.07	0.06	-
Nb	15.6	16.0	12.4	14.7	20.5	15.3	13.4	8.1
Ni	2.2	2.3	1.5	1.1	2.1	1.3	4.1	7.1
Pb	58	16	5876	2372	33	182	571	148
Rb	185	168	141	174	252	174	142	153.3

Sample	GS-28 -655.1	GS-28 -664.6	GS-28 -681	GS-28 -683.7	GS37B -0925.7	GS37B -0948.4	GS37B -0998	GS-25A -580
Laboratory	Actlabs	Actlabs	Actlabs	Actlabs	Actlabs	Actlabs	Actlabs	ACME
Rock Type	ash tuff/ sed	chloritic ash <1% pyrite	sericite altered ash tuff	chloritic ash tuff	felsic tuff/ sed	felsic tuff/ sed	grey tuff/ sed	felsic tuff
Sb	0.5	0.7	3.4	1.1	0.2	1.4	2.4	0.7
Sc	12.3	14.6	10.6	12.4	15.4	13.9	13	10
Se	-0.5	-0.5	-0.5	5.6	-0.5	-0.5	-0.5	-
Sn	6.6	7.0	19.9	3.1	4.3	2.1	2.2	0.5
Sr	15	12	17	12	49	8	23	16.6
Ta	1.16	1.12	0.93	1.11	1.59	1.18	0.95	1.2
Th	15.5	15.7	12.7	15.1	22.4	18.5	13.3	7.5
Tl	2.00	3.32	5.94	12.1	4.05	1.49	2.08	0.2
U	4.48	4.52	3.68	4.34	5.02	5.22	3.80	2.8
V	-5	-5	7	-5	-5	-5	-5	31
W	3	-1	-1	2	4	4	4	5.1
Y	46	44	40	47	58	57	44	26.6
Zn	3959.7	141.8	5620.5	2958.5	57.0	76.1	236.5	1514
Zr	320	325	275	316	363.8	290.8	282.3	121
La	47.1	54.0	48.2	54.1	67.2	59.1	45.7	20.2
Ce	99.9	113	99.1	113	145	121	95.0	41.2
Pr	11.3	12.4	10.7	12.3	16.2	13.4	10.4	4.74
Nd	41.1	46.6	40.4	45.9	61.2	49.9	38.3	18.9
Sm	9.11	9.77	8.69	9.68	13.98	10.90	8.30	4.4
Eu	1.40	1.15	1.89	1.90	1.73	1.12	1.11	0.76
Gd	8.47	8.86	8.01	9.04	12.29	10.21	7.47	4.04
Tb	1.54	1.60	1.39	1.56	2.09	1.82	1.33	0.59
Dy	8.98	8.95	7.99	9.08	12.0	10.5	7.85	3.96
Ho	1.89	1.76	1.58	1.85	2.35	2.10	1.60	0.89
Er	5.87	5.60	4.96	5.92	7.27	6.52	5.04	2.57
Tm	0.894	0.856	0.738	0.871	1.09	0.988	0.753	0.38
Yb	5.44	5.35	4.64	5.30	6.45	5.96	4.49	2.67
Lu	0.839	0.782	0.709	0.831	0.979	0.909	0.701	0.39
La_n/Lu_n	0.595	0.732	0.721	0.689	0.727	0.688	0.690	0.549
Tot REE	243.8	270.5	239.0	271.4	349.6	294.7	228.0	105.7

Major oxides in wt %.
All trace elements in ppm except S (wt %), Au (ppb), and Hg (ppb).
Values preceded by a negative sign are below detection limits.

Table 5. Lithogeochemical data from the Little River Formation, Gilmour Brook South area, Bathurst Mining Camp *(table continues on next page)*.

Sample	GS37B -0457.44	GS37B -0671	GS37B -0680.6	GS-25A -461	GS-39A -650.5	GS-28 -603.5	GS37B -0482.2	GS-23 -523
Laboratory	Actlabs	Actlabs	Actlabs	ACME	ACME	Actlabs	Actlabs	ACME
Unit	LRb	LRb	LRb	LRb	LRs	LRs	LRs	LRs
Rock Type	lapilli tuff	mafic volcanic	mafic volcanic	mafic volcanic	shale	shale-sandstone	black shale	black shale
SiO_2	56.34	40.77	43.77	43.13	53.09	57.24	81.94	66.61
Al_2O_3	18.24	14.75	14.99	14.45	15.14	20.06	5.01	16.23
Fe_2O_3	6.32	14.67	11.75	12.73	6.68	8.48	4.58	3.5
MnO	0.095	0.252	0.204	0.17	0.07	0.107	0.027	0.26
MgO	2.64	4.16	4.36	5.77	4.37	2.38	0.88	3.43
CaO	2.19	10.42	8.3	9.62	7.08	0.14	0.49	0.59
Na_2O	4.00	2.31	5.09	2.66	1.22	0.26	0.14	0.13
K_2O	2.87	0.79	1.36	0.34	3.01	4.81	1.23	4.6
TiO_2	2.259	2.377	2.245	2.54	0.8	1.126	0.268	0.37
P_2O_5	0.55	0.33	0.32	0.26	0.09	0.12	0.07	0.04
LOI wt %	3.42	8.47	6.46	8.1	8.3	4.11	4.43	3.8
TOTAL wt %	98.94	99.29	98.84	99.8	99.95	98.82	99.05	99.82
TOT/C wt %	-	-	-	1.57	1.65	-	-	0.19
S	0.97	0.01	0.01	< .01	0.39	1.10	3.26	0.02
Ag	0.7	0.6	0.5	0.05	0.05	0.7	-0.3	0.05
As	2	1	1	9.5	11.7	364	19	9.7
Au	3	3	1	0.25	0.25	5	4	0.25
Ba	770	-20	126	44	658	696	412	2177
Be	3	2	2	-	-	4	2	-
Bi	2.6	0.8	1.0	0.05	0.1	4.1	0.3	0.3
Br	-0.5	-0.5	-0.5	-	-	-0.5	-0.5	-
Cd	1.5	1.8	1.7	0.05	0.05	1.2	1.1	0.1
Co	23.4	57.1	44.5	41.3	20.6	25.8	18.9	8.2
Cr	102	68.8	99	82.1	143.7	128	50	27.4
Cs	2.2	0.3	4.4	0.3	4.4	4.5	1.1	3
Cu	29	8	89	30.8	28.8	35	50	18.7
Ga	34	22	19	19.7	21.9	34	9	21.7
Ge	1.6	1.6	1.4	-	-	1.5	-0.5	-
Hf	14.1	4.5	4.4	4.5	4.1	5.0	1.6	8.8
In	-0.1	-0.1	-0.1	-	-	-0.1	-0.1	-
Ir	-2	-2	-1	-	-	-2	-3	-
Mo	5	-2	-2	1.1	0.4	4	27	0.5
Na	3.03	1.72	4.28	-	-	0.19	0.08	-
Nb	50.7	21.2	20.5	19.7	11.2	20.0	8.3	21
Ni	28.2	48.6	57.6	48.1	110.9	58.6	91.8	16.3
Pb	5	-3	5	1.6	9.7	10	12	35.6
Rb	84	12	34	10.8	98.2	253	38	182.4
Sb	-0.1	0.6	1.8	0.8	0.5	1	2.6	3.8
Sc	35.8	35.3	39.2	31	15	22.7	7	17

Sample	GS37B -0457.44	GS37B -0671	GS37B -0680.6	GS-25A -461	GS-39A -650.5	GS-28 -603.5	GS37B -0482.2	GS-23 -523
Laboratory	Actlabs	Actlabs	Actlabs	ACME	ACME	Actlabs	Actlabs	ACME
Unit	LRb	LRb	LRb	LRb	LRs	LRs	LRs	LRs
Rock Type	lapilli tuff	mafic volcanic	mafic volcanic	mafic volcanic	shale	shale-sandstone	black shale	black shale
Se	-0.5	-0.5	-0.5	-	-	-0.5	-0.5	-
Sn	2.5	-1.0	-1.0	0.5	0.5	9.6	-1.0	12
Sr	187	195	302	258.2	214	29	34	31.2
Ta	3.47	1.33	1.32	1.3	0.3	1.58	0.29	1.2
Th	7.69	1.56	1.56	1.6	8.7	15.8	3.20	19.9
Tl	2.05	0.12	0.36	0.05	0.1	3.10	0.95	0.2
U	3.56	0.44	0.34	0.6	2.7	3.65	8.78	0.7
V	193	238	230	310	116	135	78	26
W	-1	-1	-1	1.8	1.1	4	3	3.2
Y	92	28	26	30.9	26.6	41	15	53.2
Zn	109.5	102.4	82.0	86	92	102.5	62.0	64
Zr	490	170	163	165.6	143.3	152	57	290.8
La	57.1	19.7	17.2	14.8	34.1	64.0	18.8	55.1
Ce	128	45.7	40.0	33.4	65.9	130	41.1	111.1
Pr	16.4	5.51	5.07	4.24	7.53	14.6	4.31	11.79
Nd	69.3	24.5	22.4	20.4	30.3	54.0	17.3	44.7
Sm	17.19	6.31	5.73	5.6	5.9	11.02	3.86	9
Eu	4.22	2.36	2.06	2.01	1.17	2.51	0.78	1.38
Gd	17.45	6.34	5.75	5.75	4.44	9.30	3.66	8.35
Tb	3.05	1.06	0.98	0.89	0.69	1.54	0.55	1.23
Dy	18.0	6.05	5.48	5.6	4.3	8.50	2.99	8.52
Ho	3.72	1.17	1.06	1.16	0.91	1.69	0.56	1.9
Er	11.5	3.31	3.05	2.78	2.42	5.13	1.63	4.84
Tm	1.70	0.462	0.415	0.47	0.45	0.746	0.222	0.76
Yb	10.4	2.78	2.60	2.47	2.7	4.56	1.39	5.04
Lu	1.60	0.413	0.401	0.38	0.39	0.685	0.210	0.81
La$_N$/Lu$_N$	0.379	0.505	0.455	0.413	0.926	0.990	0.945	0.721
Tot REE	359.8	125.7	112.2	99.9	161.2	308.5	97.4	264.5

Major oxides in wt %.

All trace elements in ppm except S (wt %) and Au (ppb).

Values preceded by a negative sign are below detection limits.

Lrb = mafic volcanic sample; Lrs = sedimentary sample.

Table 6. Lithogeochemical data from the Patrick Brook Formation, Gilmour Brook South area, Bathurst Mining Camp *(table continues on next page).*

Sample	GS-28-795	GS-17-511	GS-17-516	GS-25A-729.8	GS-25A-733.7-F	GS-25A-733.7-M
Laboratory	Actlabs	ACME	ACME	ACME	ACME	ACME
Rock Type	shale-wacke	sandstone	black shale	wacke	shale	siltstone
SiO_2	65.2	81.6	53.85	72.76	62.76	68.69
Al_2O_3	14.41	6.71	22.77	14.41	18.76	14.34
Fe_2O_3	5.45	5.99	8.36	2.2	5.99	6.96
MnO	0.093	0.05	0.05	0.02	0.04	0.04
MgO	2.47	0.96	1.94	1.07	1.27	1.43
CaO	1.9	0.65	0.16	0.68	0.13	0.22
Na_2O	0.28	0.17	0.65	2.77	0.36	0.4
K_2O	4.6	1.53	6.26	3.3	5.08	3.5
TiO_2	0.596	0.57	1.19	0.19	1.1	0.97
P_2O_5	0.16	0.34	0.07	0.25	0.06	0.11
LOI wt %	3.72	1.2	4.4	2.2	4.2	3.2
TOTAL wt %	98.89	99.81	99.82	99.88	99.82	99.92
TOT/C wt %	-	0.08	0.25	0.07	0.3	0.16
S	0.39	1	1.04	0.31	0.68	1.02
Ag	-0.3	0.1	0.05	0.1	0.1	0.1
As	15	17.2	36.4	2.9	14.6	12.1
Au	-2	0.25	0.8	0.25	0.25	0.25
Ba	243	172	821	262	551	407
Be	3	-	-	-	-	-
Bi	7.3	0.3	0.4	1.1	0.4	0.3
Br	-0.5	-	-	-	-	-
Cd	1.0	0.2	0.05	0.1	0.1	0.1
Co	14.2	12.8	24.7	4	16.8	18.9
Cr	45.9	47.9	89.0	13.7	41.1	54.8
Cs	9.9	3.8	12.4	5.4	6.2	4.2
Cu	19	32.9	53.5	12	42.9	45.9
Ga	23	13.7	38.6	21.9	29	20.1
Ge	1.9	-	-	-	-	-
Hf	5.6	12.1	4.7	2.9	7.5	9.5
Hg	-1	0.01	0.005	0.01	0.01	0.005
In	-0.1	-	-	-	-	-
Ir	-2	-	-	-	-	-
Mo	-2	0.8	0.4	0.4	1.6	0.7
Na	0.19	-	-	-	-	-
Nb	15.3	11.6	22.4	16.8	20.1	17.1
Ni	27.8	29.5	54.4	8.4	48.2	37
Pb	14	22.4	17.7	14	22.3	16.1
Rb	288	86.3	316.6	188.4	243.1	162.6
Sb	1.1	0.4	1.3	0.1	0.1	0.1
Sc	11.5	8	21	4	19	15
Se	-0.5	-	-	-	-	-
Sn	3.6	4.0	2.0	2	0.5	0.5

Sample	GS-28-795	GS-17-511	GS-17-516	GS-25A-729.8	GS-25A-733.7-F	GS-25A-733.7-M
Laboratory	Actlabs	ACME	ACME	ACME	ACME	ACME
Rock Type	shale-wacke	sandstone	black shale	wacke	shale	siltstone
Sr	58	54.2	85.1	57.5	40	32.1
Ta	1.46	0.6	1.5	2.1	1.1	0.9
Th	10.3	11.7	20.2	5.1	16.4	13.6
Tl	3.39	0.1	0.1	0.1	0.1	0.1
U	4.44	2.7	4.6	7.7	4.5	4.2
V	59	43	188	22	141	95
W	4	4.5	3.1	5.6	4.4	2.8
Y	24	47.8	53.8	16.7	46.2	47.3
Zn	98.0	138	115	55	88	115
Zr	175	428	179.4	74.2	255.1	337.2
La	31.9	37.4	68.3	10.5	59.3	50.1
Ce	65.3	86.3	133	21.2	119.5	100.3
Pr	7.20	9.71	15.2	2.52	13.22	11.51
Nd	26.9	45.6	60.1	9.7	56.4	48.5
Sm	5.83	10.7	12.3	2.9	10.3	9.5
Eu	1.11	2.03	2.29	0.41	2.05	1.66
Gd	4.98	11.07	10.04	2.87	8.89	8.2
Tb	0.86	1.44	1.29	0.61	1.36	1.29
Dy	4.93	8.09	9.41	3.06	8.51	7.76
Ho	0.95	1.48	1.84	0.54	1.69	1.56
Er	2.86	3.78	4.53	1.24	4.54	4.53
Tm	0.411	0.56	0.81	0.22	0.71	0.65
Yb	2.69	3.4	4.82	1.24	4.21	4.78
Lu	0.404	0.52	0.78	0.16	0.73	0.68
$\mathrm{La}_n/\mathrm{Lu}_n$	0.836	0.762	0.928	0.695	0.861	0.781
Tot REE	156.3	222.1	324.7	57.2	291.4	251.0

Major oxides in wt %.
All trace elements in ppm except S (wt %), Au (ppb), and Hg (ppb).
Values preceded by a negative sign are below detection limits.

Table 7. Lithogeochemical data from the Tomogonops Formation, Gilmour Brook South area, Bathurst Mining Camp *(table continues on next page)*.

Sample	GS37B-0361.2	GS-23-126	GS-25A-193	GS-25A-196	GS-25A-304	GS-25A-369
Laboratory	Actlabs	ACME	ACME	ACME	ACME	ACME
Rock Type	calcareous siltstone	black shale	black shale	sandstone	shale and siltstone	grey shale
SiO_2	45.77	88.11	79.97	61.64	57.2	59.73
Al_2O_3	11.42	2.93	5.55	15.38	15.38	16.24
Fe_2O_3	4.99	3.38	4.34	6.83	8.84	7.77
MnO	0.095	0.01	0.08	0.34	0.16	0.07
MgO	3.62	0.34	1.13	3.33	4.1	4.09
CaO	14.92	0.08	2.42	2.52	2.57	2.21
Na_2O	1.52	0.34	0.36	1.5	1.47	1.45
K_2O	1.96	0.61	1.26	2.95	3.27	3.02
TiO_2	0.64	0.14	0.28	0.88	0.85	0.88
P_2O_5	0.1	0.02	0.04	0.11	0.15	0.09
L0I wt %	13.61	3.9	4.4	4.2	5.7	4.2
TOTAL wt %	98.65	99.9	99.87	99.77	99.78	99.82
TOT/C wt %	-	1.52	1.58	0.68	1.69	0.62
Ag	-0.3	0.1	0.1	0.1	0.1	0.05
As	10	16.7	25.2	34.1	12.7	14.2
Au	3	0.25	1	0.25	0.25	0.7
Ba	237	200	252	492	491	389
Be	2	-	-	-	-	-
Bi	4.1	0.1	0.1	0.4	0.3	0.2
Br	-0.5	-	-	-	-	-
Cd	1.1	0.6	0.4	0.05	0.3	0.1
Co	20.7	11.6	12.9	79.2	38.3	26.5
Cr	158	20.5	54.8	95.8	164.3	130.0
Cs	2.2	1.3	2.5	5	5.7	4.3
Cu	25	36.3	34.4	454.3	73.5	52.5
Ga	17	6.2	9.3	19.8	21.5	22.9
Ge	1.0	-	-	-	-	-
Hf	3.5	0.7	1.5	4.8	5.4	4.1
Hg	-1	0.005	0.01	0.005	0.005	0.005
In	-0.1	-	-	-	-	-
Ir	-2	-	-	-	-	-
Mo	-2	15.8	15.3	0.9	11.2	0.6
Na	1.13	-	-	-	-	-
Nb	10.2	2.7	6.8	12.7	13.9	11.1
Ni	87.7	61.4	62.5	110.2	123.3	116.6
Pb	12	11.3	17.8	31	24.9	22.8
Rb	81	22.2	46.2	103.6	112.1	118.2
S	0.20	2.58	2.92	2.21	3.3	0.69
Sb	0.4	2.2	3.6	0.2	1.3	0.5
Sc	14.2	3	6	16	18	19
Se	-0.5	-	-	-	-	-

Sample	GS37B-0361.2	GS-23-126	GS-25A-193	GS-25A-196	GS-25A-304	GS-25A-369
Laboratory	Actlabs	ACME	ACME	ACME	ACME	ACME
Rock Type	calcareous siltstone	black shale	black shale	sandstone	shale and siltstone	grey shale
Sn	-1.0	0.5	3	0.5	0.5	0.5
Sr	383	32.5	162.9	253.1	186.9	107
Ta	0.61	0.05	0.2	0.8	0.7	0.6
Th	6.39	1.8	3.4	11.1	10.7	8.2
Tl	0.69	0.1	0.2	0.05	0.1	0.1
U	1.68	5.8	8	2.9	5.5	3.4
V	81	94	81	149	177	157
W	-1	6	6	2	10.5	1.2
Y	19	8.1	24.6	28	32	26.7
Zn	47.9	47	48	89	118	100
Zr	125	32	55.4	154.6	192.9	140.2
La	27.6	6.6	15.1	35.9	38.2	34.9
Ce	57.2	14	32.2	83.3	81.8	69.7
Pr	6.39	1.52	3.66	8.34	8.71	7.73
Nd	23.9	7.1	16.4	32.3	37.5	34.7
Sm	4.95	1.4	4.2	6.9	7	6.5
Eu	1.13	0.35	0.69	1.61	1.48	1.6
Gd	4.14	1.15	3.48	5.3	6.43	5.19
Tb	0.70	0.17	0.57	0.78	0.98	0.72
Dy	3.87	1.1	3.95	5.25	5.65	4.64
Ho	0.75	0.23	0.73	1.01	1.15	0.99
Er	2.33	0.71	2.19	2.72	2.72	2.64
Tm	0.331	0.12	0.36	0.43	0.49	0.41
Yb	2.05	0.58	2.1	2.76	3.08	2.63
Lu	0.310	0.13	0.37	0.43	0.43	0.45
La_n/Lu_n	0.942	0.538	0.432	0.884	0.941	0.822
Tot REE	135.7	35.2	86.0	187.0	195.6	172.8

Major oxides in wt %.
All trace elements in ppm except S (wt %), Au (ppb), and Hg (ppb).
Values preceded by a negative sign are below detection limits.

ACKNOWLEDGEMENTS

Thank you to Larry Pitre for help with Gemcom® and to Warna Downey and David MacDonnell for help at the core shed. Thanks also to the Brunswick Mining and Smelting Corporation Limited for providing access to drill cores. This paper has benefited from critical reviews by Les Fyffe, Reg Wilson, and Steve McCutcheon, all of the Geological Surveys Branch, New Brunswick Department of Natural Resources.

REFERENCES

Banville, R. 2001. Report of work on the Narrows property. New Brunswick Department of Natural Resources; Minerals Policy and Planning Division, Mineral Assessment Report 475506.

Boström, K. 1973. Submarine volcanism as a source for iron. Earth and Planetary Science Letters, **9**: 348–354.

Franklin, J.M., Lydon, J.W., and Sangster, D.F. 1981. Volcanic-associated massive sulfide deposits. Economic Geology, 75th Anniversary Volume, pp. 485–627.

Goodfellow, W.D., and McCutcheon, S.R. 2003. Geologic and genetic attributes of volcanic-sediment-hosted massive-sulfide deposits of the Bathurst Mining Camp, northern New Brunswick: a synthesis. *In* Massive Sulfide Deposits of the Bathurst Mining Camp, New Brunswick, and Northern Maine. *Edited by* W.D. Goodfellow, S.R. McCutcheon, and J.M. Peter. Economic Geology Monograph **11**: 245–302.

Key Anacon Mines Ltd. 1977. Report of work on the Taylor Brook Road group for Key Anacon Mines Ltd. New Brunswick Department of Natural Resources; Minerals, Policy and Planning Division, Mineral Assessment Report 472130.

Hussey, J.J. 1992. Deep exploration of the "Brunswick Horizon," Bathurst District, northern New Brunswick. Exploration and Mining Geology, **1**: 187–195.

Langton, J.P., and McCutcheon, S.R. 1993. Brunswick Project, NTS 21 P/05 west, 21 P/04 west, Gloucester County, New Brunswick. *In* Current Research 1992. *Edited by* S.A.A. Abbott. New Brunswick Department of Natural Resources; Minerals, Policy and Planning Division, Information Circular 93-1, pp. 31–51.

Le Maitre, R.W., Bateman, P., Dudek, A., Keller, J., Lameyre Le Bas, M.J., Sabine, P.A., Schmid, R., Sorensen, H., Streckeisen, A., Wolley, A.R., and Zanettin, B. 1989. A classification of igneous rocks and glossary of terms. Blackwell, Oxford, 193 p.

Lentz, D.R. 1995. Stratigraphy and structure of the Key Anacon massive sulphide deposits compared with the Brunswick deposits, Bathurst Mining Camp, New Brunswick. *In* Geoscience Research 1994. *Compiled and edited by* J.P. Langton. New Brunswick Department of Natural Resources and Energy; Minerals, Policy and Planning Division, Miscellaneous Report 15, pp. 23–44.

Lentz, D.R. 1996. Trace-element systematics of felsic volcanic rocks associated with massive sulfide deposits in the Bathurst Mining Camp: petrogenetic, tectonic and chemo-stratigraphic implications for VMS exploration. *In* Trace Element Geochemistry of Volcanic Rocks: Applications for Massive Sulfide Exploration. *Edited by* D.A. Wyman. Geological Association of Canada, Short Course Notes, **12**: 359–402.

Lentz, D.R., and Wilson, R.A. 1997. Chemostratigraphic analysis of the volcanic and sedimentary rocks in the Heath Steele B–B5 zone area, Bathurst Mining Camp, New Brunswick: stratigraphic and structural implications. *In* Current Research, 1997-D, Geological Survey of Canada, pp. 21–33.

McCutcheon, S.R., and Walker, J.A. 2001. Volcanogenic massive sulphide deposits of the Bathurst Mining Camp. *In* Guidebook for Field Trip B7. Geological Association of Canada/Mineralogical Association of Canada, Joint Annual Meeting, St. John's, Newfoundland, May 27–30, 2001, p. 89.

McCutcheon, S. R., Walker, J. A., and McClenaghan, S.H. 2001. The geologic setting of massive sulphide deposits in the Bathurst Mining Camp: a synthesis. *In* Current Research 2000. *Edited by* B.M.W. Carroll. New Brunswick Department of Natural Resources and Energy; Minerals and Energy Division, Mineral Resources Report 2001-4, pp. 63–95.

Rogers, N., and van Staal, C.R. 2003. Volcanology and tectonic setting, Bathurst Mining Camp, Part 2: mafic volcanic constraints on back-arc opening. *In* Massive Sulfide Deposits of the Bathurst Mining Camp, New Brunswick, and Northern Maine. *Edited by* W.D. Goodfellow, S.R. McCutcheon, and J.M. Peter. Economic Geology Monograph, **11**: 181-201.

Rogers, N., van Staal, C.R., McNicoll, V., and Theriault, R. 2003a. Volcanology and tectonic setting, Bathurst Mining Camp, Part I: extension and rifting of the Popelogan Arc. *In* Massive Sulfide Deposits of the Bathurst Mining Camp, New Brunswick, and Northern Maine. *Edited by* W.D. Goodfellow, S.R. McCutcheon, and J.M. Peter. Economic Geology Monograph, **11**: 157–179.

Rogers, N., van Staal, C.R., Winchester, J.A., and Fyffe, L.R. 2003b. Provenance and chemical stratigraphy of sedimentary rocks of the Miramichi, Tetagouche, California Lake, and Fournier groups, northern New Brunswick. *In* Massive Sulfide Deposits of the Bathurst Mining Camp, New Brunswick, and Northern Maine. *Edited by* W.D. Goodfellow, S.R. McCutcheon, and J.M. Peter. Economic Geology Monograph, **11**: 111–128.

Thomas, M.D., Walker, J.A., Keating, P., Shives, R., Kiss, F., and Goodfellow, W.D. 2000. Geophysical atlas of massive sulphide signatures, Bathurst Mining Camp, New Brunswick. Geological Survey of Canada, Open File 3887 — New Brunswick Department of Natural Resources and Energy; Minerals and Energy Division, Open File 2000-4, p. 105.

van Staal, C.R. 1985. Structure and metamorphism of the Brunswick Mines area, Bathurst New Brunswick, Canada. Unpublished Ph.D. thesis, University of New Brunswick, Fredericton, New Brunswick, Canada, 484 p.

van Staal, C.R. 1994. Brunswick subduction complex in the Canadian Appalachians: record of the Late Ordovician to Late Silurian collision between Laurentia and the Gander Margin of Avalon. Tectonics, **13**: 946–962.

van Staal, C.R., and Fyffe, L.R. 1991. Dunnage and Gander zones, New Brunswick: Canadian Appalachian Region. New Brunswick Department of Natural Resources; Minerals, Policy and Planning Division, Geoscience Report 91-2, 39 p.

van Staal, C.R., Winchester, J.A., and Bédard, J.H. 1991. Geochemical variation in Middle Ordovician volcanic rocks of the northern Miramichi Highlands and their tectonic significance. Canadian Journal of Earth Science, **28**: 1031–1049.

van Staal, C.R., Wilson, R.A., Rogers, N., Fyffe, L.R., Gower, S.J., Langton, J.P., McCutcheon, S.R., and Walker, J.A. 2002. Geology, Bathurst Mining Camp and surrounding areas, New Brunswick. Geological Survey of Canada, Open File 4182, Scale 1:100 000.

van Staal, C.R., Wilson, R.A., Rogers, N., Fyffe, L.R., Langton, S.R., McCutcheon, S.R., McNicoll, V., and Ravenhurst, C.E. 2003. Geology and tectonic history of the Bathurst Supergroup, Bathurst Mining Camp, and its relationship to coeval rocks in southwestern New Brunswick and adjacent Maine — a synthesis. *In* Massive Sulfide Deposits of the Bathurst Mining Camp, New Brunswick, and Northern Maine. *Edited by* W.D. Goodfellow, S.R. McCutcheon, and J.M. Peter, J.M. Economic Geology Monograph, **11**: 37–60.

Walker, J.A., and Lentz, D.R. (in press.) The Flat Landing Brook Zn–Pb–Ag massive sulfide deposit, Bathurst Mining Camp, NTS 21 P/05 west. Exploration and Mining Geology.

Wilson, R.A., van Staal, C.R., McCutcheon, S.R., and Fyffe, L.R. 1998. Revised stratigraphic nomenclature for the Bathurst Mining Camp, northern New Brunswick. *In* Abstracts 1998: 23rd Annual Review of Activities. *Edited by* B.M.W. Carroll. New Brunswick Department of Natural Resources; Minerals, Policy and Planning Division, Information Circular 98-3.

Winchester, J.A., and Floyd, P.A. 1977. Geochemical discrimination of different magma series and their differentiation products using immobile elements. Chemical Geology, **20**: 325–343.

GEOLOGY OF THE VAL D'AMOUR FORMATION: REVISITING THE TYPE AREA OF THE DALHOUSIE GROUP, NORTHERN NEW BRUNSWICK

REGINALD A. WILSON [1], **SANDRA KAMO** [2], AND **ELLIOTT T. BURDEN** [3]

[1] Geological Surveys Branch, New Brunswick Department of Natural Resources,
P.O. Box 50, Bathurst, New Brunswick, CANADA E2A 3Z1 *(reg.wilson@gnb.ca)*
[2] Jack Satterly Geochronology Laboratory, Department of Geology,
University of Toronto, 22 Russell Street, Toronto, Ontario, CANADA M5S 3B1
[3] Department of Earth Sciences, Memorial University of Newfoundland, St. John's,
Newfoundland and Labrador, CANADA A1B 3X5

Wilson, R.A., Kamo, S., and Burden, E.T. 2005. Geology of the Val d'Amour Formation: revisiting the type area of the Dalhousie Group, northern New Brunswick. *In* Geological Investigations in New Brunswick for 2004. *Edited by* G.L. Martin. New Brunswick Department of Natural Resources; Minerals, Policy and Planning Division, Mineral Resource Report 2005-1, pp. 167–212.

The Lower Devonian section in the Campbellton–Dalhousie area, northern New Brunswick, is assigned to the Val d'Amour Formation. The Val d'Amour Formation is a 6 km thick, mainly volcanic succession that is divided into three members; in ascending order, they are the Walker Brook, Thompson Brook, and Richardsville members. These subunits generally coincide with an upward transition from mafic to intermediate to felsic compositions. The Walker Brook Member comprises basaltic and minor andesitic flows; basaltic ash and lapilli tuff; and local interbedded, calcareous, fossiliferous sedimentary rocks. The Thompson Brook Member consists mainly of andesitic to dacitic effusive rocks, andesitic lithic tuff, tuff breccia, and associated fine-grained to very coarse-grained volcaniclastic rocks. The Richardsville Member comprises pink to maroon, typically flow-layered, porphyritic rhyolite and minor volcaniclastic boulder conglomerate. The Val d'Amour Formation conformably overlies the Indian Point Formation (Chaleurs Group) and is unconformably overlain by the Campbellton Formation (Gaspé Sandstone Group). The age of the formation is constrained by ~ middle Lochkovian spores from its base and a U–Pb zircon age of 407.4 ± 0.8 Ma (early Emsian) from the Richardsville rhyolite near its top. The paleoenvironment of the unit as a whole was dominantly subaerial, although relatively abundant sedimentary rocks, pillow lavas, and hyaloclastites at Dalhousie attest to a mainly subaqueous setting for that particular area.

Composition of the Val d'Amour volcanic rocks changes from mafic at the base of the unit to felsic at the top. Intermediate rocks are abundant, especially in the Thompson Brook Member, and basalts and andesites together make up 80% of the Val d'Amour Formation. Volcanic rocks are predominantly subalkaline and define a tholeiitic

differentiation trend; the basalts display characteristics of continental tholeiites. All rocks have moderately sloping rare-earth-element (REE) profiles with light REE enrichment. On extended trace-element diagrams, they show enrichment in Cs, Rb, Ba, K, Th, and U, and depletion in Nb and Ti, similar to the patterns displayed by subduction-related (arc) volcanic rocks. However, they generally fall in within-plate fields on diagrams used to infer tectonic setting. Chemical variation within the various suites of volcanic rock is related only partly to fractional crystallization. Trace-element systematics and ratios suggest that trace-element characteristics (and the abundance of intermediate rocks) can be attributed to assimilation of upper crustal rocks and/or partial melting of a common mantle source that was variably enriched by previous subduction events.

La section du Dévonien inférieur dans la région de Campbellton-Dalhousie, notamment la Formation de Dalhousie de Clark sur la côte de la baie Eel, est rattachée à la Formation de Val d'Amour. La Formation de Val d'Amour est une succession principalement volcanique de six kilomètres d'épaisseur qui se subdivise en trois membres; ceux-ci correspondent, dans un ordre ascendant, aux membres du ruisseau Walker, du ruisseau Thompson et de Richardsville. Ces sous-unités coïncident généralement avec une transition vers le haut des compositions mafiques à intermédiaires puis à felsiques. Le membre du ruisseau Walker est constitué de coulées basaltiques et, en quantité modeste, andésitiques, de tuf à lapilli et de tuf pyroclastique basaltique, ainsi que de roches sédimentaires fossilifères, calcareuses, interlitées, locales. Le membre du ruisseau Thompson est principalement constitué de roches effusives andésitiques à dacitiques, de tuf lithique andésitique, de tuf-brèche et de roches volcanoclastiques connexes de grains fins à très grossiers. Le membre de Richardsville est composé de rhyolite porphyrique, généralement à stratification de coulée, rose à brun rougeâtre ainsi que d'une quantité restreinte de conglomérat à blocs volcanoclastique. La Formation de Val d'Amour recouvre en concordance la Formation d'Indian Point (groupe de Chaleurs) et elle est recouverte en discordance par la Formation de Campbellton (groupe du grès de Gaspé). L'âge de la formation se trouve limité par des spores provenant de sa base qui remontent approximativement au Lochkovien moyen et par une datation U-Pb sur zircon de 407,4 ± 0,8 Ma (Emsien précoce) obtenue de la rhyolite de Richardsville près de son sommet. Le paléoenvironnement de l'ensemble de l'unité était essentiellement subaérien, même si des roches sédimentaires, des laves en coussins et des hyaloclastites relativement abondantes à Dalhousie attestent d'un milieu principalement subaquatique dans ce secteur.

La composition des roches volcaniques de Val d'Amour passe de mafique, à la base, à felsique, au sommet. Les roches intermédiaires sont abondantes, spécialement à l'intérieur du membre du ruisseau Thompson; les basaltes et les andésites représentent ensemble jusqu'à 80 % de la Formation de Val D'Amour. Les roches volcaniques sont en prédominance subalcalines et définissent une lignée de différenciation tholéiitique; les basaltes affichent les caractéristiques de tholéiites continentales. Toutes les roches

présentent des profils d'éléments des terres rares (ETR) modérément inclinés avec un léger enrichissement d'ETR. Sur les schémas d'éléments traces étendus, elles affichent un enrichissement en Cs, en Rb, en Ba, en K, en Th et en U, et un appauvrissement en Nb et en Ti, à l'instar des configurations qu'accusent les roches volcaniques liées à des zones de subduction (arc). Elles s'insèrent toutefois en général dans des champs intra-plaques sur les schémas utilisés pour supposer le cadre tectonique. L'écart chimique à l'intérieur des divers cortèges de roches volcaniques est relié seulement en partie à une cristallisation fractionnée. La systématique et les ratios d'éléments traces laissent supposer que les caractéristiques des éléments traces (et l'abondance de roches intermédiaires) peuvent être attribués à une assimilation de roches crustales supérieures ou à une fusion partielle d'une source mantellique commune enrichie de façon variable par des subductions antérieures.

INTRODUCTION AND PREVIOUS WORK

Almost a century has passed since Clarke's (1909) treatise on the stratigraphy and paleontology of the Lower Devonian section at Dalhousie, northern New Brunswick, established the Dalhousie Formation as "second only to the type Helderberg as representative of that Lower Devonian stage" (Greiner 1970). Clarke, however, was not the first to describe these rocks; undoubtedly, his attention was drawn by previous reports by Logan et al. (1863), Hind (1865), Honeyman (1878), Ells (1881, 1883), and Ami (1900, 1902). The last-named author (1902) was the first to use the term Dalhousie Formation. Clarke's focus was the fossil-rich sedimentary intervals within the Dalhousie section on Eel Bay (Fig. 1). Volcanic rocks dominate the Lower Devonian sequence, however, especially farther west toward and beyond Campbellton. Howard (1926) addressed his efforts to these volcanic rocks, conducting petrographic studies, assigning informal nomenclature, and attempting to relate sequences of flows to specific source areas or vents that he rather dubiously inferred to correspond to modern topographic highs.

Alcock (1935) carried out regional surveys along the north and south shores of Chaleur Bay, including the Campbellton–Dalhousie belt (Fig. 1), but produced only a very general map that grouped all Silurian and Devonian volcanic rocks into a single unit. Those parts of Alcock's memoir concerned with the Dalhousie section are largely a repetition of Clarke's (1909) stratigraphy and paleontology, and Howard's (1926) lithological and petrographic descriptions of the volcanic rocks. No further notable investigations were carried out until those of Greiner (1970, 1974a–c), who first defined constituent formations, thus elevating Clarke's (1909) Dalhousie Formation to the Dalhousie Group. Greiner produced several geology maps of the region. He based his (1970) stratigraphy on relationships noted southeast of Dalhousie in the Jacquet River area (Fig. 1), but attempted to correlate the new units to Clarke's (1909) and Howard's (1926) section on the coast at Eel Bay. These correlations, based on a few lithological

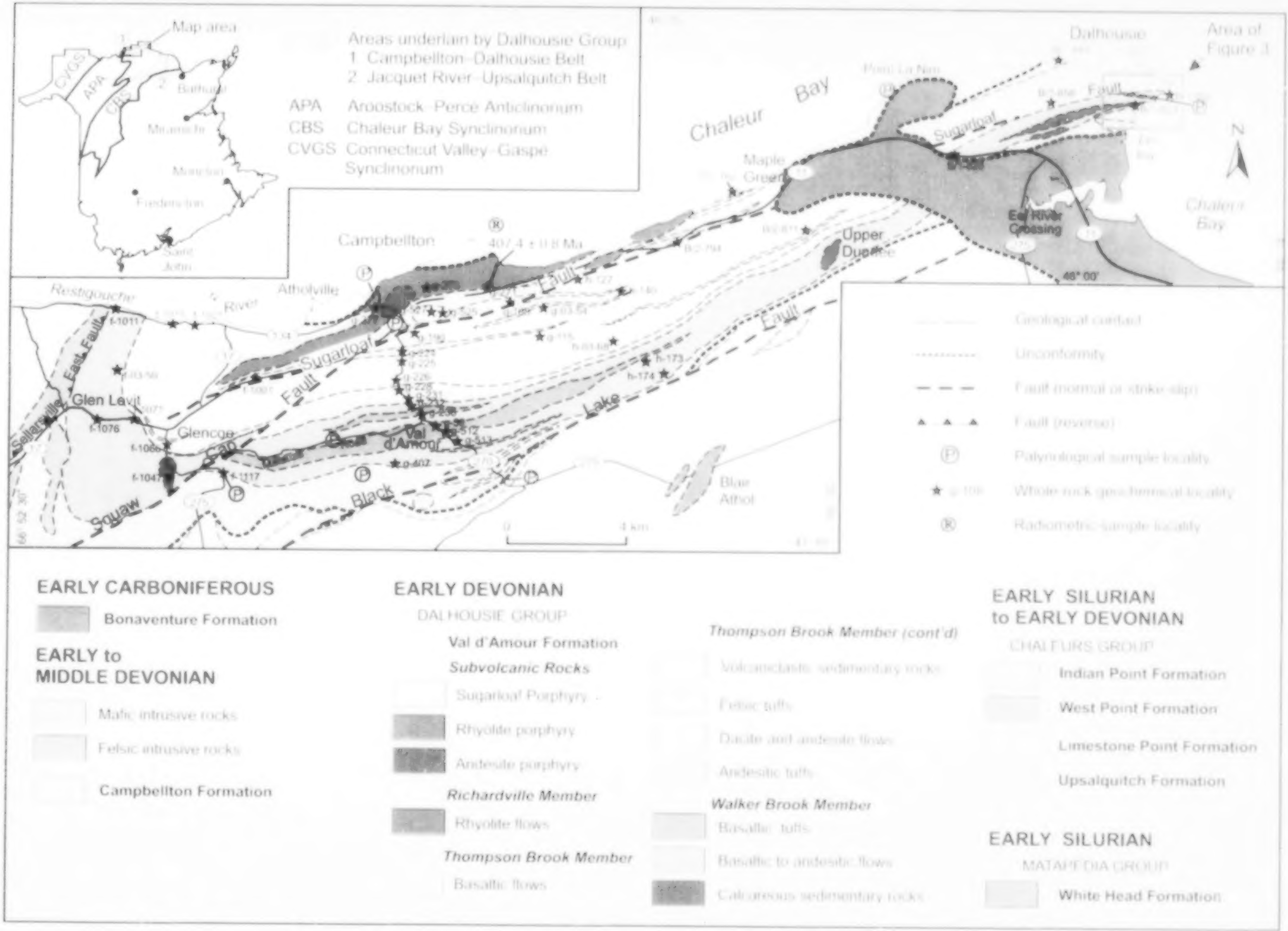
Map area
CVGS
APA
CBS
Bathurst
Miramichi
Moncton
Fredericton
Saint John
Areas underlain by Dalhousie Group
1 Campbellton–Dalhousie Belt
2 Jacquet River–Upsalquitch Belt
APA Aroostock–Percé Anticlinorium
CBS Chaleur Bay Synclinorium
CVGS Connecticut Valley–Gaspé Synclinorium
Chaleur Bay
Dalhousie
Area of Figure 3
Point La Nim
Maple Green
Campbellton
407.4 ± 0.8 Ma
Atholville
Restigouche River
Sugarloaf Fault
Upper Dundee
Eel River Crossing
Chaleur Bay
48° 00'
Glen Levit
Glencoe
Val d'Amour
Cap
Squaw
Black Lake Fault
East Fault
Sellarsville
Blair Athol
0
4 km
N
Geological contact
Unconformity
Fault (normal or strike-slip)
Fault (reverse)
Polynological sample locality
Whole-rock geochemical locality
Radiometric sample locality
EARLY CARBONIFEROUS
Bonaventure Formation
EARLY to MIDDLE DEVONIAN
Mafic intrusive rocks
Felsic intrusive rocks
Campbellton Formation
EARLY DEVONIAN
DALHOUSIE GROUP
Val d'Amour Formation
Subvolcanic Rocks
Sugarloaf Porphyry
Rhyolite porphyry
Andesite porphyry
Richardville Member
Rhyolite flows
Thompson Brook Member
Basaltic flows
Thompson Brook Member (cont'd)
Volcaniclastic sedimentary rocks
Felsic tuffs
Dacite and andesite flows
Andesitic tuffs
Walker Brook Member
Basaltic tuffs
Basaltic to andesitic flows
Calcareous sedimentary rocks
EARLY SILURIAN to EARLY DEVONIAN
CHALEURS GROUP
Indian Point Formation
West Point Formation
Limestone Point Formation
Upsalquitch Formation
EARLY SILURIAN
MATAPEDIA GROUP
White Head Formation

Figure 1. Geology of the Campbellton–Dalhousie area

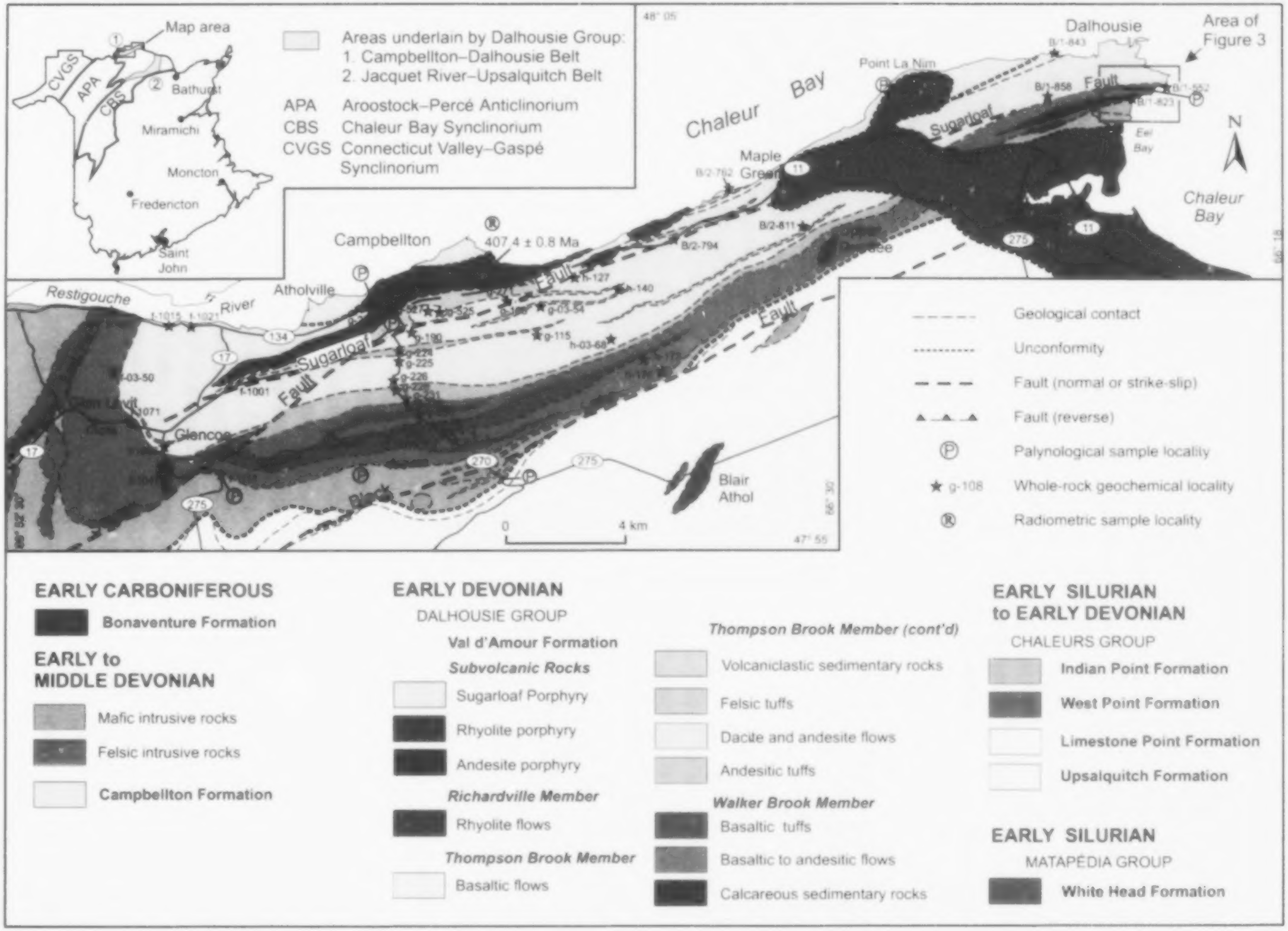
Map area
CVGS
APA
CBS
Bathurst
Miramichi
Moncton
Fredericton
Saint John
Areas underlain by Dalhousie Group:
1. Campbellton–Dalhousie Belt
2. Jacquet River–Upsalquitch Belt
APA Aroostock–Percé Anticlinorium
CBS Chaleur Bay Synclinorium
CVGS Connecticut Valley–Gaspé Synclinorium
48° 05'
Dalhousie
Area of Figure 3
Point La Nim
Chaleur Bay
Maple Green
Eel Bay
N
Chaleur Bay
Sugarloaf
Fault
Campbellton
407.4 ± 0.8 Ma
Atholville
Restigouche River
Glencoe
Blair Athol
0
4 km
47° 55'
Geological contact
Unconformity
Fault (normal or strike-slip)
Fault (reverse)
Palynological sample locality
g-108 Whole-rock geochemical locality
Radiometric sample locality
EARLY CARBONIFEROUS
Bonaventure Formation
EARLY to MIDDLE DEVONIAN
Mafic intrusive rocks
Felsic intrusive rocks
Campbellton Formation
EARLY DEVONIAN
DALHOUSIE GROUP
Val d'Amour Formation
Subvolcanic Rocks
Sugarloaf Porphyry
Rhyolite porphyry
Andesite porphyry
Richardville Member
Rhyolite flows
Thompson Brook Member
Basaltic flows
Thompson Brook Member (cont'd)
Volcaniclastic sedimentary rocks
Felsic tuffs
Dacite and andesite flows
Andesitic tuffs
Walker Brook Member
Basaltic tuffs
Basaltic to andesitic flows
Calcareous sedimentary rocks
EARLY SILURIAN to EARLY DEVONIAN
CHALEURS GROUP
Indian Point Formation
West Point Formation
Limestone Point Formation
Upsalquitch Formation
EARLY SILURIAN
MATAPÉDIA GROUP
White Head Formation

Figure 1. Geology of the Campbellton–Dalhousie area.

similarities, were rendered invalid after Greiner's stratigraphic scheme was revised following detailed mapping by Walker et al. (1993) and Walker and McCutcheon (1995). Thus, correlations between the constituent formations of the Dalhousie Group in the Jacquet River area and Clarke's (1909) Eel Bay section (assumed to be the Dalhousie Group type section) remained undefined.

Regional mapping in northern New Brunswick was carried out between 1999 and 2003 under the auspices of the Appalachian Foreland and Platform NATMAP program ("Geological Bridges of Eastern Canada") (Castonguay et al. 2003, 2004). One product of that investigation was a report on the stratigraphy and geological evolution of the Gaspé Belt in New Brunswick (Wilson et al. 2004). The report introduced the Val d'Amour Formation for rocks of the Dalhousie Group in the Campbellton–Dalhousie area; it also contained a summary of lithotypes, chemistry, and palynological and radiometric age determinations.

The purpose of the current report is to elaborate on previously presented material concerning the Val d'Amour Formation. Specifically, it offers more detailed lithological, chemical and geochronological data, describes the type section and contact relationships, and proposes a division into members based on lithological and geochemical criteria. It is evident that straightforward lithological correlations between strata of the Val d'Amour Formation and constituent units of the Dalhousie Group defined in the Jacquet River area to the southeast (Walker and McCutcheon 1995) are not possible. In the latter, existing fossil evidence indicates non-specific Early Devonian ages, and precise (e.g. radioisotopic) ages are lacking. It appears likely that the now well dated, thick Val d'Amour sequence at Campbellton–Dalhousie spans the same age range as the entire Dalhousie Group in the Jacquet River–Upsalquitch Belt (Fig. 1). However, establishing firm correlations between the two areas must await future radioisotopic dating of felsic volcanic rocks in the Jacquet River Belt.

REGIONAL SETTING

The study area is located in northern New Brunswick within the Gaspé Belt (the Matapédia Cover Sequence of Fyffe and Fricker 1987). The belt is a Middle Paleozoic successor basin that is locally unconformable on, and presumed to be underlain by, Dunnage Zone basement, as evidenced by the numerous inliers of Dunnage volcanic rocks (Wilson 2003).

The tectonic history of the Gaspé Belt began after the Late Ordovician (Caradocian) collision between the Popelogan–Victoria Arc and the Laurentian craton (van Staal 1994; van Staal et al. 1998). The Gaspé Belt generally is regarded as comprising three structural zones (see inset of Fig. 1), namely the Aroostook–Percé Anticlinorium, Chaleur Bay Synclinorium, and Connecticut Valley–Gaspé Synclinorium (Rodgers 1970). The oldest rocks in the Gaspé Belt underlie the Aroostook–Percé Anticlinorium; they consist of Upper Ordovician to Lower Silurian deep-water turbidite deposits that are broadly divided into a lower siliciclastic assemblage (Grog Brook Group) and an upper carbonate assemblage (Matapédia Group). In the study area, the uppermost part of the latter assemblage is exposed in the core of an anticline at Blair Athol (Fig. 1).

The Val d'Amour Formation occupies the Restigouche syncline, a structural subdivision of the Chaleur Bay Synclinorium at the head of Chaleur Bay (Fig. 1). The complex history of the Chaleur Bay Synclinorium is summarized by Wilson et al. (2004). The synclinorium consists of Lower Silurian to Lower Devonian rocks of the Chaleurs Group, and Lower Devonian rocks of the Dalhousie Group and Campbellton Formation. It features a Late Silurian erosional unconformity (Salinic disconformity) that, in the study area, separates the lower (Llandovery–Wenlock) and upper (Pridoli) parts of the Chaleurs Group (Fig. 1). In the Jacquet River–Upsalquitch Belt to the southeast, the unconformity lies between Wenlock–Ludlow volcanic rocks of the Chaleurs Group, and latest Silurian to Early Devonian sedimentary rocks of the Dalhousie Group. The Dalhousie Group is unconformably overlain by the Campbellton Formation along the coast of Chaleur Bay. The Chaleurs and Dalhousie groups and the Campbellton Formation all are unconformably overlain by flat-lying, coarse-grained, Carboniferous terrestrial redbeds of the Bonaventure Formation (Fig. 1).

VAL D'AMOUR FORMATION: STRATIGRAPHY AND LITHOLOGY

The Val d'Amour Formation comprises an interbedded sequence of mafic, intermediate, and felsic effusive and pyroclastic rocks, fine-grained to very coarse-grained volcaniclastic rocks, and locally interbedded fine-grained sedimentary rocks. Subvolcanic plugs and domes such as the Sugarloaf Porphyry, a dacitic volcanic neck, intrude the stratified rocks, especially in the Campbellton area. The Val d'Amour Formation forms a thick, north-dipping sequence on the south limb of the Restigouche syncline. Average dips increase from 40° at the base to 70° near the top and were obtained from measurements of interbedded sedimentary rocks, bedded tuffs, and volcanic flow-tops. The total thickness of the formation is estimated at about 5800 m in the Campbellton–Val d'Amour area, as compared with only 1900 m at Dalhousie. The sequence is interrupted by the Sugarloaf Fault in both locations, but the amount of inferred strike-slip is interpreted to be small and has a negligible effect on estimates of thickness.

To facilitate discussion of this voluminous volcanic pile, the formation has been divided into three members. From bottom to top, these are the Walker Brook, Thompson Brook, and Richardsville members (Fig. 1, 2), which consist predominantly of mafic, intermediate, and felsic volcanic rocks, respectively. All members are present in the Campbellton area, but only the Walker Brook and Thompson Brook members are recognized at the abbreviated Dalhousie section. In that section (Fig. 2, 3), the Walker

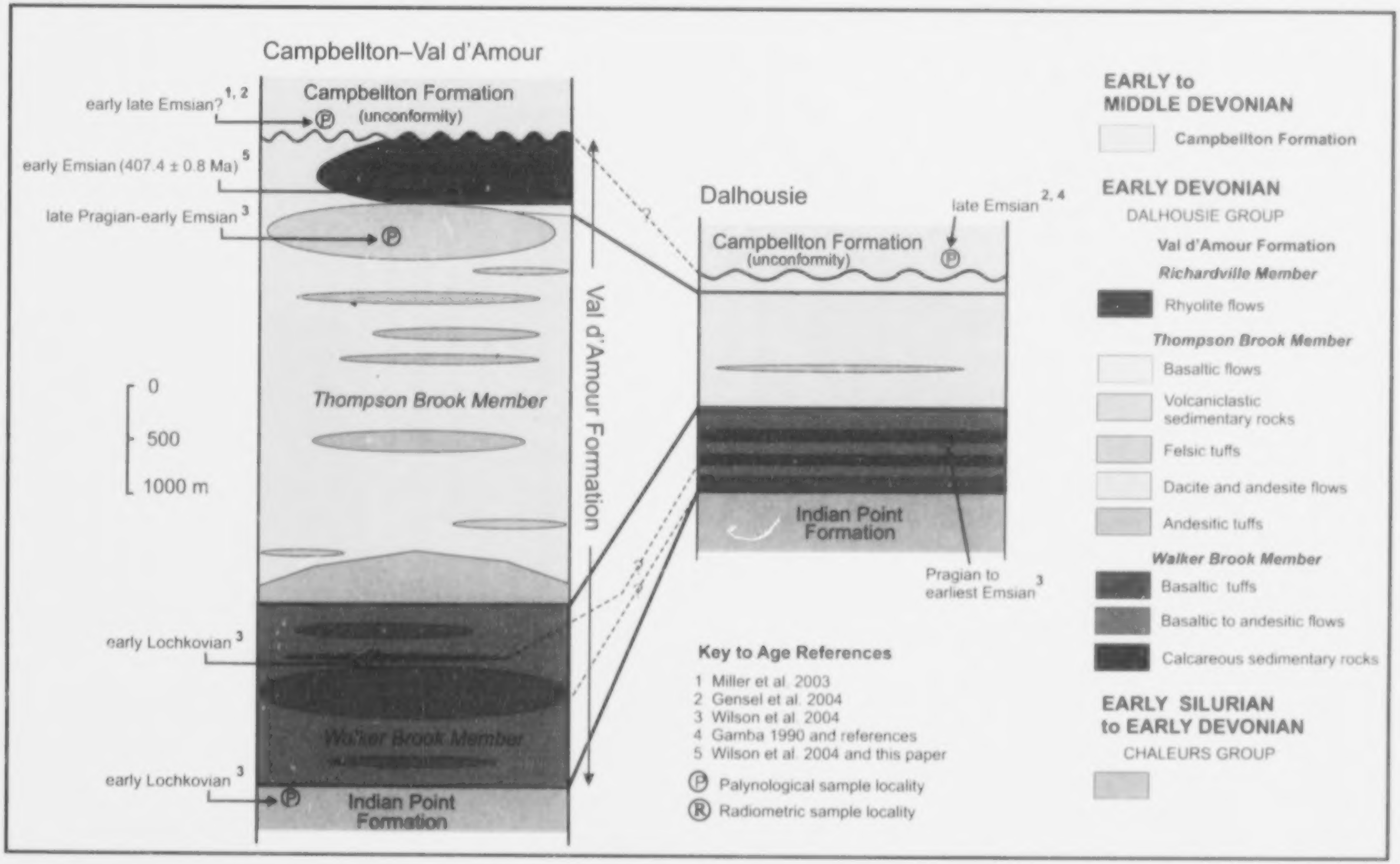
Campbellton–Val d'Amour
early late Emsian? 1, 2
Campbellton Formation
(unconformity)
early Emsian (407.4 ± 0.8 Ma) 5
late Pragian-early Emsian 3
Thompson Brook Member
0
500
1000 m
early Lochkovian 3
Walker Brook Member
early Lochkovian 3
Indian Point Formation
Val d'Amour Formation
?
Dalhousie
late Emsian 2, 4
Campbellton Formation
(unconformity)
Indian Point Formation
Pragian to earliest Emsian 3
Key to Age References
1 Miller et al. 2003
2 Gensel et al. 2004
3 Wilson et al. 2004
4 Gamba 1990 and references
5 Wilson et al. 2004 and this paper
Ⓟ Palynological sample locality
Ⓡ Radiometric sample locality
EARLY to MIDDLE DEVONIAN
Campbellton Formation
EARLY DEVONIAN
DALHOUSIE GROUP
Val d'Amour Formation
Richardville Member
Rhyolite flows
Thompson Brook Member
Basaltic flows
Volcaniclastic sedimentary rocks
Felsic tuffs
Dacite and andesite flows
Andesitic tuffs
Walker Brook Member
Basaltic tuffs
Basaltic to andesitic flows
Calcareous sedimentary rocks
EARLY SILURIAN to EARLY DEVONIAN
CHALEURS GROUP

Figure 2. Stratigraphic columns of the Val d'Amour Formation at the Campbellton–Val d'Amour type section and at Dalhousie. Columns show the proposed stratigraphic correlations between the two areas, and the palynological and radioisotopic age determinations.

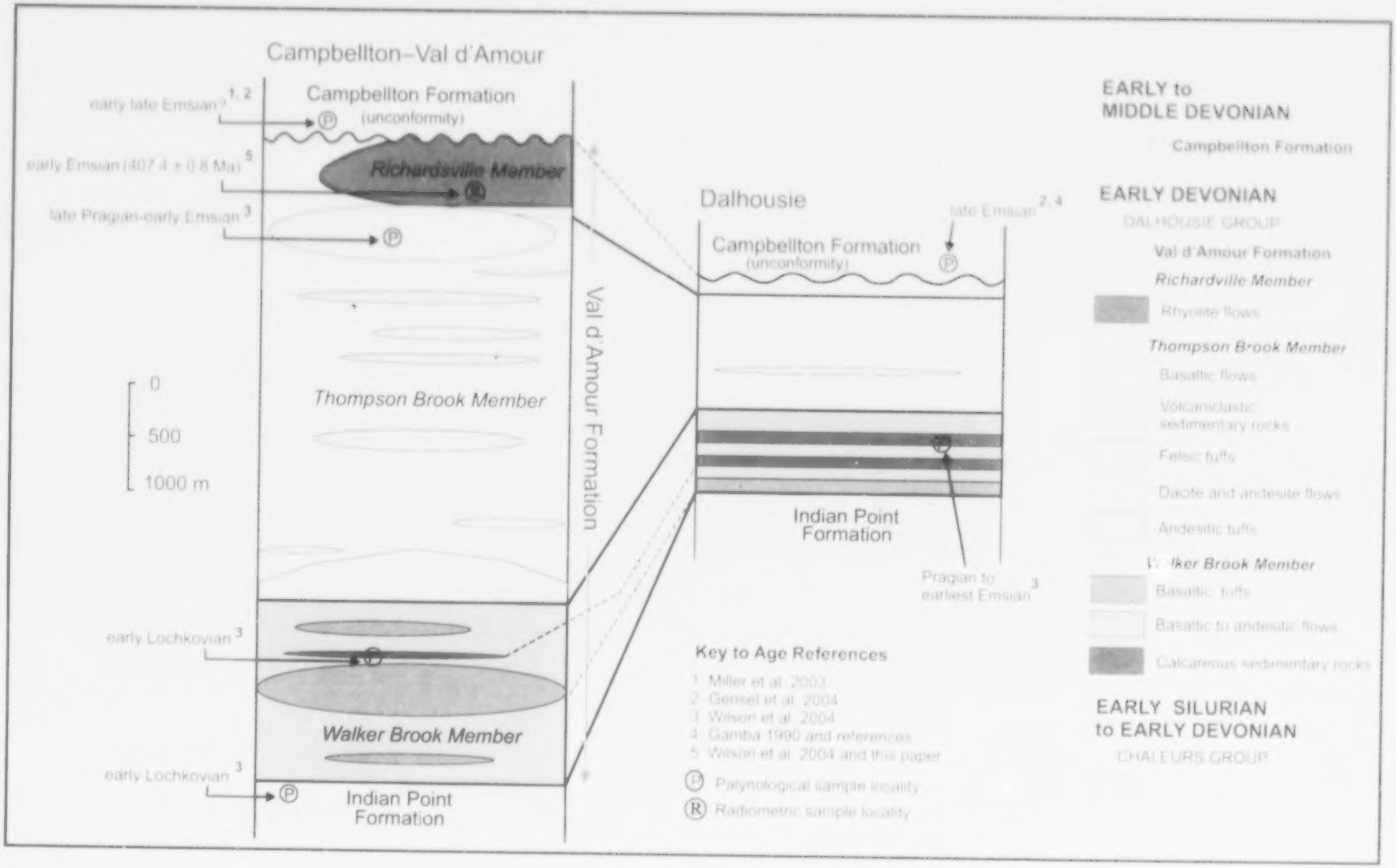
Campbellton–Val d'Amour
early late Emsian?[1, 2]
Campbellton Formation
(unconformity)
early Emsian (407.4 ± 0.8 Ma)[5]
Richardsville Member
late Pragian-early Emsian[3]
0
500
1000 m
Thompson Brook Member
Val d'Amour Formation
early Lochkovian[3]
Walker Brook Member
early Lochkovian[3]
Indian Point Formation
Dalhousie
late Emsian[2, 4]
Campbellton Formation
(unconformity)
Indian Point Formation
Pragian to earliest Emsian[3]
Key to Age References
1 Miller et al. 2003
2 Gensel et al. 2004
3 Wilson et al. 2004
4 Gamba 1990 and references
5 Wilson et al. 2004 and this paper
Ⓟ Palynological sample locality
Ⓡ Radiometric sample locality
EARLY to MIDDLE DEVONIAN
Campbellton Formation
EARLY DEVONIAN
DALHOUSIE GROUP
Val d'Amour Formation
Richardville Member
Rhyolite flows
Thompson Brook Member
Basaltic flows
Volcaniclastic sedimentary rocks
Felsic tuffs
Dacite and andesite flows
Andesitic tuffs
Walker Brook Member
Basaltic tuffs
Basaltic to andesitic flows
Calcareous sedimentary rocks
EARLY SILURIAN to EARLY DEVONIAN
CHALEURS GROUP

Figure 2. Stratigraphic columns of the Val d'Amour Formation at the Campbellton–Val d'Amour type section and at Dalhousie. Columns show the proposed stratigraphic correlations between the two areas, and the palynological and radioisotopic age determinations.

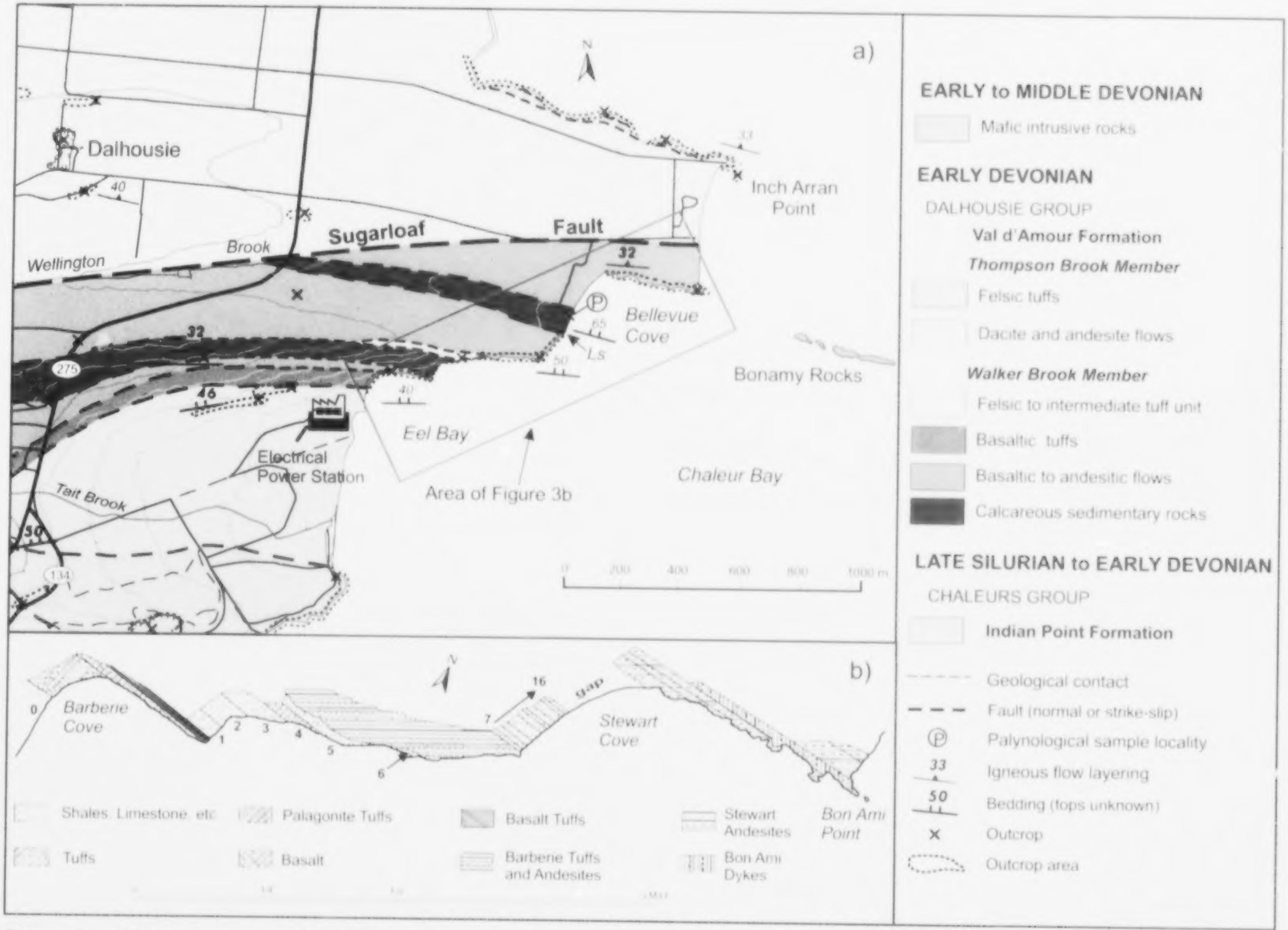
a)
N
Dalhousie
40
Wellington
Brook
Sugarloaf
Fault
32
Inch Arran Point
33
Bellevue Cove
P
65
Ls
50
Bonamy Rocks
275
32
46
40
Eel Bay
Electrical Power Station
Tait Brook
Area of Figure 3b
Chaleur Bay
50
134
0 200 400 600 800 1000 m
b)
N
0
Barberie Cove
1
2
3
4
5
6
7
16
gap
Stewart Cove
Bon Ami Point
Shales, Limestone, etc.
Tuffs
Palagonite Tuffs
Basalt
Basalt Tuffs
Barberie Tuffs and Andesites
Stewart Andesites
Bon Ami Dykes
EARLY to MIDDLE DEVONIAN
Mafic intrusive rocks
EARLY DEVONIAN
DALHOUSIE GROUP
Val d'Amour Formation
Thompson Brook Member
Felsic tuffs
Dacite and andesite flows
Walker Brook Member
Felsic to intermediate tuff unit
Basaltic tuffs
Basaltic to andesitic flows
Calcareous sedimentary rocks
LATE SILURIAN to EARLY DEVONIAN
CHALEURS GROUP
Indian Point Formation
Geological contact
Fault (normal or strike-slip)
Palynological sample locality
33
Igneous flow layering
50
Bedding (tops unknown)
Outcrop
Outcrop area

Figure 3. a) Detailed geology of the Dalhousie area. Ls = limestone bed, or bed 7 of Clarke (1909). b) Partial reproduction of Howard's (1926) map of this section. Bed numbers (1 to 16) for sedimentary rocks on the shore section are after Clarke (1909). Names of the coves shown on Howard's map are no longer in official use.

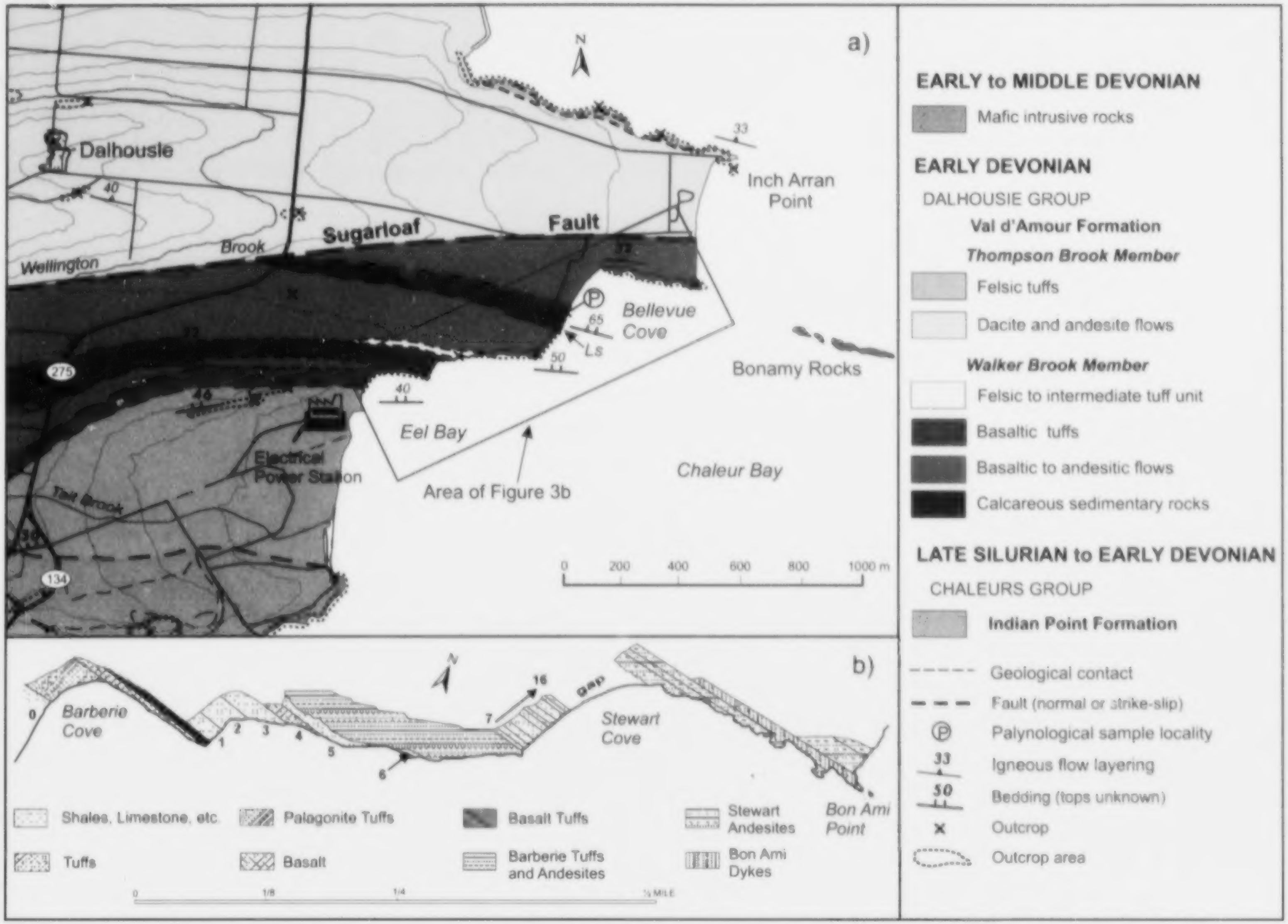
a)
N
Dalhousie
Wellington
Brook
Sugarloaf
Fault
40
33
Inch Arran Point
P
65
Ls
50
Bellevue Cove
40
Bonamy Rocks
Eel Bay
Area of Figure 3b
Chaleur Bay
Electrical Power Station
Tait Brook
275
134
46
0
200
400
600
800
1000 m
EARLY to MIDDLE DEVONIAN
Mafic intrusive rocks
EARLY DEVONIAN
DALHOUSIE GROUP
Val d'Amour Formation
Thompson Brook Member
Felsic tuffs
Dacite and andesite flows
Walker Brook Member
Felsic to intermediate tuff unit
Basaltic tuffs
Basaltic to andesitic flows
Calcareous sedimentary rocks
LATE SILURIAN to EARLY DEVONIAN
CHALEURS GROUP
Indian Point Formation
Geological contact
Fault (normal or strike-slip)
Palynological sample locality
33
Igneous flow layering
50
Bedding (tops unknown)
Outcrop
Outcrop area
b)
N
0
Barberie Cove
1
2
3
4
5
6
7
16
Gap
Stewart Cove
Bon Ami Point
Shales, Limestone, etc.
Tuffs
Palagonite Tuffs
Basalt
Basalt Tuffs
Barberie Tuffs and Andesites
Stewart Andesites
Bon Ami Dykes
0
1/8
1/4
½ MILE

Figure 3. a) Detailed geology of the Dalhousie area. Ls = limestone bed, or bed 7 of Clarke (1909). b) Partial reproduction of Howard's (1926) map of this section. Bed numbers (1 to 16) for sedimentary rocks on the shore section are after Clarke (1909). Names of the coves shown on Howard's map are no longer in official use.

Brook Member encompasses the original Dalhousie (that is, Eel Bay) section of Clarke (1909).

The proposed type section of the Val d'Amour Formation is situated along Highway 270 through the village of Val d'Amour and north to Beauvista Drive in Atholville (Fig. 1). Although the basal contact is not exposed here, many good outcrops exist along the sinuous course of Highway 270 from Highway 275 north to Sugarloaf Mountain, offering the best cross-section through the entire unit. This section also coincides with the thickest development of the Val d'Amour Formation.

Walker Brook Member

The basal unit of the Val d'Amour Formation is the Walker Brook Member, named for the brook that flows along Highway 270 through Val d'Amour. The Walker Brook Member consists of basaltic and minor andesitic flows; basaltic ash and lapilli tuffs; local basaltic hyaloclastite; and minor sedimentary rocks, and felsic tuffs and flows (Fig. 1, 3, 4a–d). Thickness is estimated to be about 1560 m. Basalts are typically dark green, dark greenish grey, or maroon, and are moderately to very amygdaloidal. Several examples of well developed spheroidal weathering were noted in basalts that form the lower part of the Walker Brook Member at the type section. West of the Squaw Cap Fault (Fig. 1), massive basalt predominates, and sedimentary rocks and mafic tuffs are absent; however, a small volume of flow-layered rhyolite crops out adjacent to the Sellarsville East Fault north of Glen Levit (Fig. 1).

Some flows are sparsely to moderately porphyritic but do not form mappable units. In contrast, a very distinctive, light green, highly porphyritic basalt at the top of the Walker Brook Member can be traced for roughly 11 km east and 11 km west of the type section on Highway 270. These flows contain 20% to 40% zoned plagioclase phenocrysts that measure up to 1 cm in diameter. Except for their fine-grained, amygdaloidal groundmass, the flows resemble intrusive rocks. In thin section, basalt textures may be hyalopilitic (glassy), trachytic, intersertal, or intergranular. Glassy types contain plagioclase microlites in an oxide-rich opaque groundmass, whereas the phenocryst population of other samples includes plagioclase (andesine or labradorite crystals, ≤ 25%, ≤ 3 mm), with or without pyroxene (≤ 10–15%, ≤ 4 mm), and with or without olivine (≤ 15%, ≤ 2 mm).

Along the coast of Eel Bay at Dalhousie, three basalt sequences (Fig. 2, 3) occur within the Walker Brook Member in the section described by Clarke (1909). The thin (approximately 15 m), lowermost unit overlies the basal "palagonite tuff" of Howard (1926) and consists of flow-brecciated basalt, columnar-jointed basalt, and basaltic hyaloclastite, overlain by sedimentary beds 1 to 3 of Clarke (1909). The middle interval represents the "Barberie andesites" of Howard (1926) and comprises about 40 m of pillow breccia and hyaloclastite (Fig. 4a), overlain by about 80 m of pillow basalt. The pillows here commonly display a concentration of amygdules near the pillow rims (Fig. 4b), and their oxidized

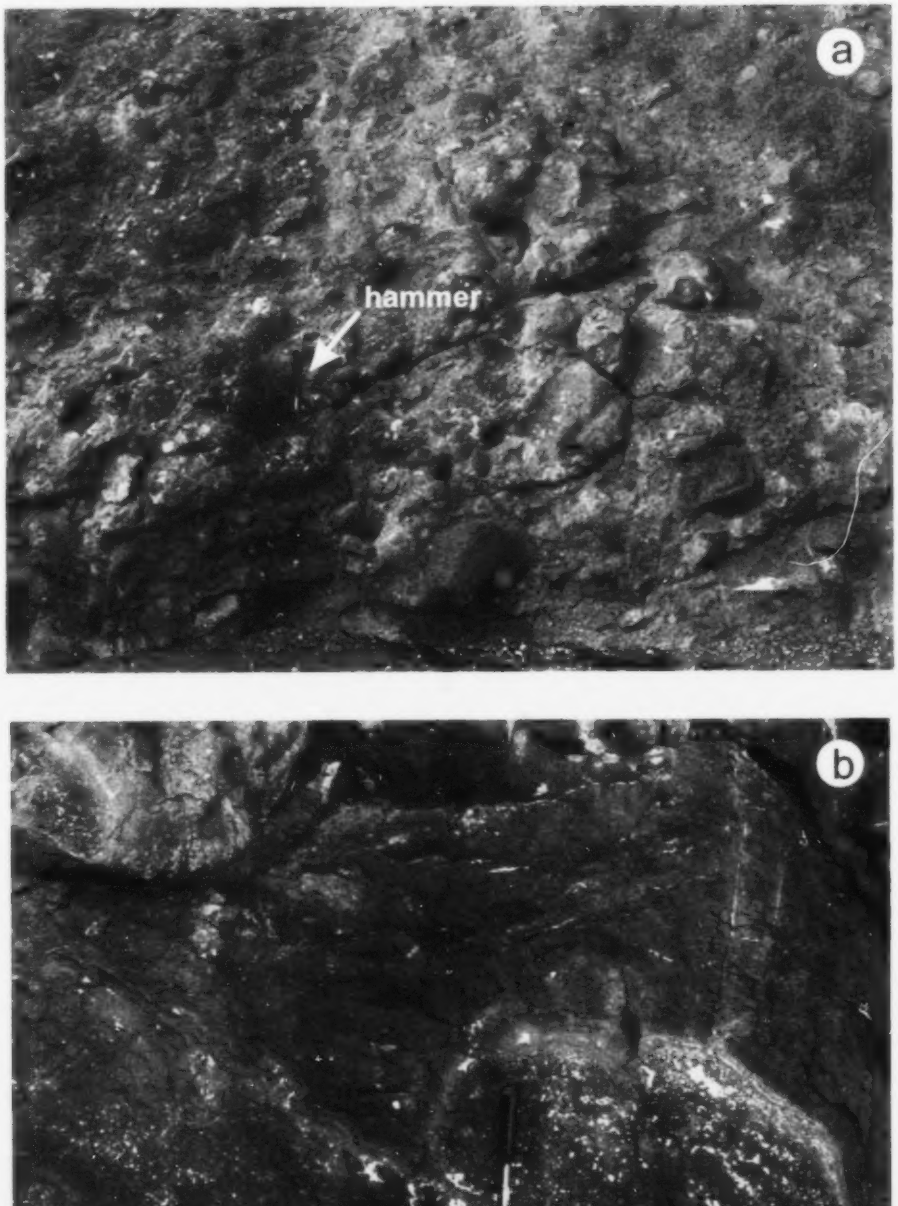

Figure 4. Lithotypes from the Walker Brook Member on Chaleur Bay coast at Dalhousie. a) Pillow breccia and hyaloclastite. Hammer handle is 37 cm long. b) Oxidized, pillowed paleosurface at the interface between successive subaqueous basalt flows. Hammer handle is 37 cm long.

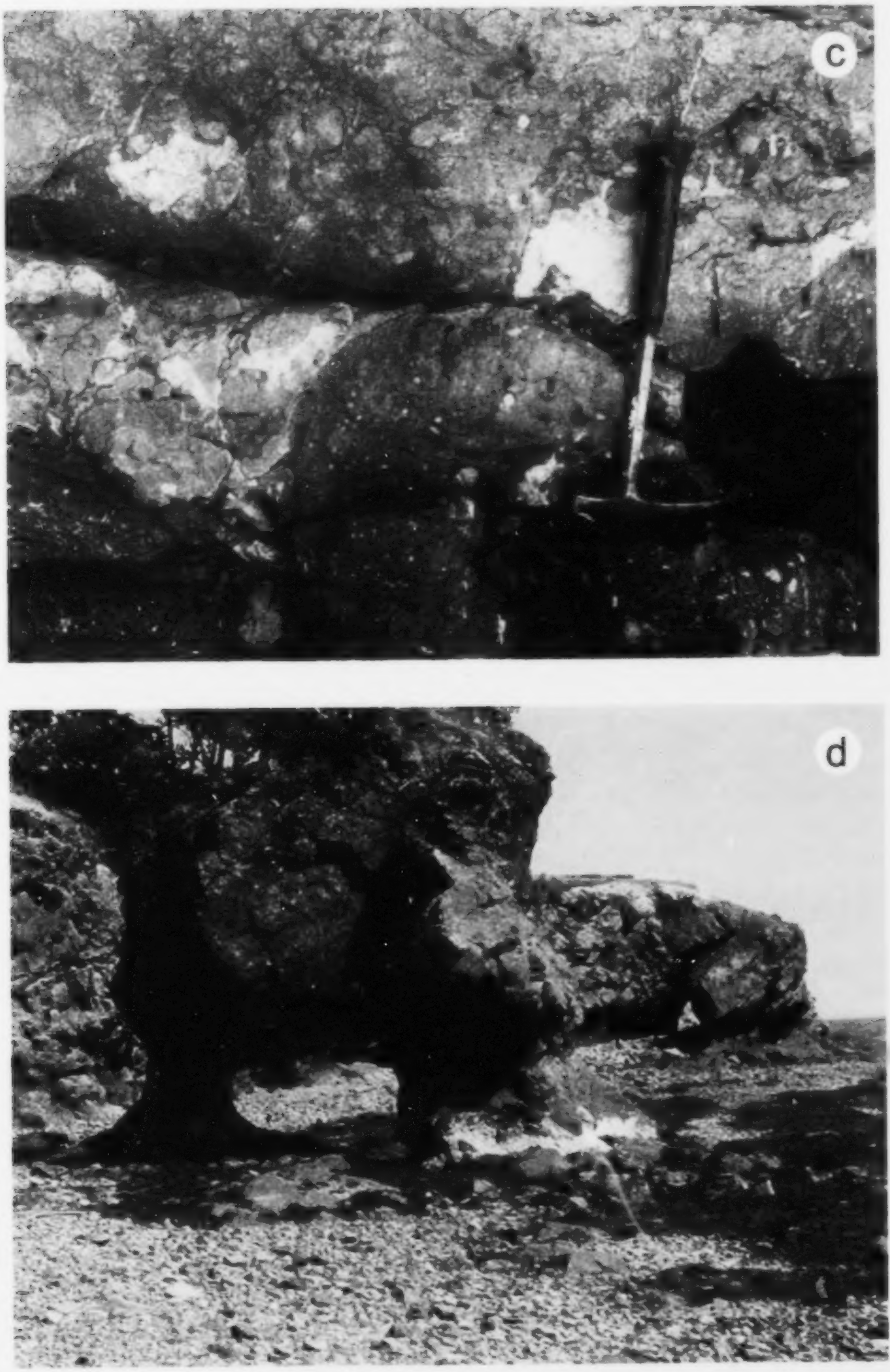

Figure 4 *(cont'd)*. Lithotypes from the Walker Brook Member on Chaleur Bay coast at Dalhousie. c) Light grey limestone (top) deposited on green pillow basalt. Hammer handle is 37 cm long. d) Basalt flows forming a 3 m high "pierced rock."

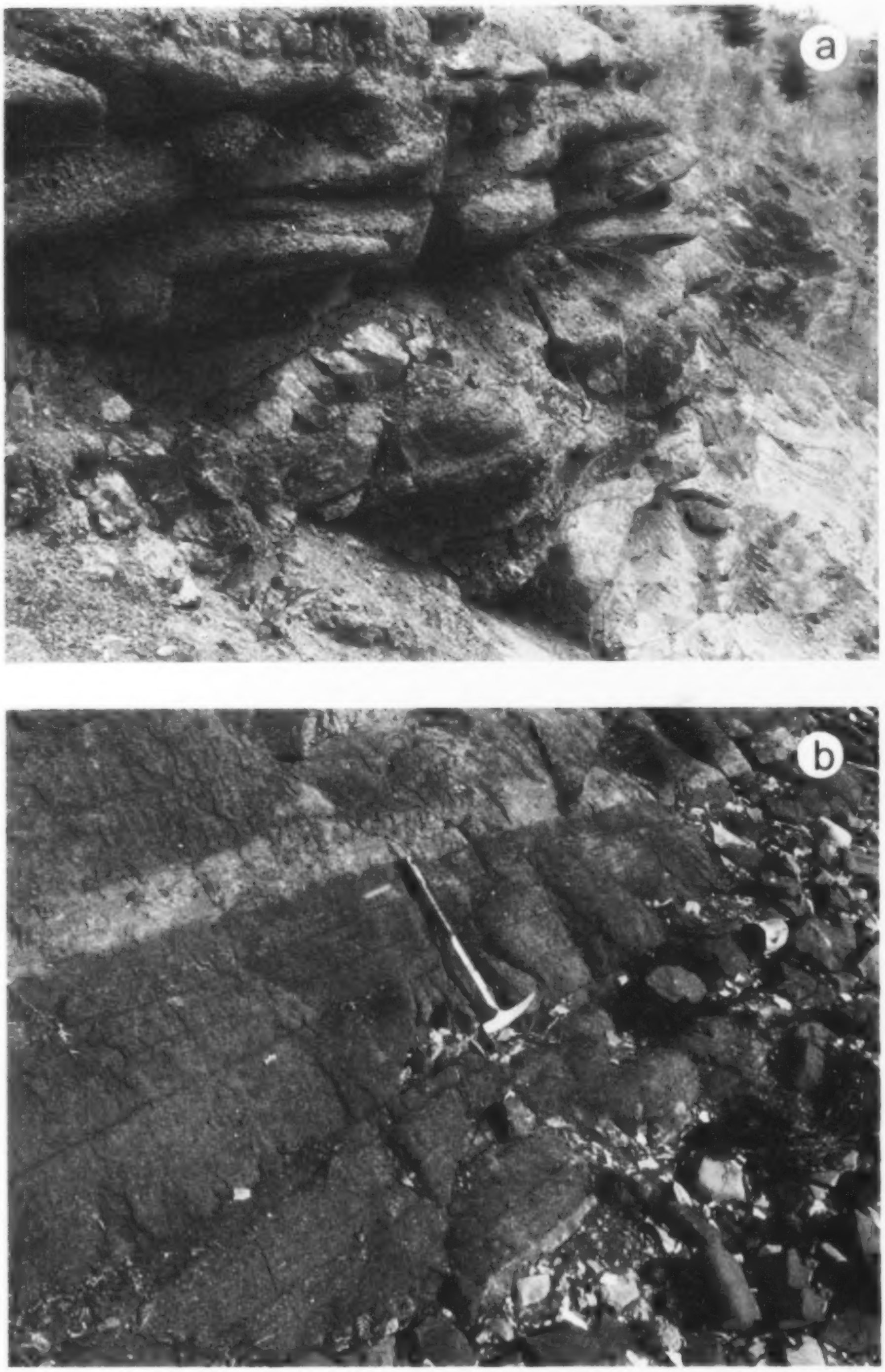

Figure 5. a) Bedded mafic ash tuff from the middle tuff unit of the Walker Brook Member at the type section on Highway 270. b) Bedded mafic tuff near the base of the Walker Brook Member on the Chaleur Bay coast at Dalhousie. Hammer handle is 37 cm long.

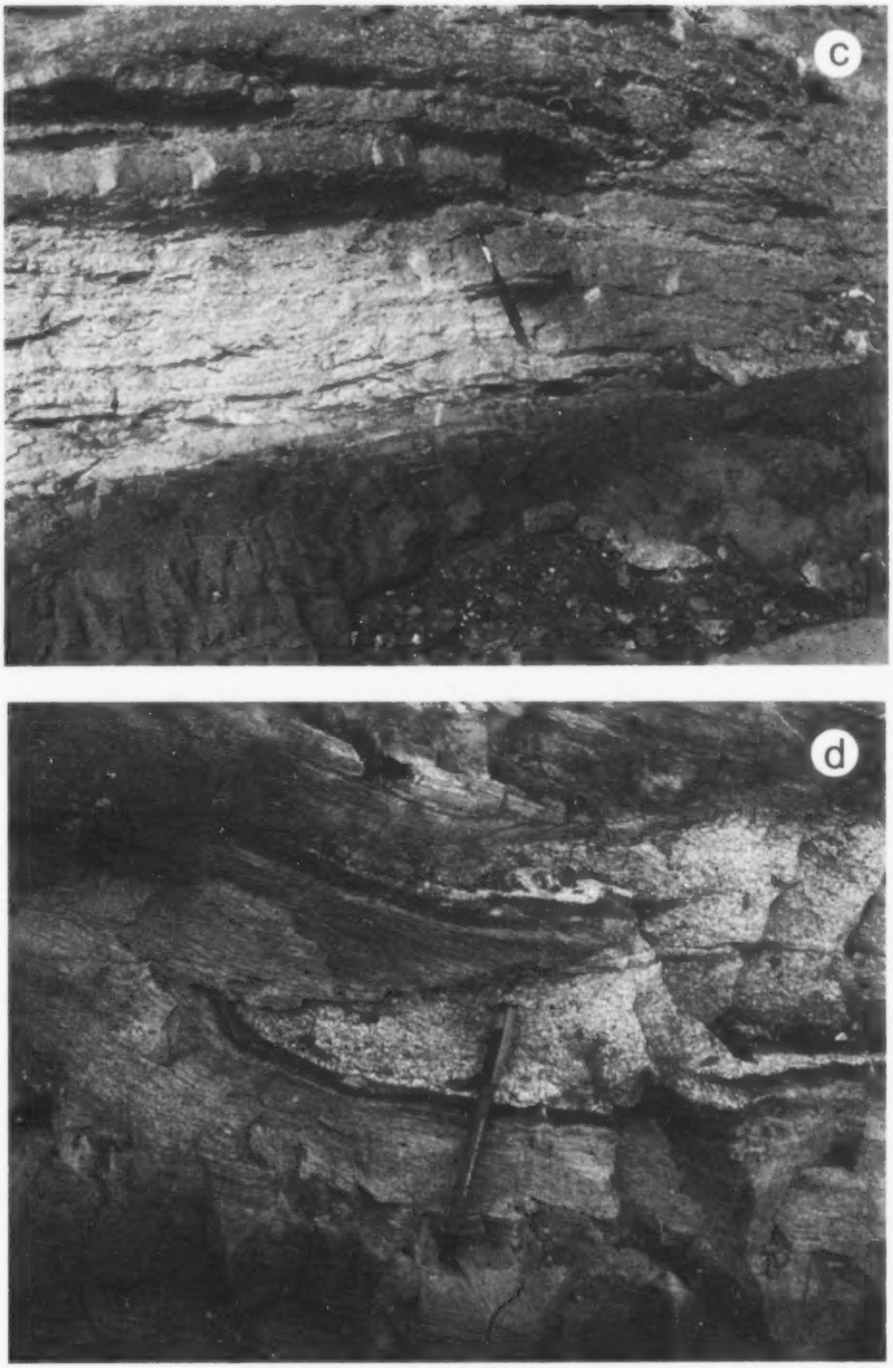

Figure 5 *(cont'd).* c) Pyroclastic flow consisting of ash tuff and pumiceous lithic–crystal tuff (greyish green), overlying lower sedimentary interval of the Walker Brook Member (brown), on the Chaleur Bay coast at Dalhousie. d) "Wedging" of a dense pyroclastic flow into underlying sedimentary rocks, Walker Brook Member, on the Chaleur Bay coast at Dalhousie. Hammer handle is 37 cm long.

paleosurfaces allow easy recognition of flow contacts. A pillowed paleosurface is also observed at the top of the "Barberie andesite" interval, where it is overlain by light grey, coral-bearing limestone (Fig. 4c) that represents bed 7 of Clarke (1909). This limestone yielded non-specific Pridolian to Early Devonian forms of conodonts. The upper mafic flows in the Walker Brook Member at Dalhousie constitute the "Stewart andesites" and "Bon Ami dykes" of Howard (1926). They consist of dark green to dark grey, massive to very amygdaloidal, locally flow-brecciated basalt (Fig. 4d) and minor volcaniclastic conglomerate. Intrusive rocks ("Bon Ami dykes") referred to by Howard (1926) were not recognized. The exposed thickness is about 60 m, but total thickness is unknown because of gaps in exposure to the north and south, and also because of possible truncation of the Walker Brook Member by the Sugarloaf Fault (Fig. 3).

Basaltic tuffs form three thin-bedded to very thick-bedded intervals that are overlain and underlain by basalt flows at the Highway 270 type section (Fig. 2). Maximum thicknesses of the lower, middle, and upper tuffs are estimated at 50, 500, and 140 m, respectively. The lower tuff is associated with green, thin-bedded mudstone and medium-bedded, parallel- or cross-laminated sandstone, and minor basalt. The middle tuff unit occurs as thin to thick, typically very friable beds comprising dark green, ash- to lapilli-sized clasts (typically ≤ 1 cm) of glassy basalt in a white to pink zeolite matrix (Fig. 5a). This tuff closely resembles the 50 m interval of thin-bedded "palagonite tuff" (Howard 1926) that constitutes the base of the Val d'Amour Formation at Eel Bay (Fig. 2, 3, 5b). Assuming a correlation between the two units, it follows that basalt flows in the lower part of the Walker Brook Member at the type section do not extend to Eel Bay (Fig. 2). In thin section, basalt lapilli have ragged to subrounded outlines, and hyalopilitic to trachytic textures of plagioclase microlites in an opaque (glassy), oxide-rich groundmass. In places, plagioclase or olivine phenocrysts are contained within the clasts.

Other pyroclastic rocks include a 6 m thick bed of pale yellowish-grey to greenish-grey felsic to intermediate tuff (Fig. 5c) that represents beds 4 and 5 of Clarke (1909). The tuff immediately underlies the middle basalt flows ("Barberie andesites") at Dalhousie and overlies the fine-grained tuffaceous sandstone (Fig. 3) representing Clarke's bed 3. The pyroclastic rocks include very thin beds of fine- to medium-grained ash at the base, overlain by a several-metre-thick bed of pumiceous lithic–crystal tuff. Emplacement as a hot, dense pyroclastic flow is inferred from baking and scouring features in the underlying sedimentary rock (Fig. 5d). Above the basal fine-grained ash, the lower part of the pyroclastic flow displays reverse grading, whereas the upper part appears to be normally graded.

Minor thicknesses of sedimentary rock are intercalated with the volcanic rocks of the Walker Brook Member at or near the type section. They include green to grey or maroon, basalt-derived volcaniclastic siltstone, sandstone, and conglomerate; thin-bedded, dark grey mudstone; and light grey, parallel-laminated sandstone. A 20 m thick interval of mudstone and sandstone between the middle and upper tuff units is well exposed on the Malauze Road west of Highway 270 (Fig. 1, 6a). Spores collected from this locality have yielded an early Lochkovian age (Fig. 2). Assuming that the correlation of the middle tuff unit with the basal "palagonite tuff" at Dalhousie is correct, the sedimentary rocks on Malauze Road probably are roughly coeval with beds 1 to 3 of Clarke (1909; Fig. 3).

Sedimentary rocks are much more abundant near Dalhousie at Eel Bay, where the two fossil-rich sedimentary sections described by Clarke (1909) comprise thin-bedded, fossiliferous, typically calcareous mudstones, and fine-grained sandstones or calcarenites. The lower section, which includes the pyroclastic flow described above, is 66 m thick and represents beds 1 to 5 of Clarke (1909). The upper section is 63 m thick and represents Clarke's beds 7 to 16 (Fig. 6b). A sample from the latter section contained a rich and diverse spore assemblage that has been dated (Wilson et al. 2004) as Pragian to early Emsian (Fig. 2, 3).

The Walker Brook Member is intruded by several small stocks of fine-grained gabbro that probably were part of the subvolcanic feeder system. Similar fine-grained intrusive rocks also intrude the upper part of the underlying Indian Point Formation. On the Chaleur Bay coast south of Dalhousie, the Indian Point Formation is intruded by a coarse-grained green teschenite or analcime gabbro (Chiswell 1979) that forms a rocky promontory. If related to Val d'Amour volcanism, this coarse-grained rock clearly represents a deeper seated part of the feeder system.

Thompson Brook Member

The Thompson Brook Member overlies the Walker Brook Member and is named for a brook that flows north into Chaleur Bay from hills just east of Campbellton. The Thompson Brook unit consists mainly of andesitic to dacitic effusive rocks; andesitic lithic tuff and tuff breccia; fine-grained to very coarse-grained volcaniclastic rocks; and minor felsic tuffs, basaltic flows, and siliciclastic sedimentary rocks (Fig. 1). The thickness of the unit at the type section is estimated at 3260 m. The contact between the Walker Brook and Thompson Brook members is defined as the base of a unit of fragmental andesite that extends from Upper Dundee to Glencoe (Fig. 1, 2). At the type section, the contact is located 860 m north of the intersection of Highway 270 with the Malauze Road (Fig. 1).

Effusive rocks of the Thompson Brook Member are typically greyish green, greyish maroon or maroon, aphyric to porphyritic andesites and dacites. About 30% to 40% of the outcrops examined consist in whole or in part of plagioclase-phyric lavas. Phenocrysts typically range in abundance from 10% to 30%, and are up to 4 mm in size. In the lower part of the unit, some andesitic flows, especially flow tops, are moderately to very amygdaloidal. Amygdaloidal flow tops are well exposed at the type section (Fig. 6c), where coalescing gas pockets have produced large cavities measuring 20 to 30 cm. The cavities are filled with a pink zeolite (Fig. 6d) that has been identified by X-ray diffraction as

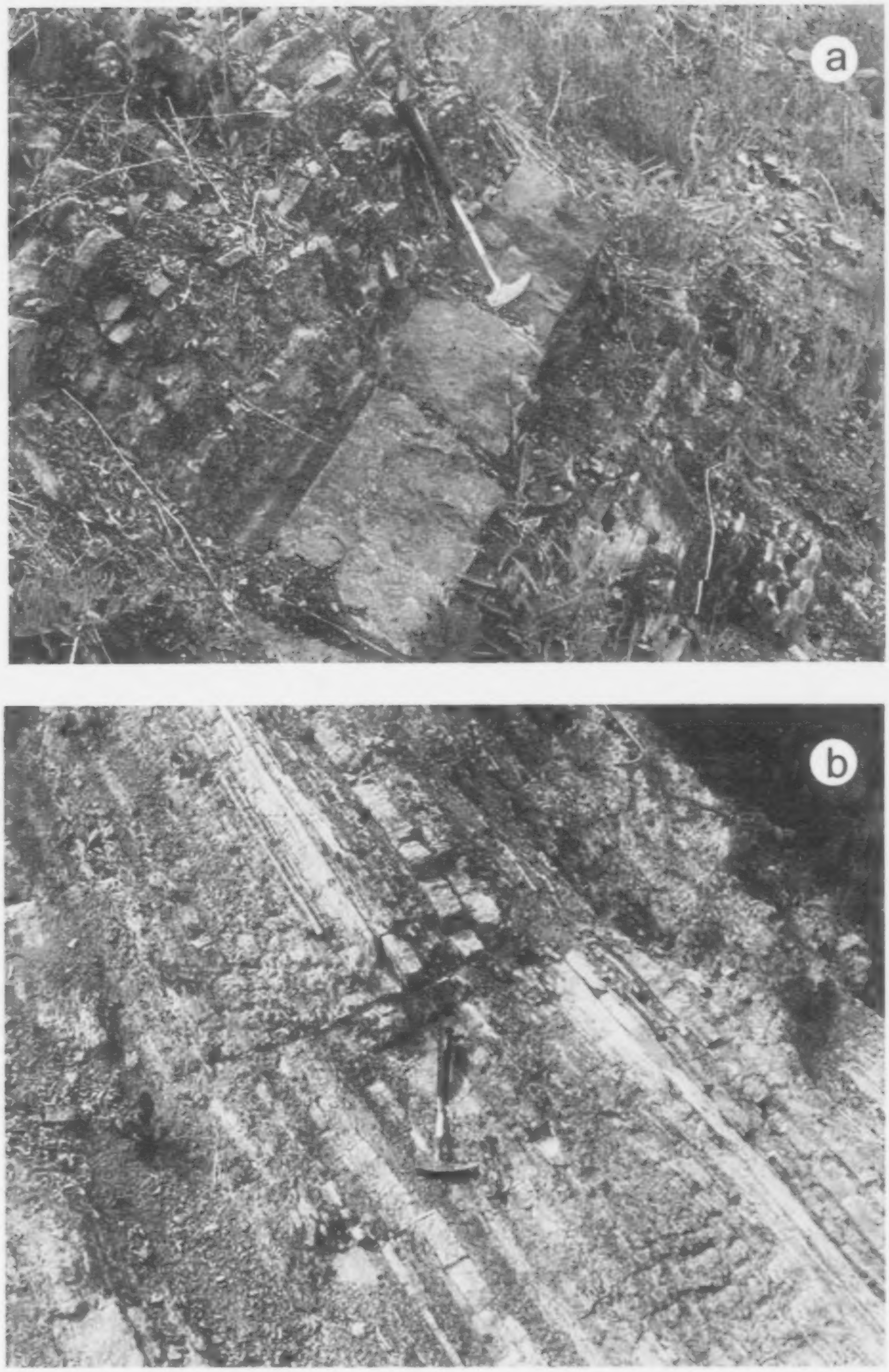

Figure 6. a) Thin-bedded mudstone (dark grey) and thicker bedded, fine- to medium-grained sandstone (light brown) of the Walker Brook Member on the Malauze Road. b) Light grey, thin-bedded, fossiliferous, calcareous mudstone and fine-grained sandstone of the Walker Brook Member (upper sedimentary interval), on the Chaleur Bay coast at Dalhousie. Hammer handle is 37 cm long.

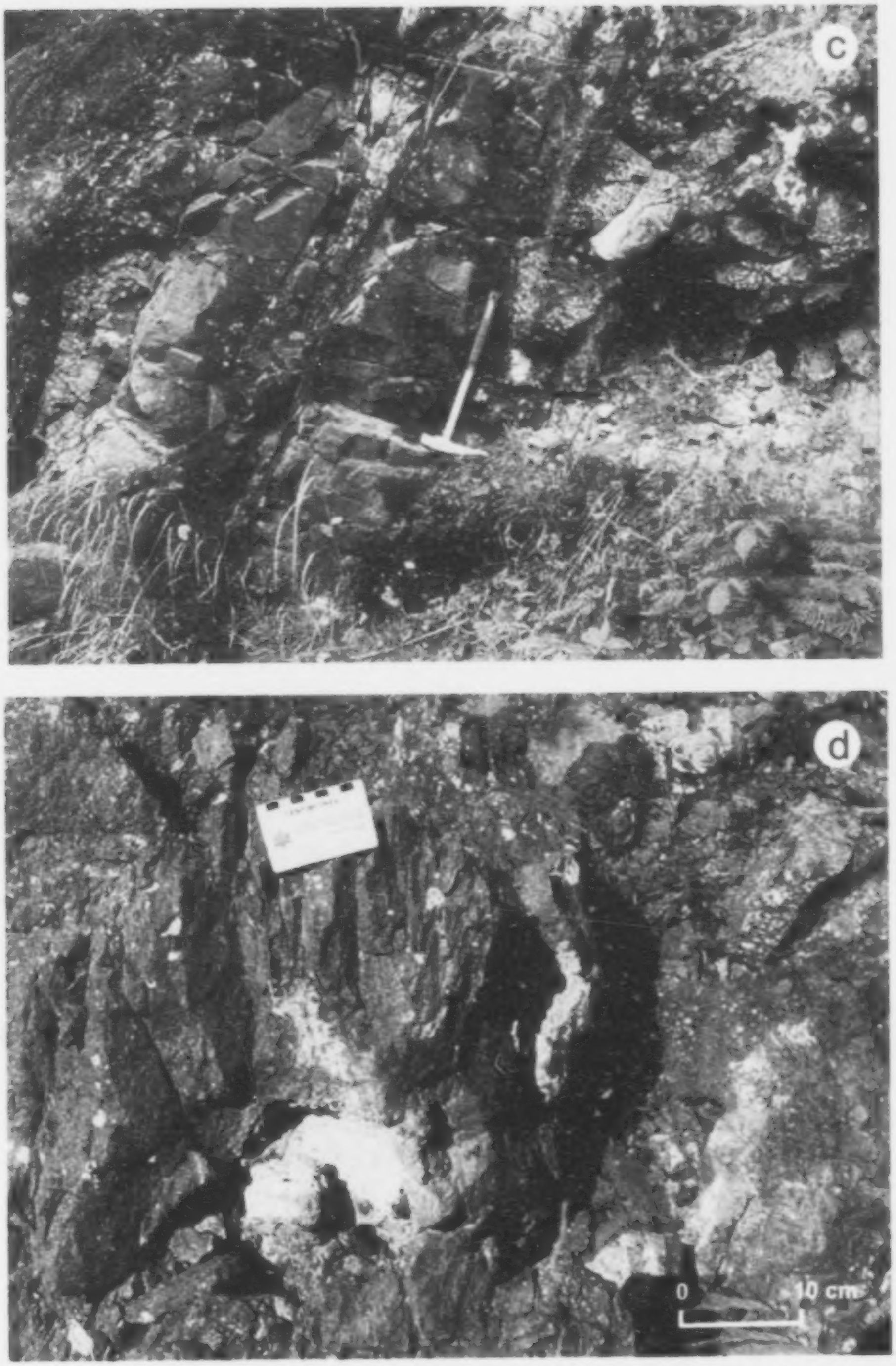

Figure 6 *(cont'd)*. c) Alternating amygdule-rich and amygdule-poor mafic flows of the Thompson Brook Member at the type section of the Val d'Amour Formation on Highway 270. The amygdaloidal zone to the right of the hammer handle is interpreted as a flow-top. d) Large, zeolite (laumontite)-filled gas pocket in amygdaloidal, andesitic flow interbedded with basal part of the intermediate tuff unit of the Thompson Brook Member at the type section on Highway 270. Hammer handle is 37 cm long.

laumontite (D. Lentz, written communication 2002). Laumontite is by far the most prevalent amygdule mineral, but others include chlorite, calcite, and celadonite.

Many andesite and dacite outcrops display a prominent, regular parting that generally dips moderately to the north, parallel to the regional structure (Fig. 7a). In thin section, this feature is recognized as a primary flow layering defined by the trachytic alignment of plagioclase microlites. Textures typically vary from trachytic to intersertal; plagioclase laths enclose a turbid to opaque (glassy) groundmass that locally contains some granular pyroxene, and that has been altered to chlorite, epidote, and/or calcite. Phenocrysts include plagioclase (andesine or labradorite: ≤ 30%, ≤ 4 mm), ± pyroxene (augite), ± hornblende (in some dacites, up to 6%), and rare olivine (in the more mafic samples).

Basalts occur sporadically within the Thompson Brook Member but are most common at or near the Chaleur Bay coast (Fig. 1), where they apparently correlate to the Maple Green andesites of Howard (1926). The basalts are dark green to dark greenish grey and typically are amygdaloidal.

Pyroclastic rocks include mainly intermediate, and minor mafic and felsic, lithic tuffs; lithic–crystal tuffs; and tuff breccias. Intermediate tuffs (Fig. 7b) form a thick (480 m at the type section) interval at the base of the Thompson Brook Member, where they are intercalated with minor basalt and andesite and also occur as several thin, discontinuous lenses within the unit. They typically are green, grey, purple or maroon, and are very well indurated, in contrast with the friable mafic lapilli tuffs in the Walker Brook Member. The Thompson Brook tuffs are clast supported and consist of angular to subrounded fragments of basalt, andesite and/or dacite (described above) in sizes generally less than 10 cm but ranging up to 50 cm (Fig. 7b).

Felsic pyroclastic rocks occur as thin, discontinuous lenses overlying the basal tuff in the lower part of the Thompson Brook Member, and near the upper part of the unit, where they are well exposed on Highway 11 (Fig. 1). They are also present on the coast near Inch Arran Point at Dalhousie (Fig. 3, 7c). The pyroclastic rocks are pink, mauve, light green, or pale maroon, include lithic or lithic–crystal lapilli tuff and tuff breccia, and contain clasts that measure up to 15 cm.

Volcaniclastic rocks are formed from reworking of primary pyroclastic or effusive volcanic material, and are recognized by better rounding of volcanic clasts and a clastic sedimentary rather than a tuffaceous matrix. They are locally interbedded in varied proportions with genetically related andesitic to dacitic tuffs but are most abundant within a separate, mappable unit at the top of the Thompson Brook Member just south of Campbellton. In this location, the unit appears as a belt that trends east-northeast–west-southwest and is centred on Sugarloaf Mountain (Fig. 1). The belt contains a roughly 500 m thick sequence of volcanic cobble–boulder conglomerate (Fig. 7d), fine- to coarse-grained tuffaceous (arkosic–lithic) sandstone, and minor fine-grained siliciclastic sedimentary rocks.

On Highway 11 just west of Sugarloaf Mountain, about 40 m of shallow-water mudstones and fine-grained sandstones (Fig. 8a) are interbedded with the volcaniclastic rocks. This interval also includes a seam of dirty coal measuring 5 to 15 cm thick. Spore sampling in these beds (Fig. 2) yielded one sample with abundant taxa of Pragian to early Emsian age (Wilson et al. 2004), the same age range obtained from spores in the upper Walker Brook Member. Presumably, spores from the latter beds date from the earlier part of the 6 million year period that spans the early Pragian to early Emsian. An early Emsian age for beds in the upper Thompson Brook Member is consistent with age determinations for the overlying Richardsville rhyolite (see **Geochronology**, below).

Volcanic cobble–boulder conglomerate occurs within the Thompson Brook Member on the coast near Maple Green (Fig. 1), where it is interbedded with minor thin-bedded, red siltstone displaying dessication cracks. These rocks are very similar to the boulder–cobble conglomerate and red mudstone interbedded with rhyolite of the Richardsville Member at Campbellton, described in the following section. If they are the same beds, then the rhyolite must pinch out to the east beneath upper Chaleur Bay.

A number of small, intermediate to felsic subvolcanic stocks and related sills and dykes intrude the upper part of the Thompson Brook Member, particularly from Highway 270 east to Maple Green (Fig. 1). Felsic subvolcanic rocks are pink, light green, or greyish-brown feldspar porphyries containing up to 25% phenocrysts of alkali feldspar. Intermediate subvolcanic rocks are typically greyish-green, greyish-maroon, or greyish-brown, massive, plagioclase-phyric dacites that are usually columnar jointed. The Sugarloaf Porphyry is a typical dacite porphyry: pinkish brown to greyish brown, containing up to 20% zoned euhedral plagioclase (andesine), 6% hornblende, and local granules of pyroxene in a turbid, microfelsitic groundmass. Finer grained parts of the porphyry display a trachytic texture of plagioclase laths, indicative of having formed in an actively flowing part of the volcanic pipe. Columnar jointing is observed near the top of the mountain, plunging about 45° in a south-southeasterly direction.

Richardsville Member

The upper part of the Val d'Amour Formation consists mainly of pink to maroon flow-layered rhyolite of the Richardsville Member, named for the east end of Campbellton, where the rhyolite underlies a prominent, east-northeasterly-trending hill. In the type area, the basal contact of the Richardsville Member is defined as the contact between the volcanic cobble–boulder conglomerate at the top of the Thompson Brook Member, and the overlying flow-layered rhyolite (Fig. 8b). At Exit 412 from Highway 11 on the east side of Campbellton, the contact between the conglomerate and rhyolite can be determined to within a few metres, although it is not presently exposed. Farther east and west, the

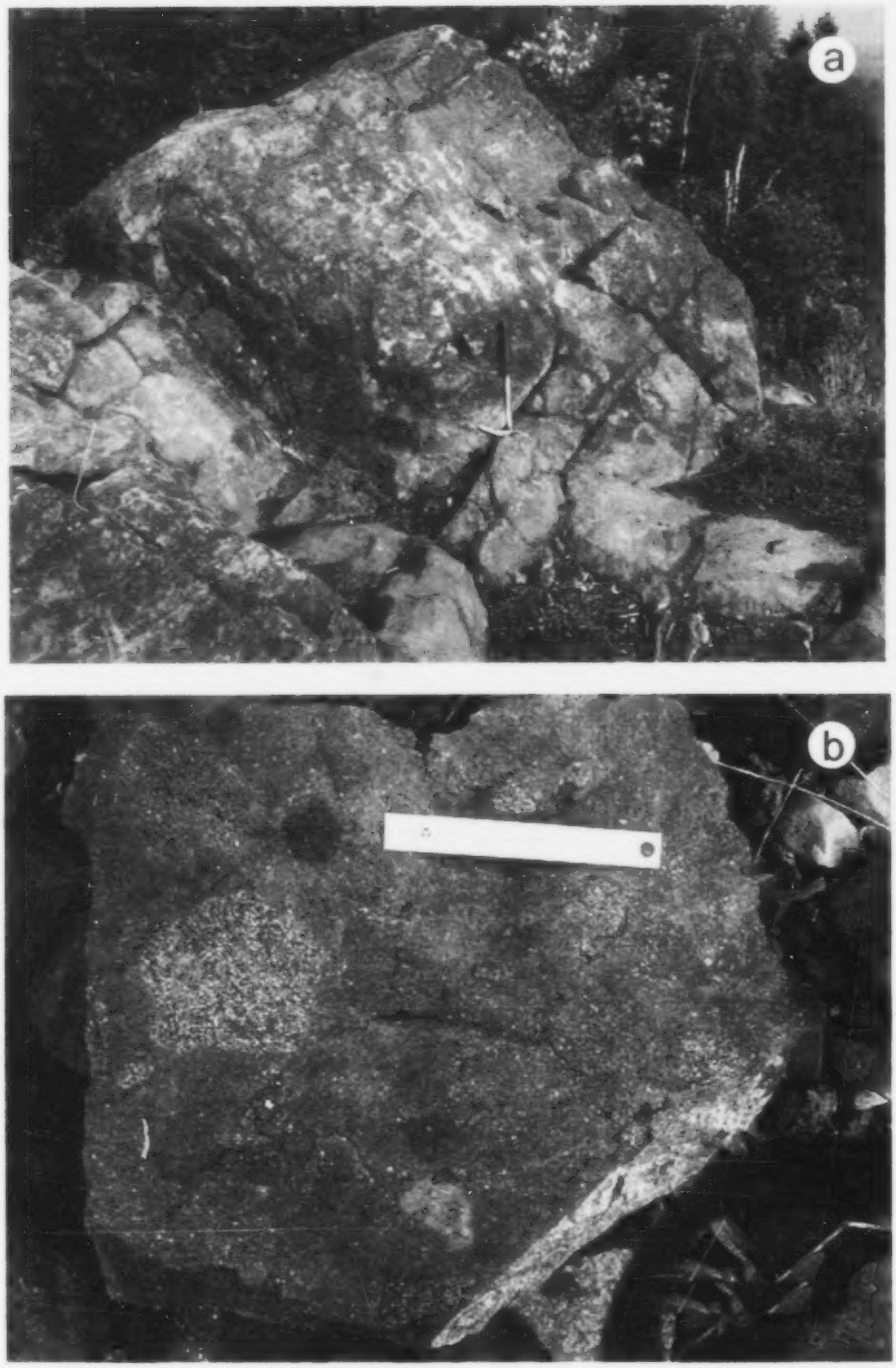

Figure 7. a) Andesitic flow of the Thompson Brook Member at Dalhousie Mountain just west of Dalhousie. The parting that dips about 45° to the left of the page (north) is a flow layering defined by trachytic alignment of plagioclase laths. b) Andesitic lithic tuff of the Thompson Brook Member at the type section on Route 270, just south of Sugarloaf Mountain. Scale is 15 cm long.

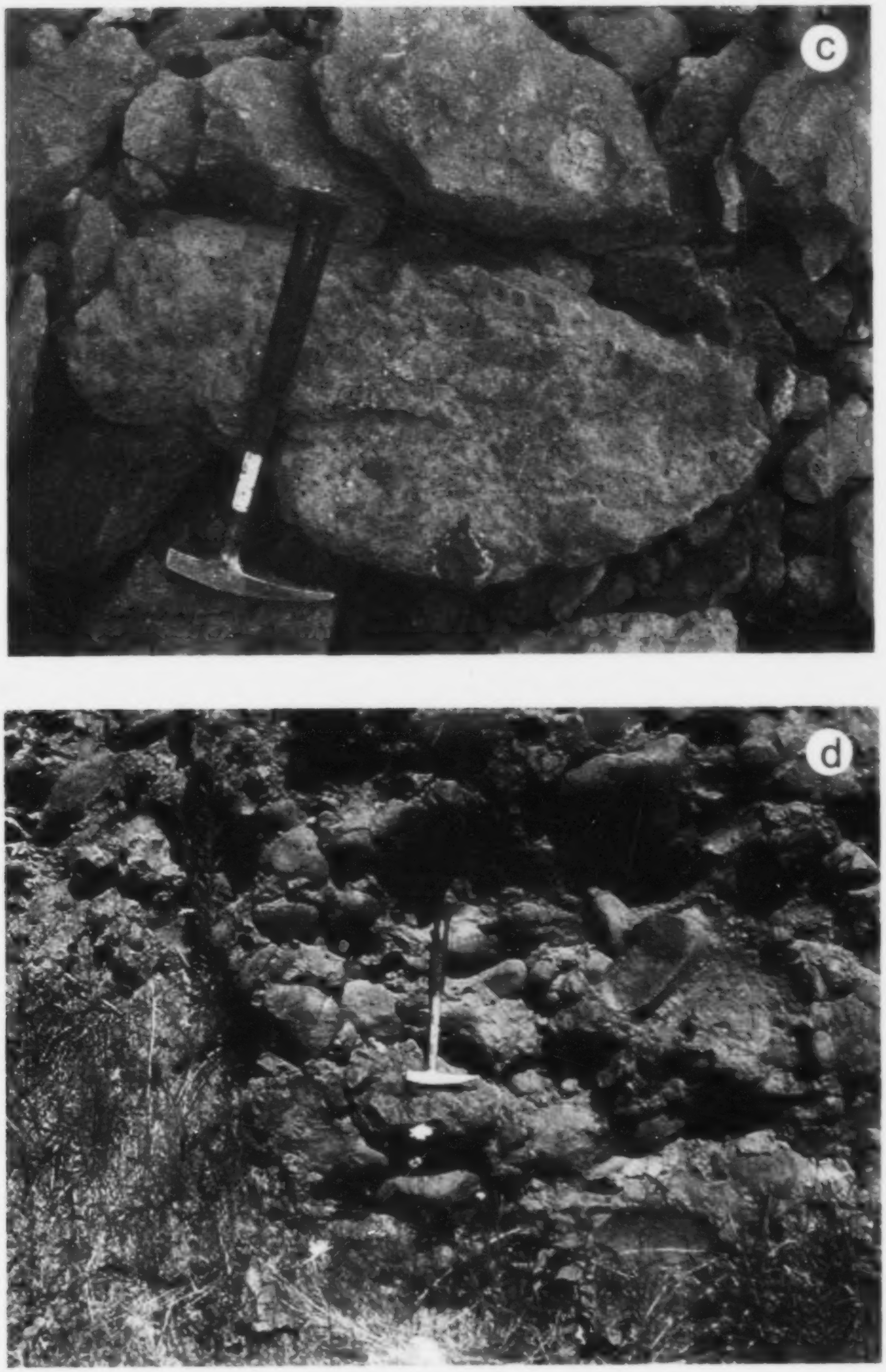

Figure 7 *(cont'd)*. c) Felsic to intermediate lithic–crystal tuff of the Thompson Brook Member near Inch Arran Point, Dalhousie. d) Volcaniclastic conglomerate at the top of the Thompson Brook Member along Highway 11 at Campbellton. Hammer handle is 37 cm long.

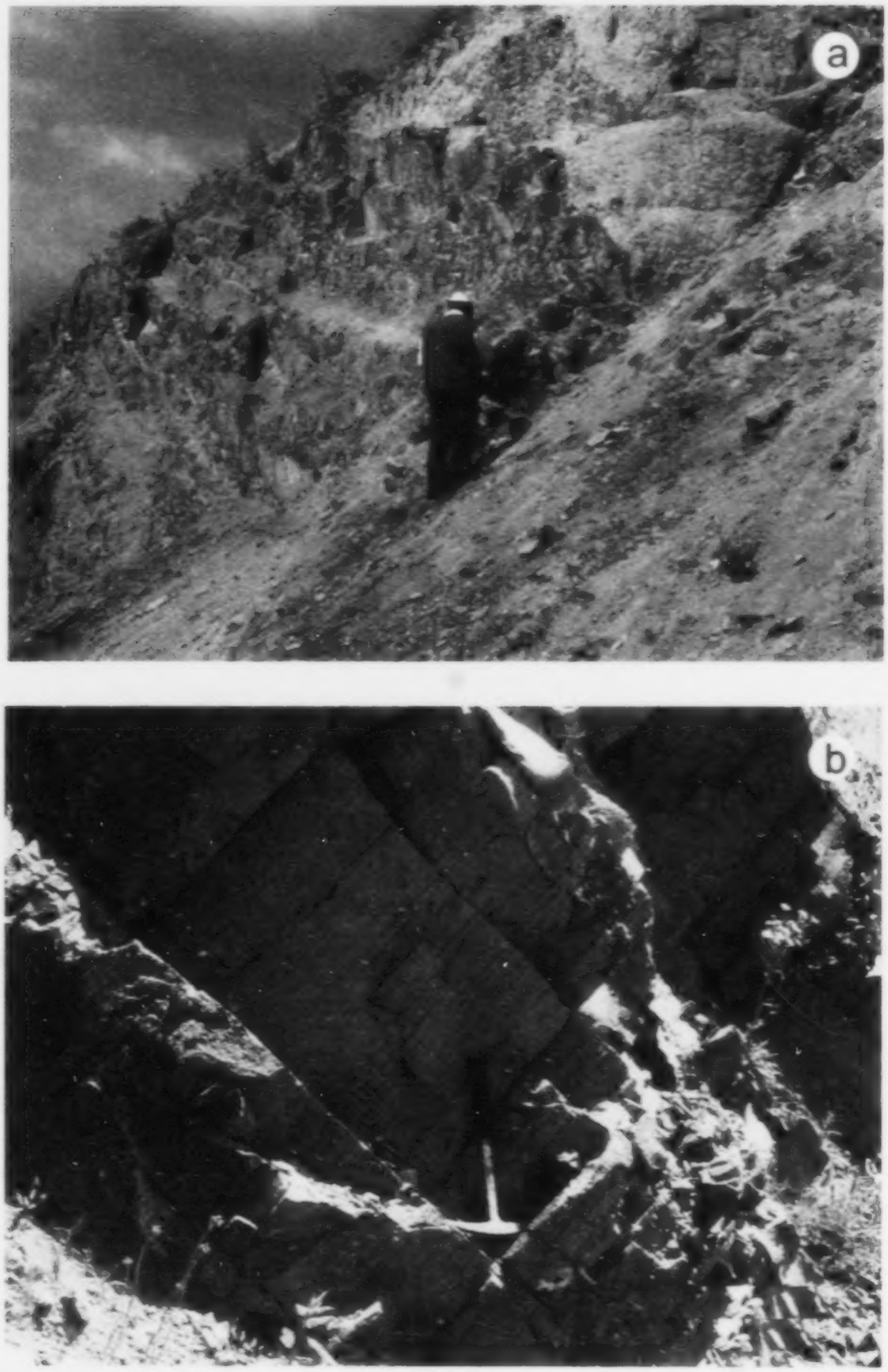

Figure 8. a) Thin-bedded mudstone and fine-grained sandstone from a volcaniclastic unit at the top of the Thompson Brook Member on Highway 11 just west of Sugarloaf Mountain. b) Flow-layered rhyolite at the base of the Richardsville Member, east side of Campbellton. Hammer is 37 cm long.

Richardsville Member overlies volcanic rocks of the Thompson Brook Member (Fig. 1). The maximum thickness of the Richardsville Member is roughly 920 m.

The Richardsville Member contains two types of rhyolite. The first is a pink, generally aphyric to sparsely feldspar-phyric, very prominently flow-layered variety that dominates the area east of Atholville and underlies much of Campbellton. In places, small phenocrysts of quartz have also been observed. Petrographic examination shows a homogenous microfelsitic groundmass containing varied quantities of euhedral alkali feldspar phenocrysts that measure 2 to 6 mm, and, in one sample, 1% to 2% embayed quartz phenocrysts that are up to 1 mm. Flow layering is consistent over considerable distances in the Richardsville area, and its orientation is similar to that of local sedimentary beds. Several felsic outcrops display a mottled alteration or bleaching that clearly overprints flow layering in some places. The alteration appears to be centred on an elliptical stock of medium to dark green, subvolcanic andesitic porphyry just northwest of Sugarloaf Mountain (Fig. 1) and therefore may be related to hydrothermal activity associated with its intrusion. The second felsic type is a porphyritic, massive to subtly flow-layered rhyolite that underlies a ridge just north of Highway 11 west of Atholville (Fig. 1). These rocks contain 10% to 25% phenocrysts of alkali feldspar measuring 1 to 6 mm. Examination of a single thin section indicated 15% euhedral phenocrysts of feldspar (5% albite, approximately 1 mm; and 10% potassic feldspar, 1 to 2 mm) in a turbid, microfelsitic groundmass containing copious fine grains and amorphous masses of opaque material.

Minor lithotypes in the Richardsville Member include local lithic–crystal tuff and tuff breccia southwest of Atholville, and a narrow belt of volcaniclastic rocks and basalt east of Atholville. The volcaniclastic rocks are volcanic cobble–boulder conglomerates, identical to those at the top of the Thompson Brook Member. They are exposed at the corner of Beauvista Drive and Du Manoire St. in Atholville, and along the railway track on the east side of Campbellton. At the former location, they are overlain by dark red mudstone. A seam of light greyish-green, tuffaceous mudstone occurs stratigraphically higher in the section on Beauvista Drive. It is rich in plant fossils and evidently marks a break between successive felsic flows (Gensel et al. 1997).

Depositional Environment

Sedimentological, palynological, and volcanological evidence indicates that generally subaerial environments dominated during deposition of the Val d'Amour Formation, except in the eastern part of the area near Dalhousie, where marine conditions prevailed. For example, sedimentary rocks are scarce in the unit as a whole, but are comparatively abundant on the coast at Eel Bay where fossiliferous, calcareous, shallow marine deposits make up about 30% of Clarke's (1909) Dalhousie section (Fig. 3). Similarly, volcanic rocks typical of subaqueous emplacement have been observed only at Bellevue Cove (pillow basalts and related hyaloclastites in the Walker Brook Member) and Inch Arran Point (dacitic(?) hyaloclastites in the Thompson Brook Member; Fig. 3). However, oxidation observed at the tops of some pillowed flows indicates that deposition occurred in relatively shallow, well aerated water. Mafic ash and lapilli tuffs of the Walker Brook Member at Val d'Amour and Dalhousie may be shallow marine deposits; they resemble the products of phreatomagmatic eruptions (e.g. maars), which typically produce well bedded accumulations of hydroclastic debris built around a volcanic vent within a lake, coastal zone, marsh, or area of abundant groundwater. In most of the study area, the transition to subaerial volcanism from marine sedimentation of the Indian Point Formation must have been abrupt, as pillow basalts and hyaloclastites are absent from the Walker Brook Member west of Dalhousie.

More than 50 species of terrestrial spores have been identified in sedimentary strata intercalated with the volcanic rocks. In general, the sedimentary rocks are thought to be freshwater in origin, which supports interpretations of a subaerial to shallow-water environment. The thin coal seam and associated plant-rich grey mudstone in the Thompson Brook Member near Sugarloaf Mountain (Fig. 7a) indicate a terrestrial environment, perhaps a marshy intermontane valley or basin; their occurrence is consistent with subaerial emplacement of most volcanic rocks.

Local thicknesses of volcaniclastic sandstone and conglomerate are inferred to have been sourced from volcanic highlands and deposited in similar basins. Volcaniclastic rocks typically form thick-bedded, immature, poorly sorted deposits that suggest minimal influence of water. For example, the thick-bedded, volcanic cobble–boulder conglomerate in the upper Thompson Brook Member at Campbellton (Fig. 7d) shows little indication of having been worked by water. The tuffaceous volcanic matrix is likely the product of in situ weathering of coarse volcanic detritus that accumulated in these intermontane valleys. Intermittent fluvial or lacustrine deposition in similar valleys may account for the sporadic, thin intervals of sedimentary rock elsewhere in the Val d'Amour Formation (aside from the fossiliferous, shallow marine sedimentary rocks on Eel Bay).

GEOCHRONOLOGY

A 20 kg sample of rhyolite collected from the Richardsville Member in Campbellton yielded zircon that was analyzed for Pb and U by Isotope Dilution Thermal Ionization Mass Spectrometry methods. Zircon was separated from the rock samples using standard heavy liquid and magnetic separation techniques. All zircon fractions were subjected to air abrasion treatment (Krogh 1982). Mineral dissolution in the presence of a mixed ^{205}Pb–^{235}U tracer followed the procedure of Krogh (1973). Chemical separation is considered unnecessary for zircon fractions weighing less than 5 micrograms and thus was not conducted on these samples. Dissolved sample solutions were dried and redissolved in 3.1N HCl, and the bulk, dissolved sample was analyzed in the mass spectrometer. Pb and U were loaded together with silica gel onto outgassed rhenium filaments. The isotopic compositions of Pb and U were measured using a single collector with a Daly pulsecounting detector in a solid-source VG354 mass spectrometer. Data were corrected for a mass discrimination of 0.07%/AMU and a deadtime correction of 21.5 nsec. The thermal source mass discrimination correction was 0.1%/AMU. Laboratory blanks for Pb and U usually are less than 1 and 0.1 pg, respectively.

In this study, the total common Pb for four of the zircon analyses had a narrow range of 0.3 to 0.9 pg. Because the low variation can be attributed to laboratory Pb, no correction was made for initial common Pb. Error estimates were calculated by propagating known sources of analytical uncertainty for each analysis. Decay constants are those of Jaffey et al. (1971). All age errors quoted in the text and table, and error ellipses in the concordia diagrams, are 2σ. Zircons occur as pale brown, equant, inclusion-rich, euhedral to rounded crystals. U–Pb analyses of four abraded, single zircon grains gave concordant and overlapping data (Fig. 9, Table 1). Calculation of the concordia age (Ludwig 2001) yielded 407.4 ± 0.8 Ma (early Emsian) with an MSWD of concordance equal to 1.0. These data provide an unequivocal zircon age that is interpreted to represent the time of rhyolite emplacement.

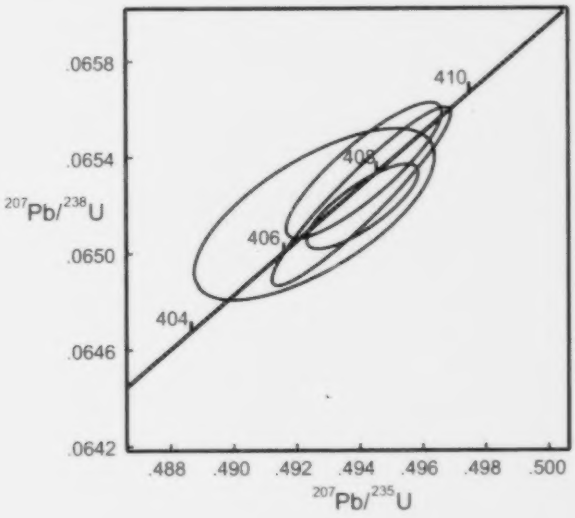

Figure 9. U–Pb concordia diagram for rhyolite from the Richardsville Member, Val d'Amour Formation.

Table 1. U–Pb isotopic data for rhyolite from the Richardsville Member, Val d'Amour Formation.

#	Wt (mg)	U (ppm)	Th/U	PbCom (pg)	^{207}Pb/ ^{204}Pb	^{206}Pb/ ^{238}U	^{207}Pb/ ^{235}U	^{206}Pb/^{238}U Age (ma)	^{207}Pb/^{235}U Age (Ma)	^{207}Pb/^{206}Pb Age (Ma)	Disc %
1	0.004	112	0.44	0.90	129.3	0.06516	0.4926	407.0±1.1	406.7±1.3	405.0±6.6	-0.5
2	0.002	186	0.60	0.25	354.9	0.06535	0.4942	408.1±0.9	407.7±0.9	405.9±3.0	-0.5
3	0.004	172	0.49	0.49	336.9	0.06520	0.4941	407.1±0.6	407.7±0.6	410.8±2.5	0.9
4	0.003	302	0.93	0.39	556.2	0.06524	0.4941	407.4±1.1	407.7±1.0	409.2±2.5	0.5

Notes: 1. All analyses are of single zircon crystals.

2. PbCom is total measured common Pb, assuming the isotopic composition of laboratory blank: ^{206}Pb/^{204}Pb = 18.221; ^{207}Pb/ ^{204}Pb = 15.612; ^{208}Pb/ ^{204}Pb = 39.360 (errors of 2%).

3. Th/U calculated from radiogenic ^{208}Pb/ ^{206}Pb and ^{207}Pb/ ^{206}Pb age assuming concordance.

4. Disc = per cent discordance for the given ^{207}Pb/^{206} Pb age.

5. Uranium decay constants are from Jaffrey et al. (1971).

CONTACT RELATIONSHIPS

The contact between the Val d'Amour Formation and underlying Indian Point Formation is exposed at two locations: south of Glencoe, and along Chaleur Bay at Dalhousie. South of Glencoe along Highway 275 (Fig. 1), pale grey, moderately to strongly calcareous, friable siltstone or fine-grained calcarenite of the Indian Point Formation is intruded by columnar-jointed diabase dykes and overlain by dark green amygdaloidal basalt of the Walker Brook Member (Wilson 2002). A conformable relationship cannot be demonstrated or disproved at this site.

At Dalhousie, sedimentary rocks of the Indian Point Formation underlie the basal "palagonite tuffs" of the Val d'Amour Formation; these beds were referred to as bed 0 by Howard (1926) and as zone 0 by Alcock (1935). Clarke (1909) did not discuss these rocks as part of the Dalhousie section proper, possibly because they are unfossiliferous and thus were of limited interest for his study. The Val d'Amour–Indian Point contact is now exposed beside the security fence of the Darlington electrical generating station (Fig. 3, 10a). Here, a conformable contact is evident between thin-bedded, calcareous mudstone and fine-grained sandstone of the Indian Point Formation, and overlying bedded mafic tuffs of the Walker Brook Member (Fig. 5b).

The foregoing conformable relationship is consistent with palynological data that indicate close similarities in age between the upper part of the Indian Point Formation and lower part of the Val d'Amour Formation (Wilson et al. 2004). In both cases, spore assemblages are assigned to the early Lochkovian *micrornatus-newportensis* zone (Richardson and McGregor 1986). Strata in Scotland containing a similar assemblage are considered late early to early late Lochkovian (Wellman 1993). As discussed previously, beds higher in the sequence, from upper parts of the Walker Brook and Thompson Brook members, are interpreted to lie within the upper Pragian through earliest Emsian *polygonalis-emsiensis* zone (Richardson and McGregor 1986), a zone that is consistent in age with the radioisotopic age obtained from the Richardsville rhyolite.

Upper contact relationships can be observed on the Restigouche River shore, northeast of the Beauvista Drive–Highway 134 intersection in Atholville. At this location, an angular discordance has been reported between felsic volcanic rocks of the Val d'Amour Formation and overlying sedimentary rocks of the Campbellton Formation (Gamba 1990; Gensel et al. 1997). That conclusion is supported here, although not the evidence previously used to reach it. For example, the steeply dipping discordant contact reported at this location by Gamba (1990) is at odds with the shallow, 20° to 25° dip seen near the base of the Campbellton Formation only 150 m farther along the shore. Moreover, the steep "contact" of Gamba (1990) is actually several exposures of a dark grey mudstone "veneer" that is present on some rhyolite outcrop surfaces. A nearby outcrop holds the key to interpreting these veneers: it features a rhyolite rockface (Fig. 10b)

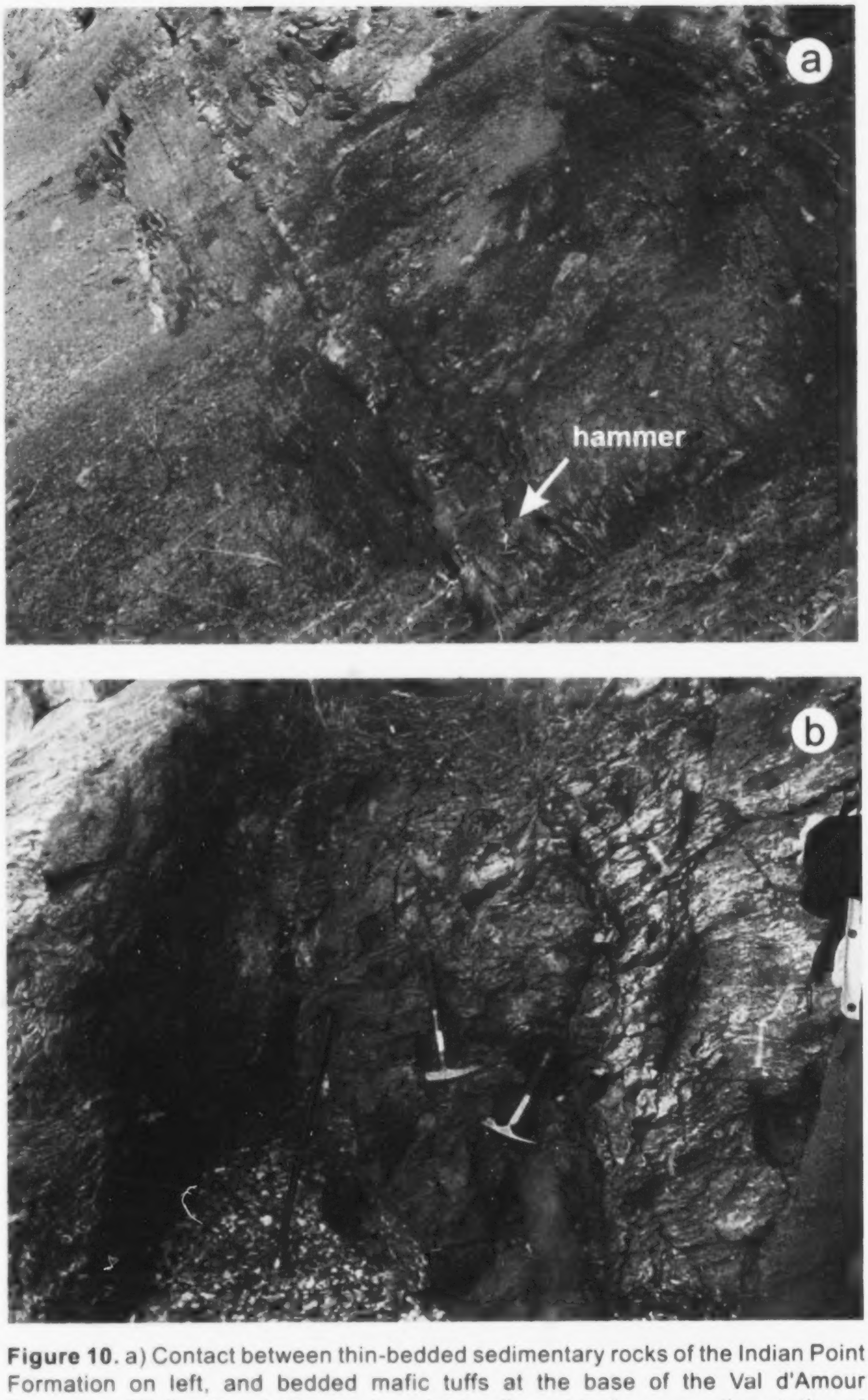

Figure 10. a) Contact between thin-bedded sedimentary rocks of the Indian Point Formation on left, and bedded mafic tuffs at the base of the Val d'Amour Formation (Walker Brook Member) on right, adjacent to the generating station at Dalhousie. Hammer lies on the contact and is 37 cm long. b) Dark grey mudstone (under hammers) of the Campbellton Formation, filling a fissure in pink-buff rhyolite (on right and left) of the Richardsville Member. Hammer in centre is 37 cm long.

indented with a deep cleft or fissure filled with the same dark grey mudstone. The veneers likely are remnants of the walls of similar fissures. The basal "breccia facies" described by Gamba (1990) does not resemble a basal conglomerate. Rather, it consists of angular rhyolite clasts in a mudstone matrix and is interpreted here as a regolith of loose rhyolite blocks that partially filled the fissures and subsequently were cemented by mudstone during sedimentation of the Campbellton Formation. The mudstone, incidentally, contains many plant fossils, a few shark spines, and rare shark teeth and fish plates. The interested reader is referred to Miller (1996) and Miller et al. (2003) and references therein for descriptions of vertebrate fauna in the Campbellton Formation.

An upper age of early Emsian for the Val d'Amour Formation has been established by using both palynological and U–Pb zircon dating methods. The presence of an unconformity is suggested by the age of the overlying Campbellton strata. Spores within the Campbellton Formation at Atholville correspond to the *annulatus-sextantii* zone of Richardson and McGregor (1986), and the presence of *Calyptosporites heisdorfensis* indicates an age of no older than late Emsian (McGregor *in* Gensel et al. 1997, p. 15). Farther east toward Point la Nim (Fig. 1), spore assemblages in the Campbellton Formation correlate best to those of late Emsian stages on the Gaspé Peninsula and in Europe (McGregor, *in* Gensel 1982, p. 652). Gamba (1990) also reported a spore-based late Emsian age for the lower part of the Campbellton Formation.

Across the Restigouche River on the Gaspé Peninsula, a late Emsian age was reported for the Lagarde Formation, which is equivalent to the lower part of the Campbellton Formation (Malo and Bourque 1993; Bourque et al. 1995). It therefore seems likely that a hiatus of perhaps several million years, corresponding to the middle Emsian, separates the Val d'Amour and Campbellton formations. It follows that the mudstone-filled fissure on the Atholville shore probably originated during extended subaerial exposure and weathering of the Val d'Amour rhyolite. An angular unconformity is also suggested by the differing bedding dips of the Campbellton Formation (15° to 30°) and the upper part of the Val d'Amour Formation (45° or greater). Furthermore, Dineley and Williams (1968, p. 243) state that the Lagarde Formation rests with "a marked discordance" on the underlying Lower Devonian volcanic rocks in the southern Gaspé Peninsula.

GEOCHEMISTRY

A total of 43 samples of volcanic rock from the Val d'Amour Formation were selected for whole-rock and trace-element analysis, including 16 samples from along and near the type section (Fig. 1). The analyses are presented in Table 2 (which appears at the end of this paper). The samples were analyzed at Activation Laboratories Limited in Ancaster, Ontario, by Lithium Metaborate/Tetraborate Fusion and Inductively Coupled Plasma–Mass Spectrometry, except for As, Au, Br, Co, Cr, Sb, Sc, and Se, which were determined by Instrumental Neutron Activation Analysis. Classification of volcanic rock types for this study was based on SiO_2 content (Table 2): < 52% for basalts, 52% to 62% for andesites, 62% to 68% for dacites, and > 68% for rhyolite. Table 2 provides analyses for two rhyolite samples. A third rhyolite sample was collected just below the contact with the Campbellton Formation within the extensive (hydrothermal?) alteration zone mentioned earlier but was discarded because of significant major-element mobility.

The Val d'Amour Formation comprises the New Brunswick equivalent of the Devonian "Ristigouche volcanics" (Burk 1964) or "Ristigouche member" of the Indian Point Formation (Bourque and Lachambre 1980) on the southern Gaspé Peninsula. As expected, the chemistry of Gaspé volcanic rocks (Laurent and Bélanger 1984; Dostal et al. 1993) resembles that of the Val d'Amour Formation. Both units contain an abundance of rocks with intermediate compositions, which distinguishes them from the dominantly bimodal suites that characterize Siluro–Devonian volcanic belts in most parts of the northern Appalachians (e.g. Dostal et al. 1989; Hon et al. 1992; Keppie and Dostal 1994; Seaman et al. 1999). When compared with the Val d'Amour Formation, however, the Restigouche basalts and andesites of Laurent and Bélanger (1984) typically contain a higher content of TiO_2, P_2O_5, Al_2O_3 and Zr, which explains why they are described as having many chemical features characteristic of an alkali rock series (Laurent and Bélanger 1984).

The lithogeochemistry of the Val d'Amour Formation shows a general progression from mafic to intermediate to felsic composition from bottom to top of the sequence. The trend is reflected in a contoured plot of Mg numbers, which measure the degree of magma evolution, and which tend to decrease (from less evolved to more evolved) from bottom to top in the stratigraphic section (Fig. 11). Yet the contour lines do not coincide precisely with the contact between the Walker Brook and Thompson Brook members, because the transition from mafic to intermediate composition is not smooth or continuous. Basalts and mafic tuffs in the lower part of the Walker Brook Member have high Mg numbers of 60 to 70 (Table 2), which is much more primitive than the 35 to 55 range reported for Devonian basalts in the southern Gaspé Peninsula (Dostal et al. 1993). Some comparatively evolved basalts with low Mg numbers also occur in the Walker Brook Member, especially west of the Squaw Cap Fault. Conversely, some basalts and andesites in the Thompson Brook Member have high Mg numbers (Fig. 11; Table 2). Farther east, in the Dalhousie area, some basalts in the Walker Brook and Thompson Brook members have low Mg numbers of 20 to 35 (Table 2). These values coincide with some of the highest TiO_2 abundances (2.3% to 3.0%) in the Val d'Amour Formation.

On a Nb/Y vs Zr/TiO_2 diagram, Val d'Amour volcanic rocks form a continuous series from the subalkaline basalt field through to the rhyolite/rhyodacite boundary (Fig. 12). Most samples are subalkaline, except for dacitic rocks of the Sugarloaf Porphyry, which plot well into the trachyandesite field because of their low Y content (Table 2). On a total alkali–MgO–FeO^t diagram (not shown) and on bivariate plots of FeO^t/MgO vs FeO^t and

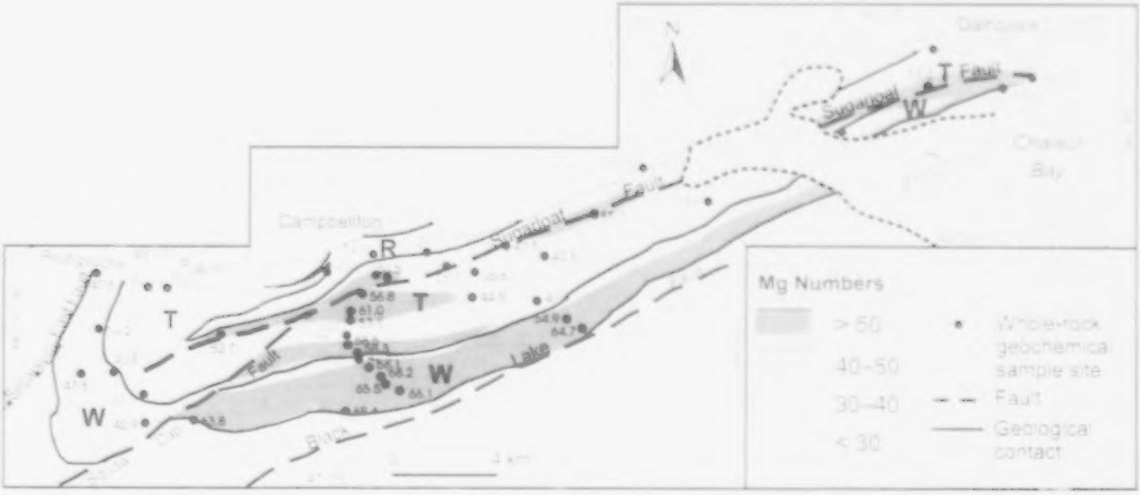
N
Dalhousie
Chaleur
Bay
Campbellton
Sugarloaf
Fault
R
T
W
Lake
Black
Mg Numbers
> 50
40–50
30–40
< 30
Whole-rock geochemical sample site
Fault
Geological contact
0
4 km

Figure 11. Contoured Mg numbers for analyzed samples of volcanic rock from the Val d'Amour Formation. Mg number = 100 x (mol. MgO) / (mol. MgO + mol. FeO). R = Richardsville Member. T = Thompson Brook Member. W = Walker Brook Member.

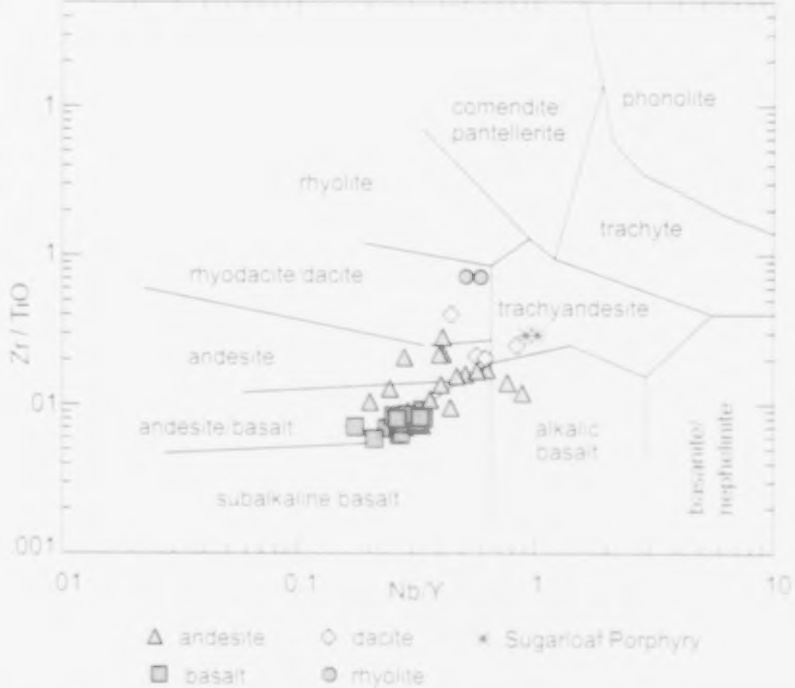

Figure 12. Nb/Y vs Zr/TiO discrimination diagram (from Winchester and Floyd 1977) for volcanic rocks of the Val d'Amour Formation.

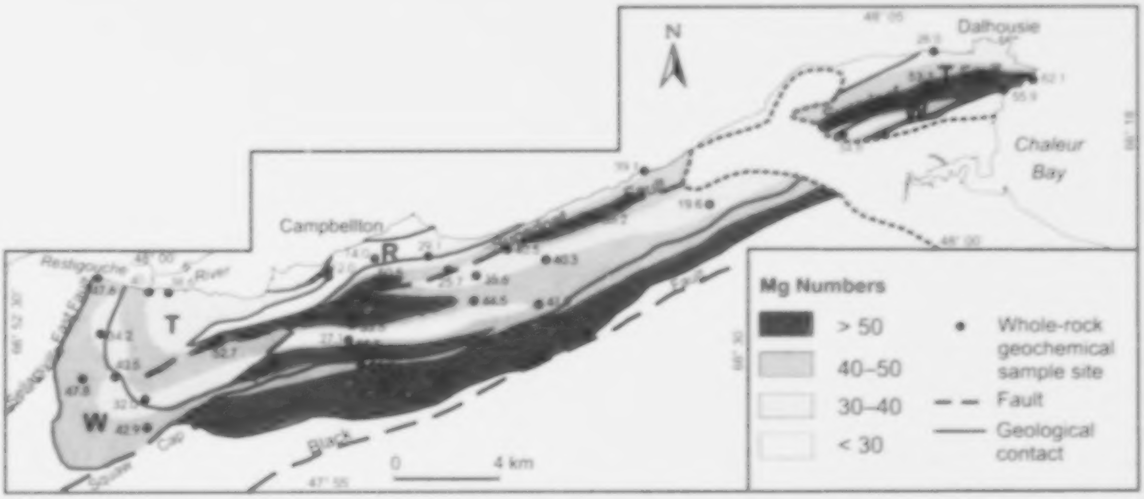
N
Dalhousie
Chaleur Bay
Campbellton
Restigouche River
R
T
W
48° 05'
48° 00'
47° 55'
Mg Numbers
> 50
40–50
30–40
< 30
Whole-rock geochemical sample site
Fault
Geological contact
0
4 km

Figure 11. Contoured Mg numbers for analyzed samples of volcanic rock from the Val d'Amour Formation. Mg number = 100 x (mol. MgO) / (mol. MgO + mol. FeO^{t}). R = Richardsville Member, T = Thompson Brook Member, W = Walker Brook Member.

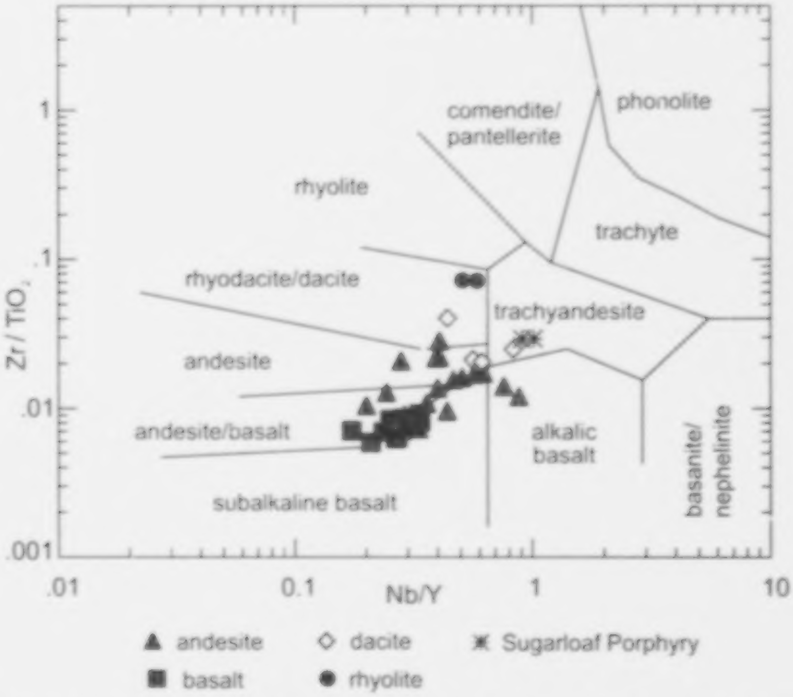

Figure 12. Nb/Y vs Zr/TiO$_2$ discrimination diagram (from Winchester and Floyd 1977) for volcanic rocks of the Val d'Amour Formation.

SiO_2 (Fig. 13a, b). Val d'Amour basalts and andesites straddle the calc-alkaline and tholeiitic fields. However, FeO^t/MgO correlates positively to FeO^t and TiO_2, displaying a typical tholeiitic differentiation trend (Fig. 13a, c). The negative correlation of FeO^t/MgO with Cr, Sr, and Al_2O_3 (Fig. 13d–f) is consistent with fractionation of olivine, possibly clinopyroxene (reported as a phenocryst phase by Howard 1926 and Dostal et al. 1993), and plagioclase.

Basalts and andesites from the Val d'Amour Formation have moderately sloping rare-earth-element (REE) profiles with flat heavy REE (HREE), enriched light REE (LREE), and an average La–Yb ratio of 5.7 in basalts and 8.8 in andesites (Fig. 14a–c). Basalt profiles show great uniformity, whereas andesites are more varied and display a greater range in absolute REE concentrations (Fig. 14a, b). Average REE profiles for dacites and rhyolites show slightly steeper slopes, although the profiles are broadly similar to those for basalts and andesites, especially in the HREE (Fig. 14c). The average La–Yb ratio for all dacites excluding the Sugarloaf Porphyry is 16.1, whereas the two rhyolite samples show a flatter profile. The rhyolites are slightly enriched in HREE (average La–Yb ratio is 12.9) when compared with dacites and also display a negative Eu anomaly (Fig. 14c). The Sugarloaf Porphyry exhibits a strongly fractionated REE profile (average La–Yb of 38.4) because of a depletion in HREE. It shows no negative Eu anomaly (Fig. 14c) and appears unrelated to any of the analyzed volcanic rocks in the Val d'Amour Formation. An extended trace-element spidergram (Fig. 14d) normalized to primitive mantle material indicates that all groups show significant enrichment in large-ion-lithophile elements (LILE) such as Cs, Rb, Ba, Th, U, and K, and have prominent negative Nb and Ti anomalies.

Enrichment in LILE and depletion in high-field-strength elements (HFSE) such as Nb and Ti are considered typical of subduction-related volcanic rocks (Fig. 15a, b). However, on diagrams commonly used to infer tectonic setting, plots of Val d'Amour basalts and andesites overlap the within-plate and volcanic-arc or calc-alkaline basalt fields (Fig. 16a, b). Furthermore, previous studies of Siluro–Devonian volcanic rocks in the northern Appalachians have shown that, in all cases, they were generated in a within-plate, continental, extensional environment (e.g. Laurent and Bélanger 1984; Dostal et al. 1989, 1993; Hon et al. 1992; Keppie and Dostal 1994; Seaman et al. 1999).

Although fractional crystallization explains some of the observed chemical variations within the Val d'Amour Formation (Fig. 13), it does not entirely account for differences in incompatible trace-element ratios between the mafic and intermediate rocks. For example, if andesites were simply related to the basalts by fractional crystallization, all samples would present a single line on Zr vs Y and Zr vs TiO_2 plots (Fig. 17a, b). Similarly, fractional crystallization does not significantly modify ratios of incompatible trace elements such as Th, Nb, and Y and therefore cannot explain the range of Th/Nb seen on a Nb/Y vs Th/Y plot (Fig. 17c). Enrichment in LILE and LREE, and depletion in HFSE, can be

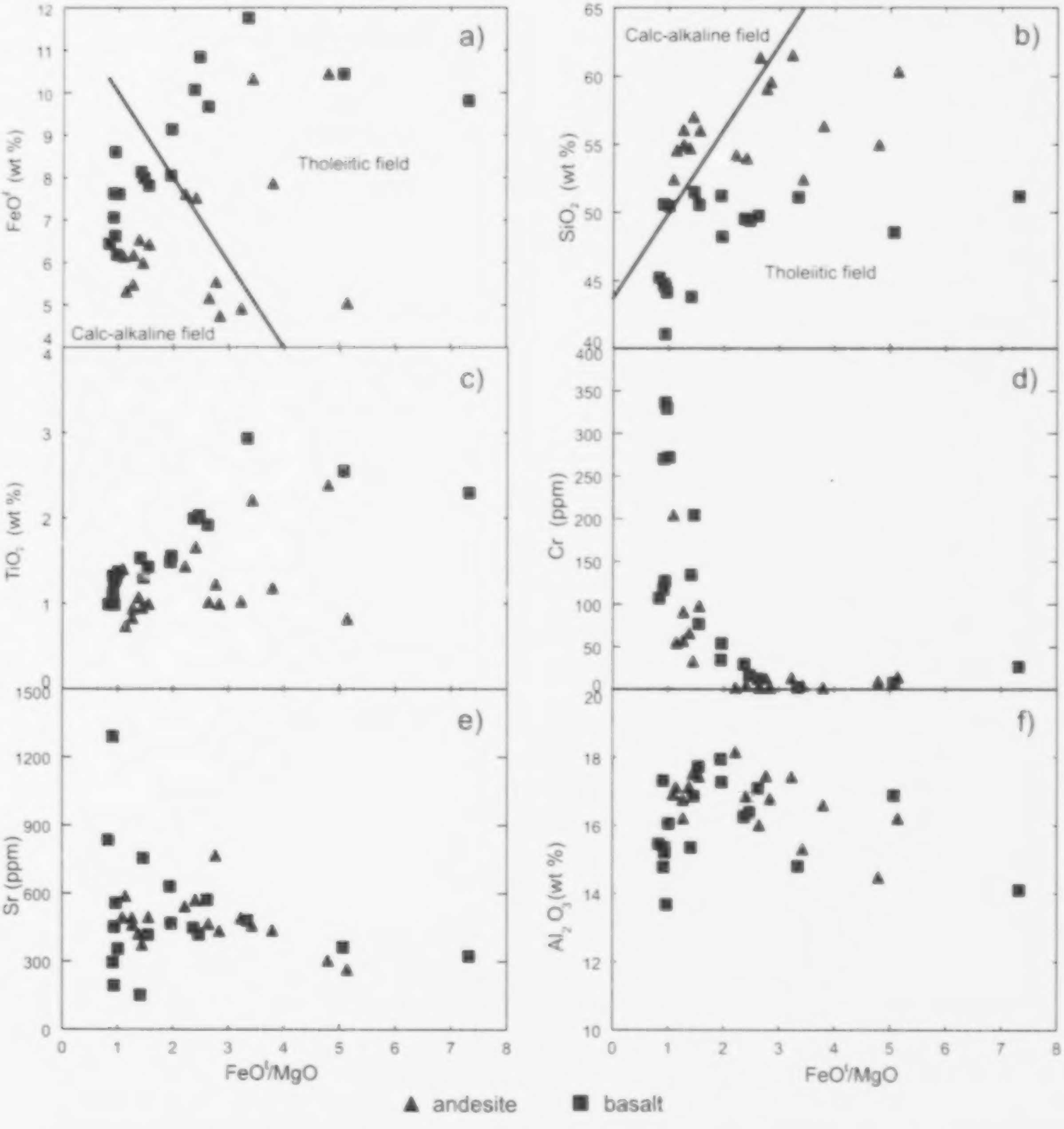

Figure 13. Bivariate diagram of FeO^t /MgO plotted against FeO^t , SiO$_2$, TiO$_2$, Cr, Sr, and Al$_2$O$_3$. Calc-alkaline and tholeiitic fields are from Miyashiro (1974).

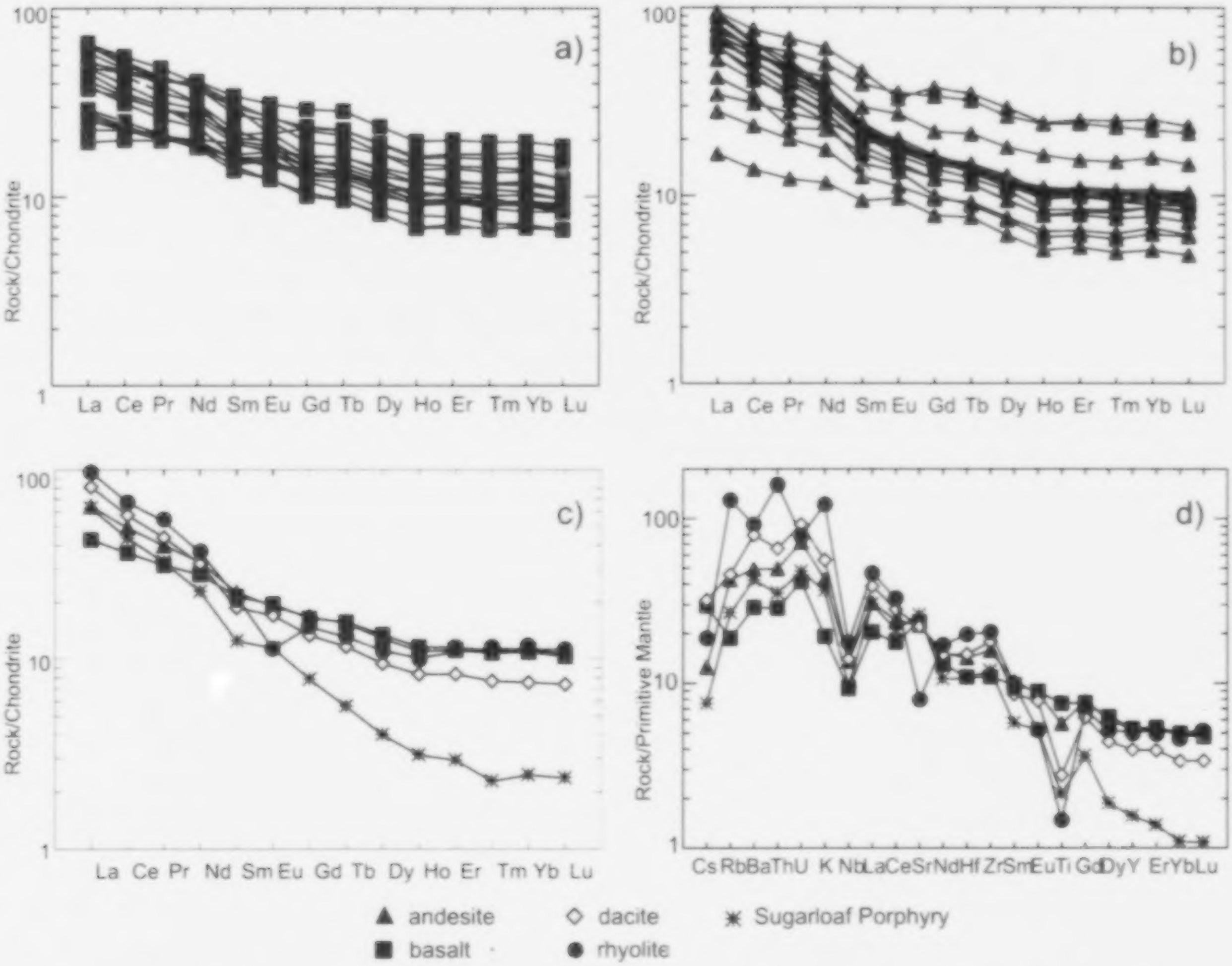

Figure 14. a) Chondrite-normalized rare-earth-element (REE) profiles for basalts of the Val d'Amour Formation. b) Chondrite-normalized REE profiles for andesites of the Val d'Amour Formation. c) Chondrite-normalized REE profiles of average Val d'Amour basalt, andesite, dacite and rhyolite, and the Sugarloaf Porphyry. Normalizing values are from Sun (1982). d) Primitive-mantle-normalized, extended-trace-element spidergram for volcanic rocks of the Val d'Amour Formation and Sugarloaf Porphyry. Normalizing values are from Sun and McDonough (1989).

associated either with a pre-existing subduction-related metasomatism of the mantle source, or with assimilation of upper crustal material. Both scenarios could account for La–Yb ratios that are high when compared with average ocean-island basalt (Fig. 15a), and Th–Yb ratios that are high when compared with mid-ocean-ridge basalt (Fig. 15b). However, we propose that the subduction–contamination model is most consistent with the trace-element data. The extensional tectonic setting suggests that magma ascent would have been relatively rapid, allowing less opportunity for crustal assimilation processes to occur. A subduction-metasomatized mantle also helps to account for the arc-type signatures present in the Val d'Amour Formation.

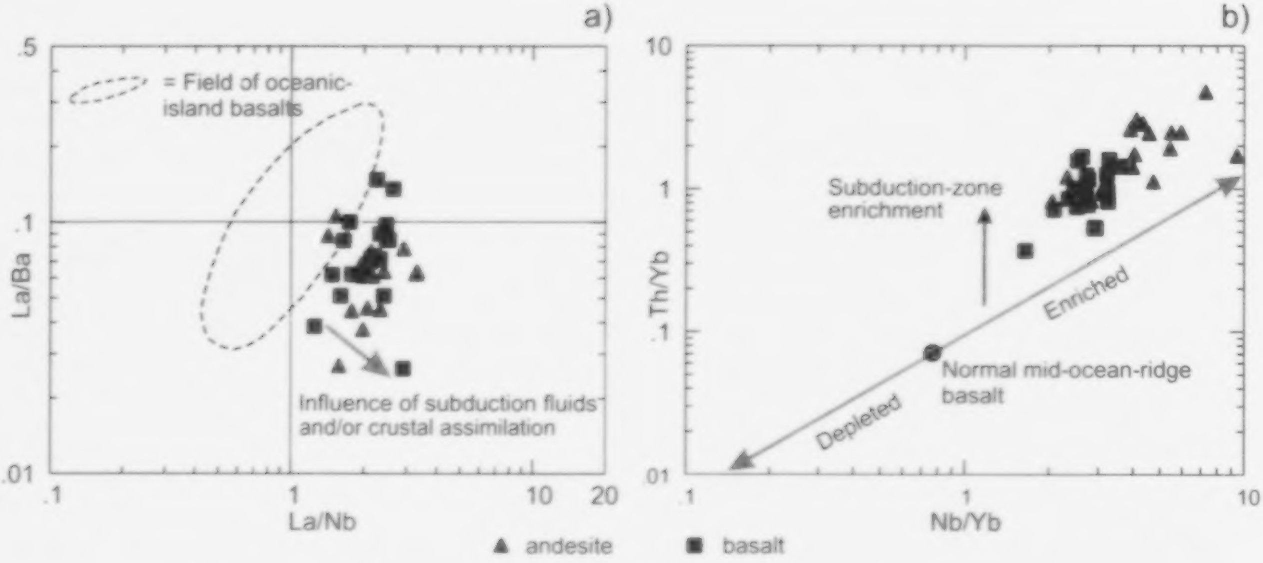

Figure 15. a) La/Ba vs La/Nb diagram for basalts and andesites of the Val d'Amour Formation, showing field of oceanic-island basalts and effects of lithospheric contamination and fluid derived from a subducted slab (after Fitton et al. 1991). b) Th/Yb vs Nb/Yb variation diagram for basalts and andesites of the Val d'Amour Formation. Blue line shows patterns of enrichment and depletion for an average normal mid-ocean-ridge basalt mantle. Black vector indicates variations caused by subduction–zone enrichment (Pearce et al. 1995).

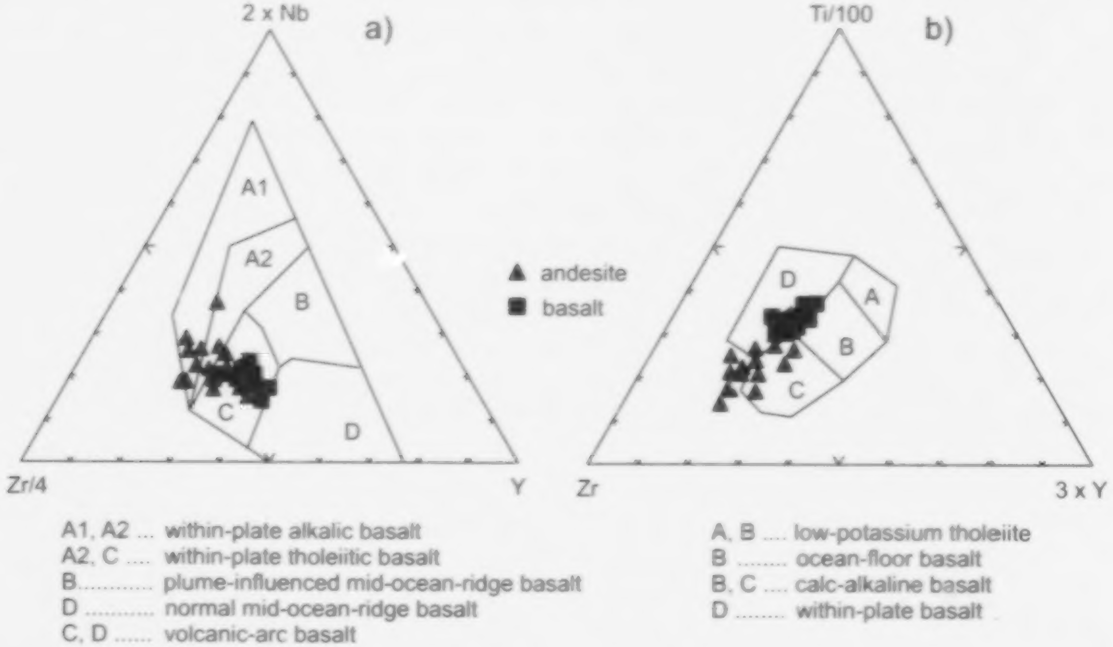

Figure 16. a) Zr–Nb–Y tectonic discrimination diagram for basalts and andesites of the Val d'Amour Formation. Fields are from Meschede (1986). b) Zr–Ti–Y tectonic discrimination diagram for basalts and andesites of the Val d'Amour Formation. Fields are from Pearce and Cann (1973).

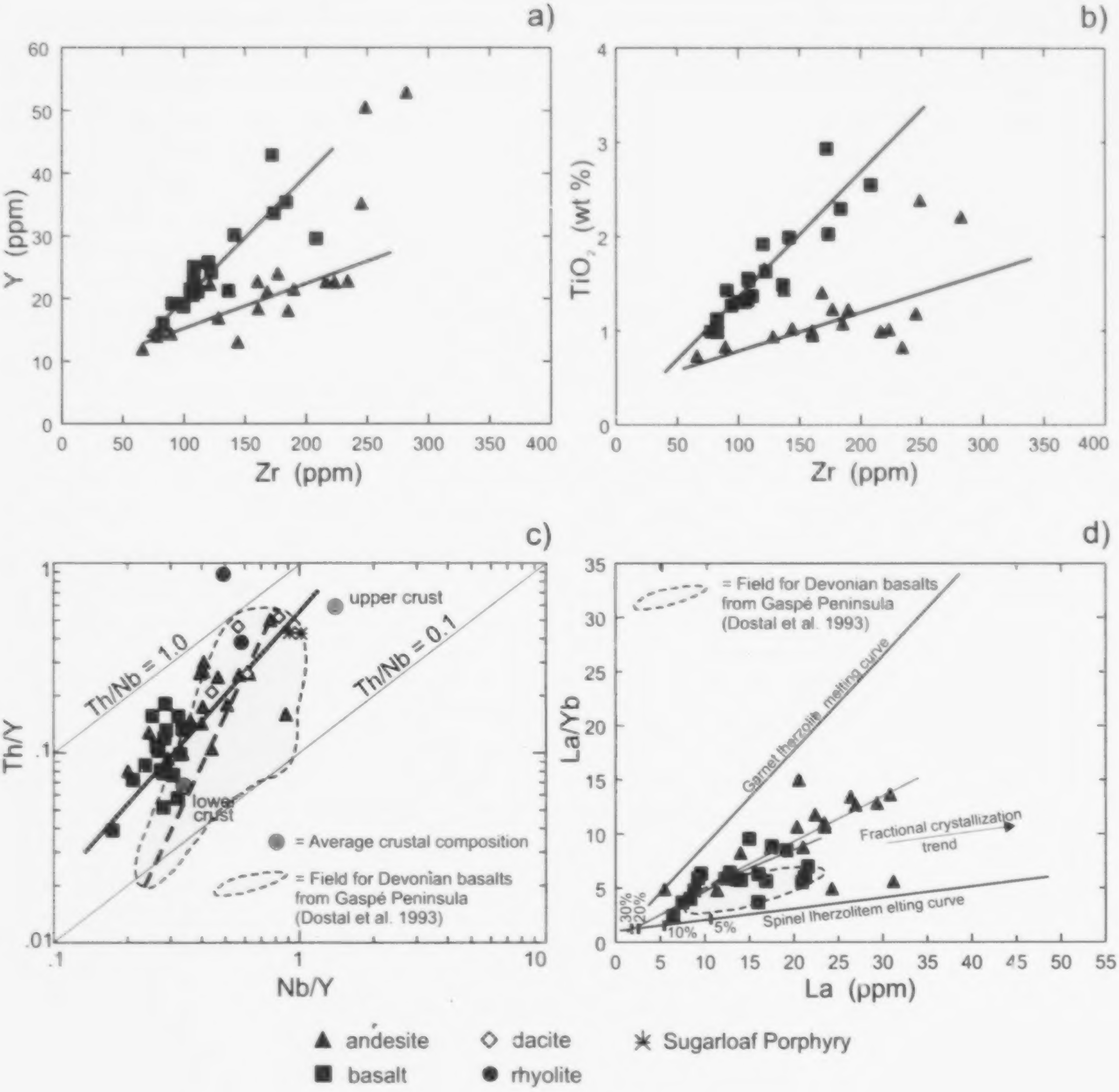

Figure 17. a) Zr vs Y bivariate plots for basalts and andesites of the Val d'Amour Formation. b) Zr vs TiO$_2$ bivariate plots for basalts and andesites of the Val d'Amour Formation. c) Nb/Y vs Th/Y variation diagram for volcanic rocks of the Val d'Amour Formation, compared with the field for Devonian basalts from the southern Gaspé Peninsula (Dostal et al. 1993). Average upper and lower crustal compositions are from Taylor and McLennan (1985). d) La vs La/Yb diagram for basalts and andesites of the Val d'Amour Formation, compared with the field for Devonian basalts from the southern Gaspé Peninsula (Dostal et al. 1993). Melting curves are from Dostal et al. (1993); numbers on the spinel lherzolite melting curve indicate per cent partial melting.

Dostal et al. (1993), in their petrogenetic study of the "Ristigouche" volcanic rocks, proposed a mechanism that involved mixing basaltic magma either with upper crustal rocks (that possess high Th–Y and Th–Nb ratios) or with melts that compositionally resemble upper continental crust. Yet Val d'Amour basalts and andesites display a much smaller range of Th/Nb than do the Ristigouche mafic rocks, which suggests that fractionation was more of a factor in the former than in the latter (Fig. 17c). Despite the evidence of contrasting crustal processes involved in petrogenesis of the Val d'Amour and Ristigouche volcanic rocks, both units evidently were generated by comparable degrees of partial melting of a common source. The La/Yb vs La diagram (Fig. 17d) illustrates that andesites and basalts from the Val d'Amour Formation overlap the field for Devonian basalts from the southern Gaspé Peninsula (Dostal et al. 1993). Both suites were formed by 20% to 30% partial melting of spinel peridotite; Dostal et al. (1993) proposed that this melting occurred at a depth of around 60 km.

CONCLUSIONS

The Val d'Amour Formation encompasses all Lower Devonian volcanic and interbedded sedimentary rocks in the Campbellton–Dalhousie area. The designated type section can be seen for 7.5 km along Highway 270 from the village of Val d'Amour through to Beauvista Drive in Atholville; the section coincides with the thickest (almost 6000 m) accumulation of volcanic rocks.

The Val d'Amour Formation is divided into three members that roughly correspond to an upward transition from mafic to intermediate to felsic composition. In ascending order, they are the Walker Brook, Thompson Brook, and Richardsville members. The Walker Brook Member comprises basaltic and minor andesitic flows; basaltic ash and lapilli tuff; and local interbedded, calcareous, fossiliferous sedimentary rocks, especially at the easternmost (exposed) limit of the unit along the shore of Eel Bay. This Eel Bay section of the Walker Brook Member coincides with Clarke's (1909) original Dalhousie "Formation" section. The Thompson Brook Member consists mainly of andesitic to dacitic effusive rocks, andesitic lithic tuff, tuff breccia, associated fine-grained to very coarse-grained volcaniclastic rocks, and minor shallow-water clastic sedimentary rocks. The Richardsville Member comprises pink to maroon, typically flow-layered, porphyritic rhyolite, and minor volcanic boulder conglomerate.

Richardsville rhyolite has yielded a U–Pb zircon age of 407.4 ± 0.8 Ma, which establishes an upper age limit for the Val d'Amour Formation and fits well with the ages of spores from just below the rhyolite and from the overlying Campbellton Formation. Palynological data, bedding attitudes, and contact relationships indicate that a middle Emsian hiatus separates the Val d'Amour Formation and the overlying, late Emsian Campbellton Formation. On the other hand, a conformable relationship between the Val d'Amour Formation and underlying sedimentary rocks of the Indian Point Formation

(Chaleurs Group) is supported by similar spore assemblages near the bottom of the former and the top of the latter unit.

Sedimentological, palynological, and volcanological evidence indicates that generally subaerial environments dominated during deposition of the Val d'Amour Formation, except in the eastern part of the area near Dalhousie, where marine conditions prevailed. For example, sedimentary rocks are scarce in the unit as a whole but are comparatively abundant on the coast at Eel Bay where fossiliferous, calcareous, shallow marine deposits make up about 30% of Clarke's (1909) Dalhousie section (Fig. 3).

Similarly, volcanic rocks typical of subaqueous emplacement have been observed only at Bellevue Cove (pillow basalts and related hyaloclastites in the Walker Brook Member) and Inch Arran Point (hyaloclastites in the Thompson Brook Member; Fig. 3). In most of the study area, the transition to subaerial volcanism from marine sedimentation of the Indian Point Formation must have been abrupt, as pillow basalts and hyaloclastites are absent from the Walker Brook Member west of Dalhousie. It is possible, however, that mafic ash and lapilli tuffs of the Walker Brook Member at Val d'Amour and Dalhousie are shallow marine deposits. They resemble the products of phreatomagmatic eruptions (e.g. maars), which typically build well bedded accumulations of hydroclastic debris around a volcanic vent within a lake, coastal zone, marsh, or area of abundant groundwater.

Volcanic rocks in the Val d'Amour Formation cover the entire compositional spectrum, featuring an abundance of intermediate rocks, especially andesites. They display characteristics of both calc-alkaline and tholeiitic series, although the basalts define a tholeiitic differentiation trend and are best described as continental tholeiites. Most volcanic rocks are feldspar-phyric, and the mafic rocks usually contain phenocrysts of olivine and/or pyroxene.

With rare exceptions, volcanic rocks are subalkaline, and mafic rocks fall in the within-plate field on diagrams used to infer tectonic setting. However, patterns of LILE and LREE enrichment, and negative Nb and Ti anomalies on trace-element spidergrams, are typical of subduction-related volcanic rocks. Although fractional crystallization can explain some of the chemical variation within and between mafic and intermediate suites, it cannot account for differences in HFSE ratios. Trace-element systematics and crude petrogenetic modelling suggest derivation by 20% to 30% partial melting of a spinel peridotite mantle source that was variably enriched by prior subduction events. The effects of subduction-related enrichment in LILE and LREE cannot be distinguished from those caused by enrichments associated with assimilation of upper crust. Nonetheless, the former scenario is believed to be more consistent with the interpreted extensional tectonic setting (e.g. Dostal et al. 1989, 1993), which implies rapid magma ascent and minimal interaction with upper crust.

Table 2. Whole-rock analyses of volcanic rocks from the Val d'Amour Formation.

Sample	**f-1011**	**f-1047**	**f-1071**	**f-1076**	**f-1117**	**g-59**	**g-225**	**g-236**	**g-407**
Rock Type	basalt	gabbro	basalt	basalt	basalt	mafic tuff	basalt	basalt	basalt
Unit	W	W	W	W	W	W	T	W	W
SiO_2	48.22	49.54	49.76	51.21	50.45	45.22	50.55	44.78	41.08
Al_2O_3	17.27	16.25	17.09	17.94	16.05	15.46	17.72	14.78	15.20
Fe_2O_3	10.15	11.19	10.74	8.94	8.46	7.15	8.68	8.47	9.55
MnO	0.21	0.19	0.10	0.07	0.14	0.09	0.18	0.14	0.10
MgO	4.65	4.25	3.69	4.13	7.52	7.73	5.04	8.32	9.13
CaO	9.54	7.85	8.57	4.81	7.81	8.26	9.53	5.97	9.43
Na_2O	3.28	3.78	3.78	4.64	2.73	1.40	3.42	4.73	1.89
K_2O	0.22	1.15	0.76	0.69	0.55	0.85	0.55	0.20	0.10
TiO_2	1.56	1.99	1.92	1.49	1.37	0.99	1.43	1.32	1.27
P_2O_5	0.23	0.32	0.25	0.26	0.22	0.12	0.17	0.19	0.15
LOI	3.50	2.00	2.00	4.66	4.32	13.08	3.11	11.18	11.51
Mg #	47.6	42.9	40.5	47.8	63.8	68.2	53.5	66.1	65.4
Cr	54	30	13	35	272	107	77	270	336
Ni	8	12	1	18	138	89	40	141	140
Co	34.0	34.0	28.0	19.0	40.0	34.4	30.2	37.2	42.0
Sc	30.6	28.2	29.2	23.5	27.2	23.2	26.6	23.4	27.7
V	244	258	318	219	203	162	204	168	180
Cu	40	23	19	22	51	53	30	46	51
Pb	2	11	2	3	2	10	2	10	7
Zn	91	85	81	76	61	58	71	62	58
Ag	0.4	0.4	0.2	0.4	0.2	0.4	0.7	0.7	0.2
S	0.010	0.003	0.002	0.397	0.011	0.016	0.009	0.040	0.001
As	3.3	3.1	3.5	2.0	2.6	2.9	2.1	2.4	0.3
Sb	0.2	0.1	0.2	0.2	0.2	0.1	0.1	0.2	0.1
Tl	0.03	0.03	0.03	0.03	0.03	0.06	0.03	0.03	0.03
Au	16.0	1.0	1.0	11.0	7.0	3.0	4.0	3.0	1.0
W	0.3	0.3	0.3	0.3	0.3	0.3	0.3	0.3	0.3
Mo	1.0	1.0	1.0	1.0	1.0	1.0	1.0	1.0	1.0
Sn	1.4	1.1	2.4	0.5	0.5	0.5	0.5	0.5	1.1
Cs	0.1	0.2	0.2	0.8	0.2	0.1	0.1	0.5	0.4
Ga	20	23	22	20	18	15	20	15	14
Rb	1	22	16	15	9	12	10	5	2
Ba	139	254	224	204	210	188	164	170	104
Sr	468	447	571	631	355	834	417	296	452
Nb	5.5	8.5	6.9	7.1	6.4	4.0	5.2	5.7	5.4
Ta	0.39	0.58	0.44	0.47	0.46	0.23	0.34	0.35	0.27
Y	23.3	30.1	25.8	21.2	21.1	14.0	19.2	20.5	19.2
Zr	108	142	120	136	111	78	91	107	94
Hf	3.0	3.7	3.1	3.5	2.6	2.3	2.8	3.0	2.4
Th	2.01	3.60	2.64	2.85	1.61	2.53	1.56	1.61	0.99
U	0.69	1.22	0.91	1.00	0.50	0.88	0.76	0.48	0.38
La	13.56	21.58	16.01	17.52	12.80	9.60	8.38	12.28	8.80
Ce	29.49	45.12	34.02	37.89	27.13	21.77	19.64	29.06	19.93
Pr	3.79	5.62	4.17	4.66	3.39	2.79	2.61	3.79	2.76
Nd	17.24	24.03	18.42	19.91	14.77	12.12	12.06	16.37	11.60
Sm	4.17	5.62	4.32	4.05	3.40	2.96	3.25	3.95	3.03
Eu	1.54	1.94	1.69	1.43	1.34	0.95	1.19	1.34	1.19
Gd	4.17	5.42	4.57	3.95	3.67	2.89	3.72	3.98	3.45
Tb	0.75	0.93	0.81	0.68	0.67	0.48	0.65	0.67	0.59
Dy	4.46	5.80	4.90	4.06	3.81	2.82	3.85	3.89	3.49
Ho	0.92	1.15	1.00	0.82	0.82	0.52	0.73	0.74	0.72
Er	2.55	3.27	2.74	2.27	2.25	1.55	2.12	2.19	2.12
Tm	0.39	0.51	0.41	0.32	0.35	0.24	0.33	0.33	0.31
Yb	2.34	3.08	2.54	1.98	1.99	1.51	2.09	2.09	1.84
Lu	0.33	0.42	0.37	0.28	0.29	0.23	0.31	0.31	0.28

Major oxides in wt %. All trace elements in ppm except S (%) and Au (ppb).

Mg # = 100 x (mol. MgO)/(mol. MgO + mol. FeO^{1}).

W = Walker Brook Member. T = Thompson Brook Member.

Table 2 *(cont'd)*. Whole-rock analyses of volcanic rocks from the Val d'Amour Formation.

Sample	**g-512**	**g-513**	**h-173**	**h-174**	**h-03-68**	**B/1-823**	**B/1-826**	**B/1-843**	**B/2-811**	**avg. basalt**
Rock Type	mafic tuff	basalt	basalt	basalt	basalt	mafic tuff	basalt	basalt	basalt	n=18
Unit	W	W	W	W	T	W	W	T	T	
SiO_2	44.55	50.59	51.49	44.15	49.41	43.80	51.12	48.54	51.19	48.09
Al_2O_3	15.35	17.31	16.85	13.68	16.39	15.35	14.80	16.88	14.10	16.03
Fe_2O_3	7.35	7.84	8.88	6.87	12.04	9.03	13.07	11.60	10.90	9.50
MnO	0.14	0.13	0.13	0.17	0.20	0.13	0.22	0.11	0.12	0.14
MgO	7.05	7.73	5.46	6.37	4.39	5.77	3.52	2.06	1.34	5.45
CaO	7.89	5.75	9.87	11.09	8.34	3.04	8.05	7.31	9.01	7.90
Na_2O	4.53	4.44	3.68	4.91	3.48	6.51	3.94	3.68	2.20	3.72
K_2O	0.35	0.95	0.41	0.20	1.00	0.10	0.54	0.90	0.93	0.58
TiO_2	0.99	1.12	1.30	1.31	2.03	1.53	2.94	2.55	2.30	1.63
P_2O_5	0.12	0.16	0.22	0.19	0.31	0.18	0.43	0.44	0.30	0.24
LOI	11.58	4.24	2.13	11.38	2.80	14.74	1.82	5.78	7.80	6.54
Mg #	65.5	66.1	54.9	64.7	41.9	55.9	34.8	26.0	19.6	53.2
Cr	127	117	204	329	17	134	3	8	27	120
Ni	72	53	111	172	18	49	3	16	8	60
Co	30.6	33.0	36.8	36.3	35.5	32.1	24.3	24.9	21.4	31.9
Sc	21.3	27.0	23.4	23.4	30.3	24.7	33.4	20.8	26.4	26.1
V	184	182	201	150	265	192	220	201	289	213
Cu	46	64	65	51	18	55	22	35	24	39
Pb	4	14	4	2	15	5	12	17	14	7
Zn	54	54	72	59	104	68	112	71	83	73
Ag	0.6	0.2	0.8	0.8	0.9	0.7	1.1	1.3	1.0	0.6
S	0.009	0.001	0.023	0.021	0.014	0.052	0.027	0.006	0.011	0.036
As	3.0	2.7	2.2	1.2	1.8	5.2	3.7	1.3	5.0	2.7
Sb	0.1	0.1	0.4	0.1	0.1	0.1	0.1	0.1	1.8	0.2
Tl	0.06	0.20	0.03	0.03	0.03	0.16	0.18	0.12	0.19	0.07
Au	1.0	1.0	4.0	1.0	1.0	1.0	1.0	1.0	2.0	3.3
W	0.3	0.3	0.3	0.3	0.3	0.3	0.3	0.3	0.6	0.3
Mo	1.0	1.0	1.0	1.0	1.0	1.0	1.0	1.0	1.0	1.0
Sn	0.5	0.5	0.5	0.5	0.5	0.5	1.7	1.6	5.2	1.1
Cs	1.6	0.9	1.0	0.2	0.1	3.7	1.0	0.2	5.8	0.9
Ga	17	15	19	13	24	16	23	22	23	19
Rb	6	25	7	3	21	2	8	18	30	12
Ba	103	573	142	194	288	104	257	168	142	202
Sr	195	1290	755	557	419	152	480	363	324	500
Nb	4.0	5.2	7.3	6.0	9.6	4.4	9.0	9.7	9.3	6.6
Ta	0.23	0.29	0.43	0.38	0.60	0.23	0.59	0.63	0.64	0.42
Y	15.8	16.1	21.4	18.7	33.6	25.1	42.9	29.6	35.4	24.1
Zr	83	82	105	100	174	108	172	209	184	122
Hf	2.3	2.2	3.0	2.7	4.8	3.1	5.2	5.3	5.4	3.4
Th	2.47	2.52	2.84	1.08	4.42	0.98	3.09	2.91	3.83	2.42
U	0.96	1.03	0.87	0.49	1.53	0.34	1.15	0.92	1.51	0.87
La	9.26	14.98	19.17	7.47	21.22	6.43	15.99	16.87	20.92	14.05
Ce	20.50	30.73	41.39	19.54	48.11	17.30	39.38	40.64	43.26	31.38
Pr	2.69	3.95	5.14	2.75	6.26	2.58	5.30	5.49	5.50	4.07
Nd	11.50	15.05	19.83	12.54	25.27	12.80	25.82	23.94	24.15	17.63
Sm	2.81	3.28	4.64	3.26	6.40	3.88	6.98	6.10	6.15	4.35
Eu	0.96	1.25	1.47	1.12	2.02	1.37	2.40	2.05	1.67	1.50
Gd	2.79	3.35	4.40	3.61	6.50	4.50	8.03	6.22	6.38	4.53
Tb	0.48	0.53	0.71	0.63	1.13	0.82	1.42	1.05	1.12	0.78
Dy	2.78	3.03	4.24	3.69	6.54	4.78	8.12	5.88	6.61	4.60
Ho	0.53	0.62	0.77	0.69	1.23	0.92	1.52	1.07	1.26	0.89
Er	1.60	1.77	2.36	2.08	3.66	2.67	4.50	3.19	3.79	2.59
Tm	0.24	0.26	0.36	0.32	0.56	0.41	0.69	0.48	0.59	0.39
Yb	1.57	1.57	2.26	2.03	3.54	2.65	4.33	2.99	3.77	2.45
Lu	0.23	0.23	0.33	0.30	0.52	0.37	0.63	0.43	0.54	0.36

Major oxides in wt %. All trace elements in ppm except S (%) and Au (ppb).

Mg # = 100 x (mol. MgO)/(mol. MgO + mol. FeO^t).

W = Walker Brook Member. T = Thompson Brook Member.

Table 2 *(cont'd)*. Whole-rock analyses of volcanic rocks from the Val d'Amour Formation.

Sample	**f-1015**	**f-1021**	**f-1066**	**f-03-50**	**g-108**	**g-115**	**g-190**	**g-224**	**g-226**
Rock Type	andesite	andesite	andesite	andesite	andesite	andesite	andesite	and. tuff	andesite
Unit	T	T	T	W	T	T	T	T	T
SiO_2	61.36	59.57	56.34	52.42	60.33	54.21	54.71	54.54	54.97
Al_2O_3	16.01	16.78	16.60	15.31	16.20	18.15	17.13	17.12	14.48
Fe_2O_3	5.73	5.27	8.73	11.47	5.60	8.46	7.26	5.90	11.61
MnO	0.11	0.09	0.16	0.20	0.08	0.16	0.15	0.08	0.20
MgO	1.95	1.67	2.07	3.01	0.98	3.43	4.74	4.65	2.18
CaO	4.34	4.94	5.55	4.06	4.54	6.93	5.28	6.47	6.45
Na_2O	4.93	4.85	4.50	5.09	3.46	4.64	4.77	3.37	4.23
K_2O	1.42	1.74	1.21	1.63	1.93	0.92	1.04	0.96	1.31
TiO_2	1.02	1.00	1.18	2.21	0.82	1.44	1.08	0.73	2.39
P_2O_5	0.29	0.26	0.60	0.52	0.21	0.26	0.27	0.09	0.40
LOI	2.46	2.42	1.86	4.35	5.87	1.15	3.89	5.72	1.53
Mg #	40.3	38.6	32.0	34.2	25.7	44.5	56.4	61.0	27.1
Cr	3	3	3	5	15	3	66	55	10
Ni	5	9	1	15	11	1	47	67	1
Co	16.0	16.0	16.0	22.3	12.0	23.0	22.2	23.0	21.0
Sc	14.0	13.3	12.2	25.8	10.8	19.0	14.2	13.8	30.1
V	115	98	83	151	77	180	121	107	168
Cu	49	21	15	62	21	42	38	36	30
Pb	2	10	10	9	9	14	11	2	9
Zn	64	65	108	139	66	73	72	52	93
Ag	1.1	1.0	0.9	1.0	0.2	0.2	0.9	0.4	0.2
S	0.007	0.004	0.006	0.016	0.001	0.001	0.007	0.008	0.001
As	2.4	8.6	4.2	2.6	4.2	2.3	2.1	1.4	2.2
Sb	0.4	0.4	0.4	0.1	0.4	0.1	0.1	0.1	0.1
Tl	0.12	0.07	0.35	0.26	0.24	0.03	0.06	0.07	0.06
Au	6.0	1.0	1.0	1.0	4.0	1.0	4.0	1.0	5.0
W	0.3	0.7	0.3	0.3	0.5	0.3	0.3	0.3	0.3
Mo	1.0	1.0	1.0	1.0	1.0	1.0	1.0	1.0	1.0
Sn	1.7	1.7	9.9	3.0	2.1	1.1	1.1	0.5	1.9
Cs	0.4	0.4	1.1	0.2	0.4	0.1	0.1	0.4	0.2
Ga	23	18	25	23	18	19	19	17	22
Rb	34	29	34	35	43	15	15	15	27
Ba	342	470	275	490	484	281	597	204	255
Sr	466	434	436	458	266	543	420	588	305
Nb	9.2	8.9	9.9	12.9	9.3	9.4	11.3	3.5	10.1
Ta	0.82	0.77	1.94	0.97	0.71	0.52	0.84	0.20	0.65
Y	22.6	22.7	35.2	52.9	22.8	21.3	18.1	11.9	50.5
Zr	223	216	245	282	234	137	185	66	249
Hf	5.0	4.8	5.4	7.2	5.4	3.3	4.5	2.1	6.1
Th	6.10	5.96	2.89	6.77	6.88	2.24	4.72	1.12	4.05
U	2.05	1.91	1.30	2.55	2.17	0.89	1.63	0.63	1.46
La	26.93	29.32	21.13	31.19	30.82	17.41	22.38	5.49	24.30
Ce	51.48	55.99	47.85	66.18	56.83	35.58	44.77	11.91	54.63
Pr	5.65	6.26	6.19	8.93	6.80	4.52	5.14	1.59	7.57
Nd	21.76	23.55	26.84	38.41	23.76	17.33	18.93	7.35	31.76
Sm	4.40	4.77	6.00	9.33	4.56	3.88	4.24	1.91	7.96
Eu	1.35	1.39	2.09	2.53	1.35	1.49	1.25	0.75	2.71
Gd	4.18	4.34	6.03	10.36	4.48	4.23	3.83	2.16	9.33
Tb	0.70	0.74	1.06	1.73	0.69	0.66	0.62	0.38	1.60
Dy	4.02	4.17	6.21	10.06	3.94	3.82	3.66	2.10	9.09
Ho	0.82	0.85	1.26	1.88	0.79	0.77	0.65	0.40	1.85
Er	2.22	2.42	3.47	5.65	2.40	2.32	1.90	1.19	5.44
Tm	0.36	0.35	0.53	0.88	0.36	0.33	0.29	0.18	0.81
Yb	2.13	2.28	3.50	5.57	2.26	1.99	1.90	1.13	4.93
Lu	0.31	0.33	0.50	0.79	0.34	0.31	0.27	0.16	0.73

Major oxides in wt %. All trace elements in ppm except S (%) and Au (ppb).

Mg # = 100 x (mol. MgO)/(mol. MgO + mol. FeO^t).

and. tuff = andesitic tuff. W = Walker Brook Member. T = Thompson Brook Member.

Table 2 *(cont'd)*. Whole-rock analyses of volcanic rocks from the Val d'Amour Formation.

Sample	**g-228**	**g-231**	**g-232**	**g-03-54**	**B/1-552**	**B/1-858**	**B/2-762**	**B/2-794**	**avg. andesite**
Rock Type	and. tuff	and. tuff	andesite	andesite	andesite	andesite	andesite	andesite	n=17
Unit	T	T	W	T	W	T	T	T	
SiO_2	56.06	54.95	53.98	61.53	52.42	56.02	59.06	57.01	56.44
Al_2O_3	16.75	16.21	16.86	17.42	16.91	17.43	17.45	17.51	16.72
Fe_2O_3	6.09	6.86	8.35	5.45	6.82	7.14	6.16	6.66	7.27
MnO	0.10	0.11	0.12	0.07	0.12	0.11	0.10	0.05	0.12
MgO	4.34	4.85	3.12	1.52	5.63	4.12	2.00	4.14	3.20
CaO	5.63	6.77	5.89	4.57	8.01	7.40	4.95	5.31	5.71
Na_2O	3.65	3.21	5.65	4.58	3.96	3.85	5.18	3.39	4.31
K_2O	1.39	1.02	0.55	1.66	1.01	1.15	1.88	0.96	1.28
TiO_2	0.83	0.94	1.66	1.02	1.41	1.00	1.23	0.95	1.23
P_2O_5	0.13	0.19	0.22	0.16	0.35	0.26	0.28	0.23	0.28
LOI	5.22	4.91	3.92	2.12	3.04	1.96	1.99	4.12	3.33
Mg #	58.5	58.3	42.5	35.6	62.1	53.3	39.1	55.2	46.6
Cr	57	91	5	14	204	98	13	33	40
Ni	51	56	5	27	130	58	16	39	32
Co	22.4	20.0	17.2	13.5	40.0	21.8	16.0	17.8	20.0
Sc	14.5	16.5	18.5	13.4	24.0	15.5	13.2	15.3	16.7
V	101	123	191	131	160	123	116	114	127
Cu	45	38	14	46	34	27	25	27	34
Pb	12	11	8	14	13	16	12	18	10
Zn	61	58	75	53	72	66	74	64	74
Ag	0.5	0.7	0.6	0.7	0.2	0.9	1.0	0.9	0.7
S	0.012	0.007	0.006	0.017	0.001	0.006	0.007	0.003	0.006
As	2.3	1.7	0.3	4.1	1.8	3.1	2.7	2.5	2.9
Sb	0.1	0.2	0.1	0.1	0.1	0.1	0.1	0.1	0.1
Tl	0.13	0.10	0.03	0.18	0.03	0.11	0.23	0.14	0.13
Au	1.0	1.0	3.0	4.0	8.0	1.0	1.0	1.0	2.6
W	0.3	0.3	0.3	0.3	0.3	0.3	0.3	0.3	0.3
Mo	1.0	1.0	1.0	1.0	1.0	1.0	1.0	1.0	1.0
Sn	0.5	0.5	1.2	1.1	1.0	1.0	1.4	0.5	1.8
Cs	0.4	0.4	0.7	0.3	0.1	0.1	0.3	0.4	0.4
Ga	16	15	20	19	17	19	18	18	19
Rb	43	29	8	42	17	24	26	20	27
Ba	207	228	107	451	298	345	521	298	344
Sr	492	461	571	491	494	495	767	373	474
Nb	5.2	6.8	7.4	10.0	18.6	11.5	10.0	10.5	9.7
Ta	0.30	0.51	0.49	0.79	1.12	0.75	0.72	0.75	0.76
Y	14.3	16.9	22.2	13.1	21.1	22.7	21.5	18.4	24.0
Zr	89	128	121	144	168	160	190	161	177
Hf	2.7	3.4	3.6	4.0	3.8	4.3	5.1	4.1	4.4
Th	2.11	2.42	2.21	6.55	3.37	4.08	5.38	4.73	4.21
U	0.94	0.94	1.09	2.26	0.99	1.42	1.82	1.62	1.51
La	9.20	14.00	11.36	20.56	26.38	23.42	23.45	20.33	21.04
Ce	20.34	29.49	26.86	38.25	50.45	44.72	49.77	40.60	42.69
Pr	2.60	2.98	3.59	4.18	6.15	5.31	5.95	4.63	5.18
Nd	11.07	14.15	15.67	15.54	22.19	20.65	23.17	17.56	20.57
Sm	2.56	3.39	4.06	3.01	4.41	4.34	4.94	3.71	4.56
Eu	0.86	1.09	1.39	1.03	1.55	1.33	1.46	1.15	1.46
Gd	2.65	3.40	4.40	2.76	4.50	4.06	4.39	3.38	4.62
Tb	0.46	0.57	0.73	0.44	0.71	0.68	0.71	0.57	0.77
Dy	2.62	3.24	4.39	2.54	4.00	3.88	3.96	3.23	4.41
Ho	0.50	0.60	0.81	0.46	0.79	0.74	0.74	0.61	0.85
Er	1.46	1.77	2.49	1.38	2.30	2.28	2.21	1.83	2.51
Tm	0.22	0.27	0.38	0.21	0.33	0.33	0.33	0.29	0.38
Yb	1.48	1.70	2.36	1.37	1.97	2.13	2.20	1.91	2.40
Lu	0.21	0.24	0.35	0.20	0.30	0.31	0.32	0.28	0.35

Major oxides in wt %. All trace elements in ppm except S (%) and Au (ppb).

Mg # = 100 x (mol. MgO)/(mol. MgO + mol. FeO^t).

and. tuff = andesitic tuff. W = Walker Brook Member. T = Thompson Brook Member.

Table 2 *(cont'd)*. Whole-rock analyses of volcanic rocks from the Val d'Amour Formation.

Sample	**f-1001**	**g-277**	**h-127**	**h-140**	**g-525**	**g-527**	**avg. dacite**	**g-273**	**g-271**	**avg. rhy.**
Rock Type	dacite	dacite	dacite	dacite	Sugarl'f	Sugarl'f	n=6	rhyolite	rhyolite	n=2
Unit	T	T	T	T	Porphyry	Porphyry		R	R	
SiO_2	63.64	63.33	63.81	62.78	63.59	65.47	63.77	74.68	69.71	72.20
Al_2O_3	16.99	16.73	17.21	15.20	15.69	15.99	16.30	13.48	14.42	13.95
Fe_2O_3	3.47	5.38	4.22	3.52	3.12	3.11	3.80	1.46	2.70	2.08
MnO	0.10	0.13	0.07	0.06	0.04	0.06	0.08	0.01	0.07	0.04
MgO	1.95	0.37	1.45	1.20	1.67	1.54	1.36	0.12	0.56	0.34
CaO	4.17	3.44	1.56	5.41	4.75	3.98	3.89	0.35	0.69	0.52
Na_2O	4.67	5.01	7.39	2.52	4.16	4.82	4.76	3.32	4.67	4.00
K_2O	0.89	2.00	1.64	1.82	0.98	1.22	1.43	4.07	3.27	3.67
TiO_2	0.79	0.89	0.71	0.52	0.47	0.45	0.64	0.29	0.36	0.32
P_2O_5	0.17	0.29	0.22	0.18	0.15	0.15	0.19	0.03	0.08	0.06
LOI	3.05	2.74	1.96	6.90	5.14	2.96	3.79	2.13	3.60	2.87
Mg #	52.7	12.0	40.5	40.3	51.5	49.5	41.1	14.0	29.1	21.6
Cr	48	3	26	8	33	20	23	3	3	3
Ni	22	1	14	5	10	11	10	1	1	1
Co	17.0	7.0	13.0	9.0	9.0	9.0	10.7	0.5	3.0	1.8
Sc	13.9	9.9	10.0	7.1	6.1	5.6	8.8	4.8	5.1	5.0
V	80	35	59	45	42	42	51	6	8	7
Cu	30	17	23	17	22	32	24	8	11	10
Pb	10	15	6	13	16	14	12	18	8	13
Zn	44	106	46	50	50	86	64	26	39	32
Ag	0.7	0.5	0.2	0.2	0.2	0.2	0.3	0.2	0.4	0.3
S	0.022	0.001	0.001	0.006	0.001	0.001	0.005	0.006	0.001	0.003
As	10.5	4.5	5.0	3.2	2.1	2.1	4.6	12.5	40.6	26.6
Sb	0.3	0.3	0.1	0.1	0.2	0.1	0.2	0.7	0.1	0.4
Tl	0.22	0.20	0.14	0.26	0.07	0.14	0.17	0.24	0.30	0.27
Au	1.0	1.0	1.0	5.0	1.0	1.0	1.7	1.0	3.0	2.0
W	0.3	0.5	0.3	0.3	0.3	0.3	0.3	0.7	0.5	0.6
Mo	1.0	1.0	1.0	1.0	1.0	1.0	1.0	1.0	2.3	1.6
Sn	2.0	2.2	0.5	0.5	1.5	0.5	1.2	2.7	1.7	2.2
Cs	0.1	0.3	0.6	3.0	0.3	0.2	0.8	0.9	0.4	0.6
Ga	16	21	17	17	18	19	18	15	19	17
Rb	18	38	23	38	15	19	25	103	60	82
Ba	692	426	836	265	269	322	468	530	756	643
Sr	356	290	977	244	535	558	493	109	226	168
Nb	7.5	15.5	7.4	9.4	7.1	6.5	8.9	9.8	15.2	12.5
Ta	0.80	1.11	0.61	0.80	0.46	0.47	0.71	0.94	1.02	0.98
Y	13.2	35.2	12.1	11.3	7.0	7.1	14.3	19.8	26.1	23.0
Zr	168	359	145	130	135	130	178	203	256	229
Hf	3.8	8.0	3.5	3.2	3.3	3.3	4.2	5.6	6.6	6.1
Th	6.11	7.36	3.16	5.73	2.95	3.02	4.72	17.32	9.97	13.65
U	1.91	2.64	1.10	2.08	0.98	1.01	1.62	1.39	1.92	1.65
La	19.17	39.50	19.53	28.59	21.14	20.20	24.69	31.08	32.84	31.96
Ce	34.68	76.78	36.79	51.08	38.44	36.64	45.74	54.81	61.53	58.17
Pr	3.65	9.09	4.54	5.53	4.33	4.13	5.21	6.32	7.61	6.96
Nd	13.51	32.55	16.06	18.32	14.74	13.89	18.18	19.94	26.26	23.10
Sm	2.69	6.42	2.99	3.13	2.61	2.44	3.38	3.68	5.01	4.34
Eu	0.98	2.09	1.14	1.02	0.91	0.85	1.17	0.67	1.06	0.87
Gd	2.56	6.61	2.86	2.68	2.25	2.07	3.17	3.41	4.76	4.08
Tb	0.46	1.07	0.41	0.39	0.28	0.27	0.48	0.56	0.75	0.65
Dy	2.60	6.17	2.18	2.04	1.39	1.35	2.62	3.26	4.33	3.80
Ho	0.53	1.23	0.42	0.38	0.24	0.24	0.51	0.66	0.89	0.78
Er	1.50	3.70	1.18	1.13	0.65	0.67	1.47	2.19	2.74	2.46
Tm	0.23	0.55	0.16	0.16	0.08	0.08	0.21	0.36	0.43	0.40
Yb	1.42	3.23	1.02	0.98	0.52	0.56	1.29	2.31	2.64	2.47
Lu	0.20	0.49	0.16	0.15	0.08	0.08	0.19	0.36	0.40	0.38

Major oxides in wt %. All trace elements in ppm except S (%) and Au (ppb).

Mg # = 100 x (mol. MgO)/(mol. MgO + mol. FeO^t).

T = Thompson Brook Member. R = Richardsville Member.

ACKNOWLEDGEMENTS

The authors thank John Langton and Steve McCutcheon of the Geological Surveys Branch of the New Brunswick Department of Natural Resources for critical review and improvement of the manuscript.

REFERENCES

Alcock, F.J. 1935. Geology of Chaleur Bay region. Geological Survey of Canada, Memoir 183, 146 p.

Ami, H.M. 1900. Synopsis of the geology of Canada (being a summary of the principal terms employed in Canadian geological nomenclature). Proceedings and Transactions of the Royal Society of Canada, Second Series, Vol. 6, Section 4, pp. 187–225.

Ami, H.M. 1902. Equisse géologique du Canada pour servir à la préparation d'un chronographe géologique du Canada et des autres parties de l'Amérique septentrionole britannique. Québec, Le Naturaliste Canadien, 60 p.

Bourque, P.-A., and Lachambre, G. 1980. Stratigraphie du Silurien et du Dévonien basal du Sud de la Gaspésie, Québec. Ministère de l'Énergie et des Ressources Québec, ES-30.

Bourque, P.-A., Brisebois, D., and Malo, M. 1995. Gaspé Belt. Chapter 4 *in* Geology of the Appalachian–Caledonian Orogen in Canada and Greenland. *Edited by* H. Williams. Geological Survey of Canada, Geology of Canada, No. 6, pp. 316–351.

Burk, C.F., Jr. 1964. Silurian stratigraphy of Gaspé Peninsula, Québec. Bulletin of the American Association of Petroleum Geologists, **48**: 437–464.

Castonguay, S., Lavoie, D., Malo, M., Tremblay, A., Brisebois, D., Lauzière, K., Dietrich, J., Carroll, J., Wilson, R., Lebel, D., McCutcheon, S., and Colman-Sadd, S. 2003. Appalachian foreland and platform architecture in Quebec, New Brunswick and Newfoundland: report of progress of the geological bridges of eastern Canada. *In* Abstracts, 2003: 28th Annual Review of Activities. *Edited by* B.M.W. Carroll. New Brunswick Department of Natural Resources; Minerals, Policy and Planning Division, Information Circular 2003-1, pp. 11–12.

Castonguay, S., Wilson, R., Brisebois, D., Desrochers, A., Malo, M., and Lavoie, D. 2004. Geologic compilation of NATMAP Transect IV, Anticosti–Gaspé–Campbellton: from the Anticosti Platform to the Gaspé Belt of northern New Brunswick. *In* Abstracts, 2004: Exploration and Mining New Brunswick. *Edited by* S.A.A. Merlini. New Brunswick Department of Natural Resources; Minerals, Policy and Planning Division, Information Circular 2004-1, pp. 5–6.

Chiswell, P.G. 1979. Differentiation trends of the teschenite sill in Dalhousie, New Brunswick. Unpublished B.Sc. thesis, Department of Geology, University of New Brunswick, Fredericton, New Brunswick, 52 p.

Clarke, J.M. 1909. The Dalhousie Formation. *In* Early Devonic history of New York and eastern North America. New York State Museum, Memoir 9, Part 2, pp. 7–51.

Dineley, D.L., and Williams, B.P.J. 1968. Sedimentation and paleoecology of the Devonian Escuminac Formation and related strata, Escuminac Bay, Quebec. *In* Late Paleozoic and

Mesozoic continental sedimentation, northeastern North America. *Edited by* G. de Vries Klein. Geological Society of America, Special Paper 106, pp. 241–264.

Dostal, J., Wilson, R.A., and Keppie, J.D. 1989. Geochemistry of Siluro–Devonian Tobique volcanic belt in northern and central New Brunswick (Canada): tectonic implications. Canadian Journal of Earth Sciences, **26:** 1282–1296.

Dostal, J., Laurent, R., and Keppie, J.D. 1993. Late Silurian–Early Devonian rifting during dextral transpression in the southern Gaspé Peninsula (Québec): petrogenesis of volcanic rocks. Canadian Journal of Earth Sciences, **30**: 2283–2294.

Ells, R.W. 1881. Report on the geology of northern New Brunswick, embracing portions of the counties of Restigouche, Gloucester and Northumberland. Geological Survey of Canada, Report of Progress for 1879–80, Part D, 47 p.

Ells, R.W. 1883. Report on the geology of northern and eastern New Brunswick and the north side of the Bay of Chaleurs. Geological Survey of Canada, Report of Progress for 1880–81–82, Part D, 24 p.

Fitton, J.G., James, D., and Leeman, W.P. 1991. Basic magmatism associated with the late Cenozoic extension in the western United States: compositional variations in space and time. Journal of Geophysical Research, **96**: 13693–13711.

Fyffe, L.R., and Fricker, A. 1987. Tectonostratigraphic terrane analysis of New Brunswick. Maritime Sediments and Atlantic Geology, **23:** 113–123.

Gamba, C.A. 1990. Sedimentology and tectonic implications of the Point La Nim and Campbellton formations, western Chaleur Bay, Maritime Canada. Unpublished M.Sc. thesis, University of Ottawa, Ottawa, Ontario.

Gensel, P.G. 1982. A new species of *Zosterophyllum* from the early Devonian of New Brunswick. American Journal of Botany, **69**: 651–669.

Gensel, P.G., Cloutier, R., and McCutcheon, S. 1997. Devonian plants and fishes of the Gaspé Peninsula, Quebec and northern New Brunswick. American Institute of Biological Sciences, Field Trip 22: August 6–11, 1997. Department of Biology, University of North Carolina-Chapel Hill, 21 p.

Greiner, H.R. 1970. Geology of the Charlo area, 21-O/16, Restigouche County, New Brunswick. New Brunswick Department of Natural Resources; Mineral Resources Branch, Map Series 70-2, 18 p.

Greiner, H.R. 1974a. Geology of Campbellton, Restigouche County, New Brunswick. New Brunswick Department of Natural Resources; Mineral Resources Branch, Plate 74-114.

Greiner, H.R. 1974b. Geology of Escuminac (west half), Restigouche County, New Brunswick. New Brunswick Department of Natural Resources; Mineral Resources Branch, Plate 74-60.

Greiner, H.R. 1974c. Geology of Oak Bay (east half), Restigouche County, New Brunswick. New Brunswick Department of Natural Resources; Mineral Resources Branch, Plate 74-61.

Hind, H.Y. 1865. A preliminary report on the geology of New Brunswick, together with a special report on the distribution of the Québec Group. Legislative Assembly, Fredericton, New Brunswick, 293 p.

Hon, R., Fitzgerald, J.P., Sargent, S.L., Schwarz, W.D., Dostal, J., and Keppie, J.D. 1992. Silurian–Early Devonian mafic rocks of the Piscataquis volcanic belt in northern Maine. Atlantic Geology, 28: 163–170.

Honeyman, D. 1878. A month among the geological formations of New Brunswick. Nova Scotian Institute of Science, Transactions, **4:** 5–21.

Howard, W.V. 1926. Devonian volcanic rocks near Dalhousie, New Brunswick. Geological Society of America Bulletin, **37**: 475–496.

Jaffey, A.H., Flynn, K.F., Glendenin, L.E., Bentley, W.C., and Essling, A.M. 1971. Precision measurement of half-lives and specific activities of ^{235}U and ^{238}U. Physical Review, **4:** 1889–1906.

Keppie, J.D., and Dostal, J. 1994. Late Silurian–Early Devonian transpressional rift origin of the Quebec Reentrant, northern Appalachians: constraints from geochemistry of volcanic rocks. Tectonics, **13:** 1183–1189.

Krogh, T.E. 1973. A low-contamination method for hydrothermal decomposition of zircon and extraction of U and Pb for isotopic age determinations. Geochimica et Cosmochimica Acta, **37:** 485–494.

Krogh, T.E., 1982. Improved accuracy of U–Pb zircon ages by the creation of more concordant systems using an air abrasion technique. Geochimica et Cosmochimica Acta, **37:** 637–649.

Laurent, R., and Bélanger, J. 1984. Geochemistry of Silurian–Devonian alkaline basalt suites from the Gaspé Peninsula, Quebec Appalachians. Maritime Sediments and Atlantic Geology, **20:** 67–78.

Logan, W.E., Murray, A., Sterry Hunt, T., and Billings, E. 1863. Geology of Canada. Geological Survey of Canada. Report of Progress from its commencement to 1863, 983 p.

Ludwig, K. 2001. Isoplot/Ex version 2.2: a geochronological toolkit for Microsoft Excel. Berkeley Geochronology Center Special Publication, No.1a, 53 p.

Malo, M., and Bourque, P.-A. 1993. Timing of the deformation events from Late Ordovician to Mid-Devonian in the Gaspé Peninsula. *In* The Acadian Orogeny: recent studies in New England, Maritime Canada, and the autochthonous foreland. *Edited by* D.C. Roy and J.W. Skehan. Geological Society of America Special Paper, **275**: 101–122.

Meschede, M. 1986. A method of discriminating between different types of mid-ocean ridge and continental tholeiites with the Nb–Zr–Y diagram. Chemical Geology, **56**: 207–218.

Miller, R. F. 1996. Note on *Pterygotus anglicus* Agassiz (Eurypterida: Devonian) from the Campbellton Formation, New Brunswick. Atlantic Geology, **32**: 95–100.

Miller, R.F., Cloutier, R., and Turner, S. 2003. The oldest articulated chondrichthyan from the Early Devonian period. Nature, **425:** 501–504.

Miyashiro, A. 1974. Volcanic rock series in island arcs and active continental margins. American Journal of Science, **274**: 321–357.

Pearce, J.A., and Cann, J.R. 1973. Tectonic setting of basic volcanic rocks determined using trace element analyses. Earth and Planetary Science Letters, **19**: 290–300.

Pearce, J.A., Baker, P.E., Harvey, P.K., and Luff, I.W. 1995. Geochemical evidence for subduction fluxes, mantle melting and fractional crystallization beneath the South Sandwich island arc. Journal of Petrology, **36**: 1073–1109.

Richardson, J.B., and McGregor, D.C. 1986. Silurian and Devonian spore zones of the Old Red Sandstone continent and adjacent regions. Geological Survey of Canada, Bulletin 364.

Rodgers, J. 1970. The Tectonics of the Appalachians. John Wiley and Sons, New York.

Seaman, S.J., Scherer, E.E., Wobus, R.A., Zimmer, J.H., Sales, and J.G. 1999. Late Silurian volcanism in coastal Maine: the Cranberry Island series. Geological Society of America Bulletin, **111:** 686–708.

Sun, S.S. 1982. Chemical composition and origin of the Earth's primitive mantle. Geochimica et Cosmochimica Acta, **46**: 179–192.

Sun, S.-S., and McDonough, W.F. 1989. Chemical and isotopic systematics of oceanic basalts: implications for mantle composition and processes. *In* Magmatism in the ocean basins. *Edited by* A.D. Saunders and M.J. Norry. Geological Society Special Publication No. 42, pp. 313–345.

Taylor, S.R., and McLennan, S.M. 1985. The Continental Crust: Its Composition and Evolution. Blackwell Scientific, Boston, Massachussetts.

van Staal, C.R. 1994. Brunswick subduction complex in the Canadian Appalachians: record of the Late Ordovician to Late Silurian collision between Laurentia and the Gander margin of Avalon. Tectonics, **13**: 946–962.

van Staal, C.R., Dewey, J.F., Mac Niocaill, C., and McKerrow, W.S. 1998. The Cambrian–Silurian tectonic evolution of the northern Appalachians and British Caledonides: history of a complex, west and southwest Pacific-type segment of Iapetus. *In* Lyell:.The Past is the Key to the Present. *Edited by* D.J. Blundell and A.C. Scott. London: The Geological Society, Special Publication 143, pp. 199–242.

Walker, J.A., Gower, S., and McCutcheon, S.R. 1993. Antinouri Lake–Nicholas Denys project, Gloucester and Restigouche counties, New Brunswick. *In* Current Research. *Compiled and edited by* S.A. Abbott. New Brunswick Department of Natural Resources and Energy; Mineral Resources, Information Circular 93-1, pp. 58–70

Walker, J.A., and McCutcheon, S.R. 1995. Siluro–Devonian stratigraphy of the Chaleur Bay synclinorium, Northern New Brunswick. *In* Current Research 1994. *Compiled and edited by* S.A.A. Merlini. New Brunswick Department of Natural Resources and Energy; Minerals and Energy Division, Miscellaneous Report 18, pp. 225–244.

Wellman, C. 1993. A Lower Devonian sporomorph assemblage from the Midland Valley of Scotland. Transactions of the Royal Society of Edinburgh, Earth Sciences, **84**: 117–136.

Wilson, R.A. 2002. Geology of the Squaw Cap area (NTS 21 O/15d, e, f), Restigouche County, New Brunswick. *In* Current Research 2001. *Edited by* B.M.W. Carroll. New Brunswick Department of Natural Resources and Energy; Minerals, Policy and Planning Division, Mineral Resource Report 2002-4, pp. 155–196.

Wilson, R.A. 2003. Geochemistry and petrogenesis of Ordovician arc-related mafic volcanic rocks in the Popelogan Inlier, northern New Brunswick. Canadian Journal of Earth Sciences, **40**: 1171–1189.

Wilson, R.A., Burden, E.T., Bertrand, R., Asselin, E., and McCracken, A.D. 2004. Stratigraphy and tectono-sedimentary evolution of the Late Ordovician to Middle Devonian Gaspé Belt in northern New Brunswick: evidence from the Restigouche area. Canadian Journal of Earth Sciences, **41:** 527–551.

Winchester, J.A., and Floyd, P.A. 1977. Geochemical distribution of different magma series and their differentiation products using immobile elements. Chemical Geology, **20**: 325–343.

ISSN0548-4014
ISBN1-55396-354-7
Price:$19.00